The University of Southern Mississippi

The Aquila Digital Community

Dissertations

Spring 5-2017

Polyisobutylene Telechelic Prepolymers by In Situ End-Quenching and Post-Polymerization Modifications

Bin Yang
University of Southern Mississippi

Recommended Citation

POLYISOBUTYLENE TELECHELIC PREPOLYMERS BY *IN SITU* END-

QUENCHING AND POST-POLYMERIZATION MODIFICATIONS

by

Bin Yang

A Dissertation
Submitted to the Graduate School
and the School of Polymers and High Performance Materials
at The University of Southern Mississippi
in Partial Fulfillment of the Requirements
for the Degree of Doctor of Philosophy

Approved:

_____
Dr. Robson F. Storey, Committee Chair
Professor, Polymers and High Performance Materials

_____
Dr. Derek L. Patton, Committee Member
Associate Professor, Polymers and High Performance Materials

_____
Dr. James W. Rawlins, Committee Member
Associate Professor, Polymers and High Performance Materials

_____
Dr. Jeffrey S. Wiggins, Committee Member
Associate Professor, Polymers and High Performance Materials

_____
Dr. Jason D. Azoulay, Committee Member
Assistant Professor, Polymers and High Performance Materials

_____
Dr. Karen S. Coats
Dean of the Graduate School

May 2017

Published by the Graduate School

THE UNIVERSITY OF
SOUTHERN
MISSISSIPPI.

ABSTRACT

POLYISOBUTYLENE TELECHELIC PREPOLYMERS BY *IN SITU* END-

QUENCHING AND POST-POLYMERIZATION MODIFICATIONS

by Bin Yang

May 2017

This volume focuses on the development of telechelic polyisobutylene (PIB)

prepolymers by combining end-capping of living carbocationic polymerization of

isobutylene (IB) with suitable reactants and post-polymerization modifications.

Alkylation kinetics of PIB *tert*-chloride with alkoxybenzenes using either $TiCl_4$ or $AlCl_3$

were investigated. Quantitative *para*-position end-capped products were only achieved if

the alkoxybenzene/$AlCl_3$ molar ratio was greater than unity; while no such molar ratio is

required for $TiCl_4$, but the alkylation rate was slower than $AlCl_3$ under the same

conditions. Photopolymerization kinetics analysis of PIB triphenol tri(meth)acrylates

with low and high M_ns, and control aliphatic PIB triol triacrylate with similar high M_n

showed that Darocur 1173 afforded the highest photopolymerization rate and conversion.

Kinetics analysis also indicated despite of end-functionality and acrylate structure,

photopolymerization rate for PIB prepolymers with high M_ns, attributed to reduced

diffusional mobility, resulting in decreased rate of termination and autoacceleration.

Structure-property relationships indicated the T_g of PIB networks decreased as the M_n of

PIB macromer increased regardless of end-group type, and thermal stability remained

constant regardless of end-group type. Tensile properties were characteristic of weak

rubbery networks. Quantitative synthesis of PIB telechelic prepolymers with various

types of epoxides, including aliphatic and phenyl glycidol ether, *exo*-olefin epoxide, and

cyclohexene epoxide have been developed through post modifications. A novel method for PIB chain end functionalization was developed whereby living PIB is end-capped with the bulky comonomer, 4-(4-allyloxyphenyl)-2-methyl-1-butene (AMB) at full IB conversion. Addition is readily limited to one or two comonomer units per chain end at a low [AMB]/[chain end] ratio. The mechanism suggested that upon addition of AMB, the resulting carbocation tends to undergo terminative chain transfer consisting of alkylation of the 4-allyloxyphenyl ring at C2, *via* a five-membered cyclic intermediate. Grubbs 3rd generation mediated ROMP of PIB (oxa)norbornene macromonomers *via* a grafting "through" methodology were conducted successfully, producing PIB bottlebrush polymers with controlled molecular weight and low dispersities. Both ^{1}H NMR and SEC kinetics analyses showed pseudo-first-order kinetic behavior for these macromonomers. Besides, both kinetic studies demonstrated that the ROMP propagation rate of PIB norbornene is at least 2.2 times greater than that of PIB oxanorborne macromonomer.

ACKNOWLEDGMENTS

DEDICATION

This work is dedicated to my parents for their endless love, care, and support for all paths I chose to pursue.

Finally, much gratitude to my family and friends for their much appreciated support and understanding.

TABLE OF CONTENTS

LIST OF TABLES

LIST OF ILLUSTRATIONS

xiii

LIST OF SCHEMES

CHAPTER I - BACKGROUND

1.1 Polyisobutylenes

Polyisobutylene (PIB) is a chain growth, addition polymerization product of the monomer isobutylene (IB), which is exclusively polymerizable by cationic mechanism. PIB possesses remarkable properties,[1-6] such as strong adherence, high flexibility, good thermal and oxidative stability, low gas permeability, good energy damping and solvent resistance, and biostability/biocompatibility.[7-9] PIB is very flexible with a low glass transition temperature around -70°C; thus it demonstrates elastomeric properties within a wide range of application temperatures. With regard to its physical state, PIB is a tacky, clear, viscous liquid if its molecular weight (MW) is below 100 kDa;[10] above this threshold it is a "solid" elastomer because of high chain entanglement density. Such physical entanglements alone do not make PIB a useful rubber. Like most other hydrocarbon elastomers, including natural rubber, it must be crosslinked (i.e., vulcanized) to possess proper strain recovery and resistance to creep. However, unlike natural rubber and other diene-monomer-based elastomers, PIB possesses no backbone unsaturations to serve as sites for sulfur vulcanization or other chemical crosslinking reactions. This issue was resolved by copolymerizing IB with a small fraction of isoprene (2-3 mol%) to form the commercial elastomer known as butyl rubber.[11-12]

The acid-catalyzed oligomerization of isobutylene at room temperature in the presence of the Lewis acid BF_3 was discovered in the 1870s by Bulterov *et al.*[13] Not until the 1930s was it realized that PIB molecular weight increased as polymerization temperature decreased and that temperatures < -10°C were necessary for the preparation of other than oligomeric PIBs using a BF_3 catalyst;[14] this insight enabled the preparation

of PIB with high molecular weight at -100°C. [15] Later, PIBs with MW around 300k Da were developed using the refined isobutylene/ethylene/BF_3 system and branded as Oppanol® (BASF) and Vistanex® (Exxon); these products were used to improve oxidative resistance of natural rubber. Although it was generally known that lower temperatures enabled high MW by suppressing chain transfer to monomer, unlike the anionic polymerizations demonstrated by Szwarc in 1956,[16] cationic polymerizations of isobutylene did not lend themselves to molecular weight control by manipulation of the monomer/initiator stoichimetry. Thus, development of the controlled/living polymerization of IB was slow. In the early 1980s, the first conditions for living carbocationic polymerization (LCP) of IB were realized by Kennedy *et al.*[17] Their system provided control over initiation, and propagation was sustained without appreciable chain transfer or termination until full consumption of IB monomer. All LCP systems, including the original system of Kennedy, belong to the type of living polymerization systems known as reversible-deactivation polymerizations.[18] The development of LCP of PIB enabled the synthesis of "telechelic" PIBs, which are low to medium molecular weight PIBs possessing chemical functionality at the chain ends; although many different functional groups can be fitted to the chain ends of PIB through post-polymerization modification, the reactions required to do so are often tedious and/or expensive.

The fundamental and major focus of this dissertation is on the development of novel telechelic PIB prepolymers by combining living carbocationic polymerization of PIB with post-polymerization modifications. Thus, relevant reviews will cover conventional and living carbocationic polymerization, chain end functionalization (post-polymerization and in situ), telechelic PIB prepolymers, and bottleneck brush polymers.

1.2 Living Carbocationic Polymerization of Isobutylene

1.2.1 Commercial Polyisobutylenes

Although living carbocationic polymerization of PIB has been realized for almost 30 years, most current low MW PIBs are still manufactured using conventional non-living processes, where chain transfer to monomer is the dominant chain terminating reaction affording a mixture of unsaturated termini.[19] These conventional polymerization systems consist of an $AlCl_3$ or BF_3 catalyst in conjunction with protic initiators, such as water or alcohols, in a hydrocarbon solvent at moderately low temperatures (e.g. -10 °C). PIBs synthesized by $AlCl_3$ coinitiators yield terminal unsaturations consisting predominantly of internal double bonds, namely tri- and tetra-substituted olefins, with only a small fractions of the more reactive and more desirable *exo*-olefin (methyl vinylidene) end groups. In contrast, BF_3-catalyzed PIBs possess 70-90% *exo*-olefin termini and are hence referred to as highly reactive PIB (HRPIB).[20-21] BASF markets HRPIB possessing 80-85% *exo*-olefin end groups under the trademark of Glissopal®, which is used to prepare oil additives by hydroformylation and subsequent reductive amination to yield primary amine terminated PIBs, sold under the trademark Kerocom®. Since commercial PIBs are produced using chain transfer dominated processes, these materials typically possess a mixture of end groups are inherently limited to linear monofunctional chains. Thus, controlled synthesis of telechelic PIBs with mono- to multi- chain end functionality and more complicated architectures must rely on the living carbocationic polymerization technique.

1.2.2 Living Carbocationic Polymerization of Isobutylene

Contrary to the synthesis of conventional PIBs, living polymerization proceeds in the absence of chain transfer and termination. Endeavors towards living carbocationic polymerization of IB were primarily performed in the Kennedy laboratory at The University of Akron. The first step toward living IB polymerization was the development of a difunctional *initiator*-transfer agent (inifer)[22] system consisting of *p*-dicumyl chloride initiator/chain transfer agent (the "inifer") and BCl_3 coinitiator. Although such systems were free of chain transfer to monomer, they suffered from poor control due to overly fast kinetics and heterogeneity caused by precipitation of the formed PIB in the polar solvent medium. Later, tertiary ether[23] and ester[17] initiators were discovered to afford better control, and $TiCl_4$ coinitiator was developed for use in less-polar solvent media, thereby enabling homogeneous systems.[24-25] For both BCl_3 and $TiCl_4$ systems, termination by transfer of a chloride ion from the counterion to the carbenium ion, i.e., ion pair collapse, was known to occur and to form dormant *tert*-chloride (*tert*-Cl) terminated chain ends. It was proposed that similar ligand exchange reactions between ether- and ester-based initiators occurred, resulting in generation of "electron donating" species *in situ*.[26] It was further suggested that the *in situ*-generated "electron donating" species stabilized the growing carbocation center and thus imparted control over the polymerization. At about the same time, it became popular to use external electron donors such as DMSO or pyridine to provide controlled polymerization. Interestingly, Faust proposed that the sole purpose of these external electron donors was to scavenge protic impurities from the system. However, it was known that common ion salt precurors, such as tetrabutyl ammonium chloride (TBACl), would also increase the livingness of IB polymerization,

4

by combination of $TiCl_4$ with the chloride ion to form the ammonium $Ti_2Cl_9{}^{\ominus}$ ion pair, which suppressed ion pair dissocation and shifted the chain end equilibrium toward lower ionicity. Storey *et al.* [27] confirmed that external electron donors such as pyridines indeed scavenged protic impurities, but they disagreed that this was their sole role and pointed out that products of proton scavenging were ammonion salts. Thus these authors suggested that external electron donors and common ion salts worked in the same way, that is, by generating common ions, thus suppressing the formation of free ions, resulting in the living polymerization of IB.

cationation

initiation

propagation

(reversible) termination
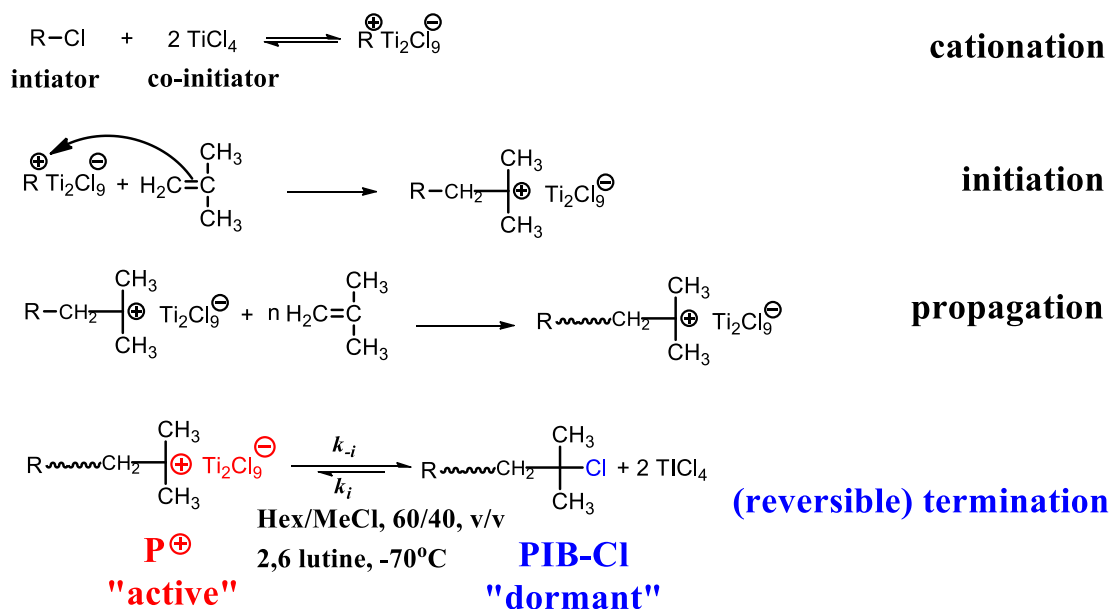
Scheme 1.1 Mechanism of living carbocationic polymerization of IB.

To date, mechanistic understanding of living carbocationic polymerization of IB has matured,[28] as illustrated in Scheme 1.1 for the specific case of $TiCl_4$-co-initiated systems. The goal of precise MW control and narrow PDI has three prerequisites: control of initiation, realization of reversible termination, and inhibition of chain transfer to either monomer or polymer, all of which have been addressed effectively. First, the dimer of

5

co-initiator TiCl$_4$ abstracts the chloride from the initiator to create an ion pair; this step is called cationation. In the second step, termed initiation, an IB monomer attacks the carbocation to initiate the polymerization. In the propagation step, multiple IB monomer additions occur to propagate a long PIB chain. As propagation proceeds, IB monomers are consumed. In the absence of transfer reactions, the degree of polymerization of the chains is equal to the concentration of consumed monomer divided by the concentration of R-Cl initiators. The termination reaction shown in the last step gives *tert*-Cl chain ends through ion pair collapse, which is a reversible process and very important for polymerization control. The maintenance of a large proportion of reversibly terminated chains allows suppression of the typically very high polymerization rates encountered in traditional cationic polymerizations. Upon purposeful destruction of the TiCl$_4$ catalyst, after the polymerization is complete, the chain ends are typically uniformly *tert*-Cl, and many *in situ* and *ex situ* PIB chain end functionalizations start with this characteristic end group.

Similar to other living polymerization techniques such living radical and anionic polymerization, living carbocationic polymerization has been employed to create sophisticated architectures such as block[29-35] and star[36-37] copolymers.

1.3 Functionalization of Polyisobutylenes

Terminally-functionalized (i.e., telechelic) PIBs enable the preparation of more complex materials for advanced applications, such as lubricant additives,[38] adhesives,[39] surface modifiers, [40] biomaterials, [9] and coatings. [41] To achieve the best properties and material performance, telechelic PIBs with nearly quantitative end group functionality are desired. Generally, two approaches have been applied for the chain end functionalization

of PIB, post-polymerization modifications and *in situ* functionalization. The latter

technique is the main focus of this dissertation, but a combination of the two approaches

has also been employed to expand the variety of end groups possible.

1.3.1 Post-Polymerization Modification

As previously mentioned, the end-functional groups of industrial PIBs are mainly

70-90% *exo*-olefin with the balance consisting of various minor olefinic structures. The

early difunctional PIBs by Kennedy *et al.*[42] consisted of *tert*-Cl-terminated PIB, which

were subjected to post-polymerization dehydrochlorination to form nearly 100% *exo*-

olefin-terminated PIB. Thus, *exo*-olefin-terminated PIB was a commonly available chain

end functionality and a convenient intermediate for further functionalization. Industrially,

exo-olefin-terminated PIB has been largely used to prepare an important intermediate,

polybutenylsuccinic anhydride (PIBSA) *via* thermal-ene reaction of the terminal

unsaturation with maleic anhydride. PIBSA is further transformed to a

polybutenylsuccinimide, which is used as an ashless dispersant in lubricating oils to

eliminate sludge or varnish accumulation on engine surfaces.

Kennedy *et al.*[43] reported the synthesis of hydroxyl-terminated PIB by

hydroboration-oxidation of *exo*-olefin terminated PIB. Kennedy *et al.* [44] also prepared

exo-olefin epoxide by direct epoxation of the olefin moiety with a strong peracid. The

obtained epoxide-terminated PIB was subjected to an acid-catalyzed isomerization to

form aldehyde,[45] which was subsequently converted to hydroxyl-terminated PIB by

reduction. Many further PIB chain end functionalities were obtained by modification of

hydroxyl-terminated PIB, such as allyl,[46] carboxylic acid,[47] isocyanate,[48-49] amine,[50-51]

etc.
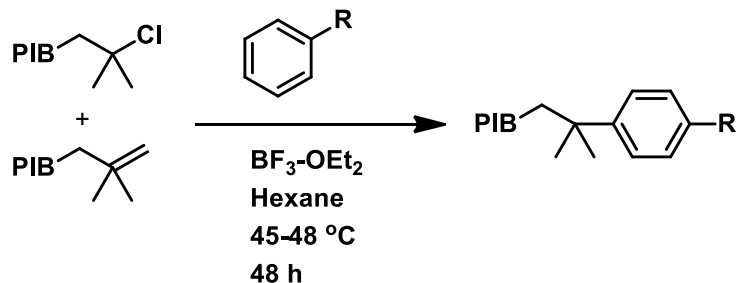
Scheme 1.2 Friedel-Crafts alkylation of *tert*-Cl and *exo*-olefin terminated PIB with phenolic and benzene derivatives.

Exo-olefin and *tert*-Cl groups have been subjected to Friedel-Crafts alkylations, as shown in Scheme 1.2. Kennedy *et al.* demonstrated alkylation of both *exo*-olefin- and *tert*-Cl terminated-PIBs with phenol,[52] anisole,[53] benzene, toluene, and xylene[54] using a boron trifluoride etherate (BF$_3$-OEt$_2$) catalyst under reflux at 45-48°C for 48 h. The resulting phenol-terminated PIB was then converted to phenyl glycidyl ether[55] by reacting with epichlorohydrin. Di/trifunctional phenyl glycidyl ether-terminated PIBs showed good curability with triethylene tetramine for crosslinked network formation.[56]

Although post-polymerization modifications such as those described above are somewhat tedious and often require stringent conditions to obtain quantitative chain end functionalization, some routes have proven to be adaptable to direct *in situ* functionalization of living PIB. For instance, the alkylation of *exo*-olefin and *tert*-Cl terminated PIB with phenolic derivatives paved the way for direct chain-end functionalization by end-quenching living IB polymerizations at full monomer conversion with alkoxybenzenes.

1.3.2 *In-Situ* Functionalization

The development of living carbocationic polymerization of IB has led to new methods for direct functionalization of living PIB chain ends. Two main approaches

have been pursued: initiation from functional initiators, and termination of the living

polymerization by a suitable nucleophile at full monomer conversion (end-quenching).

1.3.2.1 Functional Initiators

Although numerous types of functional initiators have been investigated, the types

of appealing initiators are limited due to the strict requirements of living cationic

polymerization and various side reactions. Also, most functional initiators require

protection of the desired functionalities during the polymerization. For example, Puskas

et al.[57] developed initiators containing latent hydroxyl groups masked as epoxides.

Hydroxyl functionality at the initiation site was obtained by induced ring opening of the

epoxide moiety in the presence of $TiCl_4$. Unfortunately, the initiation efficiency remained

low due to epoxide rearrangement, such as formation of aldehydes and polyethers. For

example, the maximum efficiency for 1,2-epoxycyclohexane initiator was 48%, and

while higher monomer concentration leads to higher efficiency, it also risks decreasing

livingness of the polymerization.[58-59] Furthermore, functional initiators only provide

functionality at the initiation site; the growing PIB chain end retains a *tert*-Cl group,

which requires subsequent functionalization.

1.3.2.2 *In-Situ* Functionalization

Since chain transfer and termination are negligible for living carbocationic

polyermerization of IB, PIB carbocation chain end remains active for a long period of

time even at full IB monomer consumption. This implies a great potential for direct chain

end functionalization by immediate addition of a nucleophilic reagent (quencher).

However, direct functionalization is often challenging due to the low concentration of the

active PIB carbocation chain ends, and the tendency for nucleophiles to complex and/or

react with the Lewis acid. In living carbocationic polymerization of IB, reaction

conditions (especially solvent polarity) have been purposefully designed so that the

chain-end ionization equilibrium constant of [active PIB $^{\oplus}$]/[dormant *tert*-Cl] is very

small, on the order of 10^{-7} M^{-2}. This reduces the rate of polymerization allowing for

synthetic manipulations and is beneficial for precise MW control and narrow PDI.

However, when a nucleophile is added, the intended reaction with the PIB carbocation is

often scarce, and the nucleophile may react with the more abundant Lewis acid instead.

This tends to drive the aforementioned chain-end ionization equilibrium back toward the

dormant *tert*-Cl form. Therefore, the nucleophiles that have been successfully used for

functionalization are limited to those which do not react with a Lewis acid co-initiator. If

a "hard" σ-nucleophile quenching agent is used, such as methanol or ammonia, the

resulting product will be PIB chains with *tert*-Cl end groups,[60-61] because the quencher,

instead of reacting with the carbenium ion chain ends, reacts with the far more abundant

Lewis acid.

In general, nucleophilic quenchers are designed to modify the chain ends either by

1) regiospecific elimination reaction to form *exo*-olefin or 2) addition reaction to form

some other functional group. To date, most successful quenchers (as shown in Scheme

1.3) that cause elimination at the chain ends to form *exo*-olefin PIB belong to two classes:

1) hindered bases (such as 2,5-dimethylpyrrole,[62] 2-*tert*-butylpyridine,[63] 2,2,6,6-

tetramethylpiperidine, and 1,2,2,6,6-pentamethylpiperidine),[64] and 2) (di)sulfides[65-67]

(such as di-*tert*-butyl- or diisopropylsulfide) and ethers[68] (such as diisopropyl ether).

Hindered bases are sufficiently sterically hindered to prevent complete complexation with

TiCl$_4$ but not so sterically hindered as to prevent abstraction of a β-proton from the

carbenium ion. However, for sulfide and ether quenchers, sulfonium and oxonium ion

adducts are formed first and then reacted with excess alcohol or amines to yield *exo*-

olefin. For example, Ummadisetty and Storey[68] reported the quenching reaction of $TiCl_4$

catalyzed isobutylene polymerization at -60 °C in hexane/methyl chloride (60/40, v/v)

solvent with ethers to yield *exo* olefin. They found that the yield of *exo*-olefin was

directly related to the steric bulkiness of the ether, in the order of *sec*-butyl (100%) ≈

isopropyl (100%) > *n*-alkyl (68.5−81.5%). Although such quenching technology is useful

for directly obtaining olefin groups at full conversion, industrial production may be

limited because of quencher cost and the low temperature and/or dilute systems required.
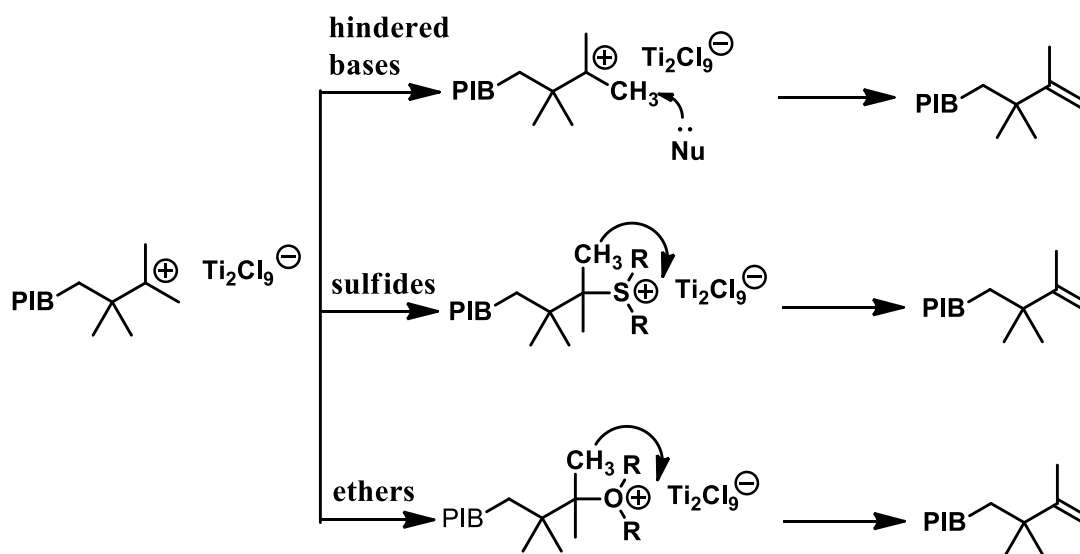
Scheme 1.3 Direct *in-situ exo*-olefin chain end functionalization by end-quenching living polymerization of IB with suitable hindered bases, sulfides, and ethers.

"Hard" σ-nucleophiles such as unhindered alcohols or amines yield *tert*-Cl groups

at the PIB chain end; thus quenchers designed to modify chain ends by addition reaction

tend to be "soft," π-nuclophiles. Two classes of π-nucleophiles have been successfully

used to cap the chain ends of $TiCl_4$-catalyzed living PIB: non-homopolymerizable olefins

such as butadiene[69] or allyltrimethylsilane,[70-72] and heterocyclic aromatics.[73-77] De and Faust[69] reported that living PIB may be quenched with 1,3-butadiene to yield quantitative allyl chloride end groups (i.e., PIB-CH$_2$-CH=CH-CH$_2$-Cl) via 1,4-monoaddition of the diene followed by immediate chlorination via counteranion collapse. Since a primary bromide group is more reactive in nucleophilic substitution, post-polymerization modifications were developed to prepare PIB-allyl bromide, including halogen exchange from PIB-allyl chloride using LiBr,[78] as well as the more complicated procedure of replacing TiCl$_4$ with a totally brominated Lewis acid system (produced from mixtures of aluminum tribromide and trimethylaluminum).[79] By using PIB-allyl-bromide as the starting material, a series of functional end groups was reported, [80] such as -OH, -NH$_2$, -COOH, -N$_3$, and -OCH$_2$C≡CH.

Highly reactive heterocyclic aromatics like thiophene[74] and *N*-substituted pyrroles[75-76] can undergo Friedel-Crafts alkylation to introduce various functional end groups onto the polymer chain. For example, Storey *et al*.[76] obtained quantitative alkylation of living PIB using either *N*-(2-chloroethyl)pyrrole or the corresponding bromo compound with either a 2-carbon or a 3-carbon tether. Later, hydroxyl-terminated PIB was obtained *in situ* using a protected *N*-(ω-hydroxyalkyl)pyrrole[77] followed by heating the reaction mixture in the presence of ethylaluminum dichloride and sulfuric acid to de-block the *tert*-butyl group. The de-blocking procedure also induced the alkylation of pyrrole by the small fraction (< 5%) *exo*-olefin chain ends formed during the alkylation, to yield exclusively hydroxyl-functionalized PIB. The primary hydroxyl groups thus obtained demonstrated excellent reactivity towards carboxylic acids and isocyanates.

More recent studies have focused on end-capping of living PIB by less reactive aromatic compounds, specifically arenes. Although alkylation of arenes has been utilized for many years in cationic polymerization, its early use was as a chain transfer/termination reaction for molecular weight control, as opposed to a method used purposefully for chain end functionalization. When the method did gain interest as a means of functionalization, living carbocationic polymerization of isobutylene (IB) was not yet well developed, so the alkylation reactions were typically carried out post-polymerization. Several papers[52-54] have reported the Friedel-Crafts alkylation of pre-formed PIB, containing *tert*-Cl and/or olefin end groups, using aromatic substrates in order to introduce quantitative functionality to the PIB chain end. For example, Bergbreiter *et al.*[81] reported successful alkylation of phenol and anisole in the presence of concentrated sulfuric acid in CH_2Cl_2 with both *exo-* and *endo*-olefin-terminated PIB after 60 h; less activated alkylbenzenes were reported to be unsuccessful.
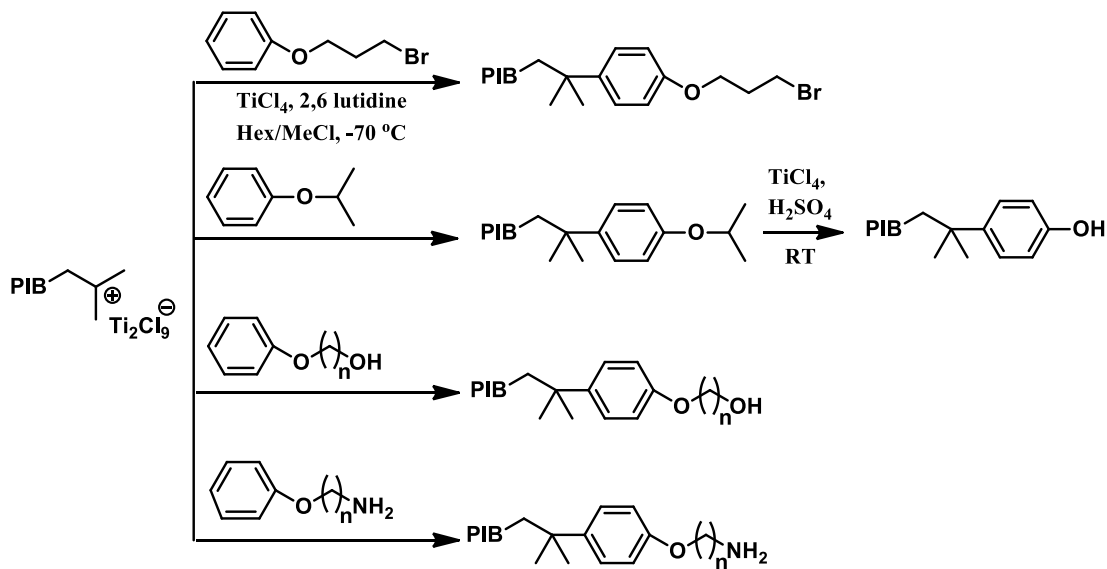
Scheme 1.4 Friedel-Crafts alkylation of *tert*-Cl terminated PIB with alkoxybenzenes for direct *in-situ* chain end functionalization.

Recently, Storey *et al.*[82-83] developed a method for direct end-capping of $TiCl_4$-catalyzed living PIB via Friedel-Crafts alkylation of various alkoxybenzene compounds, yielding quantitative end functionality in a "one pot, one step" synthesis, as shown in Scheme 1.4. This greatly reduced the difficulty of the reaction and the product isolation, and it reduced the cost by eliminating synthetic steps. Phenolic PIB was synthesized via alkylation of simple alkyl phenols such as anisole and isopropoxybenzene with subsequent *in situ* de-blocking. For anisole, cleavage of the terminal methyl ether required reaction with excess BBr_3 (6 eq. per chain end) at room temperature for 22 h. The bulkier isopropoxybenzene could be de-blocked under milder conditions, requiring only 5.5 h at room temperature with sulfuric acid and excess $TiCl_4$ (6 eq. per chain end). The alkylation reactions were tolerant of temperatures ranging from -70 to -30°C, and worked equally well with *tert*-Cl, *endo*-, and *exo*-olefin termini. When [alkoxybenzene] /[PIB] was $\geq$ 1.5, multiple alkylation of a single aromatic substrate by two or more primary PIB chains was not observed. The products were exclusively *para*-substituted, and no PIB fragmentation, degradation, or depolymerization occurred. Moreover, functionalities such as nucleophilic primary alcohol and amine could also be achieved using this one-step end-quenching strategy using correspondingly phenoxyalkyl alcohol/amine quenchers.[83] For phenoxyalkanol, if the site of alkylation, the phenyl ring, was spatially separated ($\geq$4 C) from the hydroxyl, the alkylation was successfully carried out, albeit with a higher demand for $TiCl_4$ due to titanate formation. Phenoxyalkylamine required a longer spacer between amine and phenyl ring ($\geq$6 C), but nonetheless, it could still be quantitatively alkylated with excess $TiCl_4$, despite of its tendency for complexation with both $TiCl_4$ and PIB carbenium ions. The alkylation reactions were

14

tolerant of temperatures ranging from -70 to -30°C and were uninhibited by the presence of *endo-* or *exo-*olefin termini. No over-alkylation (alkylation of a single aromatic substrate by two or more primary PIB chains resulting in coupling) or degradation/de-polymerization occurred after end-quenching according to GPC analysis.

1.4 Telechelic Polyisobutylenes

Telechelic PIBs enable the preparation of polymers various architectures, such as block, graft, brush, and star polymers, and cross-linked networks for more advanced applications. As a result of the development of *in-situ* chain end functionalization and post-polymerization modifications, a variety of useful functional groups have been introduced onto PIB chain ends, including alcohol, amine, phenol, (meth)acrylate, epoxide, azide, alkyne, thiol, olefin, isocyanate, carboxylic acid, etc. Among these functional groups, the use of (meth)acrylate and epoxide for PIB networks formation has been the main focus of this dissertation.

PIBs containing various acrylate end groups have been used to prepare graft copolymers and cross-linked networks with interesting potential applications. For example, Kennedy *et al.*[7] synthesized amphiphilic co-networks (APCNs) by copolymerizing PIB (meth)acrylates with hydrophilic monomers including hydroxyethyl methacrylate (HEMA), methacrylic acid (MAAc), dimethylaminoethyl acrylamide (DMAEMA) and dimethyl acrylamide (DMAAm). Amphiphilic co-networks (APCNs) are two-component networks of covalently interconnected hydrophilic/ hydrophobic (HI/HO) phases, with co-continuous morphology; as such they swell both in water and hydrocarbons, and respond to changes in the medium by morphological isomerization.

PIB (meth)acrylate was first prepared by Kennedy *et al.*[84-85] from *tert*-Cl PIB by multiple post-polymerization reactions, involving dehydrohalogenation with potassium *tert*-butoxide to produce *exo*-olefin, followed by hydroboration-oxidation to produce PIB-alcohol (PIB-OH), and finally esterification by an excess of the appropriate (meth)acryloyl chloride. Kennedy also developed a synthetic method involving allyltrimethylsilane[70-71] as an *in situ* quencher of living PIB to form allyl-terminated PIB, which was used to prepare PIB (meth)acrylate by either conventional hydroboration-oxidation and (meth)acryloyl chloride esterification, or anti-Markovnikov hydrobromination followed by nucleophilic substitution with alkali metal (meth)acrylate salts. Faust *et al.*[86] prepared bromoallyl PIB *in situ*, by introducing 1,3-butadiene to methylaluminum sesquibromide-catalyzed IB polymerization. PIB methacrylate was then achieved by nucleophilic substitution of bromide by sodium methacrylate. However, this method placed into the chain an undesired internal double bond that required saturation by additional hydrogenation.

Another important functional group used extensively in industry for network formation is epoxide, which can either undergo cationic ring opening polymerization or may be reacted with amines to form epoxy-amine networks. The cationic ring opening process is not oxygen sensitive and thus offers the advantage of not requiring an oxygen-free environment or amine synergists. Faust *et al.* [41] have reported that the fracture, flexural, and tensile properties of a diglycidyl ether of bisphenol A (DGEBA)-triethylenetetramine (TETA) epoxy network are improved by the incorporation of glycidyl ether end-functional PIB as rubbery segment. Kennedy *et al.* [87]demonstrated in earlier research that such rubbery PIB soft segments greatly reduce the brittleness,

chemical sensitivity, and hydrophilicity of traditional epoxy networks, and thus could be applied in underwater coatings and wire insulation.

The synthesis of PIB-based epoxy-amine networks requires well-defined telechelic polymers with controlled molecular weight and narrow molecular weight distribution. Existing synthetic methods toward PIB epoxides are tedious and/or introduce undesirable unsaturations at the chain end. For instance, Kennedy *et al.* [88] developed an *exo*-olefin type epoxide by dehydrochlorination of tert-chloride[89] terminated PIB to obtain PIB *exo*-olefin [42] first, followed by epoxidation of the olefin. Kennedy *et al.*[56] reported the synthesis of PIB-phenyl glycidyl ether using a multistep synthetic procedure. First, PIB phenol[52] was obtained by Friedel-Crafts alkylation of phenol, used in excess, by *tert*-chloride- or *exo*-olefin-terminated PIB catalyzed by boron trifluoride etherate ($BF_3 \cdot OEt_2$). The resulting PIB phenol was then reacted with excess epichlorohydrin to achieve end capping to the exclusion of chain extension. Later, Kennedy *et al.*[90] developed a method to synthesize glycidyl-terminated PIB by the *m*-chloroperbenzoic acid epoxidation of allyl-terminated PIB, which was obtained by quenching of living PIB with allyltrimethylsilane. Recently, *Faust et al.*[41,86] developed a method to synthesize aliphatic glycidyl ether end-functional PIB by base-catalyzed SN_2 substitution of PIB allyl bromide with glycidol or by substitution of PIB alcohol with epichlorohydrin.

1.5 Bottlebrush Polymers

Recently, bottleneck brush polymers have been of great interest owing to their unique polymer topology as a result of well-defined structures, customizable dimensions, as well as special mechanical and rheological properties.[91-92] Bottleneck brush polymers

consist of macromolecular sides chains grafted to a polymer backbone and possess a chain extended conformation at sufficient graft density caused by the steric repulsions between crowded neighboring polymer branches.[93] Similarly to other macromolecular architectures, the morphology of bottleneck brush polymers can be tailored by controlling polymer composition, graft density, and side chain size to achieve cylindrical,[94-95] spherical,[96-97] or worm-like[91] morphologies. Proper selection of polymeric side chains, essential properties including stimuli-responsiveness[91,98] and amphiphilicity,[99-100] can be incorporated into the brush polymers. Due to repulsions of polymeric side chains, bottleneck brush polymers typically lack the chain entanglements displayed by most linear polymers, resulting in relatively low viscosity at even very high molecular weight.[101-102]

Methods of preparing bottleneck brush polymers generally fall into three approaches (as shown in Scheme 1.5):[103-106] "grafting from," "grafting onto," and "grafting through." The "grafting from" approach has been the most widely investigated strategy and involves introduction of initiating sites at the backbone for the polymerization of monomers to form side chains.[107-108] This approach usually involves post-polymerization modifications to form the backbone initiating species. Disadvantages of the grafting from approach are many; it typically suffers from low graft density, non-homogeneity of side chains, and uneven side chain distribution issues. Furthermore, high density of initiation sites might also cause low initiation efficiency, resulting in unreacted initiating sites remaining along the backbone.[109] The "grafting onto" approach has some advantages since it allows for preparation of backbone and side chain polymers individually,[110-112] followed by efficient coupling to form bottleneck brushes, allowing

for precise composition, size, and functionality control. In addition to the covalent bond formation at the grafting site, supramolecular interactions including coordination bonding, hydrogen bonding, or ionic interactions could also be employed for specific applications.[113-115] One major drawback of this approach is that as conversion of the coupling reaction advances, it becomes more difficult for the reaction to proceed owing to the self-repulsion of side chains, even when a high excess of side chain polymers are used.[110] Among the three approaches, the "grafting through" strategy is the most versatile route and involves preparation of macromonomers (MMs) with polymerizable end-functional groups and their subsequent polymerization, preferably by a controlled/ "living" process, to form bottleneck brush polymers.[116-118] "Grafting through" affords precise control over the backbone and side chain length, as well as high graft density; namely, 100% graft density, can be achieved since the polymerizeable moiety is inherently bound to a side chain. However, it remains difficult to achieve brush polymers with high degree of polymerization (DP) and low polydisperisity (PDI), largely due to the steric hindrance brought by the self-repulsion of polymeric side chains along with low concentration of polymerizable moieties.

Ring-opening meththesis polymerization (ROMP) provided a solution to these issues.[119-121] Numerous syntheses of bottleneck brush polymers with approximately quantitative conversion have been reported via ROMP using ruthenium-based metathesis catalysts (as shown in Scheme 1.6), owing to their fast initiation, high reactivity, and high functional group tolerance.[102-104,106,122-127] Despite recent developments on preparation of brush polymers via ROMP, synthesis of the required norbornene end-functional MMs still remains a challenge.

19
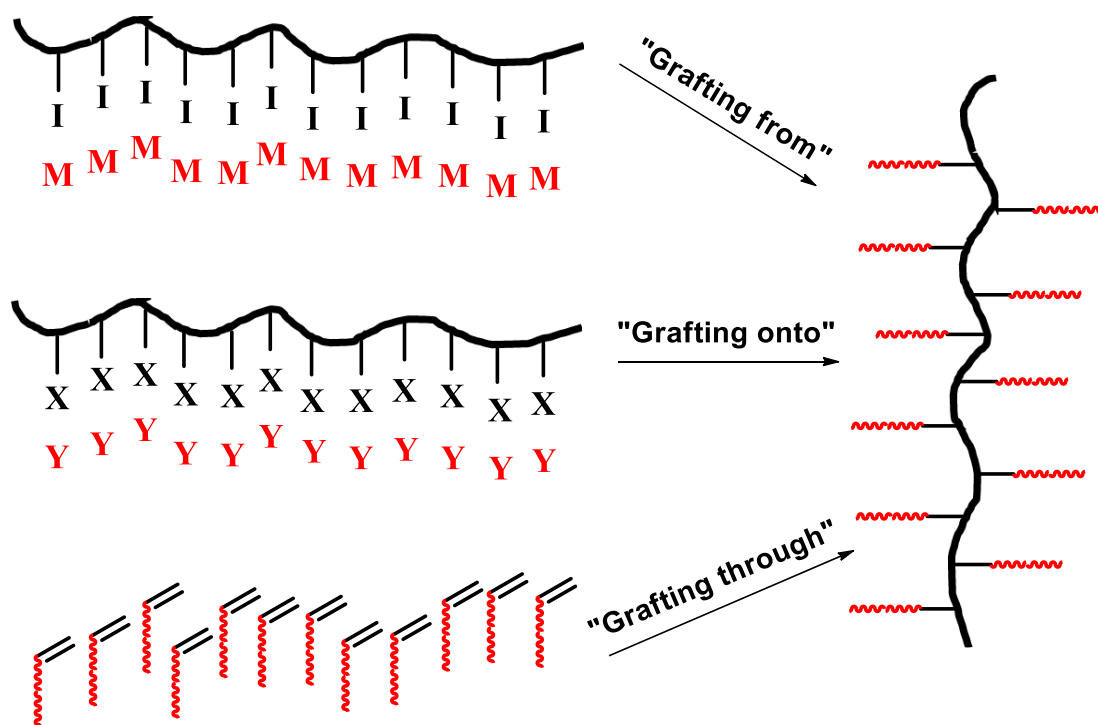
Scheme 1.5 Synthetic routes toward bottleneck brush polymers: "grafting from," "grafting onto," and "grafting through."
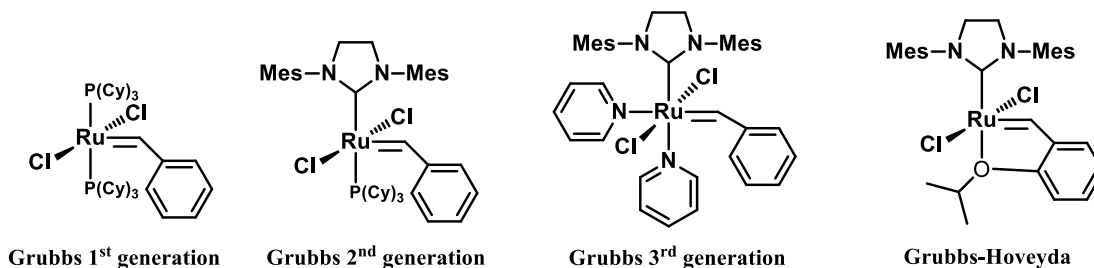
Scheme 1.6 Ruthenium-based catalysts for ROMP.

Two approaches have been utilized for the synthesis of MMs (Scheme 1.7); one is "direct-growth" (DG-MM), and the other is "growth-then-coupling" (GC-MM) as described by Xia *et al.*[128] DG-MM approach has generally been realized by using a norbornene-functional compound to initiate ring opening polymerization (ROP), NMP, or ATRP, or a norbornene-functional chain transfer agent to mediate RAFT polymerization.[104,106,129-132] However, several potential problem may arise when radical

20

polymerization methods are used. First copolymerization of the norbornen, terminal

olefin with monomers needs to be minimized;[133] second, small traces of difunctional

norbornene arising from bimolecular radical coupling generally leads to non-favored

brush branching and increased PDI of brushes.[128] GC-MM strategy allows for precise

molecular weight and PDI control over the side chains. By combining living

polymerization techniques with post-polymerization modifications, the choices of

composition, architecture, and size of side chains can be precisely tuned to govern

properties of designed brush polymers. Post-polymerization modifications need to be

carefully performed to get quantitative conversion of MMs.
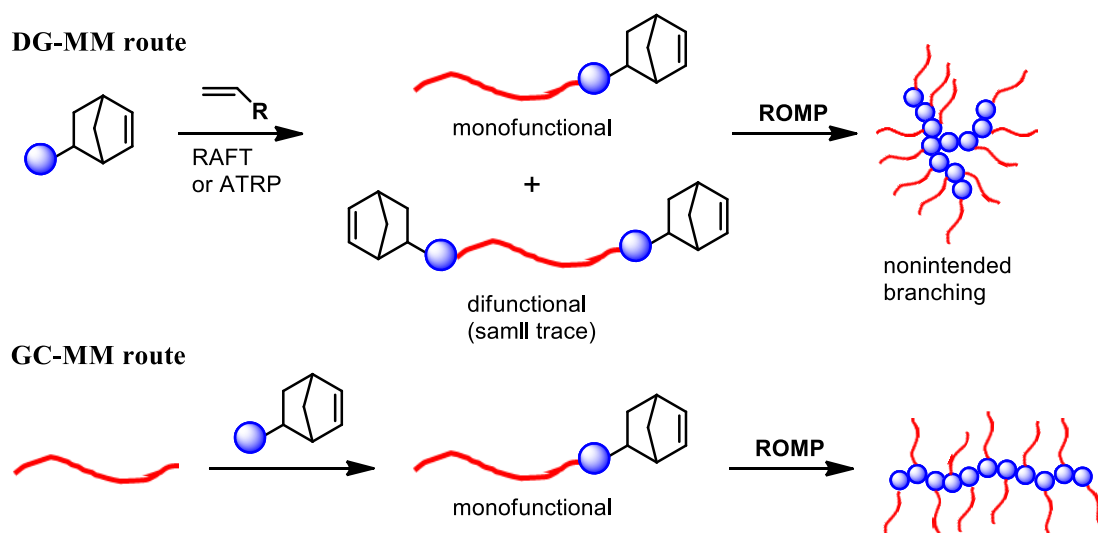
Scheme 1.7 Direct-growth (DG-MM) and growth-then-coupling (GC-MM) routes for the
synthesis of norbornene-functional macromonomers.

1.6 References

(1)   Tripathy, R.; Crivello, J. V.; Faust, R., *J. Polym. Sci., Part A: Polym. Chem.* **2013,** *51* (2), 305-317.

(2)   Puskas, J. E.; Foreman-Orlowski, E. A.; Lim, G. T.; Porosky, S. E.; Evancho-Chapman, M. M.; Schmidt, S. P.; El Fray, M.; Piątek, M.; Prowans, P.; Lovejoy, K., *Biomaterials* **2010,** *31* (9), 2477-2488.

(3)   Domján, A.; Erdödi, G.; Wilhelm, M.; Neidhöfer, M.; Landfester, K.; Iván, B.; Spiess, H. W., *Macromolecules* **2003,** *36* (24), 9107-9114.

(4)   Erdödi, G.; Iván, B., *Chem. Mater.* **2004,** *16* (6), 959-962.

(5)   Haraszti, M.; Tóth, E.; Iván, B., *Chem. Mater.* **2006,** *18* (20), 4952-4958.

(6)   Kali, G.; Vavra, S.; László, K.; Iván, B., *Macromolecules* **2013,** *46* (13), 5337-5344.

(7)   Erdodi, G.; Kennedy, J. P., *Prog. Polym. Sci.* **2006,** *31* (1), 1-18.

(8)   Puskas, J. E.; Chen, Y., *Biomacromolecules* **2004,** *5* (4), 1141-1154.

(9)   Puskas, J. E.; Chen, Y.; Dahman, Y.; Padavan, D., *J. Polym. Sci., Part A: Polym. Chem.* **2004,** *42* (13), 3091-3109.

(10)   Thomas, R.; Sparks, W.; Frolich, P. K.; Otto, M.; Mueller-Cunradi, M., *Journal of the American Chemical Society* **1940,** *62* (2), 276-280.

(11)   Thomas, R.; Lightbown, I.; Sparks, W.; Frolich, P.; Murphree, E., *Industrial & Engineering Chemistry* **1940,** *32* (10), 1283-1292.

(12)   Thomas, R. M.; Sparks, W. J., *Hydrocarbon Interpolymers Suitable for Electric Insulation and Numerous Other Uses. US 2356128, **1944**. .*

(13)   Goriainow, W.; Butlerow, A., *Justus Liebigs Annalen der Chemie* **1873,** *169* (1-2), 146-149.

(14)   Otto, M.; Mueller-Cunradi, M., *Polymerizing Isobutylene. GP 641284, **1937**.*

(15)   Otto, M.; Mueller-Cunradi, M., *Polymers of Iso-olefins. US 2203873, **1940**.*

(16)   Szwarc, M., *Nature* **1956,** *178*, 1168-1169.

(17)   Faust, R.; Kennedy, J. P., *J. Polym. Sci., Part A: Polym. Chem.* **1987,** *25* (7), 1847-1869.

(18)   Jenkins Aubrey, D.; Jones Richard, G.; Moad, G., 2009; Vol. 82, p 483.

(19)   Harrison, J. J.; Young, D. C.; Mayne, C. L., *The Journal of organic chemistry* **1997,** *62* (3), 693-699.

(20)   Samson, J. N. R., *US Patent 4605808, **1986**.*

(21)   Eaton, B. E., *US Patent 5068490, **1991**.*

(22)   Kennedy, J. P.; Smith, R. A., *J. Polym. Sci., Polym. Chem. Ed.* **1980,** *18* (5), 1523-1537.

(23)   Mishra, M. K.; Wang, B.; Kennedy, J. P., *Polym. Bull.* **1987,** *17* (4), 307-314.

(24)   Kaszás, G.; Puskás, J.; Kennedy, J. P., *Polym. Bull.* **1987,** *18* (2), 123-130.

(25)   Puskás, J.; Kaszás, G.; Kennedy, J. P.; Kelen, T.; Tüdös, F., *J. Macromol. Sci., Part A : Chem.* **1982,** *18* (9), 1229-1244.

(26)   Kaszas, G.; Puskas, J.; Chen, C.; Kennedy, J. P., *Macromolecules* **1990,** *23* (17), 3909-3915.

(27)   Storey, R. F.; Curry, C. L.; Hendry, L. K., *Macromolecules* **2001,** *34* (16), 5416-5432.

(28)   Storey, R. F.; Chisholm, B. J.; Brister, L. B., *Macromolecules* **1995,** *28* (12), 4055-4061.

(29)   Storey, R. F.; Chisholm, B. J., *Macromolecules* **1993,** *26* (25), 6727-6733.

(30)   Kennedy, J. P.; Midha, S.; Tsunogae, Y., *Macromolecules* **1993,** *26* (3), 429-435.

(31)   Ojha, U.; Feng, D.; Chandekar, A.; Whitten, J. E.; Faust, R., *Langmuir* **2009,** *25* (11), 6319-27.

(32)   Feng, D.; Chandekar, A.; Whitten, J. E.; Faust, R., *J. Macromol. Sci., Part A* **2007,** *44* (11), 1141-1150.

(33)   Strickler, F.; Richard, R.; McFadden, S.; Lindquist, J.; Schwarz, M. C.; Faust, R.; Wilson, G. J.; Boden, M., *Journal of biomedical materials research. Part A* **2010,** *92* (2), 773-82.

(34)   Martinez-Castro, N.; Lanzendorfer, M. G.; Muller, A. H. E.; Cho, J. C.; Acar, M. H.; Faust, R., *Macromolecules* **2003,** *36*, 10.

(35)   Higashihara, T.; Feng, D.; Faust, R., *Macromolecules* **2006,** *39*, 5275-5279.

(36)   Storey, R. F.; Shoemake, K. A.; Chisholm, B. J., *J. Polym. Sci., Part A: Polym. Chem.* **1996,** *34* (10), 2003-2017.

(37)   Breland, L. K.; Storey, R. F., *Polymer* **2008,** *49* (5), 1154-1163.

(38)   Hancsók, J.; Bartha, L.; Baladincz, J.; Kocsis, Z., *Lubr. Sci.* **1999,** *11* (3), 297-310.

(39)   Wang, K. S., Osborne, J. L., Hunt, J. A., Nelson, M. K. , *U.S. Patent 5,508,038, 1996*.

(40)   Zirbs, R.; Binder, W.; Gahleitner, M.; Machl, D., *Macromol. Symp.* **2007,** *254* (1), 93-96.

(41)   Tripathy, R.; Ojha, U.; Faust, R., *Macromolecules* **2011,** *44* (17), 6800-6809.

(42)   Kennedy, J. P.; Chang, V. S. C.; Smith, R. A.; Iván, B., *Polym. Bull.* **1979,** *1* (8), 575-580.

(43)   Ivan, B.; Kennedy, J. P.; Chang, V. S., *J. Polym. Sci., Polym. Chem. Ed.* **1980,** *18* (11), 3177-3191.

(44)   Kennedy, J.; Chang, V.; Francik, W., *J. Polym. Sci., Polym. Chem. Ed.* **1982,** *20* (10), 2809-2817.

(45)   Kéki, S.; Nagy, M.; Deák, G.; Lévai, A.; Zsuga, M., *J. Polym. Sci., Part A: Polym. Chem.* **2002,** *40* (22), 3974-3986.

(46)   Percec, V.; Guhaniyogi, S. C.; Kennedy, J. P., *Polym. Bull.* **1982,** *8* (11), 551-555.

(47)   Liao, T.-P.; Kennedy, J. P., *Polym. Bull.* **1981,** *5* (1), 11-18.

(48)   Wondraczek, R. H.; Kennedy, J. P., *Polym. Bull.* **1980,** *2* (10), 675-682.

(49)   Wondraczek, R. H.; Kennedy, J. P., *Polym. Bull.* **1981,** *4* (8), 445-450.

(50)   Wollyung, K. M.; Wesdemiotis, C.; Nagy, A.; Kennedy, J. P., *J. Polym. Sci., Part A: Polym. Chem.* **2005,** *43* (5), 946-958.

(51)   Kéki, S.; Nagy, M.; Deák, G.; Herczegh, P.; Zsuga, M., *J. Polym. Sci., Part A: Polym. Chem.* **2004,** *42* (3), 587-596.

(52)   Kennedy, J. P.; Guhaniyogi, S. C.; Percec, V., *Polym. Bull.* **1982,** *8* (11), 563-570.

(53)   Mishra, M. K.; Sar-Mishra, B.; Kennedy, J. P., *Polym. Bull.* **1986,** *16* (1), 47-53.

(54)   Kennedy, J. P.; Hiza, M., *J. Polym. Sci., Polym. Chem. Ed.* **1983,** *21* (12), 3573-3590.

(55)   Kennedy, J. P.; Carter, J., *Macromolecules* **1990,** *23* (5), 1238-1243.

(56)   Kennedy, J. P.; Guhaniyogi, S. C.; Percec, V., *Polym. Bull.* **1982,** *8* (11), 571-578.

(57)   Puskas, J.; Brister, L.; Michel, A.; Lanzendörfer, M.; Jamieson, D.; Pattern, W., *J. Polym. Sci., Part A: Polym. Chem.* **2000,** *38* (3), 444-452.

(58)   Song, J.; Bódis, J.; Puskas, J. E., *J. Polym. Sci., Part A: Polym. Chem.* **2002,** *40* (8), 1005-1015.

(59)   Michel, A. J.; Puskas, J. E.; Brister, L. B., *Macromolecules* **2000,** *33* (10), 3518-3524.

(60)   Walch, E.; Gaymans, R., *Polymer* **1993,** *34* (2), 412-417.

(61)   Chen, C. C.; Si, J.; Kennedy, J., *J. Macromol. Sci., Pure Appl. Chem.* **1992,** *29* (8), 669-679.

(62)   Simison, K. L.; Stokes, C. D.; Harrison, J. J.; Storey, R. F., *Macromolecules* **2006,** *39* (7), 2481-2487.

(63)   Bae, Y. C.; Faust, R., *Macromolecules* **1997,** *30* (23), 7341-7344.

(64)   Morgan, D. L.; Harrison, J. J.; Stokes, C. D.; Storey, R. F., *Macromolecules* **2011,** *44* (8), 2438-2443.

(65)   Ummadisetty, S.; Morgan, D. L.; Stokes, C. D.; Storey, R. F., *Macromolecules* **2011,** *44* (20), 7901-7910.

(66)   Morgan, D. L.; Stokes, C. D.; Meierhoefer, M. A.; Storey, R. F., *Macromolecules* **2009,** *42* (7), 2344-2352.

(67)   Ummadisetty, S.; Morgan, D. L.; Stokes, C. D.; Harrison, J. J.; Campbell, C. G.; Storey, R. F., *Macromol. Symp.* **2013,** *323* (1), 6-17.

(68)   Ummadisetty, S.; Storey, R. F., *Macromolecules* **2013,** *46* (6), 2049-2059.

(69)   De, P.; Faust, R., *Macromolecules* **2006,** *39* (20), 6861-6870.

(70)   Wilczek, L.; Kennedy, J. P., *J. Polym. Sci., Part A: Polym. Chem.* **1987,** *25* (12), 3255-3265.

(71)   Wilczek, L.; Kennedy, J. P., *Polym. Bull.* **1987,** *17* (1), 37-43.

(72)   Roth, M.; Mayr, H., *Macromolecules* **1996,** *29* (19), 6104-6109.

(73)   Hadjikyriacou, S.; Faust, R., *Macromolecules* **1999,** *32* (20), 6393-6399.

(74)   Martinez-Castro, N.; Lanzendörfer, M. G.; Müller, A. H. E.; Cho, J. C.; Acar, M. H.; Faust, R., *Macromolecules* **2003,** *36* (19), 6985-6994.

(75)   Storey, R. F.; Stokes, C. D.; Harrison, J. J., *Macromolecules* **2005,** *38* (11), 4618-4624.

(76)   Martinez-Castro, N.; Morgan, D. L.; Storey, R. F., *Macromolecules* **2009,** *42* (14), 4963-4971.

(77)   Morgan, D. L.; Storey, R. F., *Macromolecules* **2010,** *43* (3), 1329-1340.

(78)   Higashihara, T.; Feng, D.; Faust, R., *Macromolecules* **2006,** *39* (16), 5275-5279.

(79)   De, P.; Faust, R., *Macromolecules* **2006,** *39* (22), 7527-7533.

(80)   Ojha, U.; Rajkhowa, R.; Agnihotra, S. R.; Faust, R., *Macromolecules* **2008,** *41* (11), 3832-3841.

(81)   Li, J.; Sung, S.; Tian, J.; Bergbreiter, D. E., *Tetrahedron* **2005,** *61* (51), 12081-12092.

(82)   Morgan, D. L.; Storey, R. F., *Macromolecules* **2009,** *42* (18), 6844-6847.

(83)   Morgan, D. L.; Martinez-Castro, N.; Storey, R. F., *Macromolecules* **2010,** *43* (21), 8724-8740.

(84)   Iván, B.; Kennedy, J. P.; Chang, V. S. C., *J. Polym. Sci., Polym. Chem. Ed.* **1980,** *18* (11), 3177-3191.

27

(85)   Kennedy, J. P.; Hiza, M., *Polym. Bull.* **1983,** *10* (3), 146-151.

(86)   Tripathy, R.; Ojha, U.; Faust, R., *Macromolecules* **2009,** *42* (12), 3958-3964.

(87)   Kennedy, J. P.; Guhaniyogi, S., *US Patent 4429099,* **1984**.

(88)   Kennedy, J. P.; Chang, V. S. C.; Francik, W. P., *J. Polym. Sci., Polym. Chem. Ed.* **1982,** *20* (10), 2809-2817.

(89)   Kennedy, J. P.; Smith, R. A., *J. Polym. Sci., Polym. Chem. Ed.* **1980,** *18* (5), 1523-1537.

(90)   Iván, B.; Kennedy, J. P., *J. Polym. Sci., Part A: Polym. Chem.* **1990,** *28* (1), 89-104.

(91)   Lee, H.-i.; Pietrasik, J.; Sheiko, S. S.; Matyjaszewski, K., *Prog. Polym. Sci.* **2010,** *35* (1-2), 24-44.

(92)   Dalsin, S. J.; Hillmyer, M. A.; Bates, F. S., *Macromolecules* **2015,** *48* (13), 4680-4691.

(93)   Sheiko, S. S.; Sumerlin, B. S.; Matyjaszewski, K., *Prog. Polym. Sci.* **2008,** *33* (7), 759-785.

(94)   Yuan, J.; Lu, Y.; Schacher, F.; Lunkenbein, T.; Weiss, S.; Schmalz, H.; Müller, A. H. E., *Chem. Mater.* **2009,** *21* (18), 4146-4154.

(95)   Bolton, J.; Rzayev, J., *ACS Macro Lett.* **2012,** *1* (1), 15-18.

(96)   Pesek, S. L.; Li, X.; Hammouda, B.; Hong, K.; Verduzco, R., *Macromolecules* **2013,** *46* (17), 6998-7005.

(97)   Dalsin, S. J.; Hillmyer, M. A.; Bates, F. S., *ACS Macro Lett.* **2014,** *3* (5), 423-427.

(98)   Verduzco, R.; Li, X.; Pesek, S. L.; Stein, G. E., *Chem. Soc. Rev.* **2015,** *44* (8), 2405-2420.

(99)   Nese, A.; Li, Y.; Averick, S.; Kwak, Y.; Konkolewicz, D.; Sheiko, S. S.;
        Matyjaszewski, K., *ACS Macro Lett.* **2012,** *1* (1), 227-231.

(100)   Li, Y.; Zou, J.; Das, B. P.; Tsianou, M.; Cheng, C., *Macromolecules* **2012,** *45*
        (11), 4623-4629.

(101)   Iwawaki, H.; Urakawa, O.; Inoue, T.; Nakamura, Y., *Macromolecules* **2012,** *45*
        (11), 4801-4808.

(102)   Ganewatta, M. S.; Ding, W.; Rahman, M. A.; Yuan, L.; Wang, Z.; Hamidi, N.;
        Robertson, M. L.; Tang, C., *Macromolecules* **2016,** *49* (19), 7155-7164.

(103)   Radzinski, S. C.; Foster, J. C.; Chapleski, R. C., Jr.; Troya, D.; Matson, J. B., *J.
        Am. Chem. Soc.* **2016,** *138* (22), 6998-7004.

(104)   Xia, Y.; Kornfield, J. A.; Grubbs, R. H., *Macromolecules* **2009,** *42* (11), 3761-
        3766.

(105)   Radzinski, S. C.; Foster, J. C.; Matson, J. B., *Polym. Chem.* **2015,** *6* (31), 5643-
        5652.

(106)   Patton, D. L.; Advincula, R. C., *Macromolecules* **2006,** *39* (25), 8674-8683.

(107)   Runge, M. B.; Dutta, S.; Bowden, N. B., *Macromolecules* **2006,** *39* (2), 498-508.

(108)   Cheng, G.; Böker, A.; Zhang, M.; Krausch, G.; Müller, A. H. E., *Macromolecules*
        2001, *34* (20), 6883-6888.

(109)   Sumerlin, B. S.; Neugebauer, D.; Matyjaszewski, K., *Macromolecules* **2005,** *38*
        (3), 702-708.

(110)   Gao, H.; Matyjaszewski, K., *J. Am. Chem. Soc.* **2007,** *129* (20), 6633-6639.

(111)   Schappacher, M.; Deffieux, A., *Science* **2008,** *319* (5869), 1512-1515.

(112) Helms, B.; Mynar, J. L.; Hawker, C. J.; Fréchet, J. M. J., *J. Am. Chem. Soc.* **2004,** *126* (46), 15020-15021.

(113) Stupp, S. I.; LeBonheur, V.; Walker, K.; Li, L. S.; Huggins, K. E.; Keser, M.; Amstutz, A., *Science* **1997,** *276* (5311), 384-389.

(114) Antonietti, M.; Conrad, J.; Thuenemann, A., *Macromolecules* **1994,** *27* (21), 6007-6011.

(115) Ruokolainen, J.; Tanner, J.; ten Brinke, G.; Ikkala, O.; Torkkeli, M.; Serimaa, R., *Macromolecules* **1995,** *28* (23), 7779-7784.

(116) Gerle, M.; Fischer, K.; Roos, S.; Müller, A. H. E.; Schmidt, M.; Sheiko, S. S.; Prokhorova, S.; Möller, M., *Macromolecules* **1999,** *32* (8), 2629-2637.

(117) Dziezok, P.; Fischer, K.; Schmidt, M.; Sheiko, S. S.; Möller, M., *Angew. Chem. Int. Ed. Engl.* **1997,** *36* (24), 2812-2815.

(118) Ito, K.; Tanaka, K.; Tanaka, H.; Imai, G.; Kawaguchi, S.; Itsuno, S., *Macromolecules* **1991,** *24* (9), 2348-2354.

(119) Leitgeb, A.; Wappel, J.; Slugovc, C., *Polymer* **2010,** *51* (14), 2927-2946.

(120) Choi, T.-L.; Grubbs, R. H., *Angew. Chem. Int. Ed.* **2003,** *42* (15), 1743-1746.

(121) Bielawski, C. W.; Grubbs, R. H., *Prog. Polym. Sci.* **2007,** *32* (1), 1-29.

(122) Sveinbjörnsson, B. R.; Miyake, G. M.; El-Batta, A.; Grubbs, R. H., *ACS Macro Lett.* **2014,** *3* (1), 26-29.

(123) Radzinski, S. C.; Foster, J. C.; Matson, J. B., *Macromol. Rapid Commun.* **2016,** *37* (7), 616-21.

(124) Zhang, M.; Breiner, T.; Mori, H.; Müller, A. H. E., *Polymer* **2003,** *44* (5), 1449-1458.

(125)   Johnson, J. A.; Lu, Y. Y.; Burts, A. O.; Xia, Y.; Durrell, A. C.; Tirrell, D. A.; Grubbs, R. H., *Macromolecules* **2010,** *43* (24), 10326-10335.

(126)   Li, Z.; Ma, J.; Cheng, C.; Zhang, K.; Wooley, K. L., *Macromolecules* **2010,** *43* (3), 1182-1184.

(127)   Gregory, A.; Stenzel, M. H., *Prog. Polym. Sci.* **2012,** *37* (1), 38-105.

(128)   Teo, Y. C.; Xia, Y., *Macromolecules* **2015,** *48* (16), 5656-5662.

(129)   Sveinbjörnsson, B. R.; Weitekamp, R. A.; Miyake, G. M.; Xia, Y.; Atwater, H. A.; Grubbs, R. H., *Proc. Natl. Acad. Sci.* **2012,** *109* (36), 14332-14336.

(130)   Kim, J. G.; Coates, G. W., *Macromolecules* **2012,** *45* (19), 7878-7883.

(131)   Miyake, G. M.; Weitekamp, R. A.; Piunova, V. A.; Grubbs, R. H., *J. Am. Chem. Soc.* **2012,** *134* (34), 14249-14254.

(132)   Li, Y.; Themistou, E.; Zou, J.; Das, B. P.; Tsianou, M.; Cheng, C., *ACS Macro Lett.* **2012,** *1* (1), 52-56.

(133)   Cheng, C.; Khoshdel, E.; Wooley, K. L., *Macromolecules* **2007,** *40* (7), 2289-2292.

CHAPTER II – END-QUENCHING OF *TERT*-CHLORIDE TERMINATED

POLYISOBUTYLENE WITH ALKOXYBENZENES: COMPARISON

OF ALCL₃ AND TICL₄ CATALYSTS

2.1 Abstract

Alkoxybenzenes, including (3-bromopropoxy)benzene, anisole, and

isopropoxybenzene, were used to end-quench polyisobutylene, activated with either

AlCl₃ or TiCl₄ at different temperatures (-50, -25 and 0 °C) in 70/30 and 55/45 (v/v)

hexane/methylene chloride (Hex/CH₂Cl₂). Quenching reactions were performed on pre-

formed difunctional *tert*-chloride PIB, which was produced from 5-*tert*-butyl-1,3-di(1-

chloro-1-methylethyl)benzene/TiCl₄ at 70 °C in 40/60 (v/v) hexane/methyl chloride. For

(3-bromopropoxy)benzene and anisole, quantitatively end-capped products were

achieved if the alkoxybenzene/AlCl₃ molar ratio was greater than unity. Under these

conditions, alkylations were generally quantitative and occurred exclusively in the para

position; neither multiple alkylations on the same alkoxybenzene nor polymer chain

degradation were observed. Carbocation rearrangement was observed if the

alkoxybenzene/AlCl₃ molar ratio was less than unity. No such specific

alkoxybenzene/Lewis acid molar ratio was required to obtain quantitatively alkylated

products using TiCl₄ catalyst. The alkylation rate of (3-bromopropoxy)benzene with

AlCl₃ was 2.6 times faster than with TiCl₄ under the same reaction conditions. The

alkylation rate of (3-bromopropoxy)benzene was faster than that of anisole using AlCl₃.

For isopropoxybenzene quencher only, using AlCl₃ catalyst, a small fraction of *exo*-olefin

was formed during the initial stage of reaction, and the quenching reaction failed to reach

completion. Chain end functionality, a mixture of para and meta isomers (3:1), reached

only 1.72 (86.4% conversion) after 45 h. Increasing temperature to -25 and 0 °C did not greatly affect the rate of alkylation, but it did increase carbocation rearrangement and decreased regioselectivity; at 0 °C, 25% alkylation occurred at the *meta* or *ortho* positions of (3-bromopropoxy)benzene. Increasing solvent polarity to 55/45 (v/v) Hex/CH_2Cl_2 also did not greatly affect alkylation rate but increased carbocation rearrangement.

2.2 Introduction

Selection of proper catalyst is of great importance for alkylation reactions, particularly with regards to avoiding fragmentation of the PIB or the alkylated PIB product and prevention of unwanted reactions such as over-alkylation. Commonly used catalysts[1] for alkylation include Lewis acids (such as $TiCl_4$, BF_3 and BF_3 complexes, and $FeCl_3$), trifluoromethane sulfonic acid, [2] and acidic molecular sieves (such as Amberlyst 36).[3] In previous research of end-capping of living PIB with alkoxybenzenes, [1,4] $TiCl_4$ has been the preferred catalyst. However, $TiCl_4$-based alkylation systems require high $TiCl_4$/chain end (CE) ratios to achieve high alkylation rates and low temperatures to facilitate ionization by $TiCl_4$. [5] Additionally, the toxic and corrosive nature of $TiCl_4$ adds more cost due to special handling requirements and waste disposal. Therefore, there is an impetus to develop an efficient and cheap alkylation system by using other strong Lewis acids to replace $TiCl_4$ for the end-capping of living PIB with alkoxybenzenes.

Among common Lewis acids, $AlCl_3$ is perhaps the leading candidate due to its strong acidity (stronger than $TiCl_4$), good alkylation effectiveness, and low cost. Moreover, a resurgent interest in $AlCl_3$ as a catalyst to produce highly reactive (high *exo*-olefin) PIB at elevated temperature has recently occurred as a result of work by Kostjuk

and others. [6] Many attempts at using $AlCl_3$ in alkylation of cationic polymers have been

reported, but either the efficiency was low or harsh conditions and excess reagents were

required to achieve the desired effectiveness. For example, Hunter *et al.* [7] reported 40-

70% of sec-benzylic chloride-terminated polystyrene chain ends were capped by

alkylphenols using $AlCl_3$ as a catalyst at 0 or -78 °C. Bergbreiter *et al.* [8] reported the

successful alkylation of 2,6-disubstituted aniline with a mixture of *exo-* and *endo*-olefin-

terminated PIBs with $AlCl_3$ catalyst at 220 °C for 3 days. Kennedy et al. [9] obtained

bromide-terminated PIB by alkylation of 2-bromoethylbenzene or *β*-

bromoisopropylbenzene (60 times molar excess relative to *tert*-Cl PIB) *via* excess $AlCl_3$

catalyst (8 times molar excess) at temperatures ≤ -50 °C for 5 h.

R= -CH₃, -(CH₂)₃Br, -CH(CH₃)₂
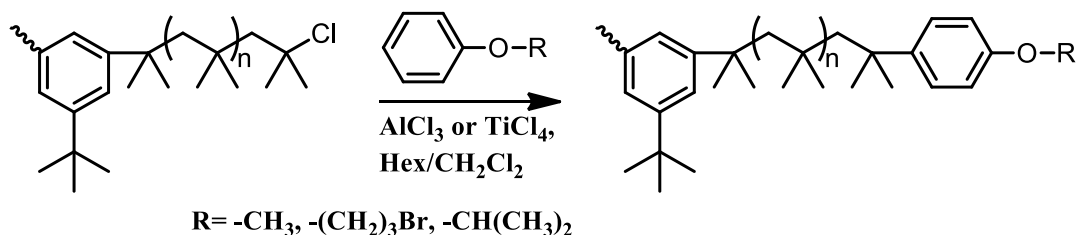
Scheme 2.1 End-quenching of difunctional *tert*-Cl PIB with alkoxybenzenes using $AlCl_3$
or $TiCl_4$ catalyst.

Herein, we compare the alkylation of a range of alkoxybenzene compounds by

preformed *tert*-chloride PIB, catalyzed by $AlCl_3$ and $TiCl_4$, at temperatures ranging from

-50 to 0 °C in 70/30 or 55/45 Hex/CH_2Cl_2 (Scheme 2.1). 3-(Bromopropoxy)benzene,

anisole and isopropoxybenzene were chosen as representative of the family of

alkoxybenzenes since bromide- and phenol-terminated PIB (derived from anisole) are

currently of great interest due to their reactivity and ease of transformation into other

useful functionalities.

2.3 Experimental

Materials. Hexane (anhydrous, 95%), methanol (anhydrous, 99.8%), methylene chloride (CH_2Cl_2) (anhydrous, 99.8%), titanium tetrachloride ($TiCl_4$) (99.9%), 2,6-lutidine (99.5%), anisole (anhydrous, 99.7%), (3-bromopropoxy)benzene (anhydrous, 98%), tetrahydrofuran (THF) (anhydrous, 99.9%), and aluminum chloride ($AlCl_3$) (anhydrous, 99%) were purchased from Sigma-Aldrich and used as received. Isopropoxybenzene (97%) was purchased from Oakwood Chemical and used as received. Magnesium sulfate ($MgSO_4$) (anhydrous) and chloroform-d ($CDCl_3$) were purchased and used as received from Fisher Scientific. Isobutylene (BOC Gases) and methyl chloride (Alexander Chemical Corp.) were dried by passing the gasses through columns of $CaSO_4$/molecular sieves/$CaCl_2$ and condensed within a N_2-atmosphere glovebox immediately prior to use. The difunctional initiator, 5-*tert*-butyl-1,3-di(1-chloro-1-methylethyl)benzene (*t*-Bu-*m*-DCC), was synthesized as previously reported [10] and stored at 0 °C.

Instrumentation. Nuclear magnetic resonance (NMR) spectra were obtained using a 300 MHz Varian Mercury[plus] NMR (VNMR 6.1C) spectrometer. All ^{1}H chemical shifts were referenced to TMS (0 ppm). Samples were prepared by dissolving the polymer in chloroform-d (5-7%, w/v) and charging this solution to a 5 mm NMR tube. For quantitative integration, 32 transients were acquired using a pulse delay of 5 s. In all cases, the signal due to the phenyl protons of the initiator (7.17 ppm, 3H, singlet) was chosen as an internal reference for functionality analysis.

Number-average molecular weights ($\overline{M_n}$) and dispersities ($Ð = (\overline{M_w}/\overline{M_n})$) were determined using a gel-permeation chromatography (GPC) system consisting of a Waters

Alliance 2695 separations module, an online multi-angle laser light scattering (MALLS) detector fitted with a gallium arsenide laser (power: 20 mW) operating at 658 nm (miniDAWN TREOS, Wyatt Technology Inc.), an interferometric refractometer (Optilab rEX, Wyatt Technology Inc.) operating at 35°C and 685 nm, and two PLgel (Polymer Laboratories Inc.) mixed E columns (pore size range 50-10^3 Å, 3 μm bead size). Freshly distilled THF served as the mobile phase and was delivered at a flow rate of 1.0 mL/min. Sample concentrations were ca. 15-20 mg of polymer/mL of THF, and the injection volume was 100μL. The detector signals were simultaneously recorded using ASTRA software (Wyatt Technology Inc.), and absolute molecular weights were determined by MALLS using a *dn/dc* calculated from the refractive index detector response and assuming 100% mass recovery from the columns.

Real-time ATR-FTIR monitoring of isobutylene polymerizations was performed using a ReactIR 45m (Mettler-Toledo) integrated with a N_2-atmosphere glovebox (MBraun Labmaster 130). Isobutylene conversion during polymerization was determined by monitoring the area above a two-point baseline of the absorbance at 887 cm^{-1}, associated with the $= CH_2$ wag of isobutylene. [11]

Isobutylene polymerization and end-quenching with (3-bromopropoxy)benzene, anisole, and isopropoxybenzene. All quenching experiments were performed on a single masterbatch PIB carrying *tert*-Cl end groups. This polymer was prepared using living polymerization of IB with *t*-Bu-*m*-DCC as initiator, carried out within a N_2-atmosphere glovebox, equipped with an integral, cryostated heptane bath, according to the following procedure. To a 1 L 4-neck round-bottom flask equipped with a mechanical stirrer, infrared probe, and thermocouple, were added sequentially 128 mL of hexane, 191 mL of

methyl chloride, 5.51 g (19.2 mmol) of *t*-Bu-*m*-DCC, and 0.149 mL (0.140 g, 1.30 mmol) of 2,6 lutidine. The mixture was allowed to equilibrate to -70°C, and then 103 mL (71.9 g, 1.28 mol) of isobutylene was charged to the reactor. The mixture was equilibrated to -70°C with stirring, and polymerization was initiated by the addition of 0.30 mL (2.8 mmol) of TiCl$_4$, followed by a second addition of 0.30 mL after 8 min. Full monomer conversion (> 98%) was reached in 35 min according to FTIR data. At the end of this time, the catalyst was destroyed by addition of excess prechilled methanol. The contents of the reaction flask were allowed to warm to room temperature, and after evaporation of methyl chloride, the polymer solution was washed with methanol and then collected by precipitation into methanol. The precipitate was collected by redissolution in fresh hexane; the solution was washed with DI water, dried over MgSO$_4$, and then vacuum stripped. Residual solvent was removed under vacuum at 40°C to yield pure difunctional *tert*-Cl PIB. The $\overline{M_n}$ determined by GPC was 3,900 g/mol, and the Đ was 1.19.

The aforementioned pre-formed difunctional *tert*-Cl PIB was used to perform a series of quenching experiments. Table 2.1 lists conditions for the quenching reactions and molecular weight and functionality data for the resulting quenched PIBs. The quenching reactions were studied as a function of quenching catalyst (AlCl$_3$ and TiCl$_4$), quencher (3-bromopropoxy benzene, anisole, and isopropoxybenzene), temperature (-50, -25, and 0 °C), and solvent polarity (Hex/CH$_2$Cl$_2$, v/v, 70/30 and 55/45). No 2,6-lutidine or other additive was used during the quenching study. A typical quenching experiment was as follows: A dry 3-neck round bottomed flask was placed into a cold heptane bath (-50°C) within an inert-atmosphere glove box. To the chilled flask was charged a solution of 1.7 g (0.44 mmol) of difunctional *tert*-Cl PIB dissolved in 38.8 mL chilled hexane and

37

16.7 mL CH_2Cl_2 (Hex/CH_2Cl_2, v/v, 70/30). Next, 0.69 mL (0.95 g, 4.4 mmol) of (3-bromopropoxy)benzene was charged to the solution, followed by 0.47 g (3.5 mmol) of $AlCl_3$. Aliquots for ^{1}H-NMR analysis were taken to monitor the conversion during the quenching reaction.

2.4 Results and Discussion

End-Quenching of tert-Cl PIB using different Lewis Acids. $TiCl_4$-catalyzed quenching of PIB carbenium ions by alkoxybenzenes is a remarkably useful synthetic technique for preparation of telechelic PIBs; however, reactivity and thus rate of alkylation is low compared to the analogous reactions with heterocyclic aromatics such as *N*-alkylpyrroles.[12] As a consequence alkoxybenzene quenching, as originally reported by Storey *et al.*,[1,4] was carried out in the relatively polar co-solvent mixture of 40/60, v/v, hexane/CH_3Cl and at relatively high catalyst concentrations ($0.05 < [TiCl_4] < 0.15$ M) in order to obtain acceptable rates of quenching at -70°C. There are several practical drawbacks to this approach. A chlorinated, polar solvent such as CH_3Cl is more hazardous to the environment and more costly than a hydrocarbon solvent. At the same time, $TiCl_4$ requires a low temperature to facilitate ionization, and the fact that it must be used at high concentration adds costs related to worker safety, corrosion of industrial equipment, and waste disposal. As mentioned earlier, $AlCl_3$ is an alternative Lewis acid candidate that could potentially address some of these disadvantages. To investigate the utility of $AlCl_3$ compared to $TiCl_4$, representative alkoxybenzene compounds, (3-bromopropoxy)benzene, anisole, and isopropoxy-benzene, were used to end-quench pre-formed difunctional *tert*-Cl PIB, at -50°C in Hex/CH_2Cl_2 (70/30, v/v), as outlined in Table 2.1.

38

The ^{1}H NMR spectrum of the starting *tert*-Cl PIB is shown in Figure 2.1A. The resonances due to the *gem*-dimethyl and methylene protons adjacent to the *tert*-Cl end groups may be observed at 1.68 and 1.96 ppm, respectively, and the resonances associated with the initiator residue may be observed at 7.17 ppm (aromatic protons) and 1.83 ppm (methylene protons of first repeat unit). End quenching was studied by sequentially charging an excess of alkoxybenzene compound and anhydrous $AlCl_3$ powder (or $TiCl_4$ as a control reaction) to the *tert*-Cl PIB in 70/30 (v/v) Hex/CH_2Cl_2 cosolvents. The relatively high non-polar, hydrocarbon solvent fraction was chosen for the reasons discussed above, and CH_2Cl_2 was selected instead of methyl chloride to potentially allow higher reaction temperatures. Progress and extent of reaction were monitored by ^{1}H NMR analysis of aliquots removed from the reactor at various times.

At -50°C in 70/30 (v/v) Hex/CH_2Cl_2 cosolvents, it was found that quantitative end-capping with (3-bromopropoxy)benzene, without detectable side reactions, could be achieved using $AlCl_3$ as catalyst, provided that the alkoxybenzene to Lewis acid ratio was larger than unity. For example, perfect bifunctionality (bromide end group) was observed in entries 1-3, Table 2.1, for which [Q]/[$AlCl_3$] was 2.5, 1.88, and 1.25, respectively. The data also show that an increasingly greater excess of quencher relative to chain ends results in increasingly shorter reaction times (see column 9, Table 2.1) as the second-order reaction becomes increasingly pseudo first-order.

Figure 2.1B shows the ^{1}H NMR spectrum of the difunctional PIB product from Entry 3, Table 2.1, which is representative. This spectrum is essentially identical to the spectrum for the control polymer produced using $TiCl_4$ catalysis (Entry 5, Table 2.1), shown in Figure 2.1C. (3-Bromopropoxy)benzene alkylation is indicated by the complete

39

disappearance of the resonances at 1.68 and 1.96 ppm due to the *tert*-Cl end groups, and appearance of new resonances at 3.60 (k, triplet), 2.30 (j, quintet), and 4.07 ppm (i, triplet) assigned to the propoxy tether and at 1.79 ppm due to the ultimate PIB methylene unit. Monoalkylation occurred exclusively *para-* to the alkoxy moiety evidenced by the clean pair of doublets at 6.83 and 7.27 ppm due to the 4-alkylated-(3-bromopropoxy)benzene moiety. Integration of these characteristic resonances (Figure 2.1B) in comparison with the aromatic initiator residual resonance at 7.17 ppm (singlet) indicated quantitative capping and formation of difunctional, telechelic primary bromine-terminated PIB.

Entry 4 of Table 2.1 is illustrative of quenching under conditions where the alkoxybenzene to Lewis acid ratio is smaller than unity; specifically, (3-bromopropoxy)benzene quenching was carried out using $[Q]/[AlCl_3] = 0.75$, i.e., $[Q] = 3 \times [CE]$, $[AlCl_3] = 4 \times [CE]$. The quenching reaction catalyzed by $AlCl_3$ becomes significantly slower under these conditions, and although the alkylated product is quantitatively functionalized, it possesses a slightly different structure due to carbocation rearrangement (Scheme 2.2, likely carbocation rearrangement pathways). [11,13]Figure 2.2 shows the ^{1}H NMR spectrum for the product. The signal intensities of the phenoxy aromatic protons (6.83 ppm) and the propoxy tether protons (3.60 and 4.07 ppm) compared to the aromatic initiator protons (7.18 ppm) are close to the theoretical values, indicating quantitiative alkylation. However, carbocation rearrangement is revealed by the many resonances between 1.60 and 1.80 ppm, as well as the irregular resonances between 0.80 and 1.00 ppm. If no carbocation rearrangement had occurred, the summed intensity of the signals at 1.79 and 1.83 ppm would be $8/3 \times$ the intensity of the aromatic

initiator proton signal at 7.18 ppm (e.g., see Figure 2.1B); instead, a summed intensity of only 5.7/3 × the initiator signal was observed. As will be discussed in greater detail below (Figure 2.3), AlCl$_3$ is apparently more active than TiCl$_4$ with respect to rate of ionization, and possibly with respect to rearrangement/fragmentation, but the resulting PIB$^+$AlCl$_4^-$ ion pairs are not necessarily more active than PIB$^+$Ti$_2$Cl$_9^-$ ion pairs with respect to the alkylation reaction. This appears to explain the greater sensitivity of the AlCl$_3$-catalyzed quenching reaction to the [Q]/[Lewis acid] ratio. With AlCl$_3$, *tert*-Cl PIB is ionized rapidly to form PIB carbocations in high concentration; if the quencher is not also present in high concentration, the PIB carbocations become starved for alkylation substrate and tend instead to undergo rearrangement reactions, such as hydride and methide shifts. The rearranged carbocations apparently also undergo alkylation reactions, albeit much more slowly, until all chains become alkylated; however, the structure of the polymer chain at the point of attachment of the phenoxy moiety is necessarily different.

Plots of PIB end group functionality vs. alkylation reaction time better illustrate these points. Figure 2.3A shows disappearance of *tert*-Cl functionality and Figure 2.3B shows appearance of (3-bromopropoxy)phenyl functionality for entries 3, 4, and 5 of Table 2.1. Entries 3 and 4 compare systems for which [Q]/[AlCl$_3$] is above (1.25) and below (0.75) unity, respectively, and entry 5 provides a comparative TiCl$_4$-catalyzed system for which [Q]/[TiCl$_4$] = 1.25. For [Q]/[AlCl$_3$] < unity, *tert*-Cl end groups were completely gone within the first 30 min, but alkylation proceeded much more slowly, requiring 48 h for completion (△). However, for [Q]/[AlCl$_3$] > unity, disappearance of *tert*-Cl and alkylation proceeded more nearly at the same rate, and alkylation proceeded smoothly to completion (×). Importantly, the data in Figure 2.3 show that AlCl$_3$ can be a

more effective catalyst than TiCl$_4$ under the same conditions; the AlCl$_3$ system required only 17.7 h for completion; whereas the TiCl$_4$ system required 30 h (Figure 2.3B).

Closer analysis of the data in Figure 2.3A and 2.3B shows that for AlCl$_3$ catalyst, even when [Q]/[AlCl$_3$] > unity (×), the disappearance of *tert*-Cl functionality is more rapid than the appearance of bromide functionality. In comparison, for TiCl$_4$ under the same conditions (○), the disappearance of *tert*-Cl functionality is almost synchronous with the appearance of bromide functionality. Since AlCl$_3$ is a much stronger Lewis acid, the accumulation of a slowly reacting intermediate resulting from carbenium ion rearrangement still happens, even in a less polar solvent system. However, alkylation apparently still occurs slowly through isomerized tertiary and possibly secondary chloride structures arising from AlCl$_3$-catalyzed rearrangement, as evidenced by the ^{1}H NMR spectrum (Figure 2.2).

Figure 2.4 shows GPC refractive index traces of pre-quench *tert*-Cl PIB (solid line in each case) and post-quench PIB under the various conditions in Table 2.1. In general, except for a slight shift to lower elution volume due to addition of quencher moieties, the GPC traces prior to and after quenching were nearly indistinguishable, and the curves indicate that no coupling or degradation reactions occurred during alkylation using either AlCl$_3$ or TiCl$_4$ catalysts under a variety of conditions.

End-Quenching of tert-Cl PIB with different quenchers using AlCl$_3$ catalyst. In addition to (3-bromopropoxy)benzene, quenching was also carried out using two additional alkoxybenzene quenchers, anisole and isopropoxybenzene. Anisole performed predictably, yielding quantitative end-capping under conditions of [Q]/[CE] = 5 and [AlCl$_3$]/[CE] = 4, in 70/30 (v/v) Hex/CH$_2$Cl$_2$ solution at -50°C (Table 2.1, entry 6).

42

Figure 2.1D shows the ^{1}H NMR spectrum of the resulting difunctional PIB bearing

anisole end groups. Evidence of anisole alkylation is given by the disappearance of the

resonances at 1.68 and 1.96 ppm due to the *gem*-dimethyl and methylene protons of the

ultimate repeat unit in *tert*-Cl PIB. Monoalkylation occurred exclusively *para* to the

alkoxy moiety as evidenced by the resonance for the ultimate PIB methylene unit

adjacent to anisole at 1.79 ppm, and by resonances at 6.82 (doublet), 7.27 ppm (doublet),

and 3.79 ppm (singlet) due to the alkylated anisole moiety. Integration of these

characteristic resonances in comparison to the aromatic initiator residual resonance at

7.17 ppm (singlet) indicated quantitative capping and formation of difunctional,

telechelic anisole-terminated PIB.

However, for isopropoxybenzene at the same reaction conditions (entry 9),

alkylation was incomplete and the product consisted of a mixture of isomers. The

reaction was also complicated by elimination at the PIB chain end during the early stages.

As shown in Figure 2.5A, a small fraction of *exo*-olefin was observed during the initial

stage of reaction (15 min) evidenced by characteristic resonances at 4.64 and 4.85 ppm.

Interestingly, elimination was entirely regiospecific, with no *endo*-olefin detected (no

peak at 5.15 ppm; see Figure 2.5B, Supplementary Information). Early-reaction

elimination such as this has not been observed by us with isopropoxybenzene in the

presence of TiCl$_4$, but we have shown that non-aromatic, sterically hindered ethers, *e.g.*,

diisopropyl ether, do affect regiospecific elimination (exclusively *exo*-olefin) at the PIB

chain end with TiCl$_4$. [14] After 45 h, no *exo*-olefin remained, but only 62.5% of the chain

ends carried the expected *para*-alkylated product as indicated by the integrated ratio of

the methine proton of the isopropoxy group (heptet, 4.51 ppm) compared to the protons

of the aromatic initiator residue (singlet, 7.17 ppm) (Figure 2.5B). However, the presence of an additional, minor isomer was indicated by a second heptet centered at 4.62 ppm, which has been tentatively assigned to the *meta*-substituted product. Based on the intensity of the 4.62 heptet, 22.7% of the chain ends carried this structure, providing a total alkylation conversion of 86.2%.

Figure 2.6 compares the rates of quenching observed with anisole and (3-bromopropoxy)benzene (isopropoxybenzene was not compared due to *exo*-olefin formation), catalyzed by $AlCl_3$. The alkylation of (3-bromopropoxy)benzene is faster than that of anisole under identical conditions, and this agrees with a previous report by Storey *et al.* [1] in which the same relative reactivity for these two quenchers was observed using $TiCl_4$ catalyst at -70°C in 40/60 (v/v) Hex/CH_3Cl. However, analysis of the data in Figure 2.6A and 2.6B shows that the disappearance of *tert*-Cl functionality is more rapid than the appearance of alkoxybenzene functionality, especially in the case of (3-bromopropoxy)benzene. This suggests accumulation of rearranged structures (carbenium ion rearrangement) with decreased reactivity due to steric hindrance. However, this interpretation is not supported by the fact that the ^{1}H NMR spectra of the products (Figures 2.1B and 2.1D) are clean and show the proper integrated intensity of the peak for the ultimate methylene unit of the PIB chain (peak e). End capping reached 100% conversion in 17.7 h for (3-bromopropoxy)benzene, whereas it required 30 h for anisole.

End-Quenching of tert-Cl PIB at different temperatures using AlCl₃ catalyst. The effect of temperature on end-quenching with (3-bromopropoxy)benzene catalyzed by $AlCl_3$ was studied under the standard conditions of Table 2.1: 70/30 (v/v) Hex/CH_2Cl_2 , [CE] = 0.016 M, [Q] = 0.080 M, and [$AlCl_3$] = 0.064 M. The results of Entries 7 and 8,

carried out at 0 and -25°C, respectively, were comparable to those of Entry 3, carried out

at -50°C. Figure 2.7 shows the ^{1}H NMR spectrum of the quenched product at -25°C (A)

and 0°C (B). The principal effect of temperature was to cause a decrease in

regioselectively and possibly an increase in carbocation rearrangement. Alkylation did

not occur exclusively *para* to the alkoxy moiety at 0°C; *meta* and possible multiple

alkylation products were formed as well, as evidenced by the new resonances at 7.53 and

7.70 ppm. Peak integration of the aromatic proton resonances suggested that the product

distribution was about 75% *para* with the balance consisting mostly of *meta*. Carbocation

rearrangement was also indicated at 0°C, as evidenced by many resonances between 1.60

and 1.80 ppm, as well as the irregular resonances between 0.80 and 1.00 ppm.

The kinetics of alkylation catalyzed by AlCl$_3$ were compared at -50, -25 and 0°C,

as shown in Figure 2.8. Overall, the rate of alkylation was higher at the higher

temperature; a functionality of 2 with respect to (3-bromopropoxy)phenyl groups

required only 7 h at 0°C compared to 8h at -25°C and 17.7 h at -50°C. The disappearance

of *tert*-Cl functionality was more rapid than the appearance of bromide functionality at all

temperatures, but the difference was especially pronounced at the highest temperature.

Carbocation rearrangement occurred at the higher temperatures, as well. The effect of

temperature was more significant for carbocation rearrangement as compared to rate of

alkylation, suggesting that activation energy of ionization with AlCl$_3$ is higher than that

for alkylation. At the highest temperature (0°C), fast ionization occurred to produce a

high concentration of PIB carbocations, but the rate of alkylation was relatively slower.

Hence, the PIB carbocations that were yet to undergo alkylation tended to undergo

rearrangement reactions, such as hydride and methide shifts, which were evidenced by the multiple resonances between 1.60 and 1.80 ppm in the ^{1}H NMR spectrum.

As shown in Figure 2.4D, the product obtained at 0°C displayed a slight shift to higher elution volume in GPC analysis, as well as a slight molecular weight distribution broadening, indicating some portion of the starved PIB carbocations might have undergone chain scission reactions.

End-Quenching of tert-Cl PIB using AlCl₃ catalyst in different concentrations. End-capping was carried out by charging an excess of (3-bromopropoxy)benzene (5 eq per chain end) and AlCl$_3$ (2 and 4 eq per chain end) to pre-formed di-functional *tert*-Cl PIB in 70/30 (v/v) Hex/CH$_2$Cl$_2$ solution at -50°C (entries 10 and 3, respectively). Progress of alkylation as a function of time is shown in Figure 2.9. Analysis of the data shows that the disappearance of *tert*-Cl functionality was more rapid than the appearance of bromide functionality at an AlCl$_3$ concentration of 4 eq per chain end; while the disappearance of *tert*-Cl functionality corresponded to the appearance of bromide functionality at AlCl$_3$ concentration of 2 eq per chain end. This suggests no accumulation of carbenium ions, and less likelihood of carbenium ion rearrangement at the lower AlCl$_3$ concentration as compared to the higher. The end-capping reaction reached 100% conversion in 17.7 and 43.6 h for concentration of AlCl$_3$ at 4 and 2 eq per chain end, respectively.

End-Quenching of tert-Cl PIB using AlCl₃ catalyst in solvents with different polarity. End-capping was carried out by charging an excess of (3-bromopropoxy)benzene (5 eq per chain end) and AlCl$_3$ (4 eq per chain end) to pre-formed di-functional *tert*-Cl PIB in 70/30 and (55/45) (v/v) Hex/CH$_2$Cl$_2$ solution at -50°C

46

(entries 3 and 11, respectively). The reaction carried out in the more polar solvent mixture was accompanied by carbocation rearrangement, as evidenced by the many resonances between 1.60 and 1.80 ppm, as well as the irregular resonances between 0.80 and 1.00 ppm (Figure 2.10). Moreover, carbocation rearrangement caused an observable loss in the integrated intensity of the peak due to the ultimate methylene unit of the PIB chain (1.79 ppm). The summed integration of the latter peak plus the methylene peak nearest the initiator fragment (1.83ppm) should be consistent with 8 total protons (see Figure 2.1B), but in Figure 2.10 it is only 5.93.

Progress of alkylation as a function of time for entries 3 and 11 is shown in Figure 2.11. Analysis of the data shows that the disappearance of *tert*-Cl functionality is more rapid than the appearance of bromide functionality in either cosolvent system. Interestingly, the disappearance of *tert*-Cl functionality in the 55/45 solvent system was faster than in the 70/30 solvent system; however, the rate of appearance of the alkylated product showed exactly the opposite trend. This suggests that accumulation of less reactive structures occurred to a greater extent in the more polar solvent system, resulting in slower alkylation. End capping reached 100% conversion in 17.7 and 19 h in 70/30 and 55/45, v/v, Hex/CH$_2$Cl$_2$ solvent systems, respectively.

Kinetics of end-quenching. The rate of AlCl$_3$ or TiCl$_4$-catalyzed alkoxybenzene alkylation of *tert*-Cl PIB may be described by the following second-order rate equation:

$$\frac{\mathrm{d}p}{\mathrm{d}t} = k_\mathrm{c} K_\mathrm{eq}[\mathrm{LA}]^n [\mathrm{PIBCl}]_0 (1-p)(M-p) \qquad (2.1)$$

where, p is conversion of *tert*-Cl chain ends, k_c is the rate constant for alkylation, [PIBCl]$_0$ is the initial chain end concentration, [LA] is the effective concentration of AlCl$_3$ or TiCl$_4$ available for participation in the ionization equilibrium, M is the ratio of

47

the initial alkoxybenzene concentration to the initial *tert*-Cl chain end concentration

([alkoxybenzene]/[PIBCl]$_0$), and K_{eq} is the ionization equilibrium constant. No basic

additives like 2,6-lutidine were used allowing the effective [LA] to be the initial

concentration of Lewis acid. Eq 1 may be integrated to yield

$$\ln\left(\frac{M-p}{M(1-p)}\right) = k_c K_{eq}[\text{LA}]^n[\text{PIBCl}]_0(M-1)t \qquad (2.2)$$

Figure 2.12 shows data (only experiments with no carbocation rearrangement

were chosen) for alkylation of (3-bromopropoxy)benzene and anisole using AlCl$_3$ or

TiCl$_4$ at -50 and 0°C in 70/30 (v/v) Hex/CH$_2$Cl$_2$, plotted according to eq 2. Analysis of

the plots shows that the rate of alkylation is heavily dependent on the identity of the

Lewis acid, the identity of the quencher, and the concentration of the Lewis acid. The

fastest rate was for alkylation of (3-bromopropoxy)benzene at 0°C (◇), but *meta*- and/or

ortho-alkylated products were also obtained. The alkylation of (3-bromopropoxy)benzene

at -50°C (×) was slightly slower than at 0°C; however, exclusively *para*-alkylated

product was obtained at the lower temperature. The rate of alkylation of anisole was 2

times slower than that of (3-bromopropoxy)benzene using AlCl$_3$ catalyst. This indicates

that a longer alkyl tether helps to minimize electronic and steric hindrance during the

alkylation reactions. The alkylation rate of (3-bromopropoxy)benzene with AlCl$_3$ was 2.6

times faster than with TiCl$_4$, which is due to the high ionization rate produced by AlCl$_3$,

inherent to its substantially electron-poor nature (stronger Lewis acid strength). The

alkylation rate of (3-bromopropoxy)benzene with AlCl$_3$ at 4 eq per chain end was 5 times

faster than with TiCl$_4$.

2.5 Conclusions

Quenching of living PIB by alkoxybenzenes (alkylation) provides a versatile method for direct chain end functionalization or the introduction of useful reaction sites for further functionalization. Here we have investigated the alkylation of several alkoxybenzenes by PIB carbocations, produced from pre-formed *tert*-Cl PIB using either $AlCl_3$ (experimental catalyst) or $TiCl_4$ (control). $AlCl_3$, the stronger Lewis acid, has several potential advantages over $TiCl_4$. $AlCl_3$ is less expensive, and it may be more environmentally friendly due to lower toxicity and corrosivity, and higher catalytic activity in hydrocarbon solvents at elevated temperatures compared to $TiCl_4$.

In general, we found that $AlCl_3$, relative to $TiCl_4$, tends to promote rapid ionization, while not necessarily providing rapid alkylation, and this can cause accumulation of carbenium ions and concomitant side reactions such as carbenium ion rearrangement. However, under properly optimized conditions ($[Q]/[AlCl_3] \geq 1$, -50°C in 70/30 (v/v) Hex/CH_2Cl_2), the rate of alkylation of (3-bromopropoxy)benzene or anisole with $AlCl_3$ was observed to be 2.6 times faster than with $TiCl_4$ under the same conditions, and to yield regiospecific (*para* isomer only), quantitatively functionalized PIBs.

The rate of alkylation with $AlCl_3$ did not vary greatly with increasing temperature (to -25 and 0°C) or with increasing solvent polarity (to 55/45 (v/v) Hex/CH_2Cl_2); however, both of these changes increased the incidence of carbocation rearrangement and lessened regiospecificity (minor amounts of *meta* and *ortho* isomers). The rearranged carbocations were capable of quantitative alkylation but at a lower rate.

For isopropoxybenzene quencher only, using $AlCl_3$ catalyst, a small fraction of *exo*-olefin was formed during the initial stage of reaction, and the quenching reaction

49

failed to reach completion; chain end functionality was a mixture *para* and *meta* isomers (3:1) and reached only 1.72 (86.4% conversion) after 45 h.

The experiments reported herein were performed using a pre-formed *tert*-Cl-terminated PIB, which facilitated comparison of different quenching conditions using a common precursor. The method may be easily adapted to an *in situ* process, consisting first of living polymerization of isobutylene catalyzed by $TiCl_4$, followed, after complete monomer conversion, by addition of the alkoxybenzene and $AlCl_3$ catalyst. The $TiCl_4$ catalyst concentration required for living polymerization is relatively low, and the $AlCl_3$ alkylation catalyst may be simply added to the $TiCl_4$ catalyst already present.

2.6 Acknowledgements

2.7 References

(1)   Morgan, D. L.; Martinez-Castro, N.; Storey, R. F., *Macromolecules* **2010,** *43* (21), 8724-8740.

(2)   Olah, G. A.; Batamack, P.; Deffieux, D.; Török, B.; Wang, Q.; Molnár, Á.; Surya Prakash, G. K., *Appl. Catal., A* **1996,** *146* (1), 107-117.

(3)   Kolp, C. J., *US Patent 5,663,457* **1984**.

(4)   Morgan, D. L.; Storey, R. F., *Macromolecules* **2009,** *42* (18), 6844-6847.

(5)   Vasilenko, I. V.; Frolov, A. N.; Kostjuk, S. V., *Macromolecules* **2010,** *43* (13), 5503-5507.

(6)   Kostjuk, S. V.; Yeong, H. Y.; Voit, B., *J. Polym. Sci., Part A: Polym. Chem.* **2013,** *51* (3), 471-486.

(7)   Hunter, B. K.; Redler, E.; Russell, K. E.; Schnarr, W. G.; Thompson, S. L., *J. Polym. Sci., Polym. Chem. Ed.* **1983,** *21* (2), 435-445.

(8)   Hongfa, C.; Su, H.-L.; Bazzi, H. S.; Bergbreiter, D. E., *Org. Lett.* **2009,** *11* (3), 665-667.

(9)   Keszler, B.; Chang, V. S. C.; Kennedy, J. P., *J. Macromol. Sci., Part A : Chem.* **1984,** *21* (3), 307-318.

(10)   Storey, R. F.; Choate, K. R., *Macromolecules* **1997,** *30* (17), 4799-4806.

(11)   Storey, R. F.; Curry, C. L.; Brister, L. B., *Macromolecules* **1998,** *31* (4), 1058-1063.

(12)   Morgan, D. L.; Storey, R. F., *Macromolecules* **2010,** *43* (3), 1329-1340.

(13)   Dimitrov, P.; Emert, J.; Hua, J.; Keki, S.; Faust, R., *Macromolecules* **2011,** *44* (7), 1831-1840.

(14)   Ummadisetty, S.; Storey, R. F., *Macromolecules* **2013,** *46* (6), 2049-2059.

2.8 Tables and Figures for Chapter II

Table 2.1

Conditions and results for Lewis acid-catalyzed end-quenching of *tert*-Cl PIB[a] with alkoxybenzenes.

Entry	Quencher (Q)	Catalyst	Temp (°C)	Hex/CH$_2$Cl$_2$	[Q]/ [CE]	[Catalyst]/ [CE]	Time (h)	F[b]	$\overline{M_n}$[c]	PDI
1	3-BPB[d]	AlCl$_3$	-50		10	4.0	5	2.0	4,500	1.16
2	3-BPB	AlCl$_3$	-50		7.5	4.0	7	2.0	4,500	1.14
3	3-BPB	AlCl$_3$	-50		5.0	4.0	17.7	2.0	4,300	1.15
4	3-BPB	AlCl$_3$	-50		3.0	4.0	48	2.0	5,000	1.29
5	3-BPB	TiCl$_4$	-50		5.0	4.0	30	2.0	4,300	1.15
6	anisole	AlCl$_3$	-50	70/30	5.0	4.0	30	2.0	4,200	1.17
7	3-BPB	AlCl$_3$	0		5.0	4.0	8	2.0	3,500	1.28
8	3-BPB	AlCl$_3$	-25		5.0	4.0	43.6	2.0	5,100	1.23
9	IPB[e]	AlCl$_3$	-50		5.0	4.0	45	1.72	4,800	1.20
10	3-BPB	AlCl$_3$	-50		5.0	2.0	43.6	2.0	4,200	1.16
11	3-BPB	AlCl$_3$	-50	55/45	5.0	4.0	19	2.0	5,000	1.26

[a][chain end] = [CE] = 0.016 mol/L; [b]number-average functionality; [c]g/mol (GPC); [d](3-bromopropoxy)benzene; [e]isopropoxybenzene.
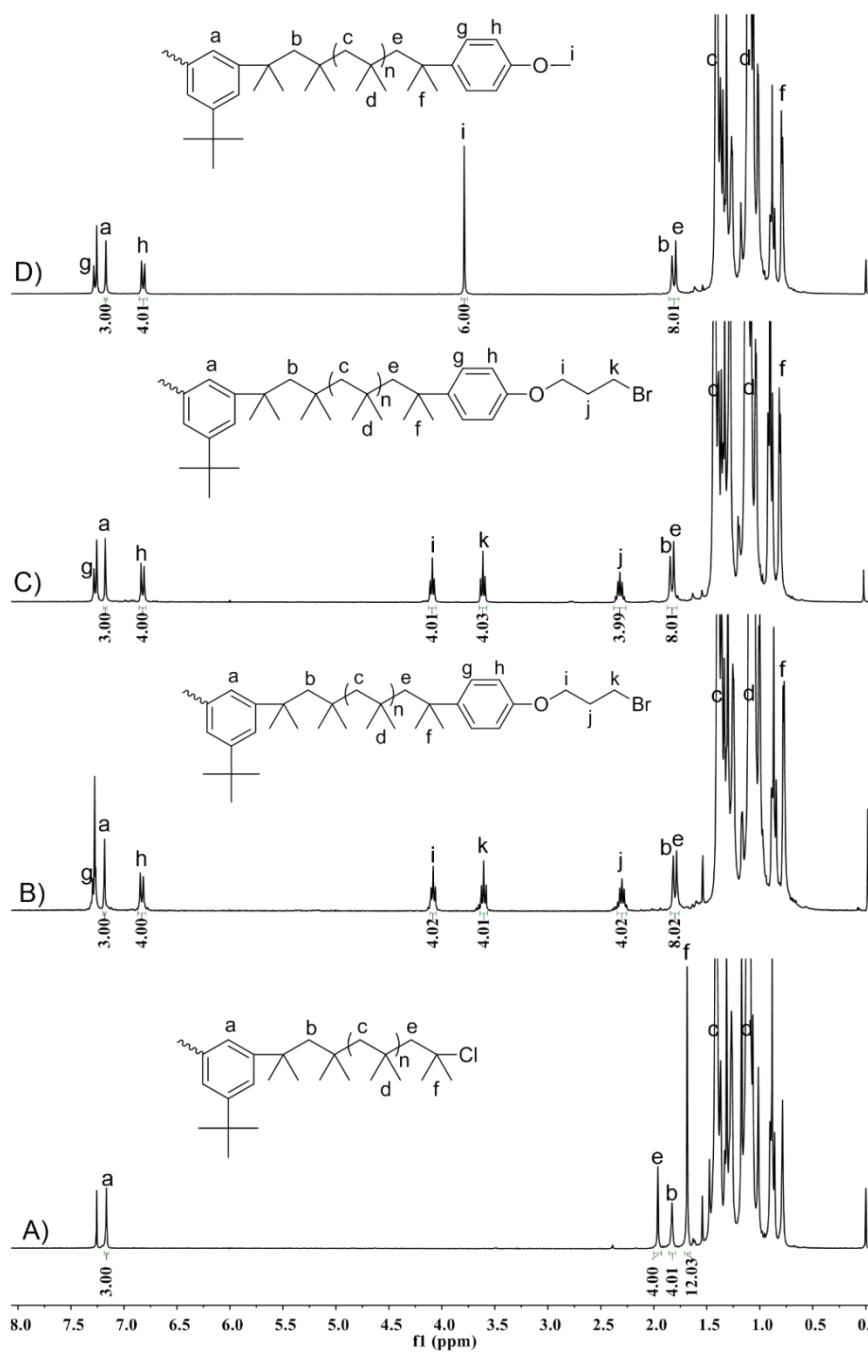
Figure 2.1 ^{1}H NMR (300 MHz, CDCl$_3$, 25°C) spectra of telechelic PIBs.

A) pre-quench *tert*-Cl PIB with peak integrations; B) α,ω-bis[4-(3-bromopropoxy)phenyl]PIB with peak integrations obtained by end-quenching with (3-bromopropoxy)benzene using AlCl$_3$ (Entry 3, Table 2.1); C) α,ω-bis[4-(3-bromopropoxy)phenyl]PIB obtained by end-quenching with (3-bromopropoxy)benzene using TiCl$_4$ catalyst (Entry 5, Table 2.1); D) α,ω-bis(4-methoxyphenyl)PIB obtained by end-quenching with anisole using AlCl$_3$ catalyst (Entry 6, Table 2.1). For spectra B-D, [Q] = 5×[CE], [Lewis Acid] = 4×[CE].
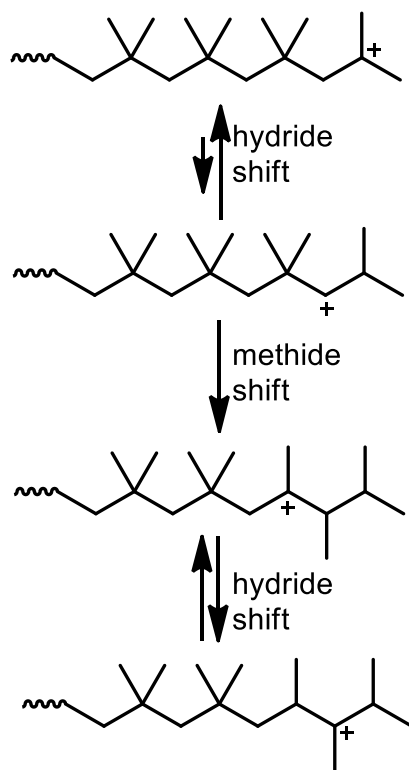
Scheme 2.2 Mechanism of PIB carbocation rearrangements.
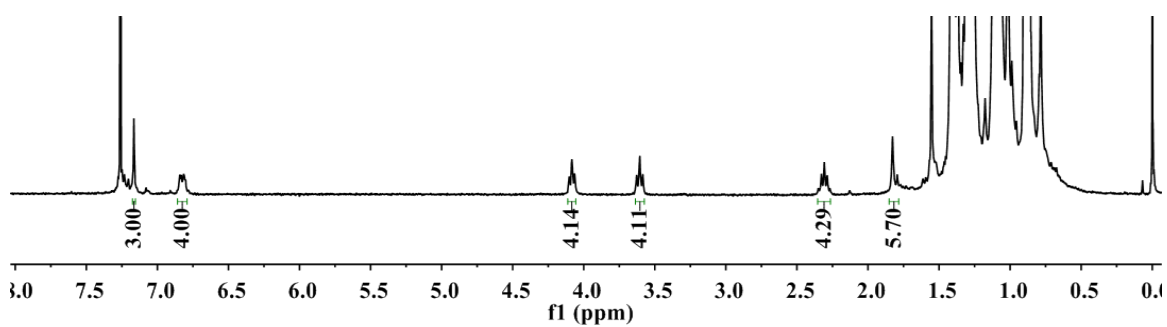
Figure 2.2 ^{1}H NMR (300 MHz, CDCl$_3$, 25 °C) spectrum of the product of Entry 4, Table 2.1. [Q]/[AlCl$_3$] =0.75.
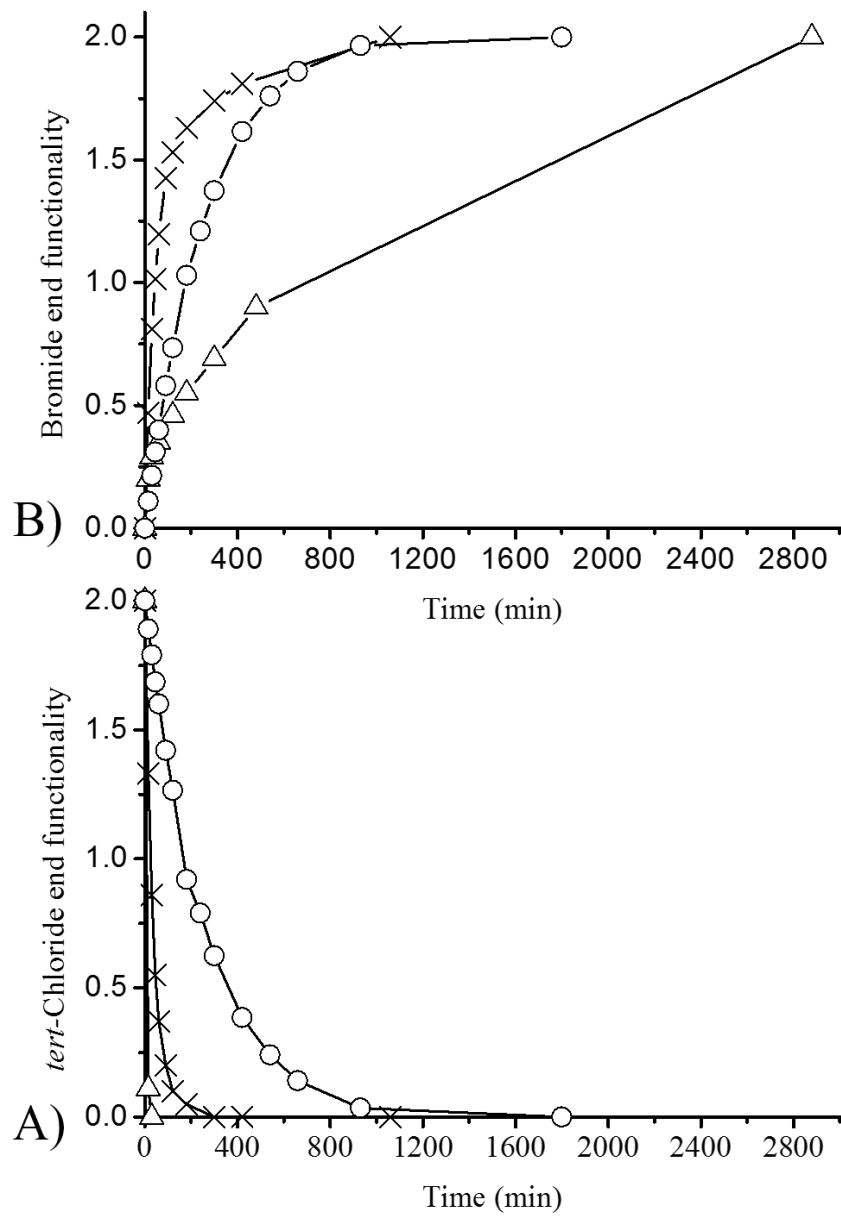
Figure 2.3 Functionality of PIB chain ends, (A) *tert*-Cl and (B) (3-bromopropoxy)phenyl, as a function of time for end-quenching of pre-formed *tert*-Cl PIB with (3-bromopropoxy)benzene

At -50°C in 70/30 (v/v) Hex/CH$_2$Cl$_2$, with [CE] = 0.016 M. [Q]/[AlCl$_3$] = 1.25 (×), [Q]/[AlCl$_3$] = 0.75 (△), [Q]/[TiCl$_4$] = 1.25 (○).

56
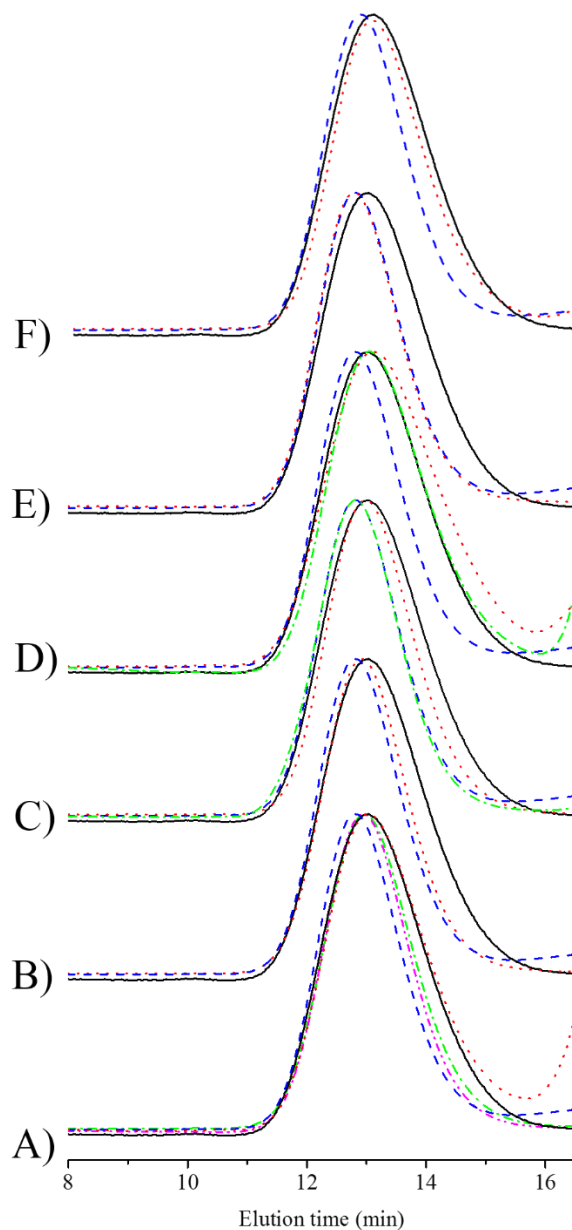
Figure 2.4 GPC refractive index traces of pre-quench *tert*-Cl PIB (black solid line in each case) and post-quench PIB (colored dot and dash lines).

Reaction conditions are -50°C, 70/30 (v/v) Hex/CH_2Cl_2, (3-bromopropoxy)benzene as quencher, $AlCl_3$ as Lewis acid catalyst, [Q] = 0.080 M, [$AlCl_3$] = 0.064 M, [CE] = 0.016 M, unless otherwise stated. (A) variation of [Q] at constant [$AlCl_3$], [Q]/[$AlCl_3$] = 2.5 (green), 1.88 (magenta), 1.25 (blue), and 0.75 (red); (B) variation of Lewis acid, $AlCl_3$ (blue) and $TiCl_4$ (red); (C) variation of quencher, (3-bromopropoxy)benzene (blue), anisole (red), and isopropoxybenzene (green); (D) variation of temperature, -50°C (blue), -25°C (green), and 0°C (red); (E) variation of [$AlCl_3$] at constant [Q], [$AlCl_3$] = 4[CE] (blue) and 2[CE] (red); and (F) variation of solvent polarity, Hex/CH_2Cl_2, v/v, 70/30 (blue) and 55/45 (red).

57
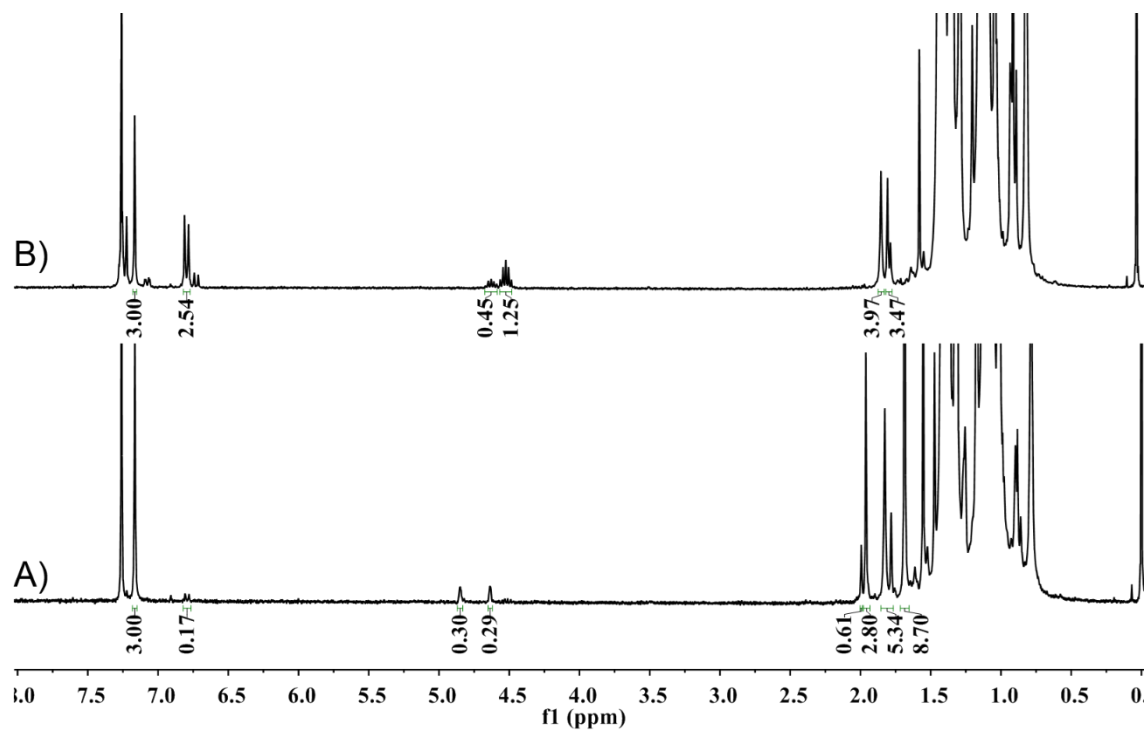
Figure 2.5 ¹H NMR (300 MHz, CDCl₃, 25°C) spectra of pre-formed *tert*-Cl PIB after quenching with isopropoxybenzene for (A) 15 min and (B) 45 h.

(Table 2.1, entry 9). [CE] = 0.016 M, [isopropoxybenzene] = 0.080 M, [AlCl₃] = 0.064 M.
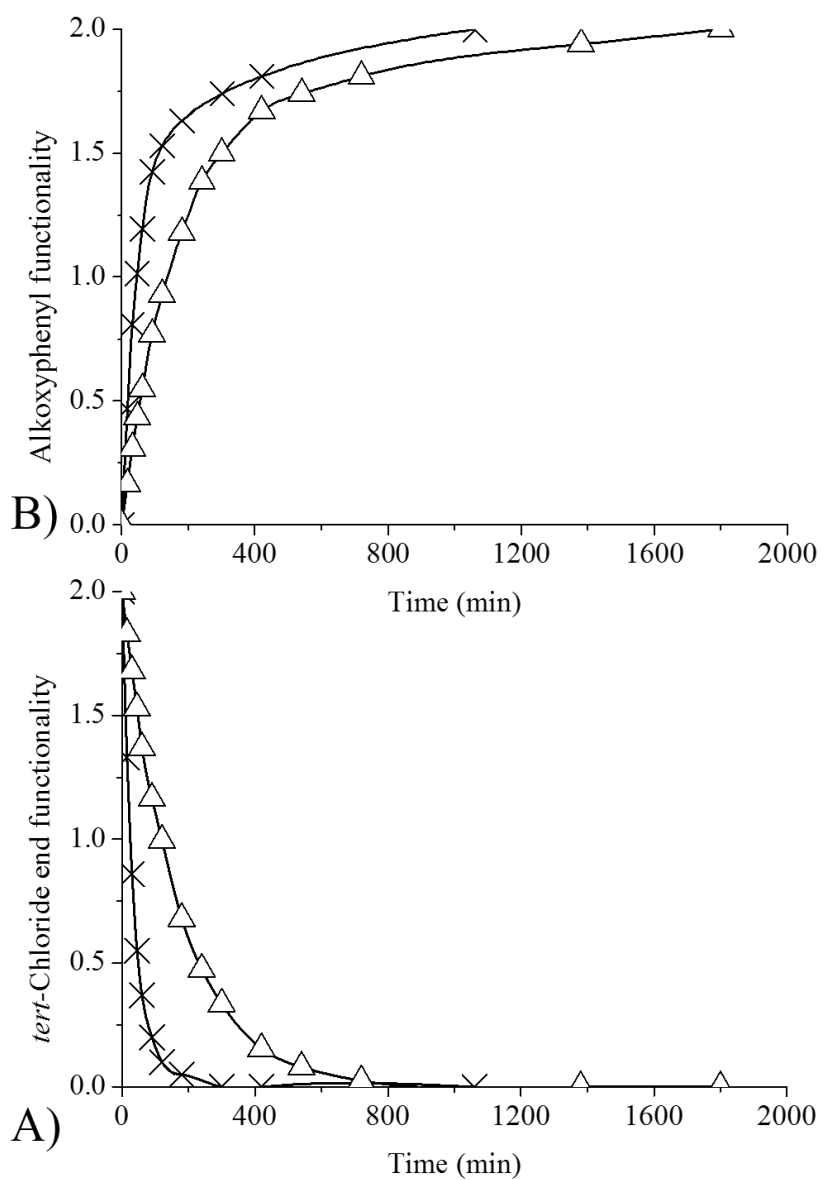
Figure 2.6 Functionality of PIB chain ends, (A) *tert*-Cl and (B) alkoxyphenyl, as a function of time for end-quenching of *tert*-Cl PIB with (3-bromopropoxy)benzene (×) or anisole (△).

Using AlCl$_3$ catalyst. -50°C, 70/30 (v/v) Hex/CH$_2$Cl$_2$, [CE] = 0.016 M, [AlCl$_3$] = 0.064 M, [Q] = 0.080 M.
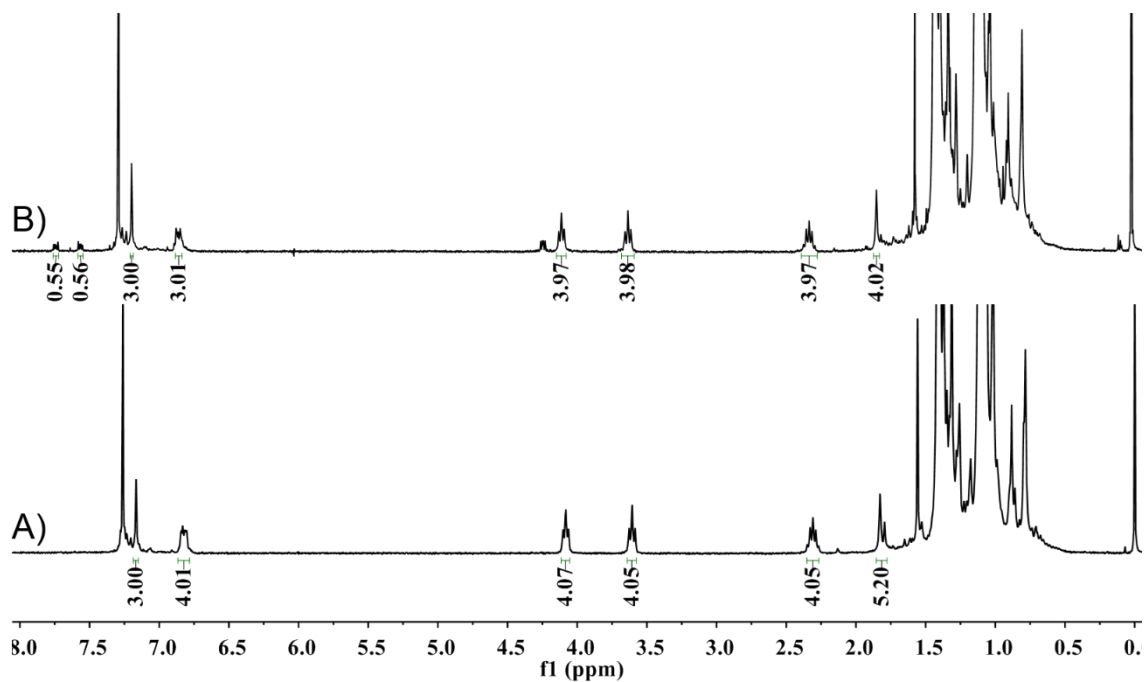
Figure 2.7 ^{1}H NMR (300 MHz, CDCl$_3$, 25°C) spectra of PIBs end-quenched with (3-bromopropoxy)benzene, catalyzed by AlCl$_3$: (A) -25°C (Entry 8, Table 2.1), and (B) 0°C (Entry 7, Table 2.1).

[CE] = 0.016 M, [Q] = 0.080 M, [AlCl$_3$] = 0.064 M.
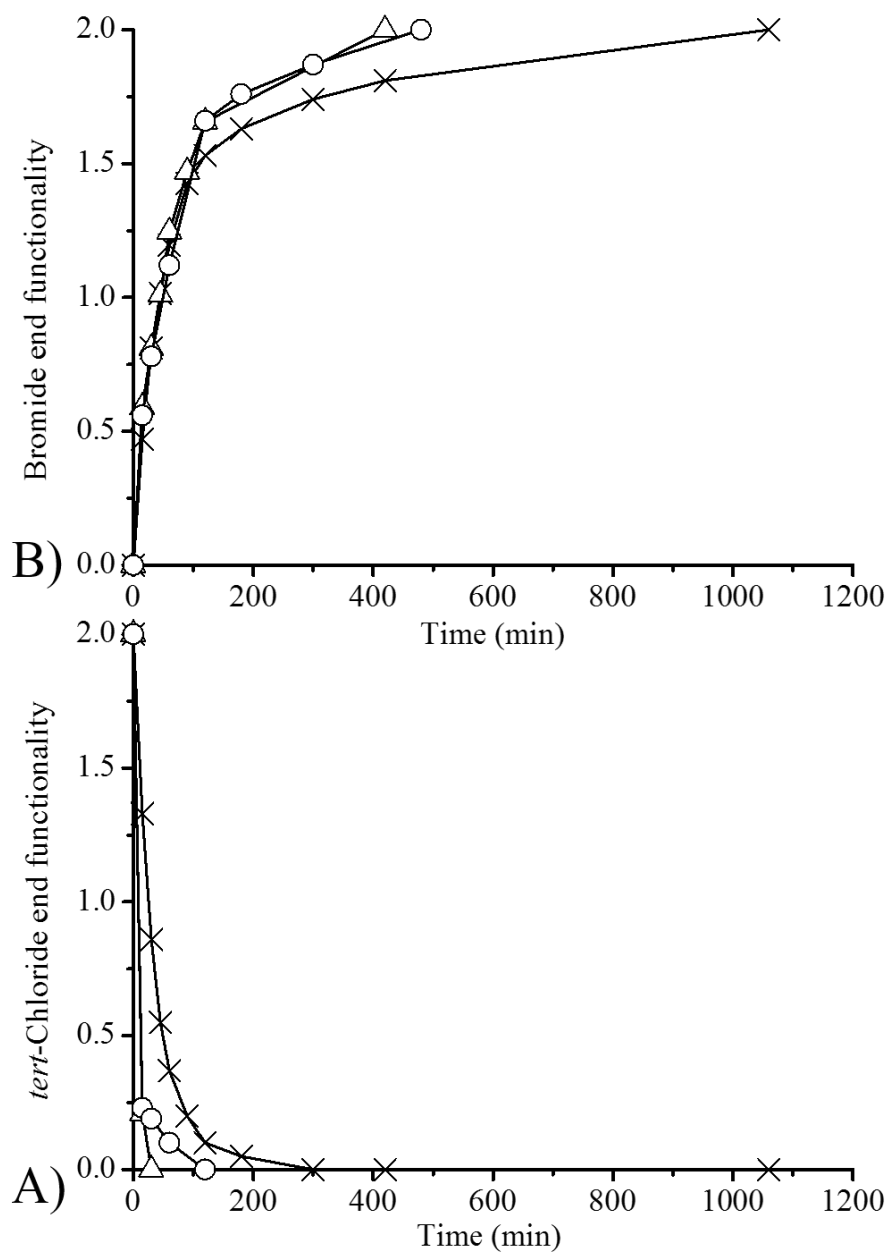
Figure 2.8 Functionality of PIB chain ends, (A) *tert*-Cl and (B) (3-bromopropoxy)phenyl, as a function of time for end-quenching of *tert*-Cl PIB at -50 (×), -25 (○) and 0°C (△) using $AlCl_3$ catalyst.

70/30 (v/v) Hex/CH_2Cl_2, [CE] = 0.016 M, [$AlCl_3$] = 0.064 M, [Q] = 0.080 M
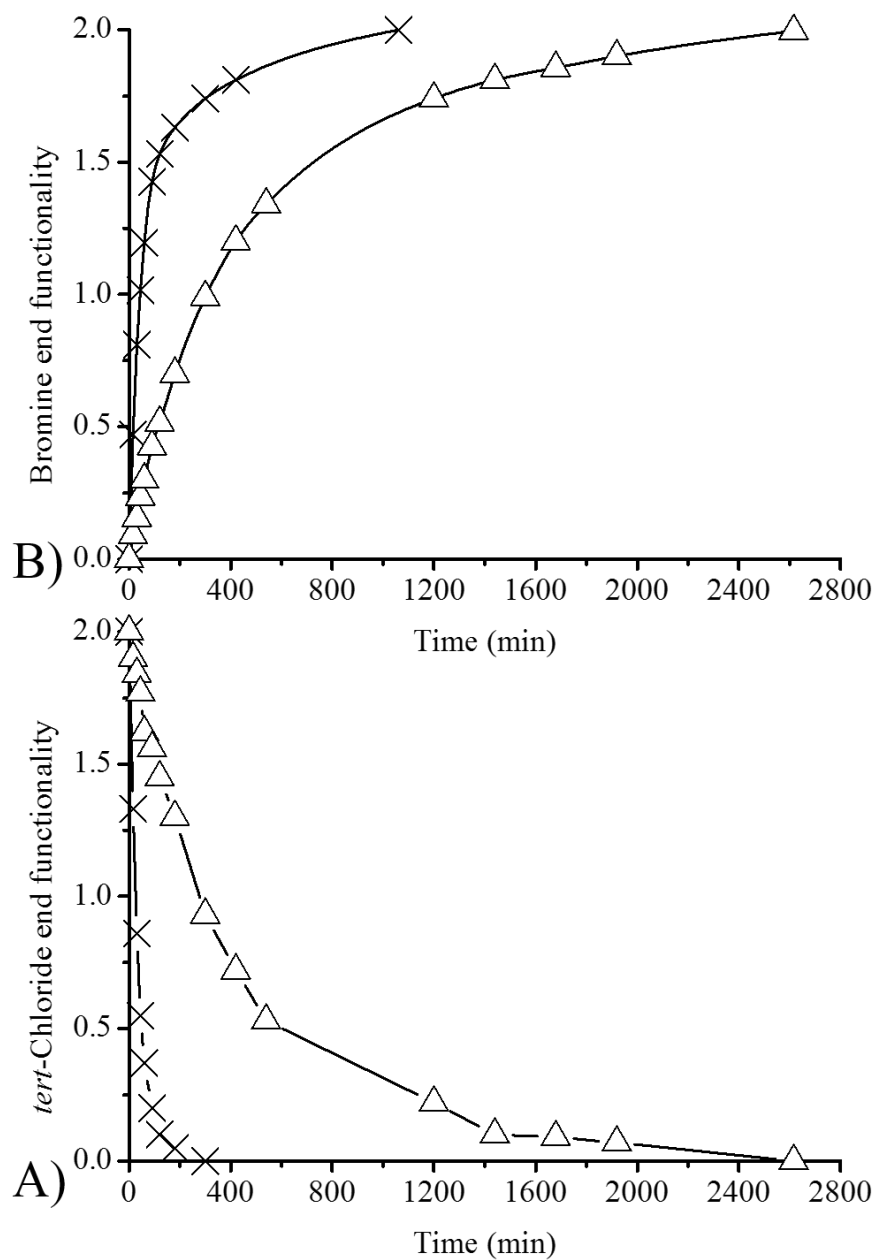
Figure 2.9 Functionality of PIB chain ends, (A) *tert*-Cl and (B) bromopropoxyphenyl, as a function of time for end-quenching of *tert*-Cl PIB with (3-bromopropoxy)benzene using AlCl$_3$ catalyst.

At 0.064 M (×) and 0.032 M (△). -50°C, 70/30 (v/v) Hex/CH$_2$Cl$_2$, [CE] = 0.016 M, [Q] = 0.08 M.
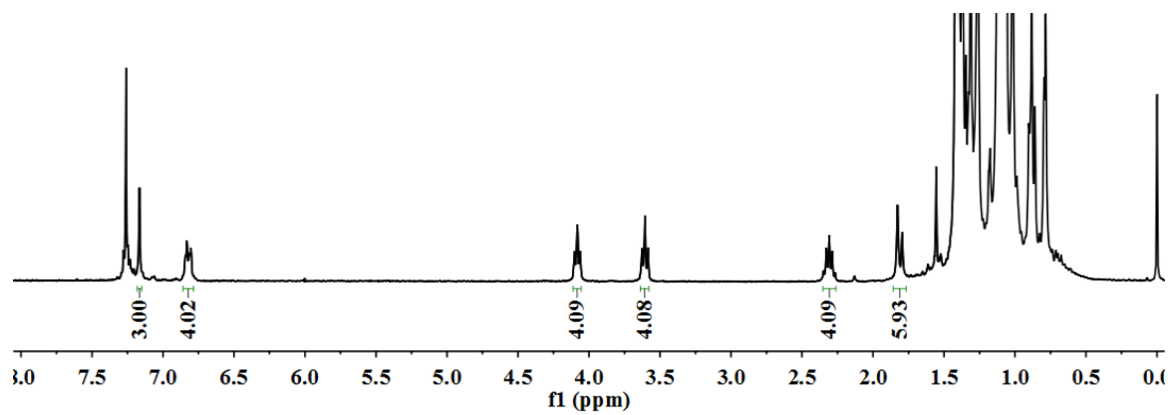
Figure 2.10 ^{1}H NMR (300 MHz, CDCl$_3$, 25°C) spectrum of the product of Entry 11, Table 2.1.

[CE] = 0.016 M, [(3-bromopropoxy)benzene] = 0.080 M, [AlCl$_3$] = 0.064 M, Hex/CH$_2$Cl$_2$, v/v, 55/45.
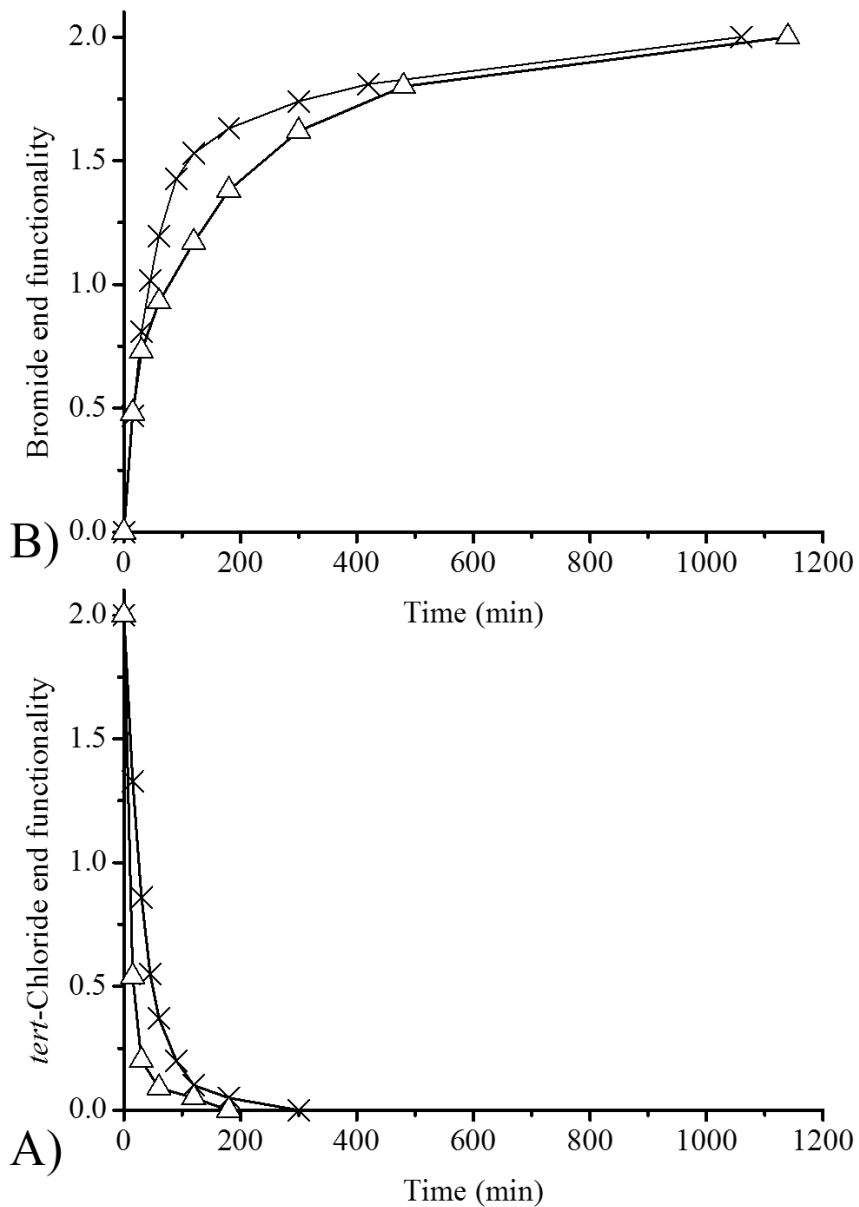
Figure 2.11 Functionality of PIB chain ends, A) *tert*-Cl and B) bromopropoxyphenyl, as a function of time for end-quenching of *tert*-Cl PIB with (3-bromopropoxy)benzene.

Using AlCl$_3$ catalyst in 70/30 (×)and (55/45) (△) (v/v) Hex/CH$_2$Cl$_2$, [CE] = 0.016 M, [Q] = 0.08 M

64
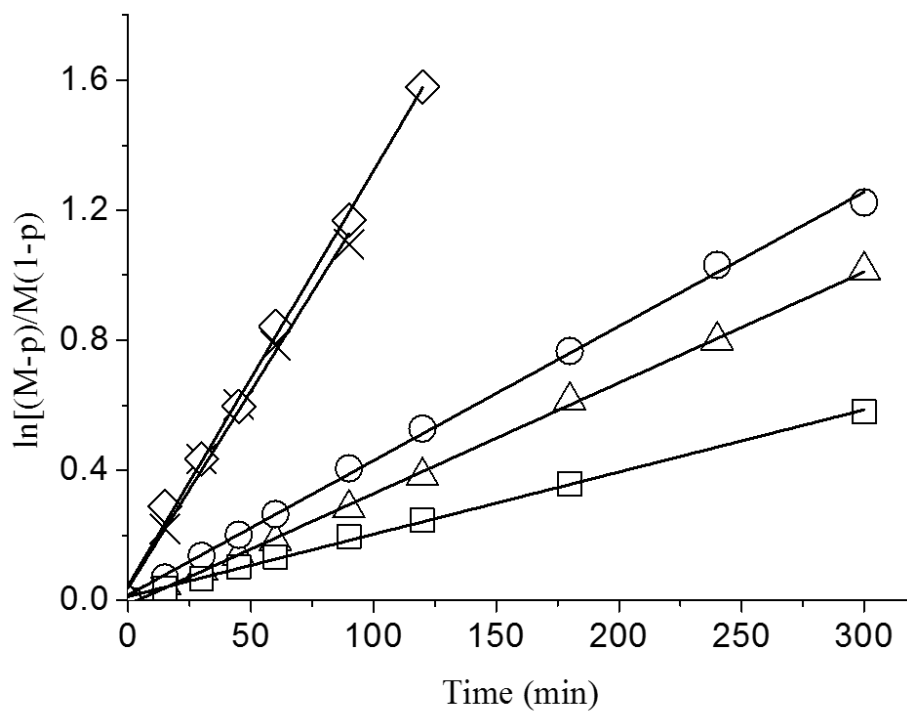
Figure 2.12 Second-order kinetic plot for alkylation of alkoxybenzenes by *tert*-Cl PIB using AlCl$_3$ or TiCl$_4$ catalyst.

At -50 or 0°C in 70/30 (v/v) Hex/CH$_2$Cl$_2$. [CE] = 0.016 M, [Q] = 0.080 M. (3-Bromopropoxy)benzene: (×) -50°C, [Q]/[AlCl$_3$] = 1.25;

(◇) 0°C, [Q]/[AlCl$_3$] = 1.25; (△) -50°C, [Q]/[TiCl$_4$] = 1.25; (□) -50°C, [Q]/[AlCl$_3$] = 2.5. Anisole: (○) -50°C, [Q]/[AlCl$_3$] = 1.25

CHAPTER III – SYNTHESIS, CHARACTERIZATION, AND

PHOTOPOLYMERIZATION OF POLYISOBUTYLENE PHENOL

(METH)ACRYLATE MACROMERS

3.1 Abstract

Polyisobutylene phenol (meth)acrylates were produced by reacting di- or triphenol-terminated PIB with (meth)acryloyl chloride. ^{1}H NMR, GPC, and MALDI-TOF MS characterization showed that meth(acrylate) end-functionality was 2 and 3, respectively, and that targeted molecular weights and relatively low polydispersities were achieved. Comparative aliphatic PIB triol triacrylate was prepared by end-quenching living polyisobutylene with 4-phenoxy-1-butyl acrylate. A photopolymerization study of PIB diphenol di(meth)acrylates with M_n about 3,000 g/mol, PIB triphenol tri(meth)acrylates with M_n about 4,000 and 10,000 g/mol, and control aliphatic PIB triol triacrylate with M_n about 10,000 g/mol was conducted. Darocur® 1173 and Irgacure® 819 and 651 photoinitiators were studied, and FTIR reaction monitoring showed that Darocur® 1173 afforded the highest rate of photopolymerization and final conversion, apparently due to its higher solubility in PIB. At $M_n \cong 4,000$ g/mol, the rate of photopolymerization and conversion of PIB triphenol triacrylate was faster than that of PIB triphenol methacrylate under the same conditions; at $M_n \cong 10,000$ g/mol, PIB triphenol triacrylate, PIB triphenol trimethacrylate, and aliphatic PIB triol triacrylate all showed the same high rate of photopolymerization, which was higher than any rate observed at $M_n \cong 4,000$ g/mol. Similarly, PIB triphenol tri(meth)acrylate at $M_n \cong 4,000$ g/mol displayed a higher rate of photopolymerization and double bond conversion than PIB diphenol di(meth)acrylate at $M_n \cong 3,000$ g/mol; although they have similar chain end

concentrations. This phenomenon was attributed to reduced diffusional mobility at higher M_n, resulting in decreased rate of bimolecular radical termination and autoacceleration. T_g of UV-cured PIB networks decreased as M_n of PIB macromer increased regardless of end-group type. Thermal stability of cured networks remained constant regardless of end-group type. Mechanical properties were characteristic of rubbery networks but weak, apparently due to low M_n and low PDI of the starting macromers and lack of chain entanglements. Networks from macromers with $M_n \cong$ 10,000 g/mol gave higher elongations, but lower Young's moduli, compared to those from macromers with $M_n \cong 4,000$ g/mol.

3.2 Introduction

Photo-cured networks have found many applications in the fields of protective and decorative coatings,[1] printing inks,[2] adhesives,[3] and dental restoratives.[4] Photopolymerization offers a number of significant advantages toward the curing of monomers, including high curing rate, low energy consumption, low operation temperature, low shrinkage, and low volatile organic compound (VOC) emission.[1,5] Acrylate (A) and methacrylate (MA) monomers are particularly useful in photo-initiated free radical polymerization because of their superior reactivity,[6] and polymers or oligomers with (M)A chain ends have been broadly used in UV curing.[5] The resulting coatings, films, and networks have excellent adhesion and mechanical, chemical, and optical properties, which make them suitable for a variety of applications.[5] UV curing of (meth)acrylate functionalized polymers such as polyesters, polycarbonates, polyurethane, polyethers, and polysiloxanes have been widely reported,[5,7] but only a few studies have reported photopolymerization of (M)A-terminated PIBs.

PIB-based networks provide remarkable properties,[8-13] such as strong adherence, high flexibility, good thermal and oxidative stability, low gas permeability, good energy damping and solvent resistance, and biostability/biocompatibility.[14-16] Preparation of PIB-based networks via UV curing requires well-defined multifunctional (M)A-terminated PIB macromers. A thorough review of the historical development of PIB (meth)acrylates has been reported in a previous paper.[17] In general, PIB (meth)acrylates have been produced by reaction of (meth)acryloyl chloride with primary hydroxyl-terminated PIB (PIB-OH)[18-20] or by reaction of alkali metal (meth)acrylates with primary bromine-terminated PIB (PIB-Br).[8,21-22] PIB-OH has mainly been obtained by hydroboration oxidation[23] of either *exo*-olefin (methyl vinylidene) or allyl PIB.[24] PIB-Br has been synthesized by 1,3-butadiene capping of living PIB to produce haloallyl PIB,[25-27] or by end-capping of living PIB with nucleophilic aromatic moieties, such as *N*-(ω-bromoalkyl)pyrrole[28] or 3-bromopropoxybenzene.[29-31] Puskas *et al.*[32] demonstrated enzyme-catalyzed methacrylation of PIB. More recently, Storey *et al.* have demonstrated a one-step, one-pot method, in which a phenoxyalkyl (meth)acrylate is added to living PIB at full monomer conversion, to achieve well defined telechelic PIB (meth)acrylates.[17]

The photopolymerization of PIB (meth)acrylates to create crosslinked networks has been studied by Faust *et al.*[8] using optical pyrometry, which has been shown to relate directly to conversion versus time data determined by RT-IR.[33] The authors demonstrated that the photopolymerization of low molecular weight aliphatic PIB-(M)A is a fast reaction and that networks with double bond conversions $\geq 95\%$ may be obtained.

The PIB (meth)acrylates discussed above are aliphatic (M)A macromers, in which the (M)A moieties are connected to the PIB chain via an aliphatic linkage. Aromatic (meth)acrylates prepared by esterification of acrylic or methacrylic acid with a phenolic compound are also readily polymerizable by radical mechanism provided that the aromatic moiety is not too bulky.[34] However, we are aware of only two research groups that have reported PIB macromers possessing an aromatic acrylate or methacrylate end group.[35-37] In both cases the authors used commercial, highly reactive PIB (HR PIB), possessing a high fraction of *exo*-olefin termini, to alkylate phenol under Friedel-Crafts conditions, followed by subsequent esterification of the phenol hydroxyl group with acryloyl or methacryloyl chloride. The resulting monofunctional, *p*-(polyisobutylene)phenyl acrylate macromers were used to produce graft copolymers in a radical-mediated, "grafting through" process.

The monofunctional PIB-phenyl acrylate macromers discussed above cannot be used to produce crosslinked networks; instead, polyfunctional analogues would be required. Although we have not found any literature reports of the latter, synthesis of the required polyfunctional PIB phenol precursors is well documented in the literature.[38-39] Recently, Storey *et al.*[30] reported synthesis of phenolic PIB via end-quenching of living PIB with alkoxybenzenes such as anisole and isopropoxybenzene followed by *in situ* de-blocking. For anisole, cleavage of the terminal methyl ether required reaction with excess BBr_3 at room temperature for 22 h. The bulkier isopropoxybenzene could be de-blocked under milder conditions, requiring only 5.5 h at room temperature with sulfuric acid and excess $TiCl_4$.
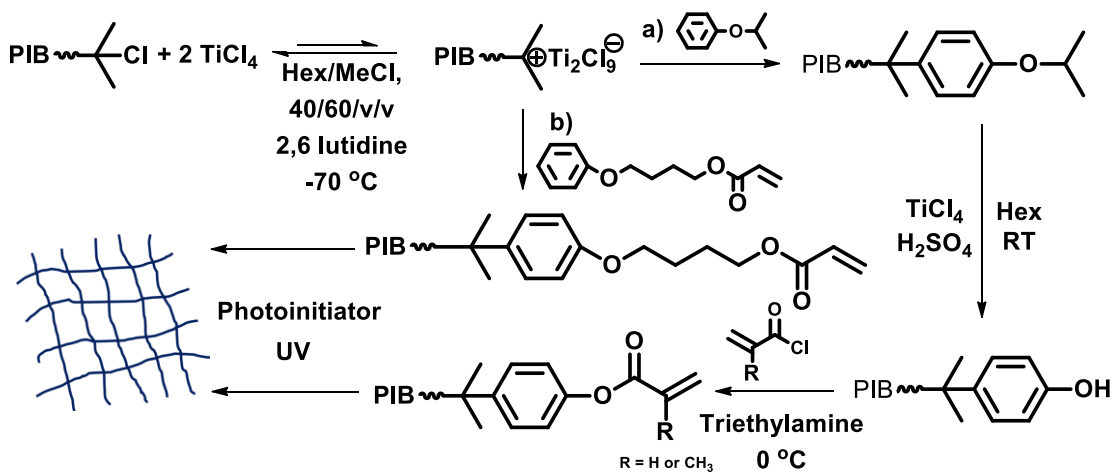
Scheme 3.1 Synthesis and UV curing of photopolymerizable PIB-(M)A macromers.

a) PIB di- or triphenol was first synthesized by direct end-quenching of living PIB with isopropoxybenzene, followed by de-blocking of isopropyl moiety. PIB phenol (meth)acrylates were then synthesized by substitution reaction with (meth)acryloyl chloride; b) for comparison, aliphatic PIB acrylate was synthesized by direct end-quenching of living PIB with 4-phenoxy-1-butyl acrylate at full IB conversion. UV-cured PIB networks were prepared by photopolymerization using a photoinitiator and broad-spectrum UV radiation centered at 365 nm.

Irgacure® 651
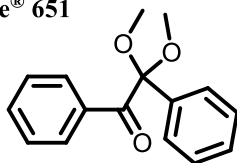
2,2-dimethoxy-1,2-diphenylethanone

Darocur® 1173
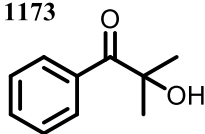
2-hydroxy-2-methyl-1-phenylpropan-1-one

Irgacure® 819
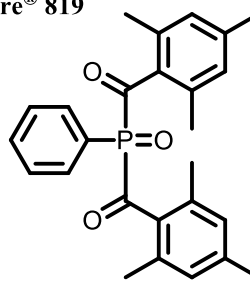
bis(2,4,6-trimethylbenzoyl)-phenylphosphine oxide

Scheme 3.2 Chemical structures of photoinitiators used, including Irgacure® 651 and 819 (solid), and Darocur® 1173 (liquid.)

Herein, we have used the end quenching method of Storey *et al.* [29-31] to synthesize di- and trifunctional telechelic PIB phenols, followed by reaction with (meth)acryloyl chloride to create aromatic PIB-(meth)acrylates, as shown in route a in Scheme 3.1. To better understand the steric effects of the phenyl ring on the photopolymerization of

(M)A terminated PIBs, a tri-functional aliphatic acrylate-terminated PIB was also synthesized (route b in Scheme 3.1). Photopolymerization kinetics of the various PIB-(meth)acrylates using different UV initiators (see Scheme 3.2) has been investigated using real-time FTIR. The effects of crosslink density and acrylate structure on the T_g of PIB networks have been analyzed by DMA. Thermal stability and mechanical properties of these PIB networks have been investigated by TGA and static tensile testing, respectively.

3.3 Experimental

Materials. Hexane (anhydrous, 95%), methanol (anhydrous, 99.8%), methylene chloride (anhydrous, 99.8%), titanium tetrachloride (TiCl$_4$) (99.9%), 2,6-lutidine (99.5%), anisole (anhydrous, 99.7%), (3-bromopropoxy)benzene (anhydrous, 98%), tetrahydrofuran (THF) (anhydrous, 99.9%), dichloromethane-d$_2$ (CD$_2$Cl$_2$), phenoxybutyric acid, borane-tetrahydrofuran complex (BH$_3$•THF, 1M), diethyl ether, potassium carbonate (K$_2$CO$_3$), and silver trifluoroacetic acid (AgTFA) were purchased from Sigma-Aldrich and used as received. Acryloyl chloride and methacryloyl chloride were purchased from Sigma-Aldrich and vacuum distilled prior to use. *Trans*-2-[3-(4-*t*-butylphenyl)-2-methyl-2-propenylidene]malononitrile (DTCB) was purchased from Tokyo Chemical Industry Co. and used as received. Isopropoxybenzene (97%) was purchased from Oakwood Chemical and used as received. Magnesium sulfate (MgSO$_4$) (anhydrous), sulfuric acid (98%), chloroform-d (CDCl$_3$) were purchased and used as received from Fisher Scientific. Photoinitiators Irgacure® 819 and 651, and Darocur® 1173 were purchased from Ciba and used as received. Isobutylene (IB, BOC Gases) and methyl chloride (Alexander Chemical Corp.) were dried by passing the gaseous reagent

71

through a column of $CaSO_4$/molecular sieves/$CaCl_2$ and condensing within a N_2-atmosphere glovebox immediately prior to use. Synthesis of the difunctional initiator, 5-*tert*-butyl-1,3-di(1-chloro-1-methylethyl)benzene (*b*DCC) has been reported.[40] The trifunctional initiator, 1,3,5-tri(1-chloro-1-methylethyl)benzene (TCC), was prepared by first synthesizing 1,3,5-tri(1-hydroxyl-1-methylethyl)benzene (TCOH) using the procedure of Mishra *et al*.,[41] followed by reaction of the latter with dry HCl at 0°C using a procedure analogous to that reported by Storey et al.[42] Both initiators were stored at 0°C prior to use. 4-Phenoxy-1-butyl acrylate was synthesized according to a previously published procedure.[17]

Instrumentation. Nuclear magnetic resonance (NMR) spectra were obtained using a 600.13 MHz Bruker Ascend (TopSpin 3.5) spectrometer. All ^1H chemical shifts were referenced to TMS (0 ppm). Samples were prepared by dissolving the polymer in either chloroform-d or dichloromethane-d_2 (5-7%, w/v) and charging this solution to a 5 mm NMR tube. For quantitative integration, 16 transients were acquired using a pulse delay of 27.3 s. In all cases, the signal due to the phenyl protons of the initiator (7.17 ppm, 2H or 3H, singlet) was chosen as an internal reference for functionality analysis.

Real-time Fourier transform infrared (RT-FTIR) monitoring of isobutylene polymerizations was performed using a ReactIR 45m (Mettler-Toledo) integrated with a N_2-atmosphere glovebox (MBraun Labmaster 130) equipped with a cryostated heptane bath.[43] Isobutylene conversion during polymerization was determined by monitoring the area above a two-point baseline of the absorbance at 887 cm^{-1}, associated with the $= CH_2$ wag of isobutylene.

Number-average molecular weights (M_n) and polydispersities (PDI = M_w/M_n) were determined using a gel-permeation chromatography (GPC) system consisting of a Waters Alliance 2695 separations module, an online multi-angle laser light scattering (MALLS) detector fitted with a gallium arsenide laser (power: 20 mW) operating at 658 nm (miniDAWN TREOS, Wyatt Technology Inc.), an interferometric refractometer (Optilab rEX, Wyatt Technology Inc.) operating at 35°C and 685 nm, and two PLgel (Polymer Laboratories Inc.) mixed E columns (pore size range 50-10^3 Å, 3 μm bead size). Freshly distilled THF served as the mobile phase and was delivered at a flow rate of 1.0 mL/min. Sample concentrations were ca. 15-20 mg of polymer/mL of THF, and the injection volume was 100μL. The detector signals were simultaneously recorded using ASTRA software (Wyatt Technology Inc.), and absolute molecular weights were determined by MALLS using a *dn/dc* calculated from the refractive index detector response and assuming 100% mass recovery from the columns.

Matrix-assisted laser desorption/ionization time-of-flight mass spectrometry (MALDI-TOF MS) was performed using a Bruker Microflex LRF MALDI-TOF mass spectrometer equipped with a nitrogen laser (337 nm) possessing a 60 Hz repetition rate and 50 µJ energy output. The PIB samples were prepared using the dried droplet method: separately prepared THF solutions of DCTB matrix (20 mg/mL), PIB sample (10 mg/mL), and AgTFA cationizing agent (10 mg/mL), were mixed in a volumetric ratio of matrix/sample/cationizing agent = 4:1:0.2, and a 0.5 µL aliquot was applied to a MALDI sample target for analysis. The spectrum was obtained in the positive ion mode utilizing the Reflector mode micro-channel plate detector and was generated as the sum of 900-1000 shots.

Attenuated total reflectance (ATR)-FTIR was used to determine the final conversion of photopolymerized films prepared for properties evaluation. ATR-FTIR spectra of the surfaces of prepared films were acquired using a Nicolet 8700 spectrometer with a gradient-angle ATR attachment and Omnic software. Spectra were taken with a resolution of 4 cm^{-1} by accumulating a minimum of 128 scans per run. Nitrogen was constantly purged through the attachment to reduce interference of CO_2 and water. Absorbances at 1638 and 1615 cm^{-1} (C=C stretching of (M)A)[44] were monitored to determine PIB phenol (meth)acrylate double bond conversion.

Photopolymerization kinetic data were obtained using transmission RT-FTIR spectroscopy by monitoring the disappearance of the (meth)acrylate absorbances at 1638 and 1615 cm^{-1}. Transmission RT-FTIR studies were conducted using a Nicolet 8700 spectrometer with a KBr beam splitter and a DTSG detector with a 320-500 nm filtered UV light source. Each sample was degassed within a vacuum oven for 30 min at room temperature and then sandwiched between two NaCl plates; the sample was then exposed to UV light while continuously purging the sample chamber with N_2. A series of scans was recorded, where spectra were taken approximately 1 scan/0.95s with a resolution of 4 cm^{-1}.

Dynamic mechanical analysis (DMA) was conducted using a Q 800 (TA Instruments) instrument in air using tensile mode. The frequency was set at 1 Hz, the pre-load static force at 0.005 N, the oscillatory amplitude at 15 µm, and the track setting at 125%. Sample dimensions were approximately 20×6.6×0.75 mm. DMA experiments were performed at a heating rate of 3°C/min and a temperature range of -120 to 80°C.

The DMA data were analyzed utilizing TA Universal Analysis software. The T_g was defined as the onset drop of the storage modulus.

Sol contents of photocured networks were determined by extraction experiments. Samples with dimension $5.0 \times 5.0 \times 0.75$ mm were cut from UV-cured networks and immersed in dry THF at room temperature. The samples were removed from THF after 48 h, dried in a vacuum oven overnight at room temperature, and weighed. Swelling in THF and vacuum drying were repeated until no further weight loss was observed.

Thermogravimetric analysis (TGA) was performed using a Q 500 (TA Instrument) thermogravimetric analyzer. The furnace atmosphere was defined by 50 mL/min N_2. Samples were prepared by loading a platinum sample pan with 10-20 mg of material. The samples were subjected to a temperature ramp of 10^oC/min from 30 to 600^oC. The degradation temperature was defined as the temperature at which 5% weight loss had occurred.

Tensile testing of PIB networks was conducted using a MTS Alliance RT/10 system and MTS Testworks 4 software. Specimens were cut into bars with dimensions of $60 \times 6.6 \times 0.75$ mm, clamped using a 500 N load cell, and tested at a crosshead speed of 5 mm/min at room temperature, following ASTM D 638.[45] Young's modulus was determined from the initial slope of the stress-strain curves. The reported values were the average of at least three different specimens.

Synthesis of phenol-terminated PIB precursors. Several phenol-terminated PIB precursor polymers were synthesized by living isobutylene polymerization/phenoxy quenching (Table 3.1) and subsequently converted to di- and trifunctional PIB phenol acrylate and methacrylate macromers (Table 3.2). Polymerization and quenching

reactions were performed within a N_2-atmosphere glovebox equipped with a cryostated heptane bath. Synthesis of 10K PIB triphenol (Entry 6,Table 3.1) is representative and was carried out as follows: To a 2 L 4-neck round-bottom flask, equipped with an overhead stirrer, thermocouple, and ReactIR probe, and immersed in the heptane bath, were added 340 mL hexane, 510 mL methyl chloride, 0.36 mL (3.1 mmol) 2,6-lutidine, 3.69 g (12.0 mmol) TCC, and 164 mL (2.04 mol) IB. The mixture was equilibrated to -70°C with stirring, and polymerization was initiated by the addition of 0.66 mL (6.0 mmol) $TiCl_4$, followed by an additional 0.66mL of $TiCl_4$ after 10 min. Essentially full monomer conversion was reached in 45 min according to RT-FTIR data, at which time 10.6 mL (72.0 mmol) isopropoxybenzene was charged to the reaction (2 eq per chain end). Additional $TiCl_4$ (6.57 mL, 59.9 mmol) was added to catalyze the quenching reaction, resulting in a total $TiCl_4$ concentration of 2 eq per chain end. The quenching reaction was allowed to proceed for 4 h, at which time the deblocking reaction to obtain phenolic PIB was begun. An additional 15.8 mL of $TiCl_4$ (resulting in a total $TiCl_4$ concentration of 6 eq relative to chain ends) and 10.6 g of H_2SO_4 (3 eq relative to chain ends) were charged to the reaction mixture, and the reactor was moved to the fume hood and allowed to warm to room temperature with evaporation of methyl chloride (about 2 h). The deblocking reaction was continued at room temperature for a total of 9 h. At the end of this time, the catalyst was destroyed by careful addition of excess methanol (~ 30 mL). The resulting polymer solution was washed with methanol and then precipitated into 1.5 L of methanol and acetone solution (methanol/acetone, v/v, 95/5). The precipitate was collected by re-dissolution in fresh hexane; the solution was washed with DI water, dried over $MgSO_4$, and then vacuum stripped. Residual solvent was removed

under vacuum at 50°C to yield pure PIB triphenol. PIB diphenol (initiated by *b*DCC) and

4K PIB triphenol precursors were prepared similarly.

Synthesis of PIB phenol (meth)acrylate macromers. Phenol-terminated PIB

precursors were reacted with either acryloyl or methacryloyl chloride to prepare the PIB

phenol (meth)acrylate macromers listed in entries 1-6 of Table 3.2. The preparation of

PIB diphenol diacrylate, which is representative, was as follows: To a scintillation vial

equipped with a magnetic stirring bar and immersed in a salt water bath were added 0.50

g PIB diphenol precursor (M_n = 2,700 g/mol, 0.37 mmol phenol groups) and 10 mL

freshly distilled THF. To the stirred solution were added triethylamine (0.154 mL, 1.11

mmol) and acryloyl chloride (0.045 mL, 0.56 mmol, vacuum distilled prior to use). Upon

addition of acryloyl chloride, the clear colorless solution immediately became cloudy.

After 2 h reaction, the THF was vacuum stripped, and the polymer was dissolved in

hexane. The resulting solution was filtered through a cotton plug and slowly added into

excess methanol to precipitate the polymer. The precipitate was redissolved in fresh

hexane, and the resulting solution was washed with DI water, dried over $MgSO_4$, and

then vacuum stripped to obtain pure PIB diphenol diacrylate. The other PIB phenol

(meth)acrylates were prepared similarly.

Synthesis of 10K aliphatic PIB triol triacrylate. An aliphatic PIB triol triacrylate

(Entry 7, Table 3.2) was prepared by direct end-quenching of living PIB with 4-phenoxy-

1-butyl acrylate following a previously published procedure.[17]

Preparation of UV Cured Networks. UV-cured networks were prepared from the

various trifunctional PIB macromers of Table 3.2, as free-standing films for analysis and

testing. The following procedure was representative: 10K PIB triphenol triacrylate (1.0

g) and photoinitiator Darocur 1173 (20 mg, 2 wt%) were added to a scintillation vial. A homogeneous solution was obtained by gently warming the mixture with stirring. The solution was transferred to a first glass plate, which had been previously cleaned with acetone, coated with release agent (Rain-X®), and fitted with a 0.75 mm Teflon® spacer. This assembly was placed in a vacuum oven at 40°C, and the solution was degassed for 1 h. After degassing, a second, clean, Rain-X®-coated glass plate was quickly placed over the sample to exclude air. Gentle pressure was applied to the resulting sandwich assembly to achieve a uniform film thickness of 0.75 mm. The sample was subsequently cured for 30 min under a medium-pressure mercury UV lamp (broad-spectrum UV radiation centered at 365 nm) at an intensity of 15 mW cm^{-2}. After UV curing, the film was gently peeled from the glass plates using a razor blade and stored in a scintillation vial prior to characterization. The final double bond conversion of the sample was determined by ATR-FTIR as described earlier.

3.4 Results and Discussion

Synthesis of phenol-terminated PIB precursors. End-quenching of $TiCl_4$-catalyzed, living IB polymerization with isopropoxybenzene at full monomer conversion, followed by addition of extra $TiCl_4$ and sulfuric acid to deblock the bulky isopropyl group, shown in Scheme 3.1(a), provided a facile procedure to produce phenol-terminated PIBs.[30] The synthetic procedure and primary structural characterization were developed and refined using a difunctional PIB sample with relatively low molecular weight (Entries 1-2 of Table 3.2). This sample configuration facilitated NMR analysis by providing a high concentration of end groups (high signal-to-noise ratio), all of which were sufficiently removed from the initiator fragment to possess a uniform chemical

shift. The ^{1}H NMR spectrum of difunctional PIB-isopropoxybenzene (M_n= 2,700 g/mol, PDI=1.19) is shown in Figure 3.1A. Exclusively monoalkylation, *para* to the alkoxy moiety, was observed, as revealed by two clean doublets at 6.79 (Ar-H, $C_{2,6}$) and 7.23 ppm (Ar-H, $C_{3,5}$). The resonance for the methine proton of the isopropyl moiety appeared as a heptet at 4.51 ppm. Figure 3.1B shows the ^{1}H NMR spectrum of difunctional phenol-terminated PIB (M_n=2,700 g/mol, PDI=1.19) after deblocking of the bulky isopropyl moiety in the presence of H_2SO_4 and extra $TiCl_4$. The resonance at 4.51 ppm disappeared, and a new singlet due to the phenolic proton appeared at nearly the same chemical shift. Quantitative phenol end-functionality was confirmed by comparing the integrated peak intensities of the phenol moiety to that of the aromatic initiator protons. Quantitative trifunctional isopropoxybenzene- and phenol-terminated PIB precursors were obtained following an analogous reaction route using TCC initiator, as indicated in the ^{1}H NMR spectra for the 10K sample (Entries 5-6, Table 3.2) in Figure 3.2A and 3.2B.) The GPC traces of difunctional (Figure 3.3) and trifunctional (Figure 3.4) isopropoxybenzene- and phenol-terminated PIBs indicated no coupling during the alkylation/quenching reaction and no degradation or depolymerization during H_2SO_4-assisted deblocking. Molecular weight and polydispersity (GPC) of isopropoxybenzene- and phenol-terminated PIB precursors are listed in Table 3.1.

Synthesis of PIB phenol (meth)acrylate macromers. The synthetic route for di- and trifunctional PIB phenol (meth)acrylate macromers is shown in Scheme 3.1(a). The quantitative end-functionality of PIB diphenol diacrylate and PIB diphenol dimethacrylate was confirmed by ^{1}H NMR as shown in Figure 3.1C and 3.1D, respectively. Evidence of formation of PIB diphenol diacrylate (Figure 3.1C, M_n = 2,900

g/mol, PDI = 1.24) was given by the appearance of chemical shifts at 5.98 (doublet), 6.31

(quartet), and 6.59 ppm (doublet), as well as the disappearance of chemical shifts at 4.51

(singlet) due to the loss of phenol. Evidence of formation of PIB diphenol dimethacrylate

(Figure 3.1D, M_n = 2,900 g/mol, PDI = 1.18) was given by the appearance of chemical

shifts at 2.05 (singlet), 5.72 (singlet), and 6.33 ppm (singlet), as well as the disappearance

of chemical shifts at 4.51 (singlet) due to the loss of phenol. Quantitative trifunctional

PIB triphenol tri(meth)acrylates were obtained following a similar reaction route, as

indicated in the ^{1}H NMR spectra for the 10K sample in Figure 3.2C and 3.2D. The GPC

traces of difunctional (Figure 3.3) and trifunctional (Figure 3.4) PIB phenol

(meth)acrylates indicated no coupling and no degradation or depolymerization during

esterification of the phenol moiety with (meth)acryloyl chloride.

MALDI-TOF MS provided a second method to determine molecular weight,

polydispersity, and end-functionality. The MALDI-TOF mass spectra of difunctional

PIB diphenol diacrylate and PIB diphenol dimethacrylate, which are representative, are

shown in Figure 3.5A and 3.5B, respectively. Each sample displayed a single, major

distribution of polymeric species, associated with Ag cations from the AgTFA

cationizing agent, differing from each other only by the number of isobutylene repeat

units. Mass spectra of the other PIB (meth)acrylates are given in Supporting Information:

4K PIB triphenol tri(meth)acrylates (Figure 3.6), 10K PIB triphenol tri(meth)acrylates

(Figure 3.7), and 10K aliphatic PIB triol triacrylate (Figure 3.8). The data from each

mass spectrum were analyzed by linear regression of a plot of mass-to-charge ratio (M/z,

assumed to be 1), measured at the maximum of each peak of the major distribution,

versus degree of polymerization (DP). The slope of this plot is theoretically equivalent to

the exact mass of the isobutylene repeat unit, 56.06 Da. The y-intercept is theoretically

equivalent to $f \times EG+I+C$, where f is the functionality of the polymer (2 or 3), EG is the

exact mass of the phenol (meth)acrylate end group, I is the exact mass of the bDCC

initiator residue, and C is the exact mass (106.91 Da) of the major isotope of the

associated Ag cation.

MALDI-TOF MS data for all of the PIB phenol (meth)acrylates and the 10K

aliphatic PIB triol triacrylate, analyzed in this manner, are summarized in Table 3.3. In

all cases, the measured value of the repeat unit molecular weight (M_{ru}) was within 0.2%

of the theoretical value (56.06 Da), and the measured value of $f \times EG+I+C$ was within

0.9% of the theoretical value. The observed close agreement between measured and

theoretical values provides strong evidence that the synthesized PIB (meth)acrylate

macromers possess the expected structure and end-group functionality. Table 3.3 also

lists M_n and PDI obtained from MALDI-TOF MS. In all cases, but especially for the

10K macromers, these values are lower than the corresponding values obtained from

GPC analysis (Table 3.2). This is a common observation and reflects the fact that

polymer chains with higher molecular weight are more difficult to desorb/ionize and thus

are under-represented at the detector.

Synthesis of 10K aliphatic PIB triol triacrylate. Quantitative ($\geq$ 98% end group

functionality) 10K aliphatic PIB triol triacrylate was obtained using our previously

published procedure,[17] shown in Scheme 3.1(b). The GPC trace and ^{1}H NMR spectrum

of this material are shown in Figure 3.2 and 3.9, respectively; from GPC analysis, it

possessed M_n = 9,900 g/mol and PDI = 1.09, as listed in Table 3.2. The MALDI-TOF

mass spectrum of 10K aliphatic PIB triol triacrylate is shown in Figure 3.8, and the M_n and PDI calculated from MALDI-TOF MS are shown in Table 3.3.

Photopolymerization kinetics of PIB macromers. RT-FTIR enabled facile and accurate measurement of the relatively rapid photopolymerization kinetics of PIB di/triphenol di/tri(meth)acrylates and aliphatic PIB triol triacrylate. Macromers were photopolymerized neat, except for the presence of photoinitiator; no reactive diluents or solvents were used. Inhibition of the photopolymerization reactions by O_2 was suppressed by degassing the sample in a vacuum oven for 30 min at room temperature and tightly sandwiching a small amount of reaction mixture between two NaCl plates and continuously purging the sample chamber with N_2.[44] 4K PIB triphenol tri(meth)acrylates (Entries 3 and 4, Table 3.2) were photopolymerized using various free radical photoinitiators, including Irgacure® 819 and 651, and Darocur® 1173. 3K PIB diphenol di(meth)acrylates, 10K PIB triphenol tri(meth)acrylates, and aliphatic PIB triol triacrylate (Entries 1-2, 5-6, and 7 Table 3.2) were photopolymerized using 1 wt% of Darocur® 1173. The conditions for photopolymerizations are listed in Table 3.4.

Effect of the photoinitiator. The suitability of a given photoinitiator and its effect on the rate of photopolymerization is dependent on its solubility/dispersibility in the monomers/polymers and its activation wavelength. The liquid photoinitiator, Darocur 1173, was observed to form a homogeneous mixture with PIB macromers; whereas the solid photoinitiators, Irgacure 651 and 819, were only partially soluble as evidenced by small portions of fine granules evenly dispersed in the bulk polymers. Figure 3.10 shows photopolymerization conversion vs. time for the 4K PIB triphenol triacrylate and trimethacrylate macromers using three different photoinitiators under the same curing

conditions (0.06 meq active radical[46]/g PIB macromer; 12 mW cm^{-2} filtered UV light, 320-500 nm.) The highest rate of photopolymerization and final double bond conversion were obtained for either macromer when Darocur 1173 was used as photoinitiator. For the methacrylate, the double bond conversion reached almost 75% in 300 s; while for the acrylate, the double bond conversion reached approximately 95% after 150 s. For a given macromer (methacrylate or acrylate), the two solid photoinitiators, Irgacure 651 and 819, produced almost identical rates of photopolymerization and final double bond conversions, and these values were lower than those produced by the liquid photoinitiator Darocur 1173. For the methacrylate, the final conversion using a solid photoinitiator was < 75%; while for the acrylate, it reached nearly 90%. Therefore, Darocur 1173 was deemed to be the most efficient photoinitiator among the three for UV curing of 4K PIB triphenol triacrylate and trimethacrylate macromers. The good solubility of Darocur 1173 (a liquid at RT) in the PIB macromers, which is facilitated by liquid-liquid diffusion, might be responsible for its high curing efficiency.

As observed in Figure 3.10, the higher rate of photopolymerization and higher final conversion of the acrylate compared to methacrylate macromer, for all three photoinitiators, is consistent with the well-known higher reactivity of acrylates relative to methacrylates in radical polymerization.[8,47-48] Higher reactivity of acrylates has been attributed to the more stable tertiary radical formed from methacrylate, as well as the rate retarding steric effect of the methyl group. In addition, acrylate monomers are reported to be less oxygen inhibited than methacrylate monomers and tend to terminate by combination of radicals, whereas methacrylates tend toward disproportionation;[49] both of these considerations cause acrylates to be more favored in photopolymerization.

Effect of photoinitiator concentration. Once Darocur 1173 photoinitiator was established to produce the fastest curing rate and highest curing efficiency, the kinetics of the photopolymerization of 4K PIB triphenol triacrylate and trimethacrylate macromers were studied with respect to photoinitiator concentration (1, 2, or 3 wt% of Darocur 1173) as shown in Figure 3.11. When the concentration of photoinitiator was increased from 1 to 2 wt%, a large increase in the rate of photopolymerization occurred, as evidenced by the initial slope of the conversion vs. time curves in Figure 3.11. However, the rate of polymerization increased only marginally as the photoinitiator concentration increased from 2 to 3 wt%. Similar observations were reported by Faust *et al.*[8] for aliphatic PIB triol (M)A. The rapid photolysis of an initiator creates a high concentration of active free radicals, which is essential for a high rate of photopolymerization (from 1 to 2 wt %), but may lead to premature termination of the photopolymerization due to competitive radical-radical coupling reactions (from 2 to 3 wt %). It can be concluded that a moderate concentration of photoinitiator does help increase the rate of photopolymerization and curing efficiency, but a higher concentration of photoinitiator doesn't guarantee a faster curing profile or may introduce defects into the networks due to high initiator residues

Effect of UV light intensity. One of the unique advantages of photopolymerizations is precise temporal control of the initiation step, by specifying both the onset and duration of light, as well as rate control, by specifying light intensity. If desired, the initiation rate can even be varied over the course of photopolymerization through adjustments in light intensity. The kinetics of the photopolymerization of 4K PIB triphenol triacrylate and trimethacrylate macromers were studied with respect to UV

light intensity (12.0, 19.5, or 29.8 mW cm^{-2}) as shown in Figure 3.12. For both

macromers, an increase in UV light intensity led not only to faster polymerization but

also to a higher curing conversion. The final conversion of the acrylate went up from

95% to almost 99%, and the final conversion of the methacrylate went up from 75% to

almost 88% when the UV light intensity increased from 12 to 29.8 mW cm^{-2}. Decker[50]

ascribed the high rate of photopolymerization and high curing efficiency originating from

high UV light intensity to two factors: (i) higher sample temperature, which results in

high polymer chain mobility and leads to high final conversion, and (ii) longer time lag

between conversion and shrinkage, which creates excess free volume and thus increases

polymer chain mobility as well.

Effect of acrylate type. The rate of radical propagation depends on the reactivity

of the monomer and the growing radical, as well as other structural factors, such as steric

effects, polarity, and resonance. With regard to steric effects, a bulky substituent on the

monomer will typically result in a lower rate of polymerization. The kinetics of

photopolymerization of three types of 10K PIB macromers, PIB triphenol triacrylate, PIB

triphenol trimethacrylate, and aliphatic PIB triol triacrylate (Entries 17-19, Table 3.4)

were studied (12 mW cm^{-2}, 1 wt% Darocur 1173) as shown in Figure 3.13. The observed

polymerization rates were very high, and under the same conditions, were significantly

higher than the rates observed with the 4K macromers, even though the double bond

concentrations in the latter were higher (See Figure 3.14, comparing Entries 5, 12, 17,

and 18 of Table 3.4.) Furthermore, the data also reveal that end group structure (acrylate

vs. methacrylate, aromatic vs. aliphatic) had no effect on polymerization rate; although it

did have a modest effect on final double bond conversion. The aliphatic PIB triol

85

triacrylate, the least bulky structure of the three, achieved the highest conversion (97%), followed by the PIB triphenol triacrylate at 95%. The most bulky structure of the three, PIB triphenol trimethacrylate, achieved the lowest conversion (93%). These results suggest that polymerization rate during the initial and intermediate stages of reaction was high and independent of end-group structure because it was largely controlled by the diffusional mobility of the reaction environment. The 10K PIB macromers are very viscous, even at the beginning of polymerization, and therefore diffusional mobility is reduced relative to the 4K macromers; the polymerizing end group also tends to be more sterically buried within the larger polymer coil. These effects result in a decreased rate of bimolecular radical termination, which induces autoacceleration.[51] Only at the later stages of the polymerization, when the final reaction conversion was approached, did the rate begin to be affected by the monomer structure, with deceleration first occurring with the bulky PIB triphenol trimethacrylate.

Effect of acrylate functionality. In general, the rate of photopolymerization should be directly proportional to the concentration of (meth)acrylate moieties. Thus, one would expect that if the concentration of polymerizable acrylate double bonds is the same, the rate of photopolymerization will be approximately the same regardless of the acrylate functionality of the polymer molecules. However, as shown in Figure 3.15 (Entries 1, 2, 5, and 12, Table 3.4), it was observed that the photopolymerization rates of 4K PIB triphenol tri(meth)acrylates are significantly faster than those of 3K PIB diphenol di(meth)acrylates, even though the acrylate double bond concentration was approximately the same for all four runs. Higher acrylate conversion was achieved for 4K PIB triphenol tri(meth)acrylates as well. These effects are attributed to the higher

86

viscosity of 4K PIB triphenol tri(meth)acrylate macromers, which decreases the

diffusional mobility as discussed in the above section.

Properties of UV-cured PIB networks. *(Meth)Acrylate functional group*

conversion. Two methods, ATR-IR and solvent extraction, were used to characterize the

final conversion of the seven different PIB macromers (Entries 1-7, Table 3.2) after UV

curing. The ATR-IR spectra of 4K PIB triphenol trimethacrylate were chosen as a

typical example, before and after UV curing, are shown in Figure 3.16. Similarly to the

kinetics study, C=C double bond stretching absorbances at 1638 and 1615 cm^{-1} were used

to determine the final conversion of cured networks, as listed in Table 3.5. For all

samples studied, $\leq$ 2.5% of (meth)acrylate functional groups remained unreacted after

curing, and the analysis revealed that the upper and lower surfaces of the films were

approximately the same, indicating uniformly high reaction conversion and thorough

crosslinking through the full depth of the film. Likewise, the results of extraction

experiments of UV-cured PIB networks in dry THF showed that the extractables were

less than 5% (see Table 3.5), which also demonstrated high degree of crosslinking for all

macromers.

Glass transition temperature and crosslink density. Cured films from all seven

PIB macromers were characterized by dynamic mechanical analysis (DMA); plots for

storage modulus and tan delta (δ) versus temperature are shown in Figures 3.17A and

3.17B, respectively. The storage modulus vs. temperature curves in Figure 3.17A are

typical of an amorphous crosslinked network; all seven samples display a high, glassy

modulus at low temperature, followed by a precipitous drop in modulus and

establishment of a rubbery plateau region as temperature increases. The temperature of

87

onset of the drop of storage modulus is one method of determining T_g. For the series of

UV-cured PIB networks in this study, the onset of the storage modulus drop occurred in

the range -67 to -65 °C for the networks produced from the 10K PIB triphenol

tri(meth)acrylate macromers, at about -63 °C for those from the 4K PIB triphenol

tri(meth)acrylate macromers, and at about -65 °C for those from the 3K PIB diphenol

di(meth)acrylate macromers (Table 3.5.) Peak of the tan δ vs. temperature curve is the

more commonly reported value for the T_g, but this method is not easily applied to PIB

because of the presence of an intense sub-Rouse relaxation,[52-54] characteristic of PIB,

which is clearly visible between -40 and -20 °C in Figure 3.17B. While Rouse segmental

motions occur at longer time scales compared to local segmental motion associated with

the glass transition, the sub-Rouse relaxation involves segmental motion with larger

length scales but involving less repeat units than the shortest of the Gaussian

submolecules as defined by the Rouse model. Plazek *et al.*[54] identified the two separate

transitions and attributed the relaxation process at a shorter time scale to local segmental

motion, i.e., the glass transition, while the longer-time-scale relaxation was attributed to

the sub-Rouse mode. Here, we have reported the approximate temperature of the shorter

time-scale process, indicated by the position of the low-temperature shoulder of the

complex tan δ vs. temperature peak as another measure of the T_g of the cured networks

(Table 3.5.)

        For crosslinked PIB networks made from the same macromer, T_g should be

proportional to crosslink density. Crosslink density, typically defined as the reciprocal of

the average molecular weight between crosslinks (M_c), is a very important structural

parameter that governs the properties of cured thermosets. Crosslink density is controlled

by a number of factors including network topology, reaction conversion, and M_n of the monomer/macromer. In this study, the networks are simple, one component systems consisting of di/trifunctional PIB macromers; thus crosslink density is affected primarily by (M)A double bond conversion and M_n of the starting macromer.

Several methods can be used to determine the crosslink density of highly crosslinked thermosets. Swelling measurements can give absolute values of crosslink density; however, this method requires accurate values of the Flory-Huggins polymer-solvent interaction parameter, which limits its application scope. A frequently employed alternative method is to calculate M_c from the value of the rubbery plateau modulus.[55] According to the theory of rubber elasticity, crosslink density is directly proportional to the equilibrium elastic modulus as given by eq 1

$$\rho = E'/3RT \tag{3.1}$$

where, ρ is the crosslink density expressed in moles of elastically effective network chains per cubic centimeter, E' is the storage modulus of the cured network at a temperature well above T_g, R is the gas constant, and T is the absolute temperature at which the experimental modulus is determined. The same relationship may be expressed in terms of the number average molecular weight between crosslinks (M_c), as shown in eq 2,

$$M_c = 3\rho_{PIB}RT/E' \tag{3.2}$$

where, ρ_{PIB} is the density of amorphous PIB, approximately 1 g/cm^3. The values of the rubbery storage modulus, crosslink density, and M_c are tabulated in Table 3.5. All of the PIB networks displayed well-defined transition and rubbery plateau regions.

Within the rubbery plateau region, the storage modulus E′ only changed slightly with temperature.

As shown in Table 3.5, for both PIB triphenol triacrylate and PIB triphenol trimethacrylate networks, the crosslink density decreased as M_n of the macromer increased, as expected. For PIB networks produced from the 10K aliphatic PIB triol triacrylate macromer, the crosslink density and the molecular weight between crosslinks are close to those of the networks made from the 10K PIB triphenol tri(meth)acrylate macromers. The crosslink densities of networks produced from 4K PIB triphenol tri(meth)acrylate macromers was higher than those produced from 3K PIB diphenol di(meth)acrylate macromers, due to the presence of a covalent branch point in the 3-arm macromers. This resulted in a slightly higher T_g for the networks made from 4K PIB triphenol tri(meth)acrylate macromers compared to those made from 3K PIB diphenol di(meth)acrylate macromers.

Thermal Stability. The decomposition temperature of PIB networks was determined by TGA, as shown in Figure 3.18. All of the PIB networks, regardless of structure of the polymerizable moiety and functionality and molecular weight of the starting macromer, displayed approximately the same decomposition behavior, with the onset (5% mass loss) and mid-point (50% mass loss) temperatures averaging about 394 °C and 437 °C, respectively, as summarized in Table 3.5. Once the onset temperature was reached, the entire degradation process advanced rapidly and was completely finished over a narrow range of about 80 °C (at 10 °C/min). The majority component for these networks is the PIB backbone (>90 wt%); the (M)A moieties only make up a small portion (<10 wt%). Thus, network composition dictates that the degradation temperature

90

and rate of decomposition will be relatively unaffected by changes in end group moiety or M_n and functionality of the starting material.

TGA analyses of the starting PIB (meth)acrylates were also performed to compare with the corresponding cured PIB networks. The results showed that the rate of decomposition and decomposition temperature stayed nearly constant (a slight 5-10 °C increase) upon network formation, as shown in Figure 3.19 and Table 3.6. This demonstrated that the degradation profile of PIB macromers/networks is determined by the PIB backbone and relatively unaffected by the change in state (from viscous liquid to elastomeric solid.)

Tensile properties. For all PIB networks, stress-strain curves demonstrated characteristic weak elastomeric behavior, as shown in Figure 3.20, which displays a typical stress-strain curve for each PIB network. For PIB networks derived from PIB triphenol triacrylate and trimethacrylate, the Young's modulus decreased, and the strain at break increased, with an increase of M_n of the macromer, as listed in Table 3.7. For PIB networks made from 10K PIB triphenol triacrylate and trimethacrylate, strain at break was almost two times higher than the networks made from the corresponding 4K materials. As previously discussed, PIB networks composed of macromers with a higher M_n gave a lower T_g. Generally, for elastomeric materials with a similar composition, a network with a lower T_g demonstrates more rubbery behavior, i.e., higher elasticity (strain at break) and lower Young's modulus. Regardless of the structure of the end group, Young's modulus was very close for PIB networks produced from a precursor of approximately the same M_n.

The Young's Moduli of networks made from 3K PIB diphenol di(meth)acrylate macromers were close to those of networks made from 4K PIB diphenol di(meth)acrylate macromers; however, the strain at break and strength at break of the former networks were slightly lower. This effect is probably due to a lower degree of physical chain entanglements since 3K PIB diphenol di(meth)acrylates do not possess the covalent branch point that is present in the 4k triphenol tri(meth)acrylates.

Wilkes and coworkers have reported mechanical properties of PIB networks formed by ionic interactions of PIB-based telechelic ionomers of both broad[56] and narrow[52] molecular weight distribution. Strength-at-break, strain-at-break, and Young's modulus of ionomer networks produced from PIB ionomers of low PDI were similar to the present UV-cured networks, for trifunctional PIB precursors of similar M_n. However, mechanical properties of the PIB ionomers were greatly improved by increasing the PDI of the PIB ionomers, which implies that the properties of UV-cured PIB networks might also be improved by similarly increasing the PDI of PIB macromers.

3.5 Conclusions

We demonstrated that PIB diphenol and triphenol (meth)acrylate macromers can be quantitatively synthesized by reacting (meth)acryloyl chloride with phenol-terminated PIBs, which are obtained by end-quenching of living PIB with isopropoxybenzene, followed by deblocking of the bulky isopropyl moiety.

PIB phenol (meth)acrylate macromers undergo facile radical photopolymerization using a photoinitiator and the appropriate wavelength of UV/visible light. Darocur® 1173 produces the fastest rate of photopolymerization and highest extent of cure due to its good miscibility with PIB. The rate of photopolymerization can be easily tuned by

varying the concentration of photoinitiator or UV light intensity. For high molecular weight trifunctional PIB macromers, essentially identical rates of photopolymerization are observed regardless of the structure of the polymerizable moiety, and the observed rate is higher than those observed with the low molecular weight macromers, which is attributed to autoacceleration in viscous polymer systems.

Trifunctional PIB networks composed of macromers with lower M_n yielded higher crosslink density, or lower molecular weight between crosslinks, resulting in higher T_gs. For UV-cured PIB networks produced from macromers with approximately the same M_n, crosslink density and the molecular weight between crosslinks were very close, regardless of whether the polymerizable moiety was acrylate or methacrylate or whether derived from PIB phenol or PIB aliphatic alcohol. Tensile properties of the cured PIB networks were found to be characteristic of a crosslinked rubber. PIB networks derived from macromers with higher M_n gave lower Young's moduli, but higher stains at break and these properties were not influenced strongly by the structure of the (meth)acrylate moiety (aromatic vs. aliphatic) as long as the M_n of the starting PIBs were similar. In general, tensile strengths of the PIB network were low, due to the low starting M_n and lack of chain entanglements. However, we expect that the tensile properties of UV-cured PIB networks might be improved by using PIB macromers with higher PDI, which can be readily produced by various synthetic means, or by simple blending.

Photopolymerization of PIB phenol (meth)acrylates offers a convenient way to harness the excellent properties of PIB networks, such as good flexibility, strong adhesion and gas barrier properties, good thermal and oxidative stability, chemical and

93

solvent resistance, and biocompatibility. In addition to acrylate and methacrylate, the phenoxy quenching method described herein may also be used to introduce other useful functional groups, such as epoxide, azide, alkyne, etc., onto PIB chain ends, to enable the synthesis of crosslinked networks for advanced applications.

3.6 Acknowledgements

3.7 References

(1)   Bauer, F.; Decker, U.; Naumov, S.; Riedel, C., *Prog. Org. Coat.* **2014,** *77* (6), 1085-1094.

(2)   Caiger, N.; Herlihy, S., *IS&T Reporter* **2005,** *20* (4), 1-12.

(3)   Donovan, B. R.; Cobb, J. S.; Hoff, E. F. T.; Patton, D. L., *RSC Adv.* **2014,** *4* (106), 61927-61935.

(4)   Moszner, N.; Salz, U., *Prog. Polym. Sci.* **2001,** *26* (4), 535-576.

(5)   Ligon, S. C.; Husar, B.; Wutzel, H.; Holman, R.; Liska, R., *Chem. Rev.* **2014,** *114* (1), 557-589.

(6)   Oster, G.; Yang, N.-L., *Chem. Rev.* **1968,** *68* (2), 125-151.

(7)   Fuchs, Y.; Soppera, O.; Haupt, K., *Anal. Chim. Acta* **2012,** *717*, 7-20.

(8)   Tripathy, R.; Crivello, J. V.; Faust, R., *J. Polym. Sci., Part A: Polym. Chem.* **2013,** *51* (2), 305-317.

(9)   Puskas, J. E.; Foreman-Orlowski, E. A.; Lim, G. T.; Porosky, S. E.; Evancho-Chapman, M. M.; Schmidt, S. P.; El Fray, M.; Piątek, M.; Prowans, P.; Lovejoy, K., *Biomaterials* **2010,** *31* (9), 2477-2488.

(10)   Domján, A.; Erdödi, G.; Wilhelm, M.; Neidhöfer, M.; Landfester, K.; Iván, B.; Spiess, H. W., *Macromolecules* **2003,** *36* (24), 9107-9114.

(11)   Erdödi, G.; Iván, B., *Chem. Mater.* **2004,** *16* (6), 959-962.

(12)   Haraszti, M.; Tóth, E.; Iván, B., *Chem. Mater.* **2006,** *18* (20), 4952-4958.

(13)   Kali, G.; Vavra, S.; László, K.; Iván, B., *Macromolecules* **2013,** *46* (13), 5337-5344.

(14)   Erdodi, G.; Kennedy, J. P., *Prog. Polym. Sci.* **2006,** *31* (1), 1-18.

(15)   Puskas, J. E.; Chen, Y., *Biomacromolecules* **2004,** *5* (4), 1141-1154.

(16)   Puskas, J. E.; Chen, Y.; Dahman, Y.; Padavan, D., *J. Polym. Sci., Part A: Polym. Chem.* **2004,** *42* (13), 3091-3109.

(17)   Roche, C. P.; Brei, M. R.; Yang, B.; Storey, R. F., *ACS Macro Lett.* **2014,** *3* (12), 1230-1234.

(18)   Liao, T.-P.; Kennedy, J. P., *Polym. Bull.* **1981,** *6* (3), 135-141.

(19)   Kennedy, J. P.; Hiza, M., *J. Polym. Sci., Polym. Chem. Ed.* **1983,** *21* (4), 1033-1044.

(20)   Iván, B.; Almdal, K.; Mortensen, K.; Johannsen, I.; Kops, J., *Macromolecules* **2001,** *34* (6), 1579-1585.

(21)   Ummadisetty, S.; Kennedy, J. P., *J. Polym. Sci., Part A: Polym. Chem.* **2008,** *46* (12), 4236-4242.

(22)   Tripathy, R.; Ojha, U.; Faust, R., *Macromolecules* **2009,** *42* (12), 3958-3964.

(23)   Iván, B.; Kennedy, J. P.; Chang, V. S. C., *J. Polym. Sci., Polym. Chem. Ed.* **1980,** *18* (11), 3177-3191.

(24)   Iván, B.; Kennedy, J. P., *J. Polym. Sci., Part A: Polym. Chem.* **1990,** *28* (1), 89-104.

(25)   De, P.; Faust, R., *Macromolecules* **2006,** *39* (20), 6861-6870.

(26)   De, P.; Faust, R., *Macromolecules* **2006,** *39* (22), 7527-7533.

(27)   Ojha, U.; Rajkhowa, R.; Agnihotra, S. R.; Faust, R., *Macromolecules* **2008,** *41* (11), 3832-3841.

(28)   Martinez-Castro, N.; Morgan, D. L.; Storey, R. F., *Macromolecules* **2009,** *42* (14), 4963-4971.

(29) Morgan, D. L.; Storey, R. F., *Macromolecules* **2009,** *42* (18), 6844-6847.

(30) Morgan, D. L.; Martinez-Castro, N.; Storey, R. F., *Macromolecules* **2010,** *43* (21), 8724-8740.

(31) Yang, B.; Storey, R. F., *Polym. Chem.* **2015,** *6* (20), 3764-3774.

(32) Puskas, J. E.; Sen, M. Y., *Green Polymer Chemistry: Biocatalysis and Biomaterials*. American Chemical Society: 2010; Vol. 1043, p 417-424.

(33) Falk, B.; Vallinas, S. M.; Crivello, J. V., *J. Polym. Sci., Part A: Polym. Chem.* **2003,** *41* (4), 579-596.

(34) Eberhardt, M.; Mruk, R.; Zentel, R.; Théato, P., *Eur. Polym. J.* **2005,** *41* (7), 1569-1575.

(35) Malins, E. L.; Waterson, C.; Becer, C. R., *J. Polym. Sci., Part A: Polym. Chem.* **2016,** *54* (5), 634-643.

(36) Günther, W.; Maenz, K.; Stadermann, D., *Angew. Makromol. Chem.* **1996,** *234* (1), 71-90.

(37) Maenz, K.; Stadermann, D., *Angew. Makromol. Chem.* **1996,** *242* (1), 183-197.

(38) Kennedy, J. P.; Guhaniyogi, S. C.; Percec, V., *Polym. Bull.* **1982,** *8* (11), 563-570.

(39) Li, J.; Sung, S.; Tian, J.; Bergbreiter, D. E., *Tetrahedron* **2005,** *61* (51), 12081-12092.

(40) Storey, R. F.; Choate, K. R., *Macromolecules* **1997,** *30* (17), 4799-4806.

(41) Mishra, M. K.; Wang, B.; Kennedy, J. P., *Polym. Bull.* **1987,** *17* (4), 307-314.

(42) Storey, R. F.; Lee, Y., *J. Macromol. Sci., Part A* **1992,** *29* (11), 1017-1030.

(43) Storey, R. F.; Curry, C. L.; Brister, L. B., *Macromolecules* **1998,** *31* (4), 1058-1063.

(44)   Lee, T.; Cramer, N.; Hoyle, C.; Stansbury, J.; Bowman, C., *J. Polym. Sci., Part A: Polym. Chem.* **2009,** *47* (10), 2509-2517.

(45)   *ASTM D638-14, Standard Test Method for Tensile Properties of Plastics, ASTM International, West Conshohocken, PA* **2014**.

(46)   *Note: Active radical refers to the molar equivalents of polymerization active radicals supplied by the given initiator. It was assumed that Irgacure 651 supplies 1 eq active radical/mol initiator, Irgacure 819 supplies 2 eq active radical/mol initiator, and Daracur 1173 supplies 1 eq active radical/mol initiator.*

(47)   Odian, G., *Principles of Polymerization, 4th Edition*. John Wiley & Sons: Hoboken, New Jersey, USA, 2004; p 269-271.

(48)   Ehlers, F. B., J.; Vana, P, *Fundamentals of Controlled/Living Radical Polymerization*. The Royal Society of Chemistry: Cambridge, United Kingdom, 2013; p 11.

(49)   Wicks, Z. W., Jr.; Jones, F.N.; Pappas, S.P., *Organic Coatings Science and Technology, 2nd Edition*. Wiley Interscience New York, New York, USA, 1999; p 514.

(50)   Decker, C., *Polym. Int.* **1998,** *45* (2), 133-141.

(51)   White, T. J.; Liechty, W. B.; Guymon, C. A., *J. Polym. Sci., Part A: Polym. Chem.* **2007,** *45* (17), 4062-4073.

(52)   Loveday, D.; Wilkes, G. L.; Lee, Y.; Storey, R. F., *J. Appl. Polym. Sci.* **1997,** *63* (4), 507-519.

(53)   Kwee, T.; Taylor, S. J.; Mauritz, K. A.; Storey, R. F., *Polymer* **2005,** *46* (12), 4480-4491.

(54)   Rizos, A. K.; Ngai, K. L.; Plazek, D. J., *Polymer* **1997,** *38* (25), 6103-6107.

(55)   Reinitz, S. D.; Carlson, E. M.; Levine, R. A. C.; Franklin, K. J.; Van Citters, D.

        W., *Polym. Test.* **2015,** *45*, 174-178.

(56)   Bagrodia, S.; Tant, M. R.; Wilkes, G. L.; Kennedy, J. P., *Polymer* **1987,** *28* (13),

        2207-2226.

3.8 Tables and Figures for Chapter III

Table 3.1

PIB isopropoxybenzene- and phenol-terminated PIB precursors.

Entry	Sample	Funct.	M_n (g/mol)	PDI
1	3K PIB Diisopropoxybenzene	2	2,700	1.19
2	3K PIB Diphenol	2	2,700	1.19
3	4K PIB Triisopropoxybenzene	3	4,200	1.16
4	4K PIB Triphenol	3	4,300	1.15
5	10K PIB Triisopropoxybenzene	3	10,200	1.08
6	10K PIB Triphenol	3	10,000	1.10

Table 3.2

PIB phenol acrylate and methacrylate macromers.

Entry	Sample	Funct.	$M_{n,NMR}$ (g/mol)	$M_{n,GPC}$ (g/mol)	PDI
1	3K PIB diphenol diacrylate	2	2,840	2,900	1.24
2	3K PIB diphenol dimethacrylate	2	2,880	2,900	1.18
3	4K PIB triphenol triacrylate	3	4,210	4,300	1.18
4	4K PIB triphenol trimethacrylate	3	4,290	4,500	1.17
5	10K PIB triphenol triacrylate	3	10,200	10,100	1.11
6	10K PIB triphenol trimethacrylate	3	10,200	10,200	1.12
7	10K aliphatic PIB triol triacrylate	3	10,000	9,900	1.09

Table 3.3

MALDI-TOF MS Data of PIB di/triphenol di/tri(meth)acrylates and PIB aliphatic triol triacrylate[a]

Sample	MW$_{theo}$ $f \times$EG+I+C[b]	MW$_{exp}$ $f \times$EG+I+C	Diff.	M$_n$	PDI	M$_{ru}$[c]
3K PIB diphenol diA	617.18	620.94	3.76	1897	1.04	56.13
3K PIB diphenol diMA	645.21	651.00	5.79	1891	1.05	56.08
4K PIB triphenol triA	749.20	751.85	2.65	2196	1.05	56.11
4K PIB triphenol triMA	791.25	792.92	1.67	2108	1.04	56.16
10K PIB triphenol triA	749.20	743.99	5.21	4369	1.04	56.05
10K PIB triphenol triMA	791.25	794.09	2.84	4523	1.05	56.04
10K aliphatic PIB triol triA	965.37	957.04	8.33	4710	1.06	56.02

[a]Unit for molecular weight is Da; [b]f=chain end functionality, EG = end group, I = initiator, C = Ag cation; [c]ru is repeat unit

Table 3.4

Photopolymerization of PIB triphenol tri(meth)acrylate and aliphatic PIB triol triacrylate under various conditions.

Entry	Macromer	Photoinitiator		UV intensity[a]	Conv. (%)	Time (s)
		Type	(wt%)			
1	3K PIB diphenol diacrylate	Daro 1173	1	12	90	300
2	3K PIB diphenol dimethacrylate	Daro 1173	1	12	72	450
3		Irga 651	1.56	12	91	200
4		Irga 819	1.28	12	91	200
5		Daro 1173	1	12	95	150
6	4K PIB Triphenol Triacrylate	Daro 1173	1	19.5	96	100
7		Daro 1173	1	29.8	97	80
8		Daro 1173	2	12	96	80
9		Daro 1173	3	12	98	80
10		Irga 651	1.56	12	62	400
11		Irga 819	1.28	12	62	400
12		Daro 1173	1	12	75	350
13	4K PIB Triphenol Trimethacrylate	Daro 1173	1	19.5	87	250
14		Daro 1173	1	29.8	92	150
15		Daro 1173	2	12	84	400
16		Daro 1173	3	12	85	400
17	10K PIB Triphenol Triacrylate	Daro 1173	1	12	95	70
18	10K PIB Triphenol Trimethacrylate	Daro 1173	1	12	93	70
19	10K Aliphatic PIB Triol Triacrylate	Daro 1173	1	12	97	70

[a]mW cm^{-2}

Table 3.5

Dynamic viscoelastic properties, crosslink densities, and thermal stability of UV cured PIB networks.

	PIB Dihpenol Diacrylate	PIB Diphenol Dimethacrylate	PIB Triphenol Triacrylate		PIB Triphenol Trimethacrylate		Aliphatic PIB Triol Triacrylate
	3K	3K	4K	10K	4K	10K	10K
Unreacted[a] (M)A %	1.8	2.2	1.2	1.9	2.0	2.3	2.5
Extractable wt% (THF)	1.1	1.9	4.0	4.4	0.7	3.5	3.6
T_g (E′ drop), °C	-65.6	-64.1	-62.7	-66.6	-63.2	-67.3	-64.9
$T_g{}^{b}$ (tan δ shoulder), °C	-55.7	-54.2	-47.0	-53.5	-48.3	-56.2	-55.0
Tan δ peak value	1.21	1.14	1.16	1.41	1.12	1.40	1.34
E'^{c}, MPa	2.20	2.51	3.41	2.38	3.05	2.12	2.67
ρ, mmol/cm^3	0.302	0.343	0.471	0.344	0.426	0.310	0.383
M_c, g/mol	3,311	2915	2,123	2,907	2,350	3,221	2,610
Decompostion temp (start[d]), °C	388	391	400	397	393	396	395
Decompostion temp (mid point[e]), °C	430	441	445	434	441	432	437

[a]Determined by ATR-FTIR, [b]low temperature shoulder of the complex tan δ vs. temperature peak, [c]storage modulus at the rubbery plateau, [d]5% PIB network weight loss, [e]50% PIB network weight loss.

Table 3.6

Thermal stability of the starting PIB (meth)acrylate macromers.

Sample	Decomposition Temp (start[a]), °C	Decomposition Temp (mid point[b]), °C
3K PIB diphenol diacrylate	381	427
3K PIB diphenol dimethacrylate	385	424
4K PIB triphenol triacrylate	387	430
4K PIB triphenol trimethacrylate	383	429
10K PIB triphenol triacrylate	381	420
10K PIB triphenol trimethacrylate	381	418
10K aliphatic PIB triol triacrylate	380	418

[a]5% PIB starting macromer weight loss, [b]50% PIB starting macromer weight loss.

Table 3.7

Tensile properties of UV-cured PIB networks.

Cured PIB network	M_n (g/mol)	Young's Modulus (MPa)	Strain-at-break (%)	Strength-at-break (MPa)	E'[a] (MPa)
3K PIB diphenol diA	2,900	2.34	15.3	0.28	2.18
3K PIB diphenol diMA	2,900	2.22	20.6	0.38	2.50
4K PIB triphenol triA	4,300	2.24	21.6	0.40	3.18
4K PIB triphenol triMA	4,500	2.35	27.8	0.51	2.77
10K PIB triphenol triA	10,100	1.51	47.6	0.52	2.18
10K PIB triphenol triMA	10,200	1.40	56.0	0.58	1.75
10K aliphatic PIB triol triA	9,900	1.62	37.7	0.55	2.67

[a] Storage modulus obtained from DMA study.
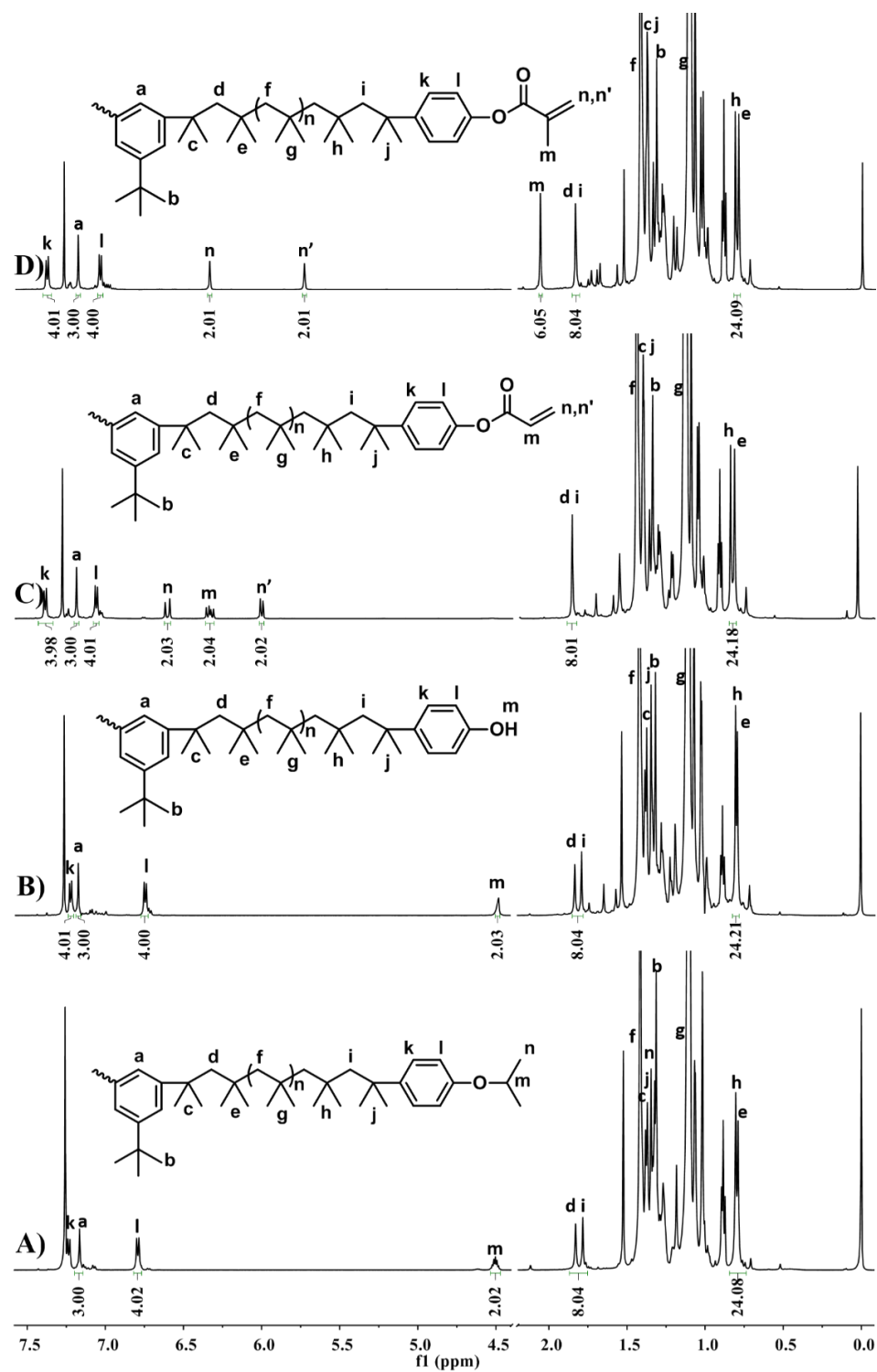
Figure 3.1 ^{1}H NMR (600 MHz, CDCl$_3$, 25 °C) spectra of difunctional PIBs with peak integrations.

(A) PIB diisopropoxybenzene; (B) PIB diphenol; (C) PIB diphenol diacrylate; (D) PIB diphenol dimethacrylate
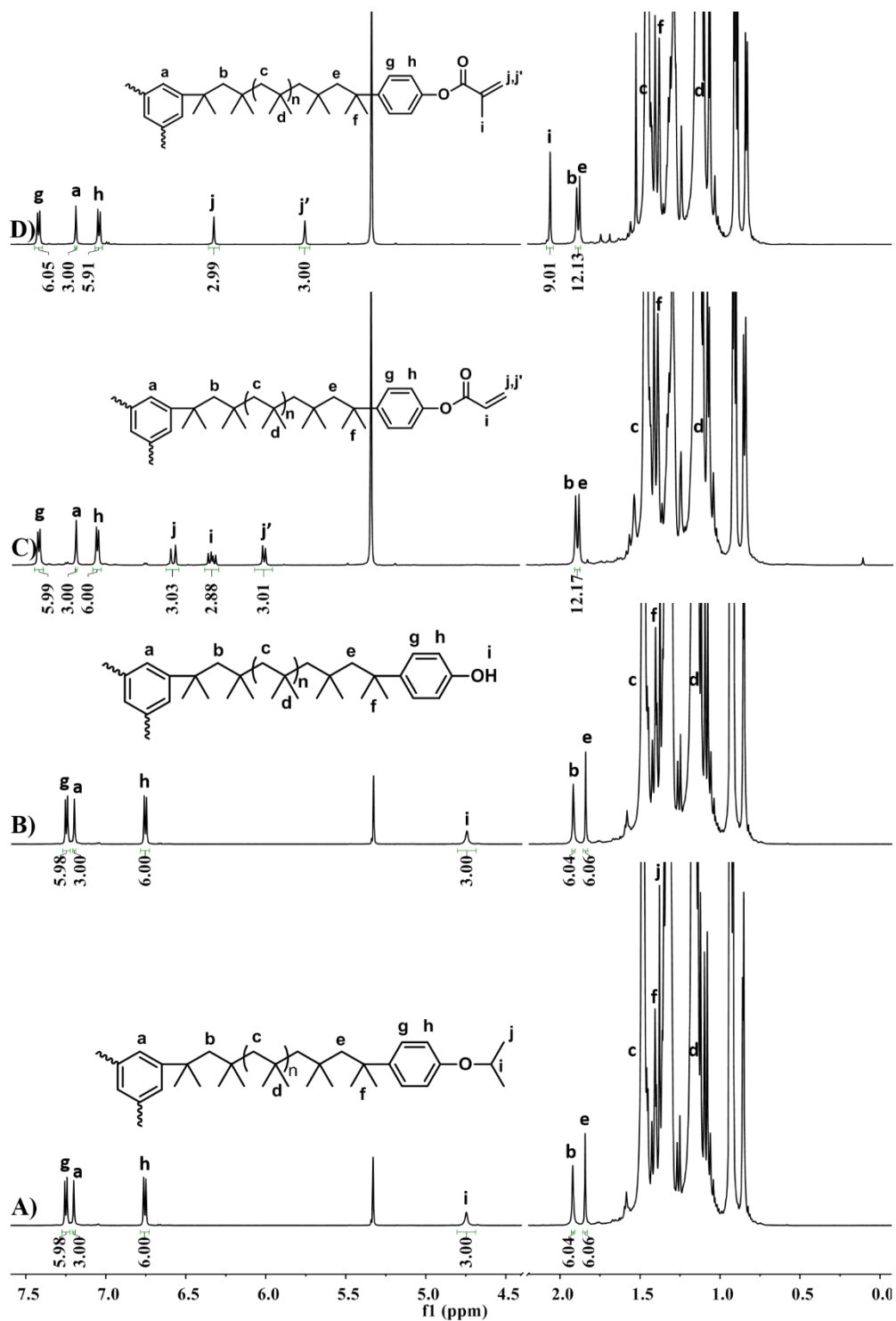
Figure 3.2 ^{1}H NMR (600 MHz, CD$_2$Cl$_2$, 23°C) spectra of 10K PIB triphenol triacrylate and trimethacrylate, and trifunctional PIB precursors, with peak integrations.

(A) PIB triisopropoxybenzene; (B) PIB triphenol; (C) PIB triphenol triacrylate; (D) PIB triphenol trimethacrylate.

106
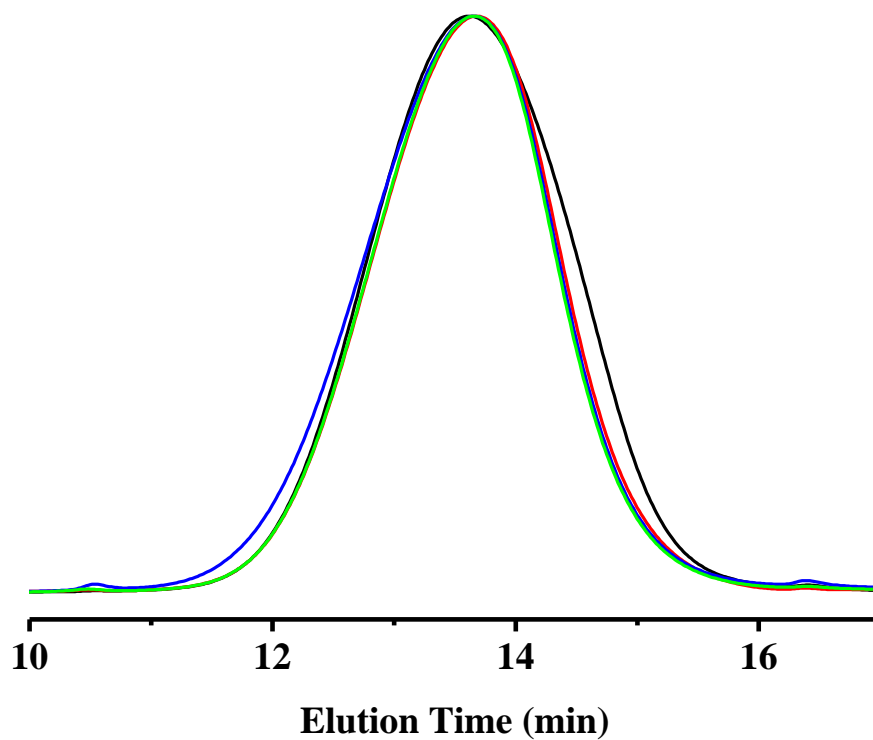
Figure 3.3 GPC traces of difunctional PIBs: PIB diisopropoxybenzene (black), PIB diphenol (red), PIB diphenol diacrylate (blue), and PIB diphenol dimethacrylate (green).
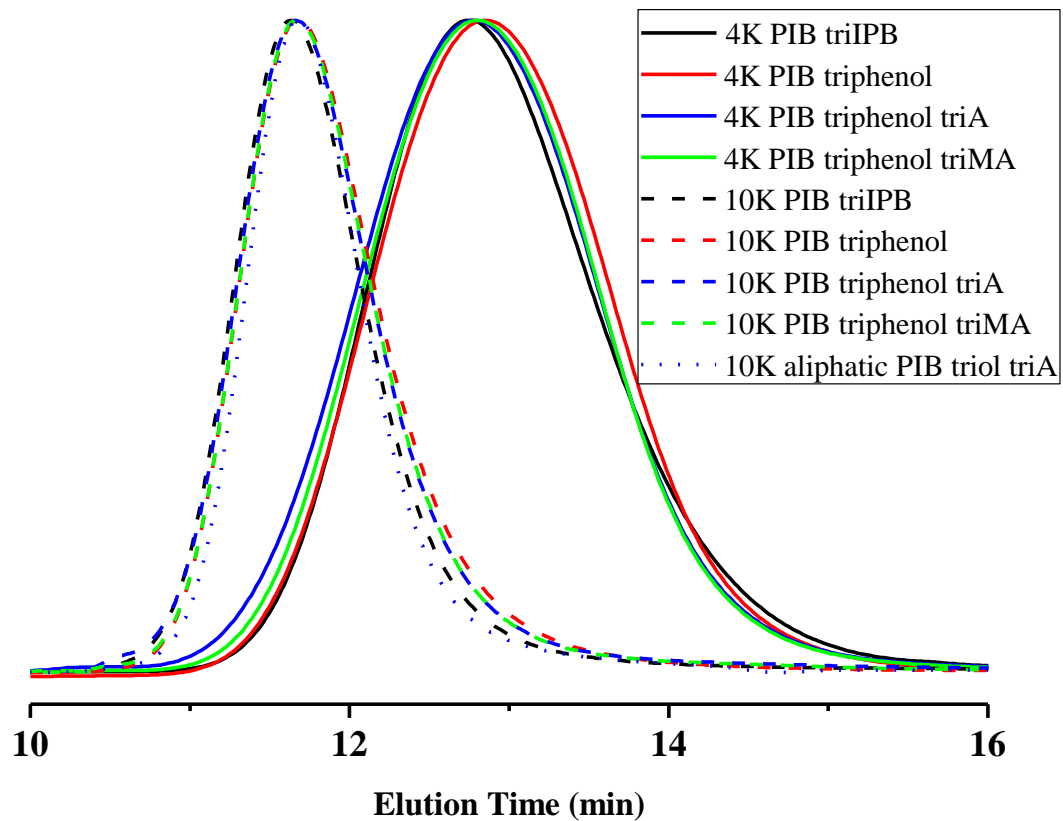
Figure 3.4 GPC traces of 4K and 10K trifunctional PIBs: PIB triisopropoxybenzene (black), PIB triphenol (red), PIB triphenol triacrylate (blue), PIB triphenol trimethacrylate (green), and aliphatic PIB triacrylate (dotted blue).
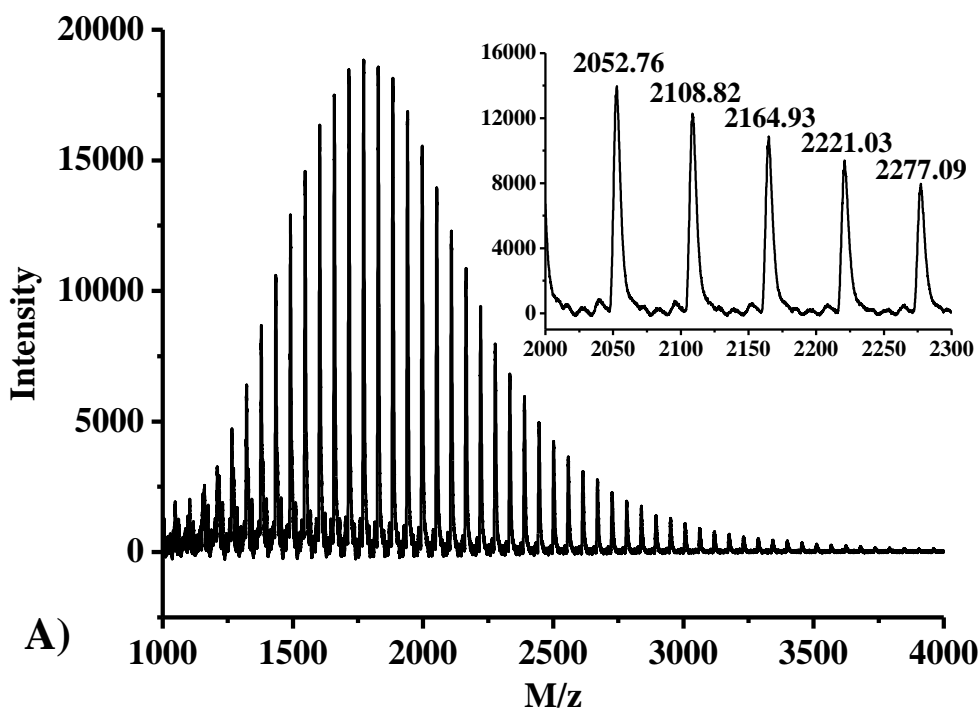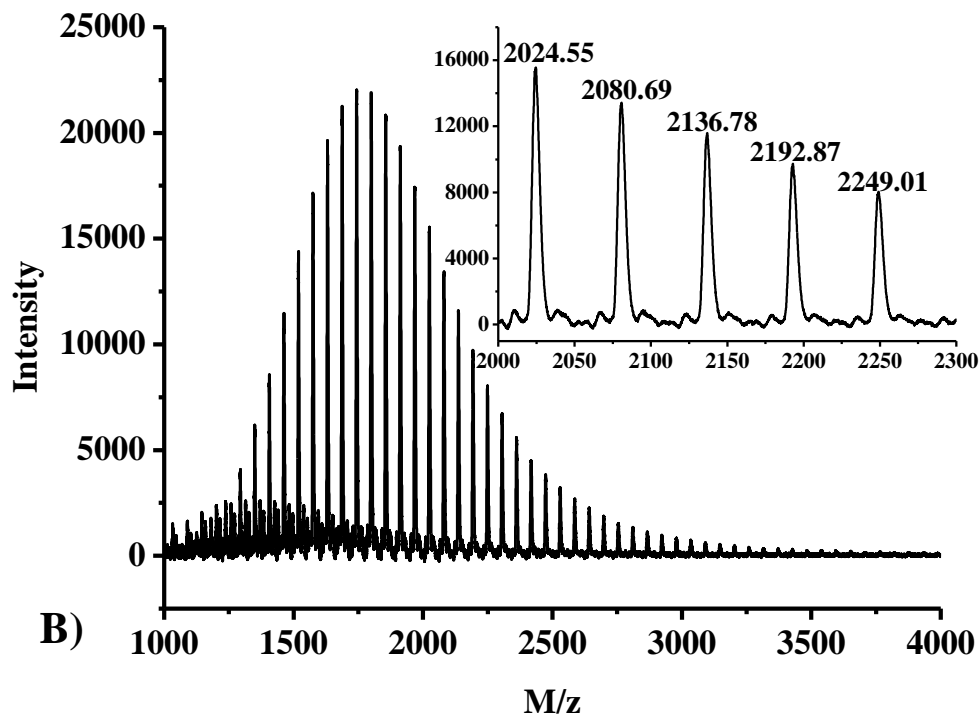
Figure 3.5 MALDI-TOF mass spectra of A) PIB diphenol diacrylate, and B) PIB diphenol dimethacrylate, prepared by the dried droplet method using DCTB as the matrix, AgTFA as the cationizing agent, and THF as the solvent.
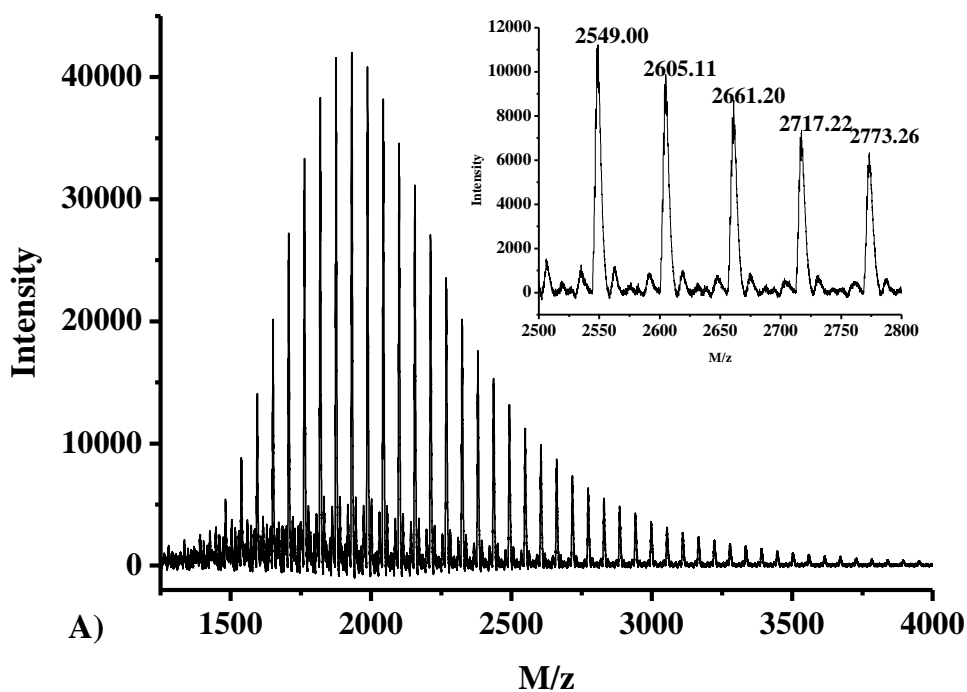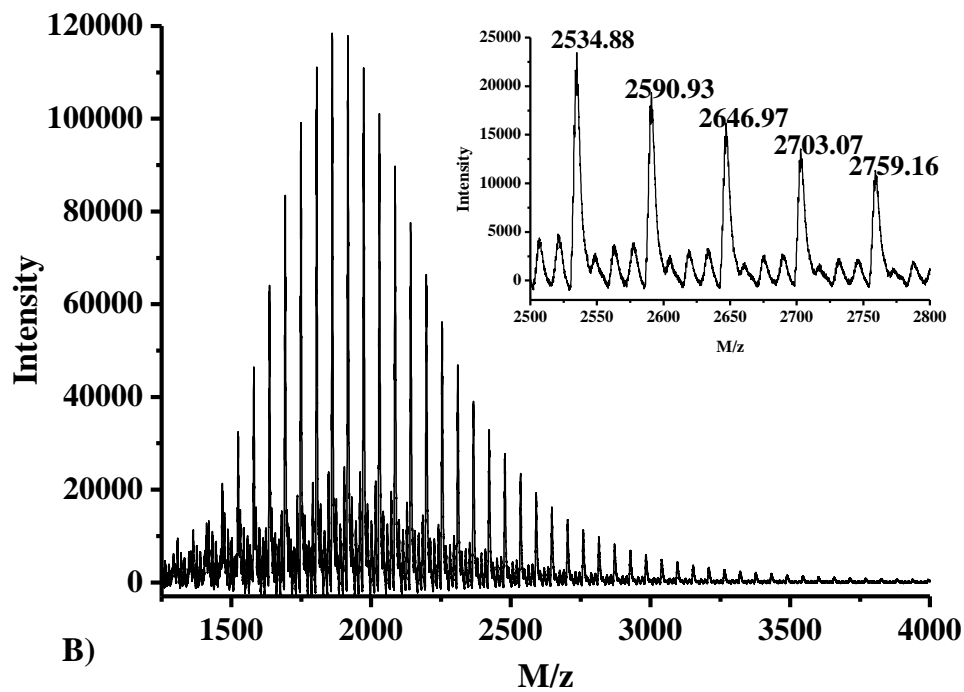
Figure 3.6 MALDI-TOF mass spectra of A) 4K PIB triphenol triacrylate, and B) PIB triphenol trimethacrylate.

Prepared by the dried droplet method using DCTB as the matrix, AgTFA as the cationizing agent, and THF as the solvent.
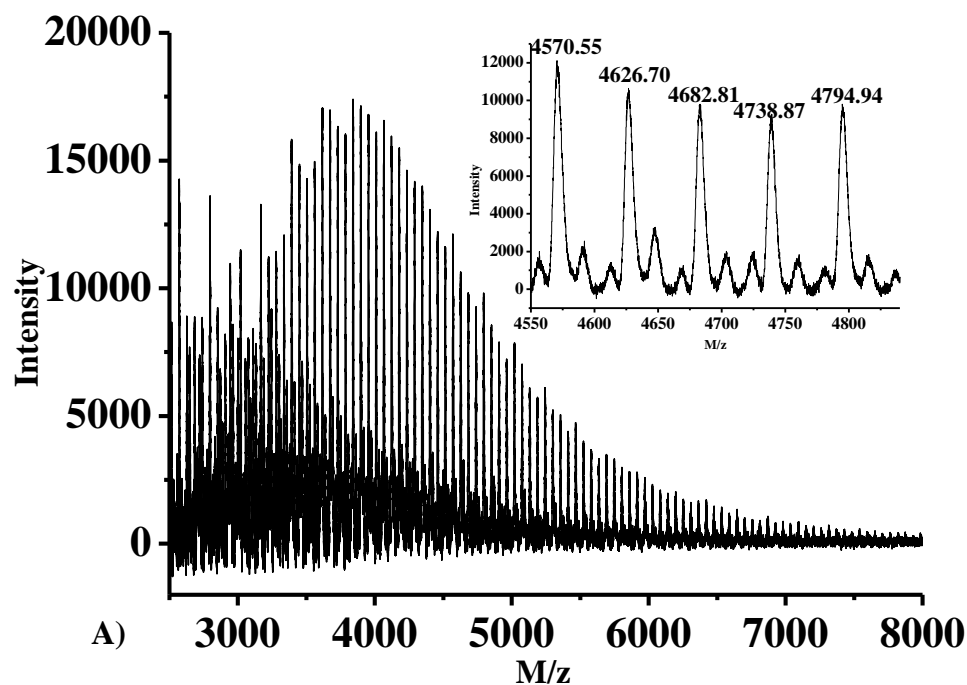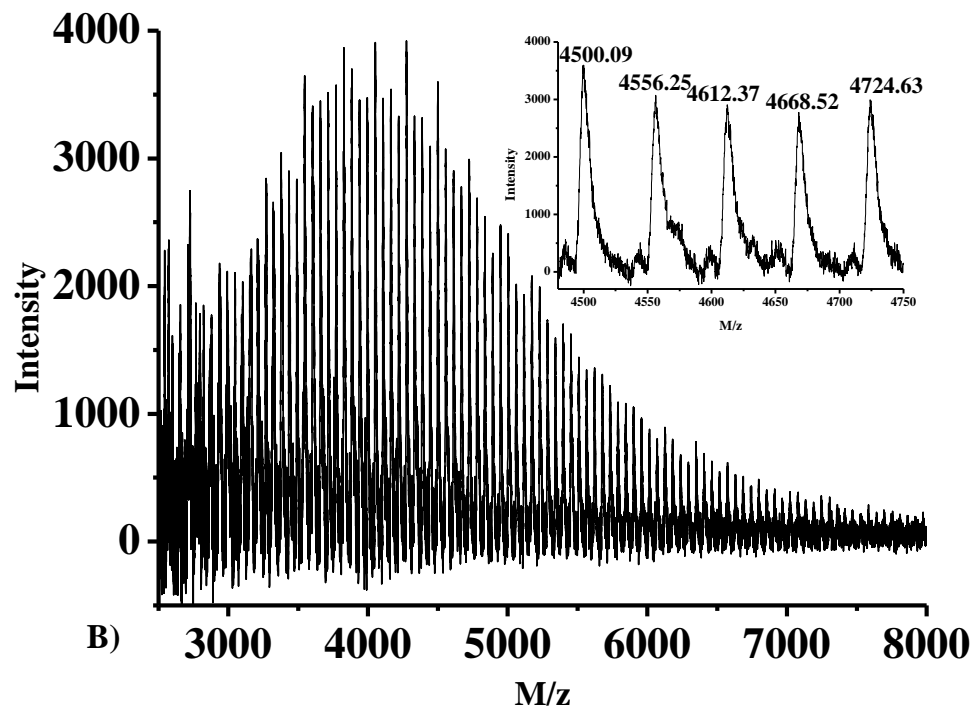
Figure 3.7 MALDI-TOF mass spectra of A) 10K PIB triphenol triacrylate, and B) 10K PIB triphenol trimethacrylate.

Prepared by the dried droplet method using DCTB as the matrix, AgTFA as the cationizing agent, and THF as the solvent.

111
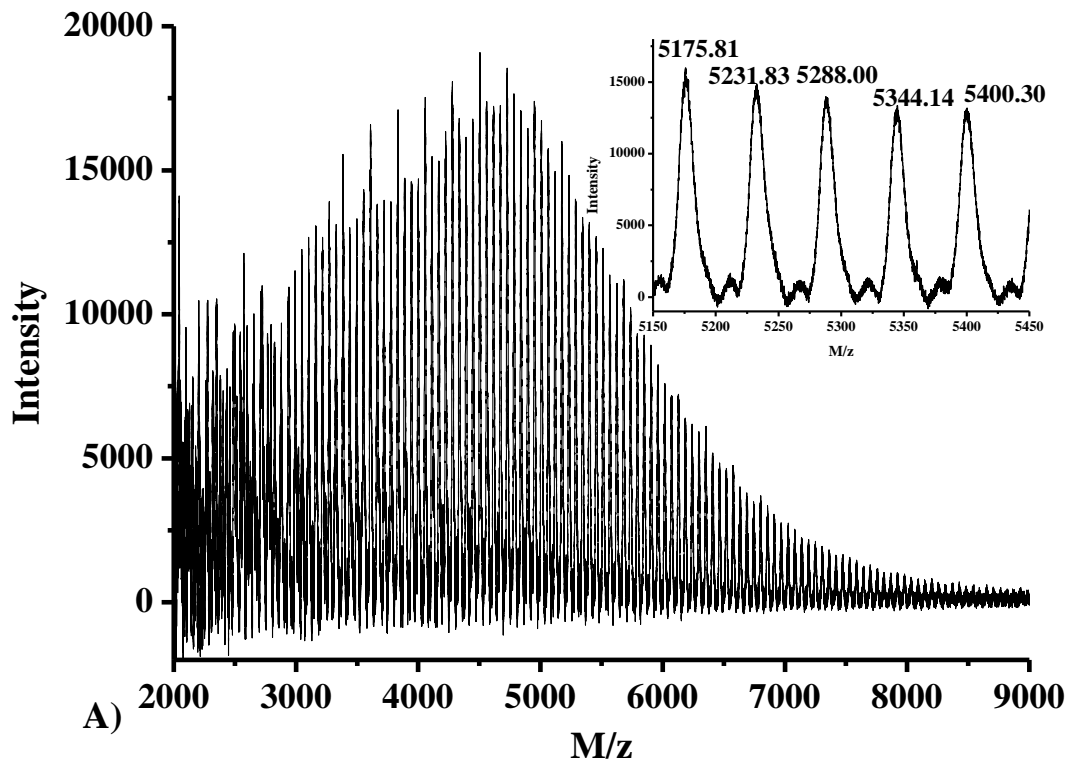
Figure 3.8 MALDI-TOF mass spectrum of 10K PIB aliphatic triol triacrylate.

prepared by the dried droplet method using DCTB as the matrix, AgTFA as the cationizing agent, and THF as the solvent.
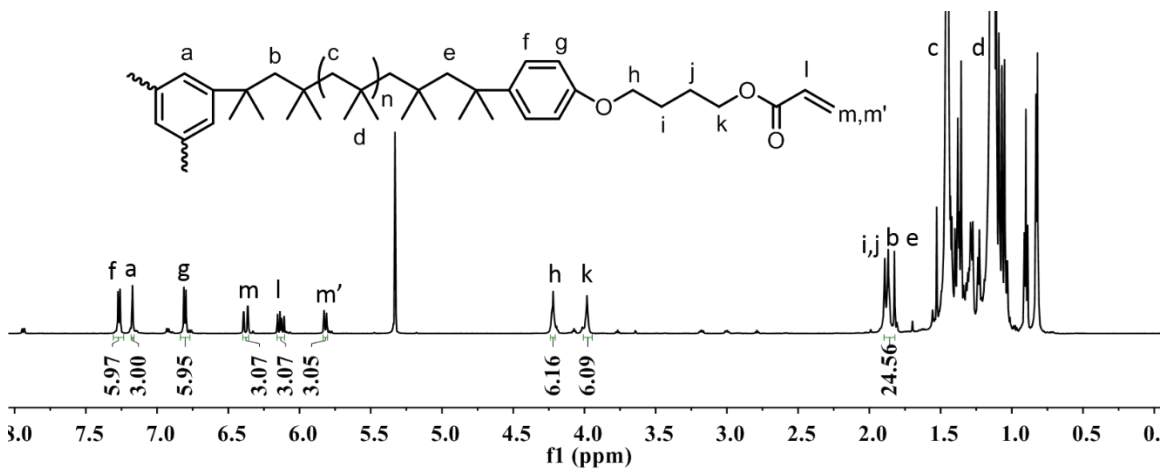
Figure 3.9 ^{1}H NMR (600 MHz, CD$_2$Cl$_2$, 23°C) spectrum of 10K aliphatic PIB triol triacrylate.

112
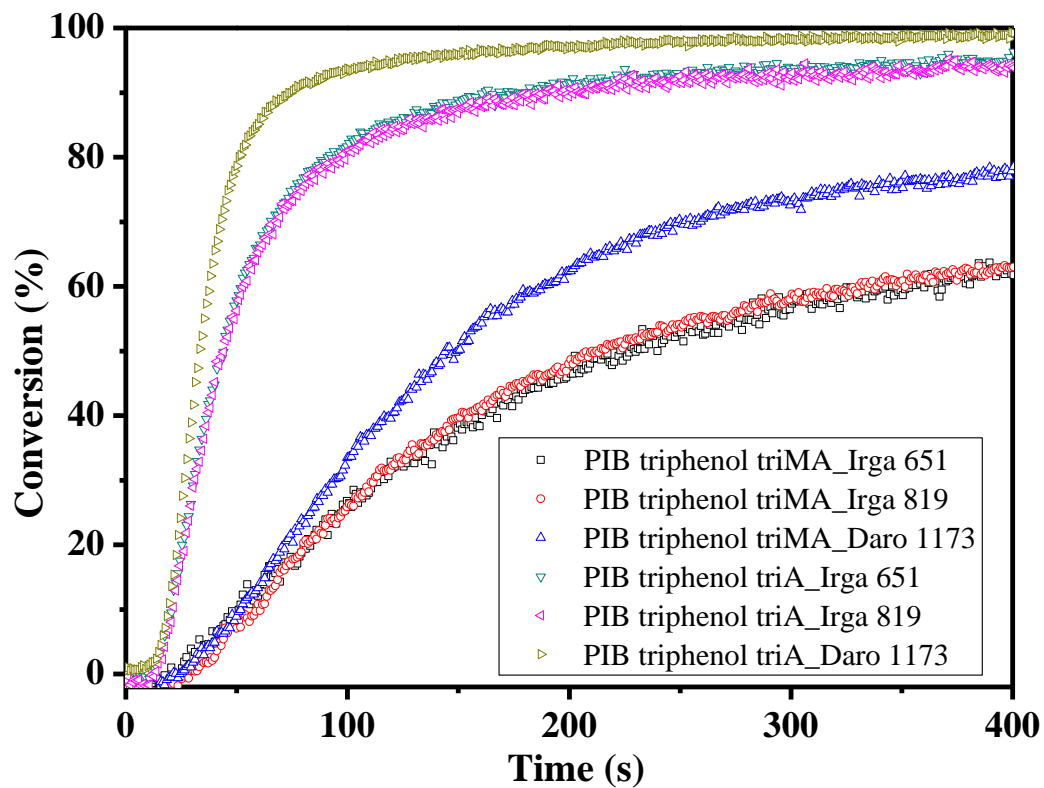
Figure 3.10 Conversion vs. time for bulk photopolymerization of 4K PIB triphenol triacrylate and trimethacrylate macromers.

Using different photoinitiators (0.06 meq active radical/g PIB macromer.) Samples were irradiated at 12 mW cm^{-2}.
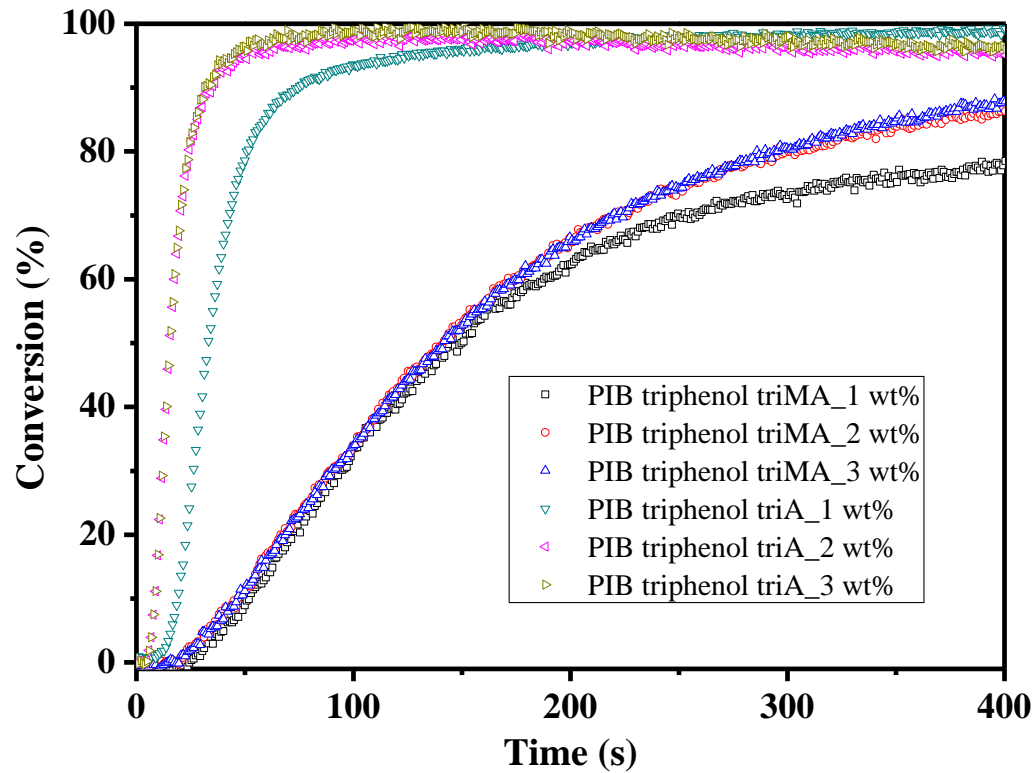
Figure 3.11 Conversion vs. time for bulk photopolymerization of 4K PIB triphenol triacrylate and trimethacrylate macromers.

Using different concentrations of Darocur® 1173 photoinitiator. Samples were irradiated at 12 mW cm^{-2}.
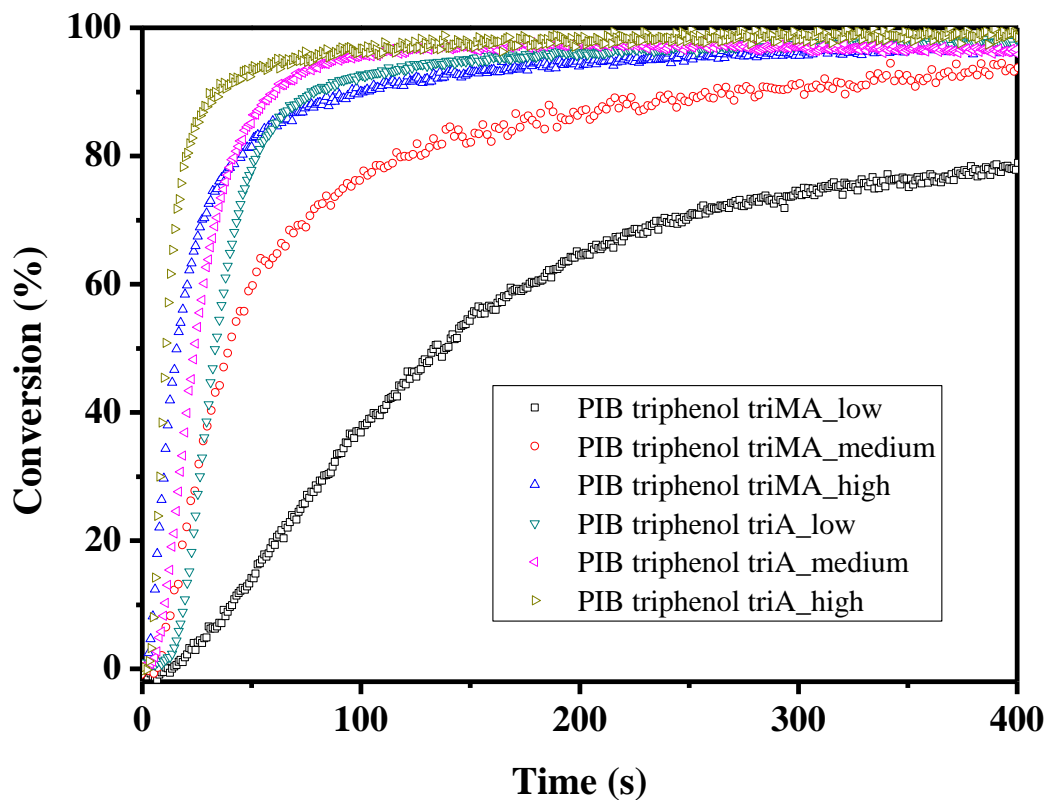
Figure 3.12 Conversion vs. time for bulk photopolymerization of 4K PIB triphenol triacrylate and trimethacrylate macromers.

Using different intensities of UV radiation (low, medium, and high radiations were 12, 19.5, and 29.8 mW cm^{-2}, respectively).

Samples contained 1 wt% Darocur® 1173 photoinitiator.
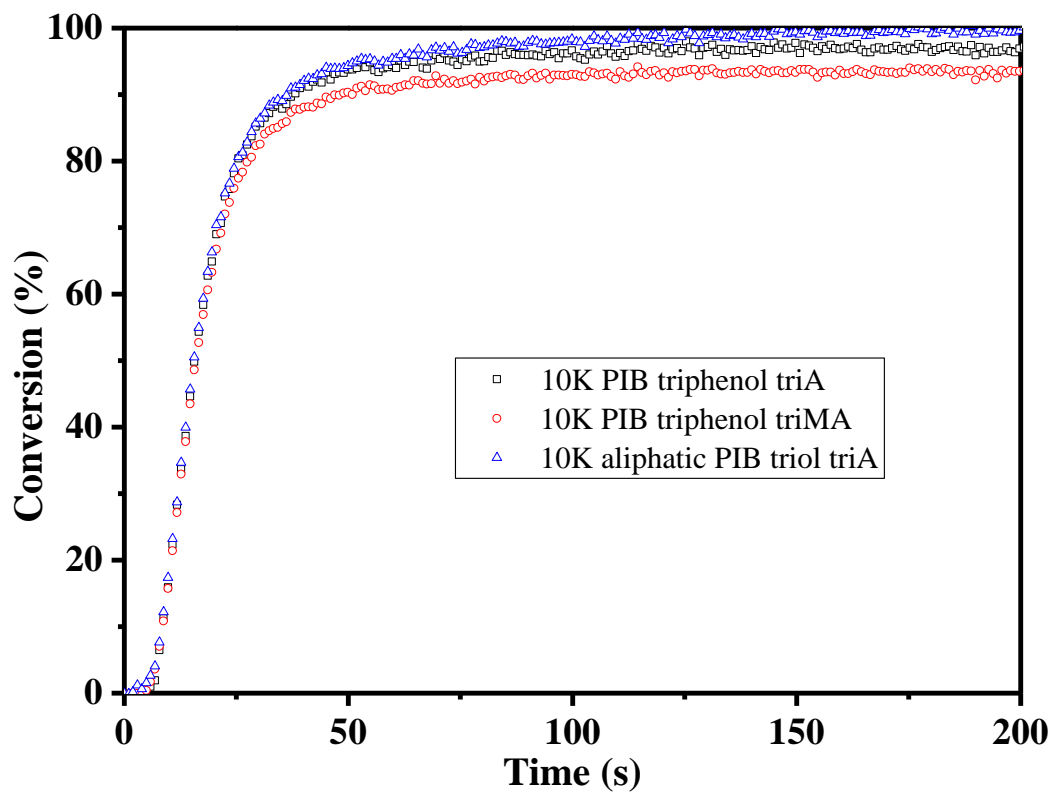
Figure 3.13 Conversion vs. time for bulk photopolymerization of 10K PIB triphenol triacrylate, 10K PIB triphenol trimethacrylate, and aliphatic PIB triol triacrylate.

Samples were irradiated at 12 mW cm^{-2} using 1 wt% of Darocur® 1173 photoinitiator.

116
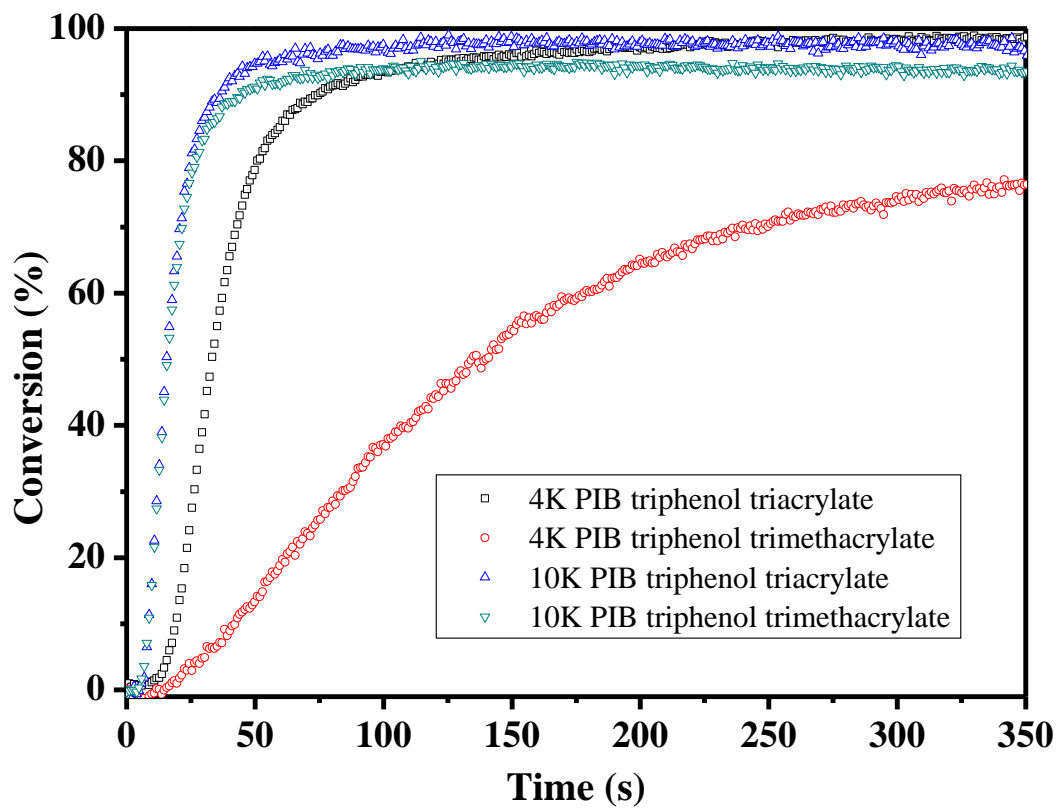
Figure 3.14 Conversion vs. time for bulk photopolymerization of 4K PIB triphenol tri(meth)acrylate and 10K PIB triphenol tri(meth)acrylate.

Samples were irradiated at 12 mW cm^{-2} using 1 wt% of Darocur® 1173 photoinitiator.
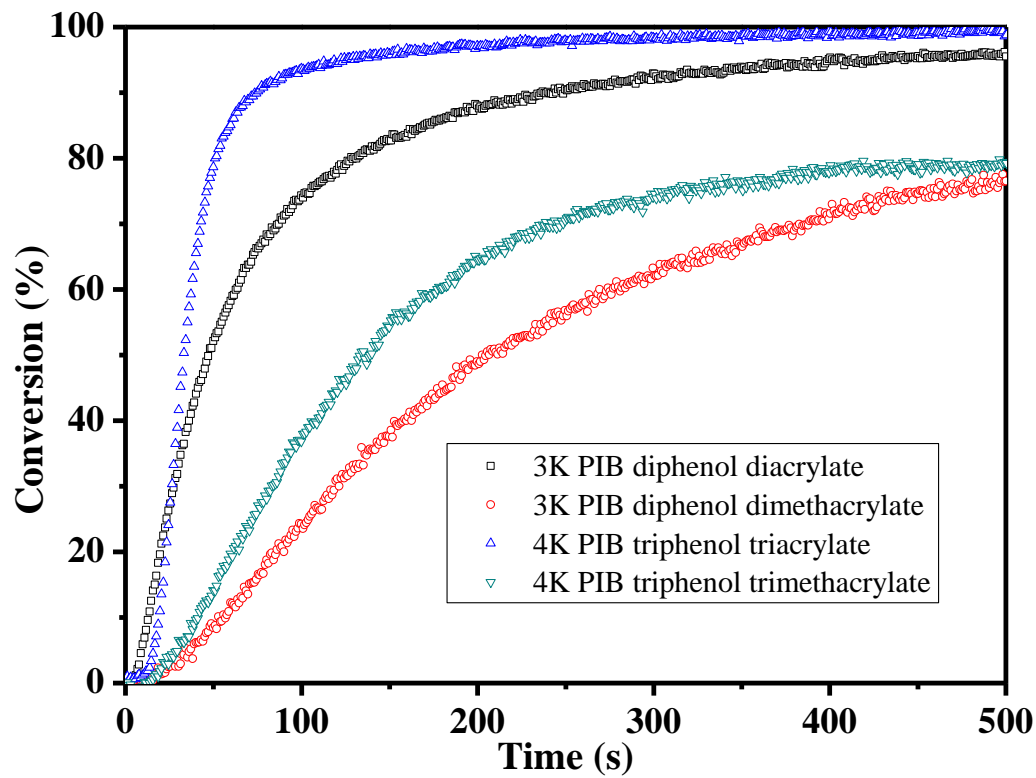
Figure 3.15 Conversion vs. time for bulk photopolymerization of 4K PIB triphenol tri(meth)acrylates and 3K PIB diphenol di(meth)acrylates.

Samples were irradiated at 12 mW cm^{-2} using 1 wt% of Darocur® 1173 photoinitiator.

1638 cm^{-1}
C=C of PIB triphenol triMA

Before Curing
UV Cured

1388 cm^{-1} PIB dimethyl wag

Wavenumbers (cm^{-1})
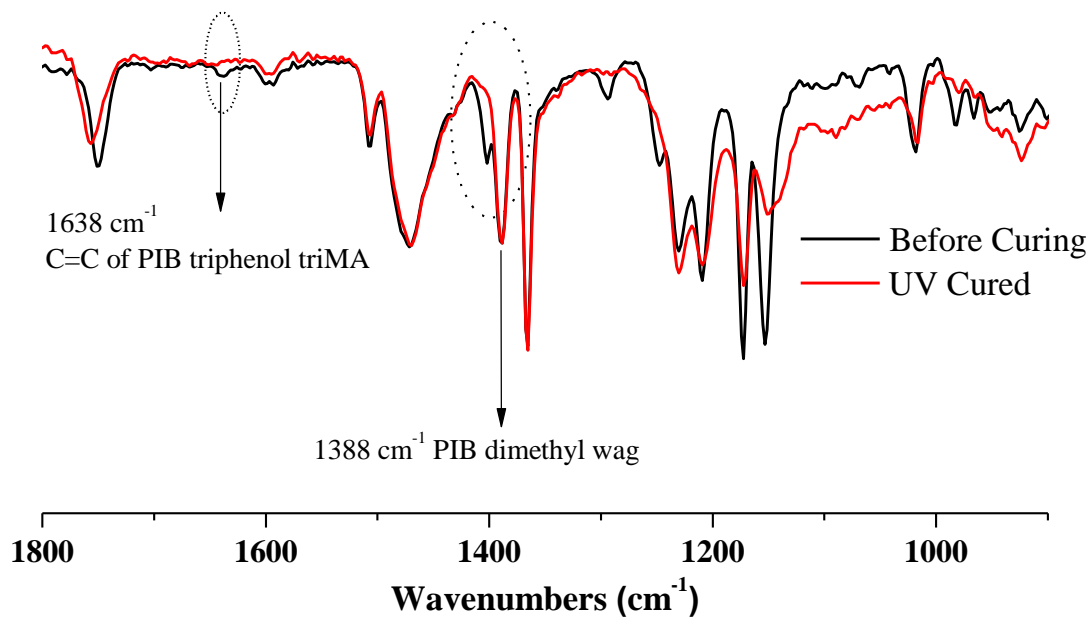
Figure 3.16 ATR-FTIR spectra of 4K PIB triphenol trimethacrylate before and after UV curing.

Sample was irradiated at 15 mW cm^{-2} using 1 wt% of Darocur® 1173 photoinitiator.
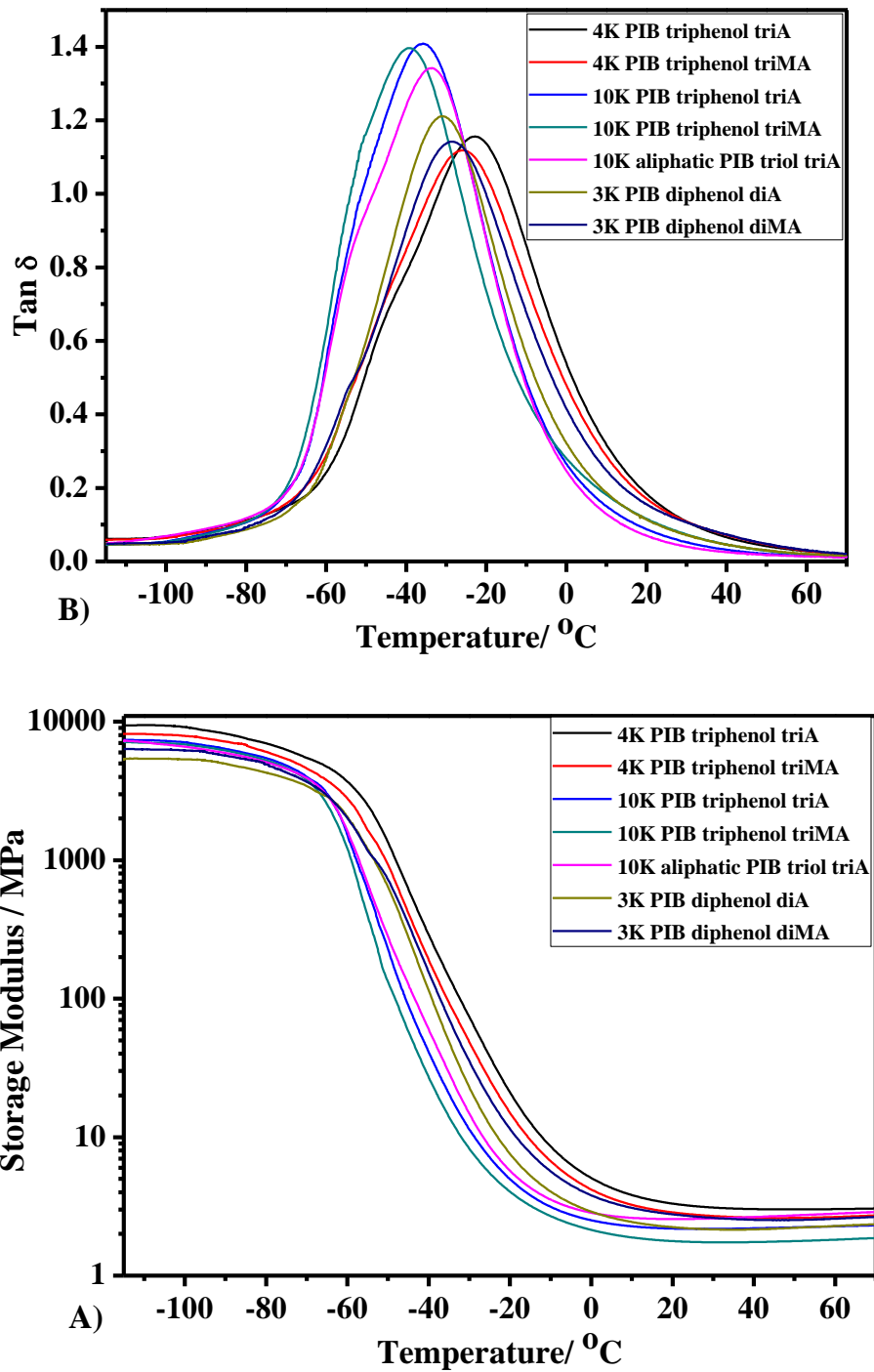
Figure 3.17 DMA analysis, A) Storage modulus versus temperature and (B) tan delta (δ) versus temperature of PIB networks produced from the seven PIB macromers.
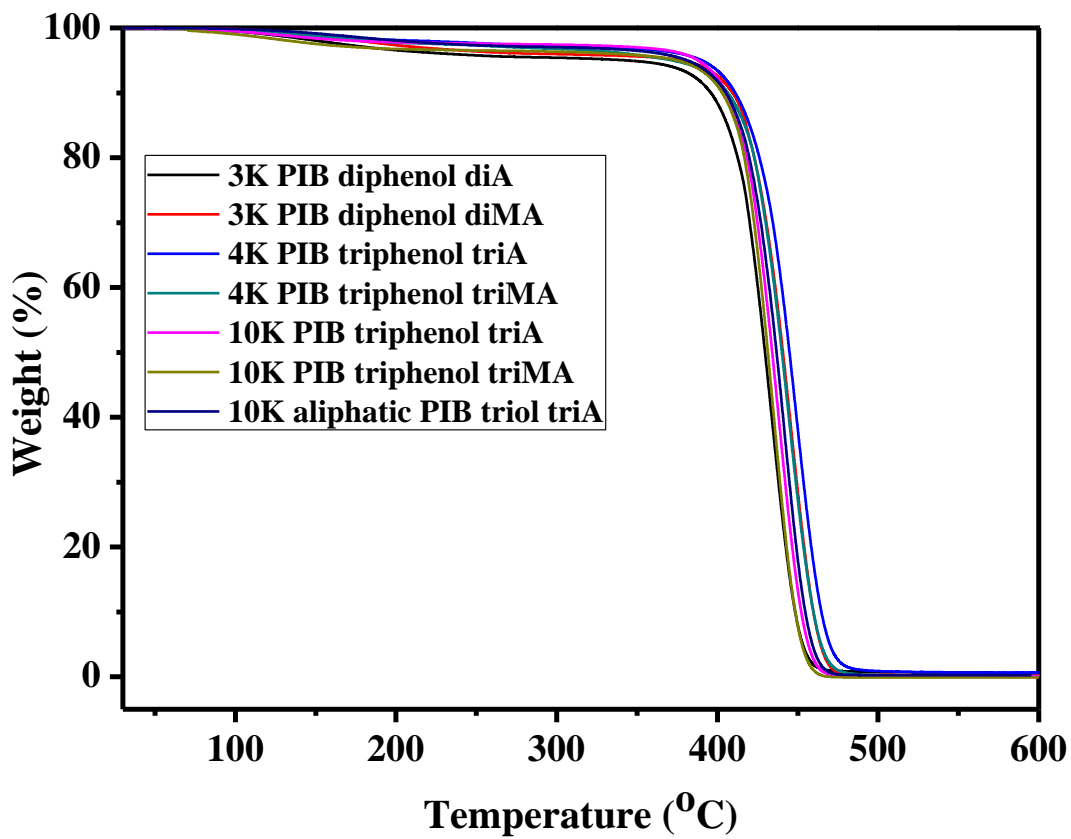
Figure 3.18 TGA analysis of PIB networks produced from the seven PIB macromers of this study.
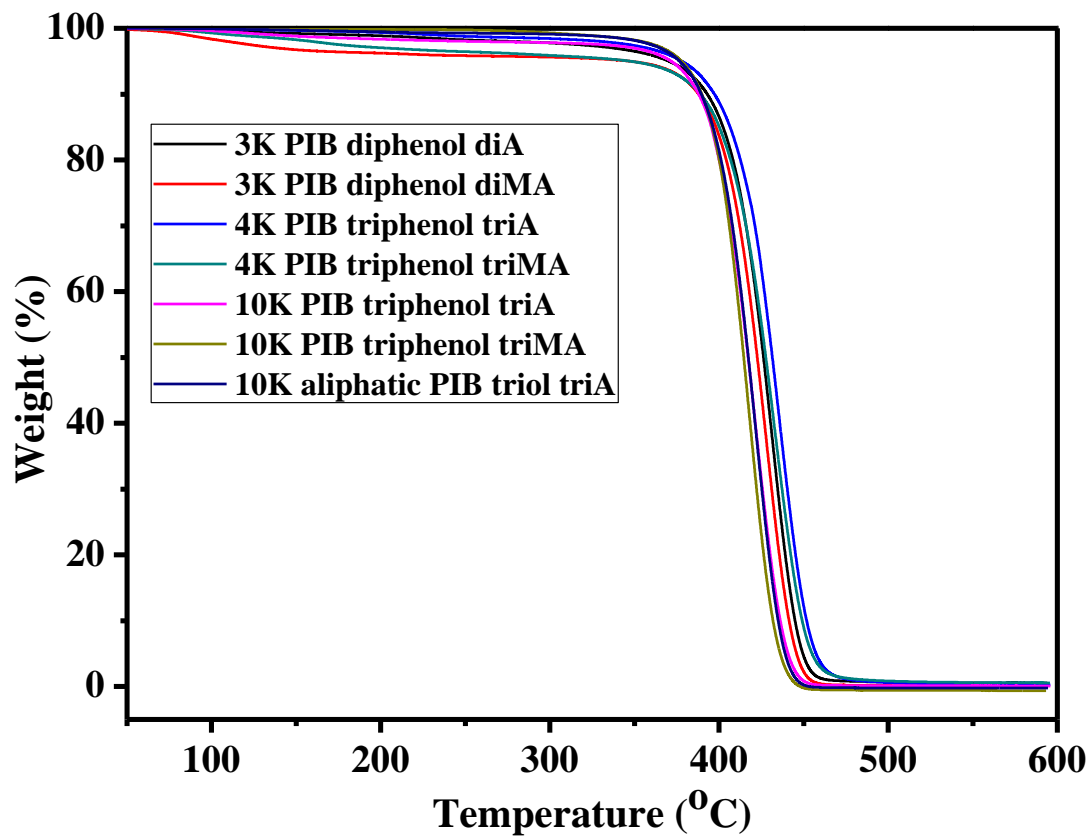
Figure 3.19 TGA analysis of seven starting PIB macromers before photocuring.
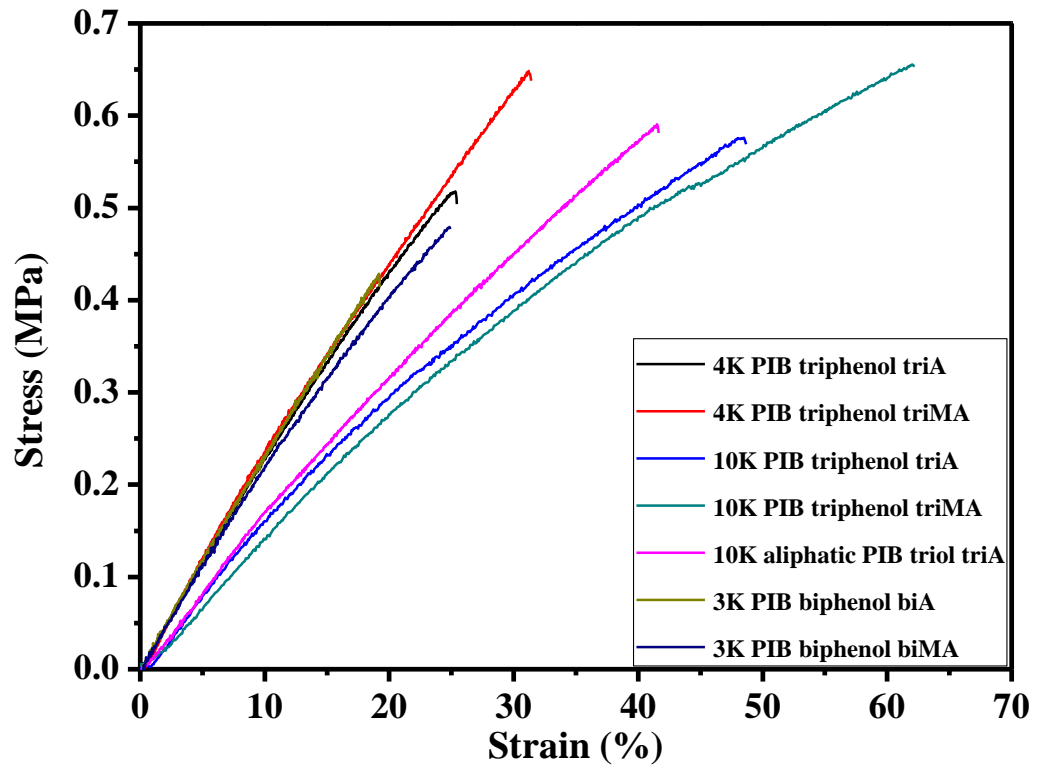
Figure 3.20 Typical stress-strain curve for each cured PIB network.

CHAPTER IV – SYNTHESIS AND CHARACTERIZATION OF NOVEL

POLYISOBUTYLENE TELECHELIC PREPOLYMERS

WITH EPOXIDE FUNCTIONALITY

4.1 Abstract

The syntheses of novel polyisobutylene telechelic prepolymers with various types of epoxide, including aliphatic glycidyl ether, phenyl glycidyl ether, ethylene oxide, and cycloaliphatic epoxide have been developed. The PIB prepolymer with aliphatic and phenyl glydicyl ether functionalities were achieved by nucleophilic substitution reaction of primary alcohol and phenol terminated PIB with epichlorohydrin, respectively. *E*xo-olefin epoxide terminated PIB was synthesized by direct epoxidation of *exo*-olefin terminated PIB with a strong oxidizing agent, *m*CPBA). The cycloaliphatic epoxide terminated PIB was obtained by nucleophilic substitution of primary bromide end-functional PIB with a premade potassium cyclohex-3-enecarboxylate salt, followed by epoxidation with *m*CPBA. ^{1}H NMR and MALDI-TOF mass spectroscopy analysis demonstrated that the functionality for all types of epoxide prepolymer was 2. Gel Permeation Chromatography (GPC) analysis showed targeted molecular weight and narrow molecular weight distribution were achieved for these prepolymers, as well as no polymer chain degradation or coupling occurred during post-polymerization modifications

4.2 Introduction

PIB based networks provide remarkable properties, such as strong adherence, high flexibility, good thermal and oxidative stability, low gas permeability, good energy

damping and solvent resistance, good insulating, and biostability/biocompatibility. Several types of PIB networks have been developed for specific applications. For example, Kennedy *et al.*[1-3] reported that PIB/polytetramethyleneoxide(PTMO) toughened polyurethanes/polyureas have significantly better mechanical properties than polyurethanes/polyureas containing highly crystalline hard segments. (Meth)acrylate based PIBs have found wide applications in biomaterials,[4] such as PIB toughened poly(methyl methcarylate) (PMMA) for bone cements,[5-6] cyanoacrylate-tipped PIB for intervertebral discs,[7] and PIB-methacrylate based amphiphilic networks for controlled drug release, artificial arteries, and first-generation immunoisolatory membranes.[4,8] Wilkes *et al.*[9] reported PIB networks formed via strong ionic interactions. Faust *et al.*[10] demonstrated the good biocompatibility of PIB/PTMO based thermoplastic urethanes (TPUs) with blood-contacting medical devices. Cationic radiation cure of PIB vinyl ether-based coatings has been applied in packaging of electronic devices and optical fibers due to the high refractive index, good adherence, and gas and moisture barrier properties of PIB networks.[11] Recently Faust *et al.*[12] and Storey *et al.*[13] reported PIB network formation by radical UV curing of (meth)acrylate end-functional PIBs to obtain PIB networks with (meth)acrylate conversion $\geq$ 95%. One major limitation of UV curing of (meth)acrylate end-functional PIBs was that an oxygen-free environment or amine synergists were required since propagating radicals can easily transfer to oxygen thereby effectively terminating the polymerization.

An important functional group used extensively in industry for network formation is epoxide, which can either undergo cationic ring opening polymerization or may be

reacted with amines to form epoxy-amine networks. The cationic ring opening process is not oxygen sensitive and thus offers the advantage of not requiring an oxygen-free environment or amine synergists. Faust *et al.* [14] have reported that the fracture, flexural, and tensile properties of a diglycidyl ether of bisphenol A (DGEBA)-triethylenetetramine (TETA) epoxy network are improved by the incorporation of glycidyl ether end-functional PIB as rubbery segment. Kennedy *et al.* [15] demonstrated in earlier research that such rubbery PIB soft segments greatly reduce the brittleness, chemical sensitivity, and hydrophilicity of traditional epoxy networks, and thus could be applied in underwater coatings and wire insulation.

A major limitation of the application of PIB-based epoxy-amine networks is the immiscibility of PIB with amines, due to the non-polar nature of the aliphatic PIB chain. One approach to this problem is to incorporate a polar oligomer into the PIB chain. For example, Faust *et al.*[14] reacted oligotetrahydrofuran (*o*THF) with primary bromide end-functional PIB to prepare PIB-*o*THF, which was then reacted with epichlorohydrin to obtain an *o*THF-modified PIB epoxide. The modified PIB epoxide showed good miscibility with DGEBA-TETA epoxy amine resin with no microphase separation observed until the content of PIB-*o*THF epoxide reached 40 wt%. However, one major concern of this approach is that the ratio of [*o*THF]/[PIB Br] must be precisely controlled, otherwise, both alcohol groups of the *o*THF might react with PIB-Br, thus leaving no alcohol group at the chain end for epoxide formation.

Another approach is to use nonpolar amines for PIB epoxy-amine network formation, for example, polyamides prepared from dimer fatty acid. The major concern

126

with this approach is the relatively high equivalent weight of these amines, which dilutes the PIB character of the resulting networks.

The synthesis of PIB-based epoxy-amine networks requires well-defined telechelic polymers with controlled molecular weight and narrow molecular weight distribution. Existing synthetic methods toward PIB epoxides are tedious and/or introduce undesirable unsaturations at the chain end. For instance, Kennedy *et al.* [16] developed an *exo*-olefin type epoxide by dehydrochlorination of tert-Cl[17] terminated PIB to obtain PIB *exo*-olefin [18] first, followed by epoxidation of the olefin. Kennedy *et al.*[19] reported the synthesis of PIB-phenyl glycidyl ether using a multistep synthetic procedure. First, PIB phenol[20] was obtained by Friedel-Crafts alkylation of phenol, used in excess, by *tert*-Cl- or *exo*-olefin-terminated PIB catalyzed by $BF_3 \cdot OEt_2$; full conversion was achieved after refluxing in hexane at 45-48°C for 48 h. The resulting PIB phenol was then reacted with excess epichlorohydrin to achieve end capping to the exclusion of chain extension. Later, Kennedy *et al.*[21] developed a method to synthesize glycidyl-terminated PIB by the *m*-chloroperbenzoic acid epoxidation of allyl-terminated PIB, which was obtained by quenching of living PIB with allyltrimethylsilane. Recently, *Faust et al.*[14,22] developed a method to synthesize aliphatic glycidyl ether end-functional PIB by base-catalyzed SN_2 substitution of PIB allyl bromide with glycidol or by substitution of PIB alcohol with epichlorohydrin. The major disadvantage of this approach is that the initial living IB polymerization/butadiene quenching reaction yields PIB-allyl chloride, which is insufficiently reactive toward SN_2 substitution reactions. A post-polymerization halogen exchange reaction using LiBr is therefore required,[23] or alternatively, the more

127

complicated procedure of replacing TiCl₄ with a totally brominated Lewis acid system

(produced from mixtures of aluminum tribromide and trimethylaluminum.)[24] Other

possible concerns are that the unsaturation of PIB-allyl bromide might bring some color

issues or be unstable towards chemicals, heat, or oxygen.
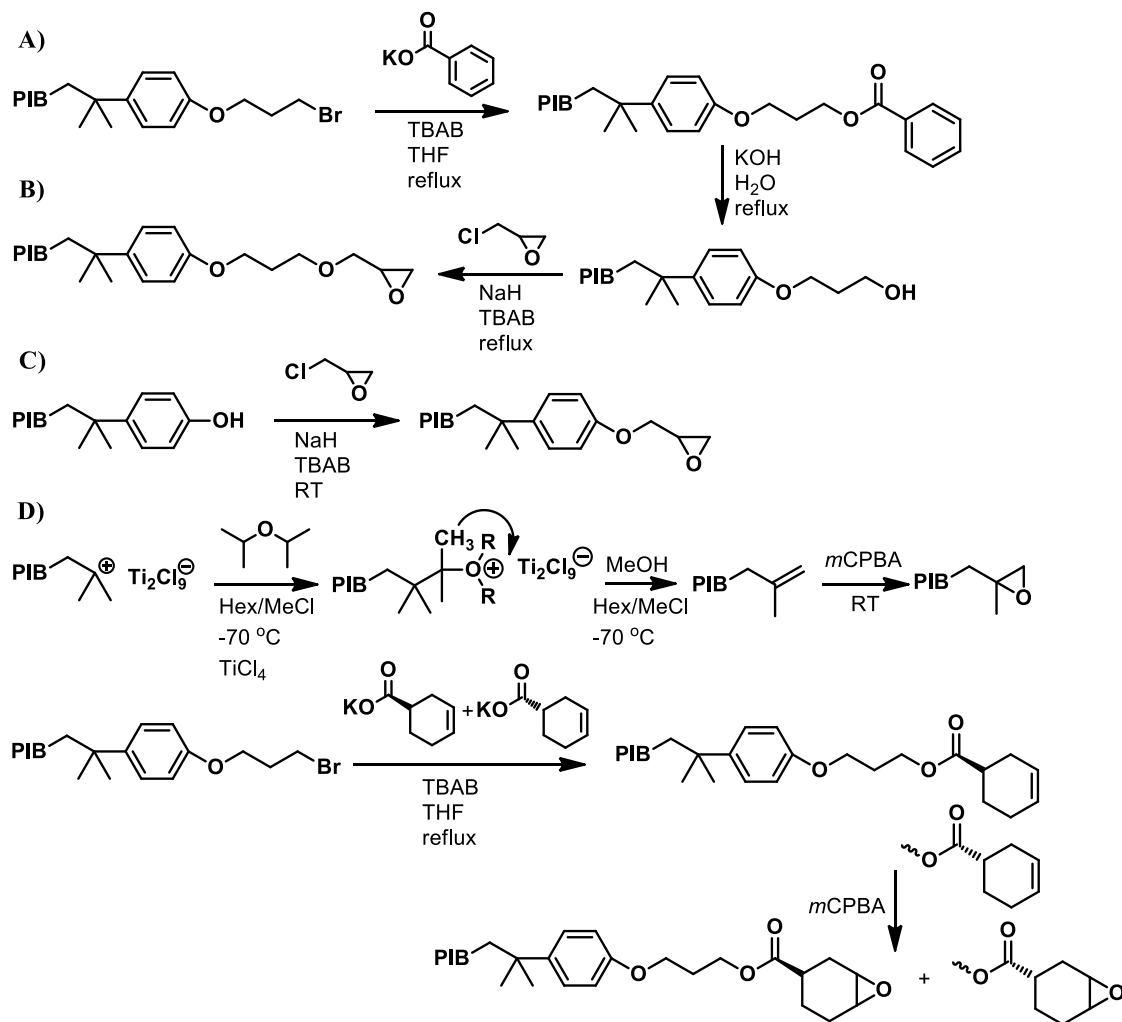
Scheme 4.1 Synthesis of PIB telechelic prepolymers with various epoxide functionalites:
A) PIB aliphatic glycidyl ether, B) PIB phenyl glycidyl ether, C) PIB *exo*-olefin epoxide,
and D) PIB cyclohexene epoxide.

     Storey *et al.* have recently developed quantitative synthesis of phenol,[13,25] *exo*-

olefin,[26] and bromide[25,27-28] end-functional PIBs by end-quenching living PIB

polymerization with suitable quenchers.[29] All these developments offer promising new routes to synthesize epoxide functional PIBs by simple nucleophilic substitution or oxidation reactions. In this study, four types of useful epoxide functional PIBs were synthesized, as shown in Scheme 4.1. PIB aliphatic and phenyl glycidyl ethers were synthesized by nucleophilic substitution reactions involving PIB alkoxide and phenolate nucleophiles, respectively, with epichlorohydrin. A non-glycidyl PIB aliphatic epoxide referred to herein as "PIB *exo*-olefin epoxide," was obtained by epoxidation of PIB *exo*-olefin with *m*CPBA. A novel PIB cycloaliphatic epoxide was achieved by nucleophilic substitution of PIB bromide with pre-formed potassium cyclohex-3-enecarboxylate , followed by epoxidation with *m*CPBA.

4.3 Experimental

Materials. Hexane (anhydrous, 95%), methanol (anhydrous, 99.8%), titanium tetrachloride (TiCl$_4$) (99.9%), 2,6-lutidine (99.5%), (3-bromopropoxy)benzene (anhydrous, 98%), heptane (99.0%), epichlorohydrin (99.0%), tertbutylammonium bromide (TBAB, 99.0%), diisopropyl ether (anhydrous, 99.0%) sodium hydride (NaH, 60% dispersion in mineral oil), dichloromethane-d$_2$ (CD$_2$Cl$_2$), chloroform (anhydrous, 99.0%), potassium carbonate (K$_2$CO$_3$, anhydrous, 99.5%), *meta*-chloroperoxybenzoic acid (*m*CPBA, ≥70% assay) and silver trifluoroacetic acid (AgTFA) were purchased from Sigma-Aldrich and used as received. Tetrahydrofuran (THF) was purchased from Fisher Scientific and distilled prior to use. *Trans*-2-[3-(4-*t*-butylphenyl)-2-methyl-2-propenylidene]malononitrile (DTCB) was purchased from Tokyo Chemical Industry Co. and used as received. Isopropoxybenzene (97%) was purchased from Oakwood

129

Chemical and used as received. Potassium benzoate (99.0%) was purchased from Alfa

Aesar and used as received. Magnesium sulfate ($MgSO_4$) (anhydrous), diethyl ether,

potassium hydroxide (KOH), 3-cyclohexene-1-carboxylic acid (racemic *exo-* and *endo-*

mixture, 97%), *N-N*-dimethylformamide (DMF), sulfuric acid (98%), acetone (99.7%),

chloroform-d ($CDCl_3$) were purchased and used as received from Fisher Scientific.

Isobutylene (IB, BOC Gases) and methyl chloride (Alexander Chemical Corp.) were

dried by passing the gaseous reagent through a column of $CaSO_4$/molecular sieves/$CaCl_2$

and condensing within a N_2-atmosphere glovebox immediately prior to use. Difunctional

initiator, 5-*tert*-butyl-1,3-di(1-chloro-1-methylethyl)benzene (*b*DCC) has been

synthesized following previous procedure[30] and stored at 0°C prior to use.

   Instrumentation. Nuclear magnetic resonance (NMR) spectra were obtained using

a 600.13 MHz Bruker Ascend (TopSpin 3.5) spectrometer. All ^{1}H chemical shifts were

referenced to TMS (0 ppm). Samples were prepared by dissolving the polymer in either

chloroform-d (5-7%, w/v) and charging this solution to a 5 mm NMR tube. For

quantitative integration, 16 transients were acquired using a pulse delay of 27.3 s. In all

cases, the signal due to the phenyl protons of the initiator (7.17 ppm, 2H, singlet) was

chosen as an internal reference for functionality analysis.

   Number-average molecular weights (M_n) and polydispersities (PDI = M_w/M_n)

were determined using a gel-permeation chromatography (GPC) system consisting of a

Waters Alliance 2695 separations module, an online multi-angle laser light scattering

(MALLS) detector fitted with a gallium arsenide laser (power: 20 mW) operating at 658

nm (miniDAWN TREOS, Wyatt Technology Inc.), an interferometric refractometer

(Optilab T-rEX, Wyatt Technology Inc.) operating at 35°C and 685 nm, and two PLgel (Polymer Laboratories Inc.) mixed E columns (pore size range 50-10^3 Å, 3 μm bead size). Freshly distilled THF served as the mobile phase and was delivered at a flow rate of 1.0 mL/min. Sample concentrations were ca. 15-20 mg of polymer/mL of THF, and the injection volume was 100μL. The detector signals were simultaneously recorded using ASTRA software (Wyatt Technology Inc.), and absolute molecular weights were determined by MALLS using a *dn*/*dc* calculated from the refractive index detector response and assuming 100% mass recovery from the columns.

Matrix-assisted laser desorption/ionization time-of-flight mass spectrometry (MALDI-TOF MS) was performed using a Bruker Microflex LRF MALDI-TOF mass spectrometer equipped with a nitrogen laser (337 nm) possessing a 60 Hz repetition rate and 50 µJ energy output. The PIB samples were prepared using the dried droplet method: separately prepared THF solutions of DCTB matrix (20 mg/mL), PIB sample (10 mg/mL), and AgTFA cationizing agent (10 mg/mL), were mixed in a volumetric ratio of matrix/sample/cationizing agent = 4:1:0.2, and a 0.5 µL aliquot was applied to a MALDI sample target for analysis. The spectrum was obtained in the positive ion mode utilizing the reflector mode micro-channel plate detector and was generated as the sum of 900-1000 shots.

Synthesis of potassium cyclohex-3-enecarboxylate. To a 250 mL one-neck round bottom flask was charged 10.8 g (78.0 mmol) of K_2CO_3 and 60 mL of diethyl ether. the round bottom was then placed into a dry ice/acetone bath. A solution of 19.6 g (155 mmol) of 3-cyclohexene-1-carboxylic acid in 50 mL of diethyl ether was prepared and

was then added to the K_2CO_3/diethyl ether slurry dropwise over a period of 60 min. The reaction was kept cold overnight. The suspension was vacuum filtered, and the remaining solid was washed with 3 fold of 60 mL of diethtyl ether. The damp salt was dried at a vacuum oven over overnight to yield a white powder(10.3 g, 73%.)

Synthesis of difunctional PIB aliphatic glycidyl ether (PIB-di-AGE). Difunctional alcohol-terminated PIB precursor (PIB-di-OH, 0.60g, M_n=4,100 g/mol, PDI=1.12) obtained by quenching living PIB with (3-bromopropoxy)benzene [25]following by reaction with benzoate/hydrolysis according to a published procedure was dissolved in 50 mL of freshly distilled THF and then transferred to a 100 mL one-neck round bottom flask. To the stirred solution were added epichlorohydrin (1.10 mL, 1.30 g), TBAB (0.048 g), and NaH (0.42g, rinsed with hexane three time prior to use to remove mineral oil). The mixture was refluxed under a dry N_2 atmosphere for 24 h. Upon completion of the reaction, the THF was vacuum stripped, and the polymer was dissolved in hexane. The resulting solution was filtered through a cotton plug and slowly added into excess methanol to precipitate the polymer. The precipitate was redissolved in fresh hexane, and the resulting solution was washed with DI water, dried over $MgSO_4$, and then vacuum stripped to obtain pure difunctional PIB aliphatic glycidyl ether.

Synthesis of difunctional PIB phenyl glycidyl ether (PIB-di-PGE). Difunctional phenol-terminated PIB precursor (PIB-di-phenol, 2.06 g, M_n=3,800 g/mol, PDI=1.22) obtained by quenching living PIB with isopropoxybenzene following a published procedure[13,25] was dissolved in 50 mL of freshly distilled THF and was then transferred to a 100 mL one-neck round bottom flask. To the stirred solution were added

132

epichlorohydrin (3.86 mL, 4.56 g), TBAB (0.44 g), and NaH (0.66g, rinsed with hexane three time prior to use to remove mineral oil.) The mixture was stirred under a dry N_2 atmosphere for 6h. Upon completion of the reaction, the THF was vacuum stripped, and the polymer was dissolved in hexane. The resulting solution was filtered through a cotton plug and slowly added into excess methanol to precipitate the polymer. The precipitate was redissolved in fresh hexane, and the resulting solution was washed with DI water, dried over $MgSO_4$, and then vacuum stripped to obtain pure difunctional PIB phenol glycidyl ether.

Synthesis of difunctional PIB exo-olefin epoxide (PIB-di-EO). Difunctional *exo*-olefin-terminated PIB precursor (PIB-di-*exo*-olefin, 0.60g, M_n=4,100 g/mol, PDI=1.12) obtained by end-quenching living PIB polymerization with diisopropyl ether[26] was dissolved in 25 mL of anhydrous $CHCl_3$ and was then transferred to a 100 mL three-neck round bottom flask. *M*CPBA (2.16 g, 70% assay) was dissolved in 25 mL of anhydrous $CHCl_3$ and was added dropwise to the PIB solution with a 30 min period. The mixture was stirred under a dry N_2 atmosphere for 6 h. Upon completion of the reaction, the $CHCl_3$ was vacuum stripped, and the polymer was dissolved in hexane. The resulting solution was filtered through a cotton plug and slowly added into excess methanol to precipitate the polymer. The precipitate was redissolved in fresh hexane, and the resulting solution was washed with DI water, dried over $MgSO_4$, and then vacuum stripped to obtain pure difunctional PIB *exo*-olefin epoxide.

Synthesis of difunctional PIB cyclohexene epoxide (PIB-di-CHE). Difunctional bromide-terminated PIB precursor (PIB-di-Br, M_n = 4,000 g/mol, PDI = 1.10) obtained

133

by end quenching of living PIB with (3-bromopropoxy)benzene[25,27-28] was converted to cyclohexene epoxide by nucleophilic substitution of bromide with cyclohexene, followed by epoxidation of cyclohexene with mCPBA. The first step was done in a solvent mixture of 50/50 (v/v) heptane/DMF to ease the purification of PIB polymers owing to the high phase selectivity for heptane.[25,31] Thus, PIB-di-Br (2.0 g) was dissolved in 30 mL of heptane. Pre-formed potassium cyclohex-3-enecarboxylate (1.54 g) and TBAB (0.3 g) were dissolved in 30 mL of DMF. The two liquids were combined in a 100 mL one-neck round bottom flask and sparged with high purity Ar for 15 min. The mixture was refluxed under a dry N_2 atmosphere for 9 h. Upon completion of the reaction, the solution was allowed to cool to room temperature causing the heptane and DMF layers to separate. The top layer containing the PIB product in heptane was collected, and the bottom layer consisting of the DMF, TBAB, and excess potassium cyclohex-3-enecarboxylate was discarded. The heptane layer was washed with DI water, dried over $MgSO_4$, and then vacuum stripped to obtain pure difunctional PIB cyclohexene. Difunctional PIB cyclohexene epoxide was then achieved by epoxidation of PIB cyclohexene with mCPBA similarly to the synthesis of PIB exo-olefin epoxide.

4.4 Results and Discussion

Synthesis of difunctional PIB aliphatic glycidyl ether. In small molecule syntheses, glycidol is commonly used to react with primary halides to obtain epoxides under basic conditions. Initially, PIB bromide was reacted with glycidol in the presence of NaH and a TBAB phase transfer catalyst under reflux in THF. Under these conditions, however, the conversion did not reach 100% after 24 h. This was attributed to poor

134

solubility of the sodium glycidoxy salt in THF in spite of the presence of phase transfer

catalyst. High effective concentration of the nucleophile is required in this reaction since

the bromide end group of PIB Br is buried within the polymer coil. An alternate route

was next attempted, involving initial conversion of PIB-Br to PIB-OH following a

literature procedure,[25] followed by a Williamson ether synthesis involving the obtained

PIB OH and epichlorohydrin activated by NaH. Full conversion of PIB-OH to PIB-

epoxide was observed to be complete within 18 h at THF reflux temperature (~67°C).

This alternative route was successful because the ionic species involved, sodium PIB-

alkoxide is well soluble in THF because of its relatively high molecular weight.

Figure 4.1 shows the ^{1}H NMR spectra of the starting difunctional PIB Br,

intermediate PIB benzoate ester, PIB OH, and product PIB aliphatic glycidyl ether.

Figure 4.1B shows the presence of the benzoate ester by multiplets at 7.43, 7.55, and 8.04

ppm, and the observed downfield shift of the terminal tether methylene unit from 3.60 to

4.52 ppm due the electron-withdrawing ester linkage. Figure 4.1C shows the spectrum of

the PIB OH in which the resonance for the methylene unit adjacent to the terminal

hydroxyl appears at 3.87 ppm. Evidence of quantitative formation of aliphatic glycidyl

ether was provided in Figure 4.1D by multiplets appearing at 3.70, 3.40, 3.14, 2.78, and

2.60 ppm, as well as the slight upfield chemical shift of peaks originally at 4.10 and 3.87

ppm to 4.04 and 3.73 ppm due to the conversion of OH to glycidyl ether.

GPC analysis in Figure 4.2A showed that no chain coupling or degradation

occurred in any of the post-polymerization modification steps. Molecular weight and

polydispersity obtained from GPC study was listed in Table 4.1.

135

Synthesis of difunctional PIB phenyl glycidyl ether. End-quenching of living PIB polymerization with isopropoxybenzene followed by detaching of the bulky propene moiety provided a simple and reliable way to quantitatively synthesize highly reactive phenol-terminated PIBs. Reaction of difunctional PIB phenol obtained by this method with epichlorohydrin was carried out in THF using a NaH base and a TBAB phase transfer catalyst. Quantitative formation of the phenyl glycidyl ether was complete after 6 h reaction at room temperature, which was a much shorter reaction time than required for the aliphatic glycidyl ether, even though the latter reaction was conducted at THF reflux temperature. More rapid conversion to the aromatic glycidyl ether is attributed to the faster deprotonation of phenol moiety.

Figure 4.3 shows the starting difunctional PIB phenol, and product PIB phenyl glycidyl ether ^{1}H NMR spectra of Evidence of quantitative conversion was given by the appearance of resonances at 4.17 and 3.96 (complex doublet of doublets), 3.36 (quintet), 2.90 (triplet) and 2.75 ppm (quartet) due to addition of the glycidyl ether moiety, as well as the disappearance of the phenolic proton resonance at 4.48 ppm (singlet). GPC analysis in Figure 4.2B showed that no chain coupling or degradation occurred during the substitution reaction.

Synthesis of difunctional PIB exo-olefin epoxide. End-quenching of living PIB with hindered ethers, such as diisopropyl ether, provides a simple and convenient route to highly reactive *exo*-olefin-terminated PIBs. Using a modification of a method originally published by Kennedy,[16] epoxdation of difunctional PIB *exo*-olefin with *m*CPBA was carried out in anhydrous $CHCl_3$ at room temperature.

136

Figure 4.4 shows the ^{1}H NMR spectra of the starting difunctional PIB *tert*-Cl, intermediate PIB *exo* olefin, and product PIB *exo*-olefin epoxide. Evidence of formation of the epoxide was given by the appearance of chemical shifts at 2.63 and 2.58 (doublet of doublets), 1.81 and 1.83 (doublet of doublets), 1.21 (singlet), 1.18 (singlet) and 0.78 ppm (singlet), as well as the disappearance of peaks at 4.64, 4.86, 2.00, and 1.79 ppm due to the conversion *exo*-olefin to oxirane.

GPC analysis in Figure 4.2C showed a small shoulder on the high molecular weight side of the main peak in the traces of the precursor PIB *exo*-olefin and the final PIB *exo*-olefin epoxide, indicating a low fraction of coupled PIB formed during end-quenching with diisopropyl ether. The coupling is likely due to the PIB *exo*-olefin attacked neighboring PIB carbocation, which would happen if the ratio of [diisopropylether]/[TiCl$_4$] was smaller than 1.1.[26] In the oxidation process, coupled olefin can also be oxided to form an internal oxirane along the PIB chain without chain cleavage.

Synthesis of difunctional PIB cyclohexene epoxide. In small molecule syntheses, carboxylic acids are commonly reacted with primary halides to obtain esters under basic conditions. Initially, cyclohex-3-ene-1-carboxylic acid was reacted with PIB primary bromide using NaH/TBAB under reflux in a 50/50, v/v, heptane/DMF cosolvent. However, conversion was less than 10% after 24 h, and the majority (90%) of the bromide was converted to PIB alkene. Apparently, under these reaction conditions, the rate of E2 elimination by basic hydride ion is faster than SN$_2$ nucleophilic substitution of Br by cyclohexenecarboxylate. This problem was solved by first converting the

137

cyclohexenecarboxylic acid to its potassium salt by neutralization with potassium carbonate. After isolation, the resulting potassium cyclohexenecarboxylate (structure was confirmed by ^{1}H NMR, Figure 4.5) was reacted with PIB-Br in the absence of hydride ion but otherwise under the same reaction conditions to yield full conversion of the desired product within 6 h.

Figure 4.6 shows the ^{1}H NMR spectra of the starting difunctional PIB primary Br, intermediate PIB cyclohexene, and the product PIB cyclohexene epoxide. In Figure 4.6B, the presence of the cyclohexene moiety is revealed by multiplets at 2.56, 2.25, 2.10, and 1.70 ppm, and the downfield shift of the terminal methylene unit of the propoxy tether from 3.60 to 4.28 ppm due the electron-withdrawing ester linkage. Quantitative formation of aliphatic glycidyl ether is demonstrated in Figure 4.6C by multiplets at 5.67, 3.22, 3.12-3.15, 2.51, 2.15-2.28, 1.95-1.98, 1.75, and 1.61 ppm, as well as the disappearance of peaks at 2.56, 2.25, 2.10, and 1.70 ppm due to the conversion of cyclohexene to cyclohexene epoxide. A mixture of *exo* and *endo* epoxides was obtained at a ratio of 2:1, which reflected the composition of the starting 3-cyclohexene-1-carboxylic acid. The chemical shift of the methine group attaching to the ester linkage of the *exo* diastereoisomer appeared at 2.51 ppm, while that of the *endo* diastereoisomer was buried in the methylene groups due to the less electron withdrawing effect of the *endo* diastereoisomer. Similar evidence was shown by the methine groups within the oxirane ring; peaks at 3.22 and 3.14 ppm, and 3.13 ppm were attributed to *exo* and *endo* diastereoisomer, respectively. GPC analysis in Figure 4.2D showed that no chain coupling or degradation occurred during the substitution and oxidation reactions.

138

End group analysis. MALDI-TOF MS provided a second method to determine molecular weight, polydispersity, and end-functionality. The MALDI-TOF mass spectra of difunctional PIB aliphatic glycidyl ether, PIB phenyl glycidyl ether, PIB *exo*-olefin epoxide, and PIB cyclohexene epoxide, are shown in Figure 4.7A-D. Each sample displayed a single, major distribution of polymeric species, associated with Ag cations from the AgTFA cationizing agent, differing from each other only by the number of isobutylene repeat units. The data from each mass spectrum were analyzed by linear regression of a plot of mass-to-charge ratio (M/z, assumed to be 1), measured at the maximum of each peak of the major distribution, versus degree of polymerization (DP). The slope of this plot is theoretically equivalent to the exact mass of the isobutylene repeat unit, 56.06 Da. The y-intercept is theoretically equivalent to $f{\times}EG{+}I{+}C$, where f is the functionality of the polymer (2 in this study), EG is the exact mass of the epoxide, I is the exact mass of the *b*DCC initiator residue, and C is the exact mass (106.91 Da) of the major isotope of the associated Ag cation.

MALDI-TOF MS data for all of the difunctional PIB epoxides, analyzed in this manner, are summarized in Table 4.2. In all cases, the measured value of the repeat unit molecular weight (M_{ru}) was within 0.2% of the theoretical value (56.06 Da), and the measured value of $f{\times}EG{+}I{+}C$ was within 0.8% of the theoretical value. The observed close agreement between measured and theoretical values provides strong evidence that the synthesized difunctional PIB epoxides possess the expected structure and end-group functionality. Table 4.2 also lists M_n and PDI data obtained from MALDI-TOF-MS. In all cases, these values are lower than the corresponding values obtained from GPC

139

analysis (Table 4.2). This is a common observation and reflects the fact that polymer chains with higher molecular weight are more difficult to desorb/ionize and thus are under-represented at the detector.

4.5 Conclusions

We have demonstrated that PIB prepolymers with aliphatic glycidyl ether, phenyl glycidyl ether, *exo*-olefin epoxide, and cycloaliphatic epoxide can be quantitatively synthesized by combining living carbocationic polymerization with one or two-step post-polymerization modifications. These reactions represent facile and quantitative syntheses of telechelic PIB prepolymers fitted with a variety of epoxide structures commonly used in industry.

Both PIB aliphatic and phenyl glycidyl ethers can be thermally cured with crosslinkers to form networks for coatings, adhesives, and sealants applications. The difunctional PIB prepolymers with *exo*-olefin epoxide and cyclohexene epoxide reported in this study may be converted to crosslinked networks using photoinitiated cationic ring opening polymerization, which is an alternate to photoinduced radical polymerization of PIB (meth)acrylates. Unlike radical polymerizations, which are typically inhibited by oxygen, cationic polymerization of PIB epoxides is not inhibited by oxygen, however, it is susceptible to moisture. In future studies, photopolymerization of PIB epoxides and vinyl ethers and structure-property relationships of the resulting networks will be investigated to expand the application of PIB networks by UV curing.

The method of combining living polymerization of PIB and post-polymerization modifications can be further expanded to include synthesis of telechelic PIB prepolymers

140

with other functionalities, such as azide, alkyne, isocyanate, alcohol, thiol, norbornene, etc. useful for the creation of thermoplastic elastomers, amphiphilic conetworks (APCNs), photocurable networks, and bottleneck brushes.

4.6 Acknowledgements

4.7 References

(1)   Jewrajka, S. K.; Yilgor, E.; Yilgor, I.; Kennedy, J. P., *J. Polym. Sci., Part A: Polym. Chem.* **2009,** *47* (1), 38-48.

(2)   Jewrajka, S. K.; Kang, J.; Erdodi, G.; Kennedy, J. P.; Yilgor, E.; Yilgor, I., *J. Polym. Sci., Part A: Polym. Chem.* **2009,** *47* (11), 2787-2797.

(3)   Erdodi, G.; Kang, J.; Kennedy, J. P.; Yilgor, E.; Yilgor, I., *J. Polym. Sci., Part A: Polym. Chem.* **2009,** *47* (20), 5278-5290.

(4)   Kennedy, J. P., *J. Polym. Sci., Part A: Polym. Chem.* **2005,** *43* (14), 2951-2963.

(5)   Kennedy, J. P.; Richard, G. C., *Macromolecules* **1993,** *26* (4), 567-571.

(6)   Kennedy, J. P.; Askew, M. J.; Richard, G. C., *J. Biomater. Sci., Polym. Ed.* **1993,** *4* (5), 445-449.

(7)   Kennedy, J. P.; Midha, S.; Gadkari, A., *J. Macromol. Sci., Part A : Chem.* **1991,** *28* (2), 209-224.

(8)   Erdodi, G.; Kennedy, J. P., *Prog. Polym. Sci.* **2006,** *31* (1), 1-18.

(9)   Loveday, D.; Wilkes, G. L.; Lee, Y.; Storey, R. F., *J. Appl. Polym. Sci.* **1997,** *63* (4), 507-519.

(10)   Cozzens, D.; Luk, A.; Ojha, U.; Ruths, M.; Faust, R., *Langmuir* **2011,** *27* (23), 14160-8.

(11)   Bahadur, M.; Suzuki, T., *US Patent 6069185* **2000**.

(12)   Tripathy, R.; Crivello, J. V.; Faust, R., *J. Polym. Sci., Part A: Polym. Chem.* **2013,** *51* (2), 305-317.

(13)   Yang, B.; Parada, C. M.; Storey, R. F., *Macromolecules* **2016,** *49* (17), 6173-6185.

(14)   Tripathy, R.; Ojha, U.; Faust, R., *Macromolecules* **2011,** *44* (17), 6800-6809.

(15)   Kennedy, J. P.; Guhaniyogi, S., *US Patent 4429099,* **1984**.

(16)   Kennedy, J. P.; Chang, V. S. C.; Francik, W. P., *J. Polym. Sci., Polym. Chem. Ed.* **1982,** *20* (10), 2809-2817.

(17)   Kennedy, J. P.; Smith, R. A., *J. Polym. Sci., Polym. Chem. Ed.* **1980,** *18* (5), 1523-1537.

(18)   Kennedy, J. P.; Chang, V. S. C.; Smith, R. A.; Iván, B., *Polym. Bull.* **1979,** *1* (8), 575-580.

(19)   Kennedy, J. P.; Guhaniyogi, S. C.; Percec, V., *Polym. Bull.* **1982,** *8* (11), 571-578.

(20)   Kennedy, J. P.; Guhaniyogi, S. C.; Percec, V., *Polym. Bull.* **1982,** *8* (11), 563-570.

(21)   Iván, B.; Kennedy, J. P., *J. Polym. Sci., Part A: Polym. Chem.* **1990,** *28* (1), 89-104.

(22)   Tripathy, R.; Ojha, U.; Faust, R., *Macromolecules* **2009,** *42* (12), 3958-3964.

(23)   Higashihara, T.; Feng, D.; Faust, R., *Macromolecules* **2006,** *39*, 5275-5279.

(24)   De, P.; Faust, R., *Macromolecules* **2006,** *39* (22), 7527-7533.

(25)   Morgan, D. L.; Martinez-Castro, N.; Storey, R. F., *Macromolecules* **2010,** *43* (21), 8724-8740.

(26)   Ummadisetty, S.; Storey, R. F., *Macromolecules* **2013,** *46* (6), 2049-2059.

(27)   Morgan, D. L.; Storey, R. F., *Macromolecules* **2009,** *42* (18), 6844-6847.

(28)   Yang, B.; Storey, R. F., *Polym. Chem.* **2015,** *6* (20), 3764-3774.

(29)   Roche, C. P.; Brei, M. R.; Yang, B.; Storey, R. F., *ACS Macro Lett.* **2014,** *3* (12), 1230-1234.

(30)   Storey, R. F.; Choate, K. R., *Macromolecules* **1997,** *30* (17), 4799-4806.

(31)   Bergbreiter, D. E.; Sung, S. D.; Li, J.; Ortiz, D.; Hamilton, P. N., *Org. Process Res. Dev.* **2004,** *8* (3), 461-468.

4.8 Tables and Figures for Chapter IV

Table 4.1

Molecular weight of various difunctional PIB epoxides.

Entry	Sample	Funct.	$M_{n,NMR}$ (g/mol)	$M_{n,GPC}$ (g/mol)	PDI
1	4K PIB aliphatic glycidyl ether	2	4,140	4,400	1.17
2	4K PIB phenyl glycidyl ether	2	4,390	4,400	1.22
3	4K PIB *exo*-olefin epoxide	2	3,820	3,900	1.13
4	4K PIB cyclohexene epoxide	2	4,270	4,300	1.10

Table 4.2

MALDI-TOF MS data of various difunctional PIB epoxides.[a]

Sample	MW_{theo} $f \times EG+I+C$[b]	MW_{exp} $f \times EG+I+C$	Diff.	M_n	PDI	M_{ru}[c]
4K PIB aliphatic glycidyl ether	737.30	739.76	2.46	2464	1.06	56.14
4K PIB phenyl glycidyl ether	621.22	623.32	2.10	2320	1.06	56.12
4K PIB *exo*-olefin epoxide	465.20	466.99	1.79	2170	1.10	56.11
4K PIB cyclohexene epoxide	873.35	875.75	2.40	2431	1.05	56.08

[a]Unit for molecular weight is Da; [b]*f*=chain end functionality, EG = end group, I = initiator, C = Ag cation; [c]ru is repeat unit.
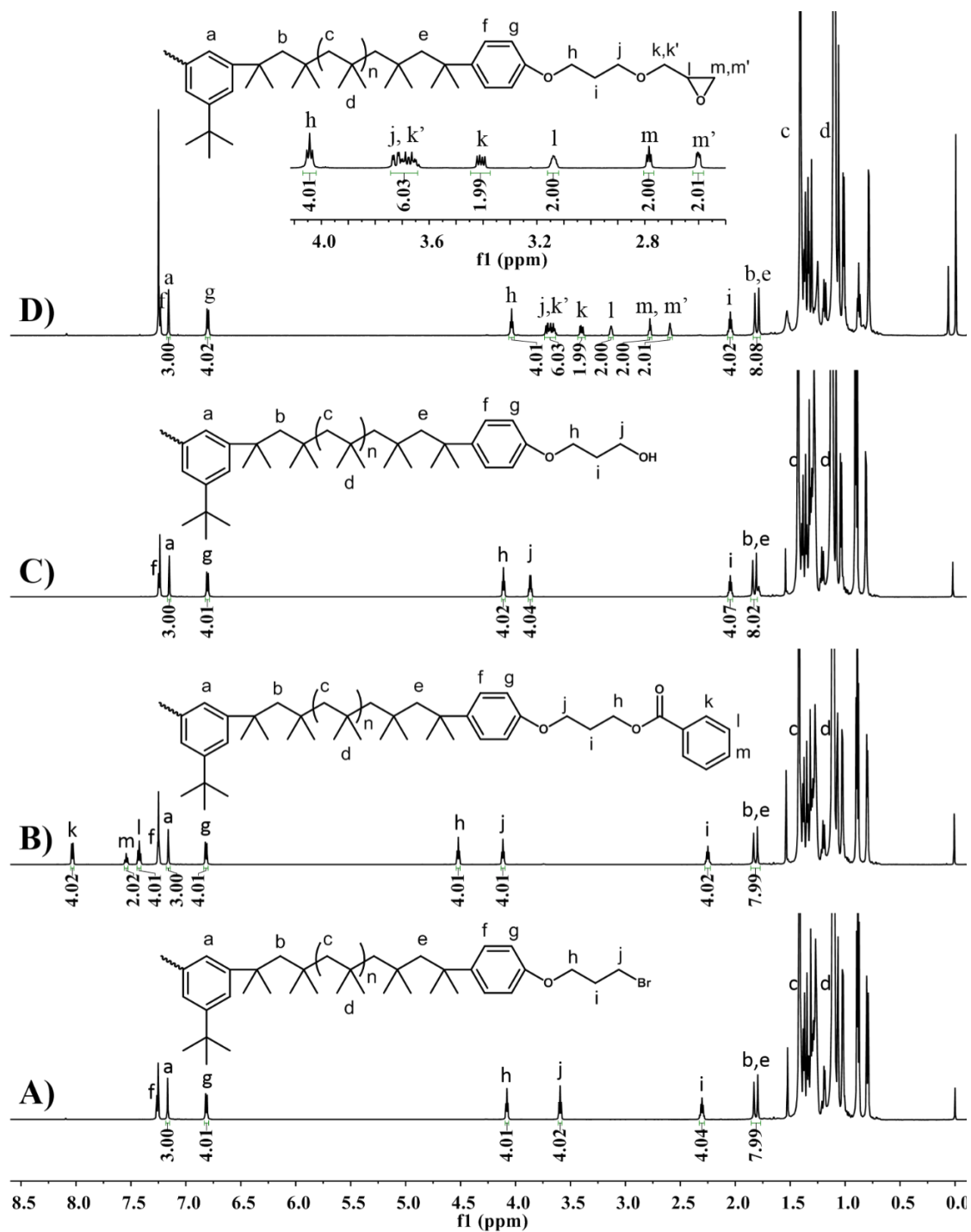
Figure 4.1 ^{1}H NMR (600 MHz, CDCl$_3$, 25°C) spectra of difunctional PIBs from Route A.

A) difunctional PIB-Br; B) difunctional PIB benzoate obtained by displacement of bromide with potassium benzoate; C) difunctional PIB-OH obtained by subsequent hydrolysis; and D) difunctional PIB aliphatic glycidyl ether obtained by Williamson ether synthesis of PIB alkoxide with epichlorohydrin.

146
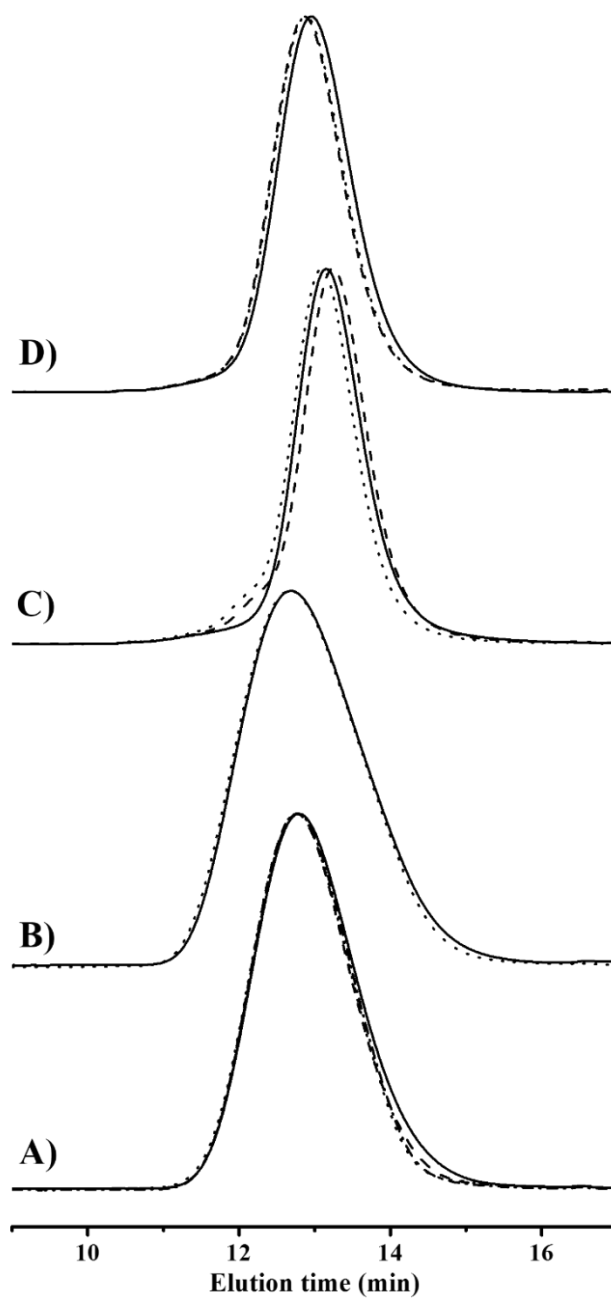
Figure 4.2 GPC refractive index traces of PIB epoxides and their starting and intermediate polymers.

A) difunctional PIB aliphatic glycidyl ether (dot), starting difunctional PIB bromide (solid), and intermediates PIB benzoate (dash dot) and PIB alcohol (dash); B) difunctional PIB phenyl glycidyl ether (dot) and starting PIB phenol (solid); C) difunctional PIB *exo*-olefin epoxide (dot), starting PIB chloride (solid) and PIB *exo* olefin (dash); D) difunctional PIB cyclohexene oxide (dot), starting PIB bromide (solid), and intermediate PIB cyclohexene (dash).

147
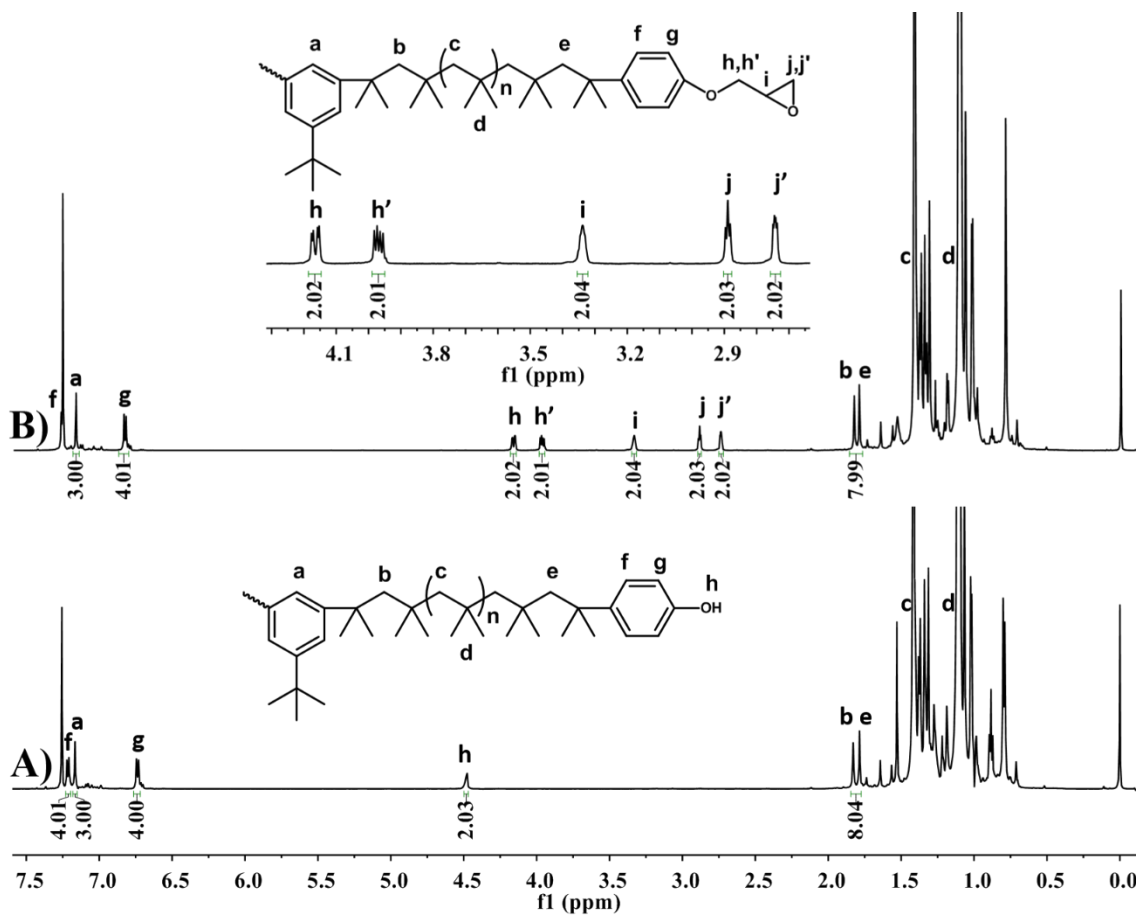
Figure 4.3 ^{1}H NMR (600 MHz, CDCl$_3$, 25°C) spectra of difunctional PIBs from Route B.

A) difunctional PIB phenol and B) difunctional PIB phenyl glycidyl ether obtained by reaction of PIB phenol with epichlorohydrin.
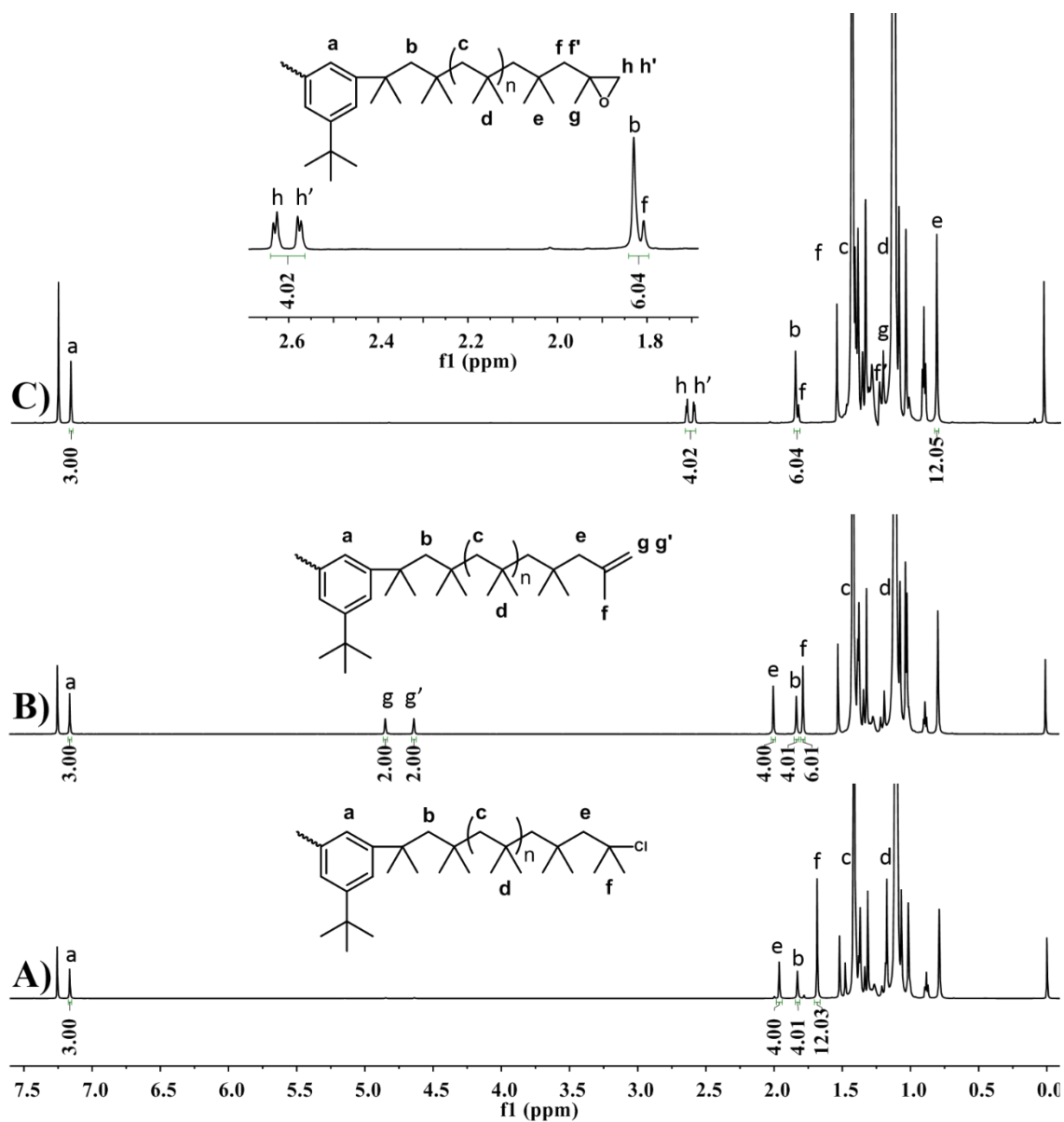
Figure 4.4 ^{1}H NMR (600 MHz, CDCl$_3$, 25 °C) spectra of difunctional PIBs from Route C.

A) difunctional PIB *tert*-chloride; B) difunctional PIB *exo*-olefin obtained by end-quenching living PIB with diisopropyl ether; and C) difunctional PIB *exo*-olefin epoxide obtained by epoxidation with *m*CPBA.

149
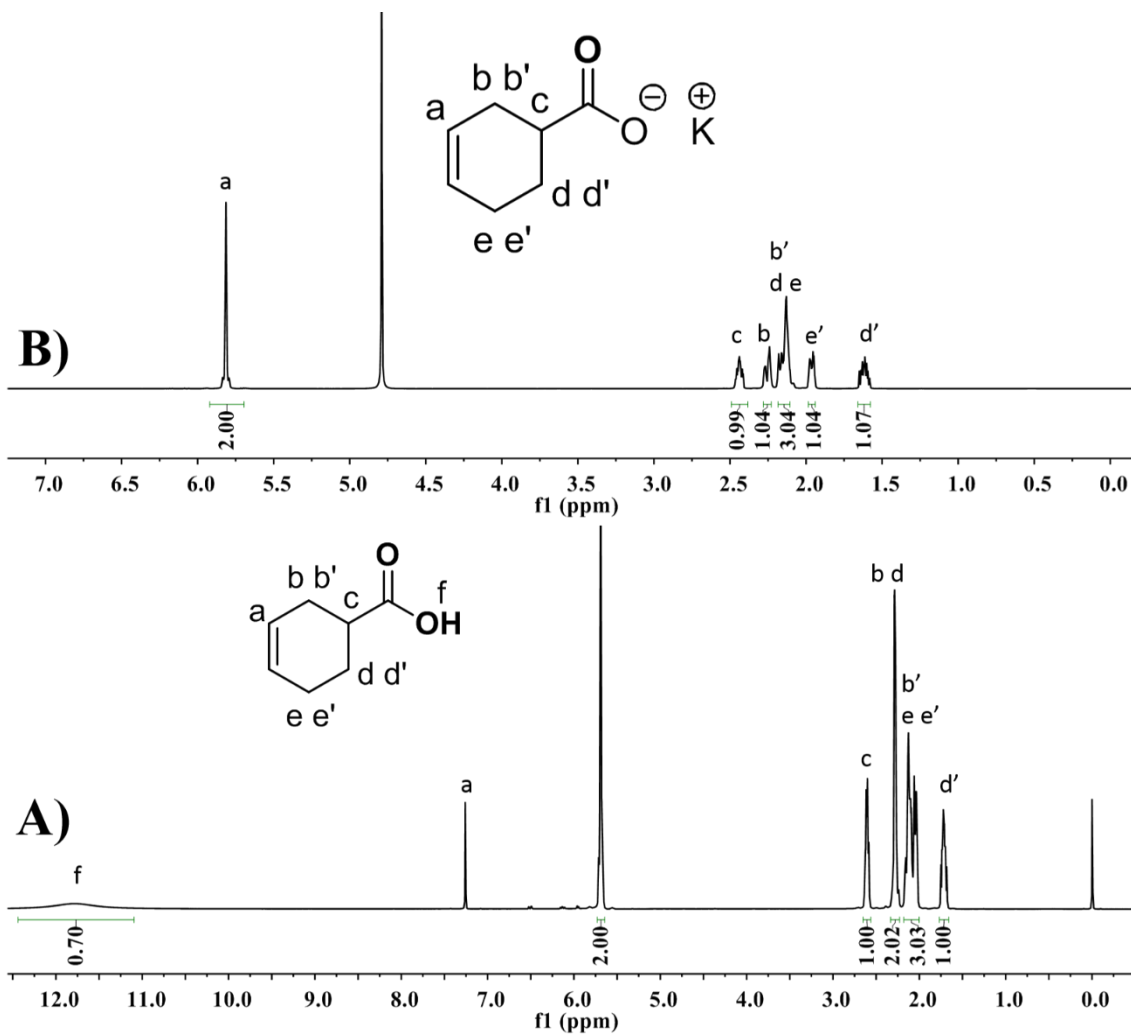
Figure 4.5 ^{1}H NMR spectra (600 MHz, 25 °C) of A) 3-cyclohexene-1-carboxylic acid (CDCl$_3$), and B) potassium cyclohexenecarboxylate (D$_2$O.)
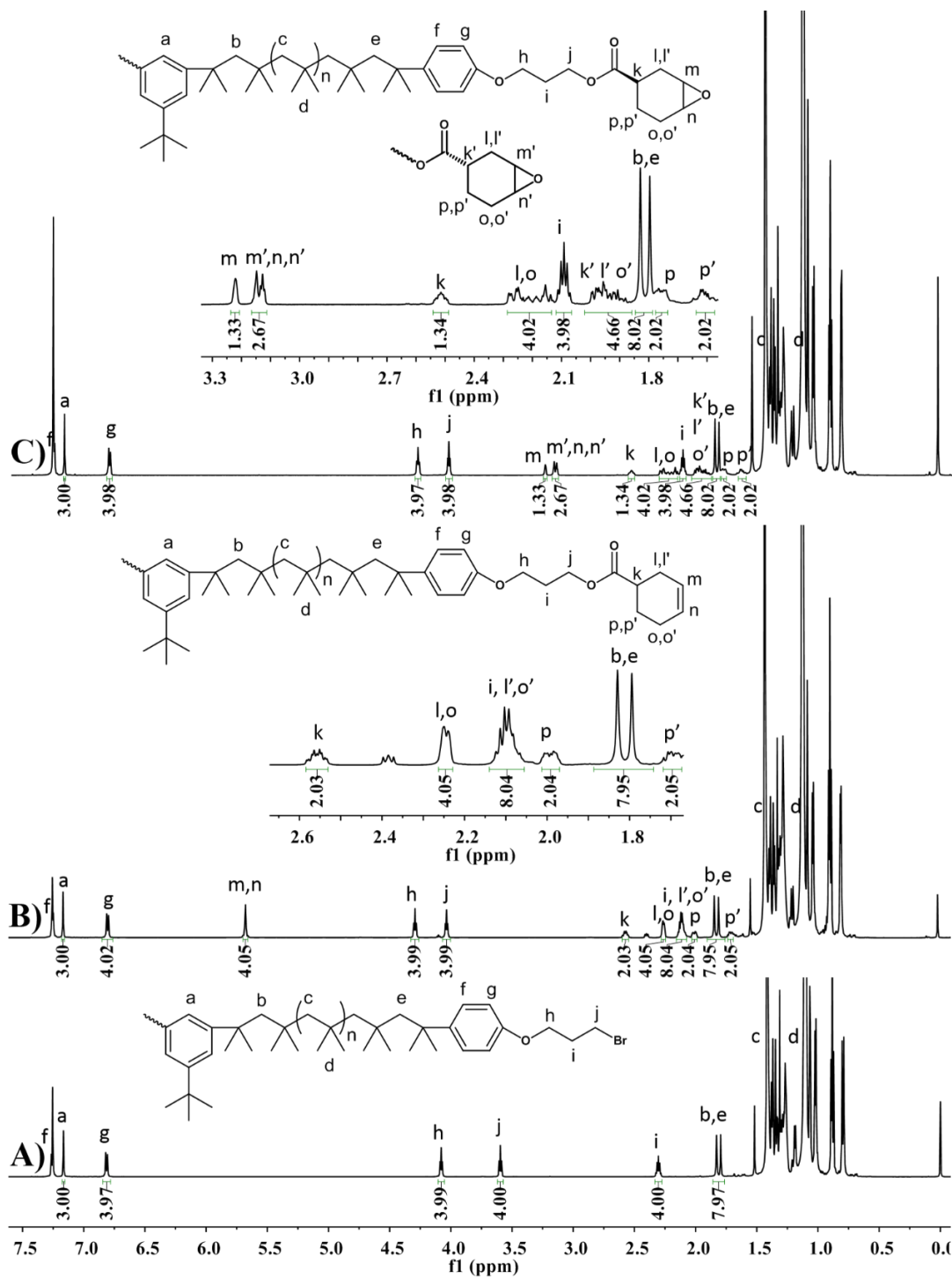
Figure 4.6 ^{1}H NMR (600 MHz, CDCl$_3$, 25 °C) spectra of difunctional PIBs from Route D.

A) difunctional PIB primary bromide; B) difunctional PIB *exo*-olefin obtained by displacement of bromide with potassium

cyclohexenecarboxylate; and C) difunctional PIB cyclohexene epoxide obtained by epoxation with *m*CPBA.

151

D)

C)
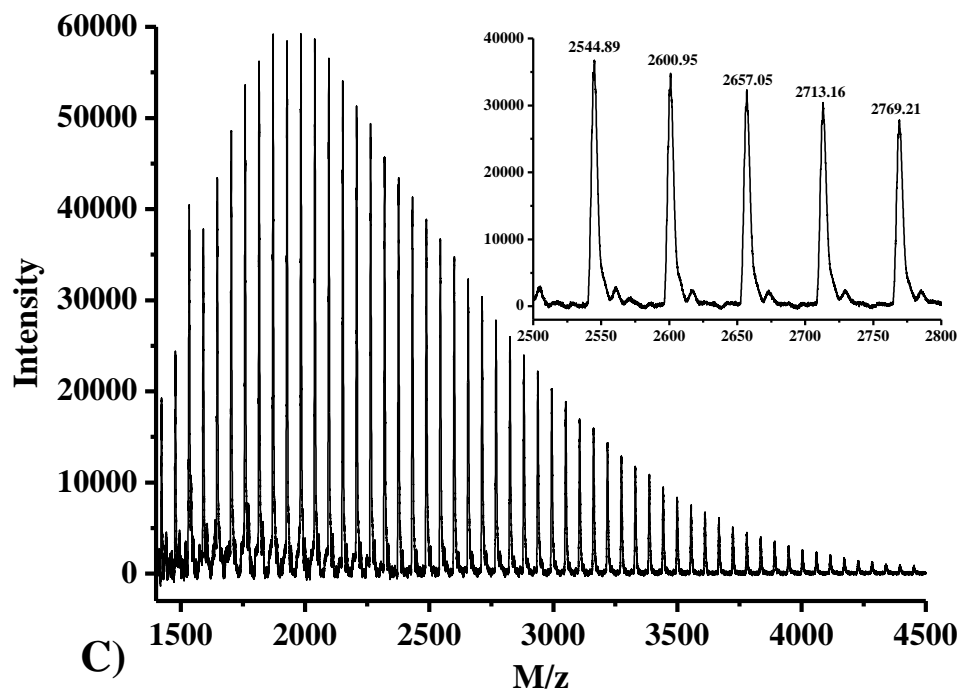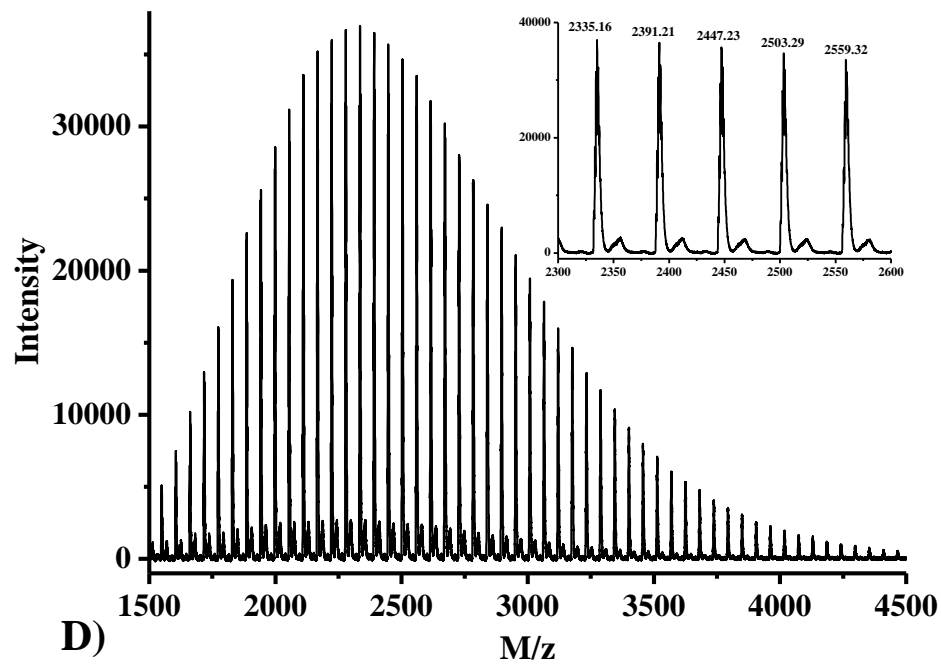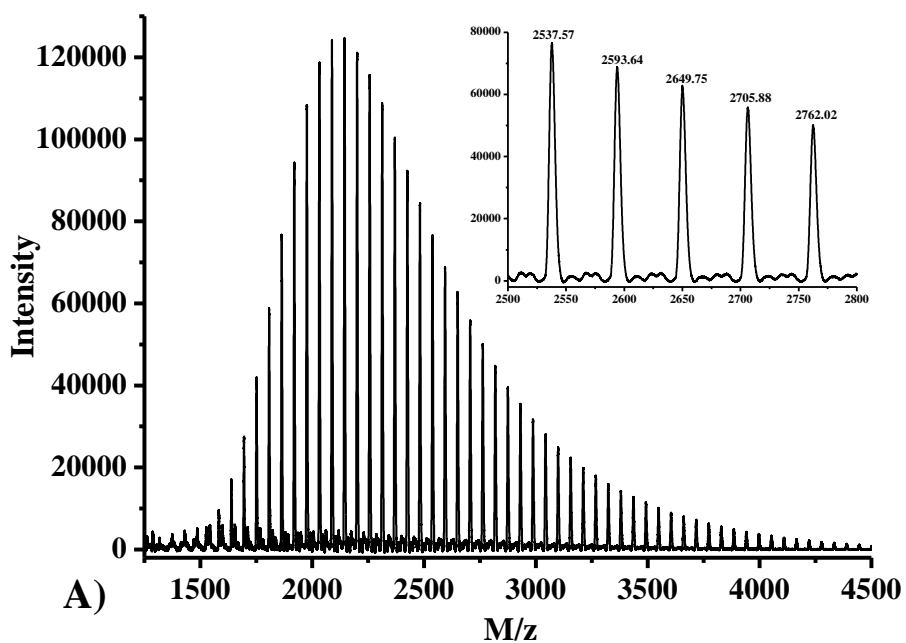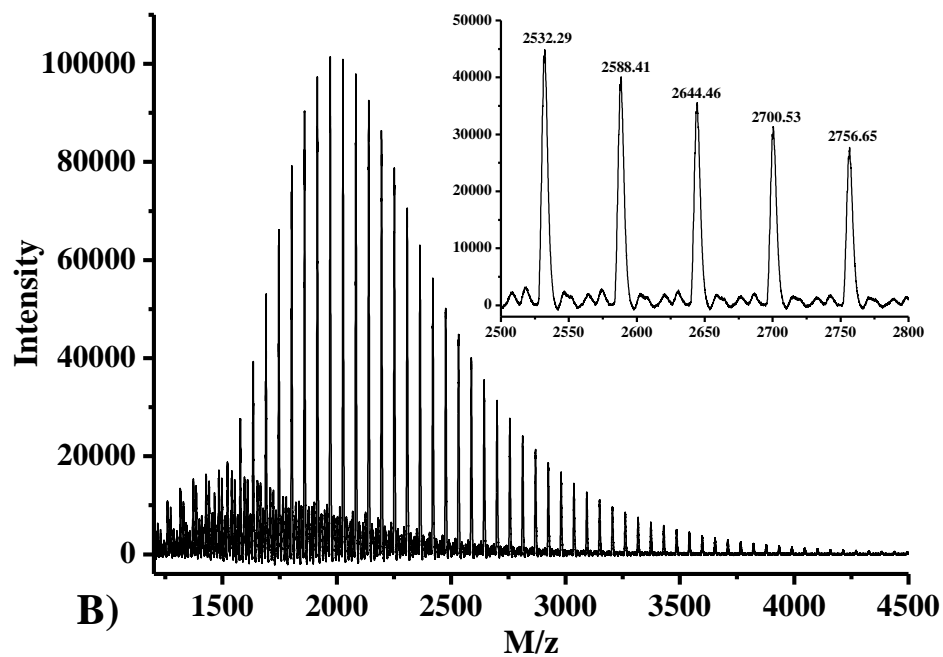
Figure 4.7 MALDI-TOF mass spectra of difunctional PIB epoxides.

A) 4K PIB aliphatic glycidyl ether, B) 3K PIB phenyl glycidyl ether, C) 4K PIB *exo*-olefin epoxide, and D) 4K PIB cyclohexene epoxide prepared by the dried droplet method using DCTB as the matrix, AgTFA as the cationizing agent, and THF as the solvent.

153

CHAPTER V – A NOVEL METHOD FOR SYNTHESIZING END-FUNCTIONAL

POLYISOBUTYLENES BY COPOLYMERIZING ISOBUTYLENE

WITH A STERIC HINDERED COMONOMER

5.1 Abstract

A novel method for chain end functionalization of polyisobutylene (PIB) was developed whereby living PIB is end-capped with the bulky comonomer, 4-(4-allyloxyphenyl)-2-methyl-1-butene (AMB) at full IB conversion. Addition is readily limited to one or two comonomer units per chain end through the use of a low [AMB]/[chain end] ratio. For [AMB]/[chain end] = 2, NMR showed that 1.2 comonomer units were added per PIB chain end, on average. Chain end structure and mechanism of formation were investigated by ^{1}H, ^{13}C, APT, DEPT, and HSQC NMR. *tert*-Chloride chain ends formed *via* PIB$^\oplus$Ti$_2$Cl$_9{}^S$ or PIB-AMB$^\oplus$Ti$_2$Cl$_9{}^S$ ion pair collapse were not observed. Olefinic chain ends formed *via β* H$^\oplus$ loss also were not detected. Instead, a cyclic end group structure was observed; upon addition of AMB the resulting carbocation tends to undergo terminative chain transfer consisting of alkylation of the 4-allyloxyphenyl ring at C2, *via* a five-membered cyclic intermediate. MALDI-TOF mass spectroscopy data indicated that no more than two comonomer units added to each chain end, as the mass spectrum consisted of only three major distinguishable distributions, structures possessing one AMB unit per chain end, one at one end and two at the other end, and two units at each chain end. MALDI-TOF-MS data confirmed the absence of *tert*-chloride and olefinic structures. GPC analysis indicated no chain fragmentation occurred during the end-capping reaction.

5.2 Introduction

Telechelic (end-functional) PIB oligomers are of great scientific and technological interest as intermediates to high-performance materials with applications in the areas of lubricant additives,[1] sealants and adhesives,[2] coatings,[3] biomaterials,[4] *etc*. With the development of living carbocationic polymerization, *in situ* functionalization of the living chain ends has greatly eased the production of end-functional polymers. *In situ* quenching of living PIB at full monomer conversion with a nucleophile that either induces elimination at[5-9] or addition to[10-21] the chain ends has been widely studied. To date, most successful quenchers that induce elimination to form *exo*-olefin PIB belong to three classes: hindered bases,[5] (di)sulfides,[6-8] and bulky ethers[9] (such as diisopropyl ether). While "hard" σ-nucleophiles such as unhindered alcohols or amines yield *tert*-chloride (*tert*-Cl) groups at the PIB chain end,[11] "soft" π-nucleophiles can be used to cap carbocations directly under living polymerization conditions to form functional chain ends other than *tert*-Cl.[18]

Three classes of π-nucleophiles have been successfully used to cap the chain ends of TiCl$_4$-catalyzed living PIB: non-homopolymerizable olefins (such as butadiene[10] or allyltrimethylsilane,[11-12]) heterocyclic aromatics,[13-17] and alkoxybenzenes.[18-21] It has been demonstrated that heterocyclic aromatics and alkoxybenzenes can undergo quantitative Friedel-Crafts alkylation with living PIB to effectively synthesize PIBs with various functional groups, such as bromide,[18,21] alcohol,[14,19] amine,[19] (meth)acrylate,[15] azide,[22] *etc.*, either by direct functionalization alone or in conjunction with subsequent post-polymerization modifications. However, these Friedel-Crafts alkylation reactions,

155

particularly those involving alkoxybenzenes, require a high concentration of $TiCl_4$

($[TiCl_4]$/[chain end] $\geq$2) to achieve acceptable rates of alkylation. In contrast, the living

carbocationic polymerization of IB requires only a low concentration of $TiCl_4$

($[TiCl_4]$/[chain end]$\leq$0.2). So ideally, it would be desirable to identify a type of

carbocationically polymerizable monomer that could be fitted with functional groups that

are non-reactive with $TiCl_4$ and that would add only once to the PIB chain end, thereby

acting as an end-capping agent. A monomer family such as this could enable a quenching

method that would eliminate the need for high concentrations of toxic and expensive

$TiCl_4$.

A typical type of sterically hindered monomer, 1,1-diphenylethylene (DPE) (and

its derivatives), can add only once to the chain end and has been widely used in living

radical[23] and anionic[24-25] polymerizations for chain end functionalization and preparation

of block copolymers and star polymers.[23-25] In carbocationic polymerization,

nonhomopolymerizable DPE derivatives have also been used for molecular design for

years.[26-28] For example, Muller *et al.*[27] reported synthesis of PIB-*b*-poly(butyl

methacrylate) (PIB-*b*-PBMA) and PIB-*b*-poly(methyl methacrylate) (PIB-*b*-PMMA) by

using PIB-DPE macroanions, which were obtained by capping the PIB chain end with

DPE, followed by metalation with Na/K or Cs alloy. Due to the low efficiency of

metalation and coupling reaction, Faust *et al.*[26,28] improved this method by using 1,3-

bis(1-phenylethenyl)benzene (meta-double DPE, MDDPE) or 1,4-bis(1-

phenylethenyl)benzene (para-double DPE, PDDPE) instead of mono DPE to cap the PIB

chain; the resulting adducts were then lithiated by *n*-butyllithium to form macroanions for preparation of block copolymers.

Another type of sterically hindered monomer is the family of 1-methyl-1-alkyl ethylenes (with an alkyl length ≥ 2C), whose reactivity or rate of carbocationic homopolymerization is generally inhibited, owning to the bulky alkyl group. Thus 1-methyl-1-alkyl ethylenes (alkyl ≥ 2C) have been used as comonomers with IB to cap the PIB chain end. To achieve effective capping, the number of consecutive additions of the comonomer to a given chain must be limited, and in many cases, the goal is a single addition. To approach this ideal, ion-pair collapse must be faster than propagation and essentially irreversible.[10] Strategies used to boost the rate of ion pair collapse have included lowering the Lewis acidity, decreasing the polarity of the solvent, and/or increasing the temperature.[29] To suppress the rate of propagation the monomer concentration must be low; however, if a single monomer charge is utilized, the minimum required stoichiometry between comonomer and growing chains may produce a comonomer concentration that is too high. In such cases, one must also employ starve-feed addition of the comonomer. Faust *et al.*[10] demonstrated that by lowering the concentration of the comonomer butadiene to around 0.05 M, a single 1,4-adduct was successfully capped to the living PIB chain end.

Bio-based cationically polymerizable monomers have gained significant recent interest from the standpoint of sustainable chemistry.[30] Raspberry ketone (Scheme 5.1A) is a naturally occurring phenolic compound known principally as the fruity aroma of red raspberries but also found in other fruits including cranberries and blackberries. Herein,

157

we describe reaction of raspberry ketone with methyltriphenylphosphonium bromide/NaH (Wittig reaction), as shown in Scheme 5.1A, to produce 4-(3-methylbut-3-en-1-yl)phenol, a common precursor to a new family of sterically hindered 1-methyl-1-alkylethylene monomers. As a representative example, we have synthesized allyl ether derivative, 4-(4-allyloxyphenyl)-2-methyl-1-butene, by reaction of the phenol with allyl bromide. To the best of our knowledge, this is the first report of the use of raspberry ketone derivatives as hindered, end-capping comonomers for synthesis of telechelic PIBs.
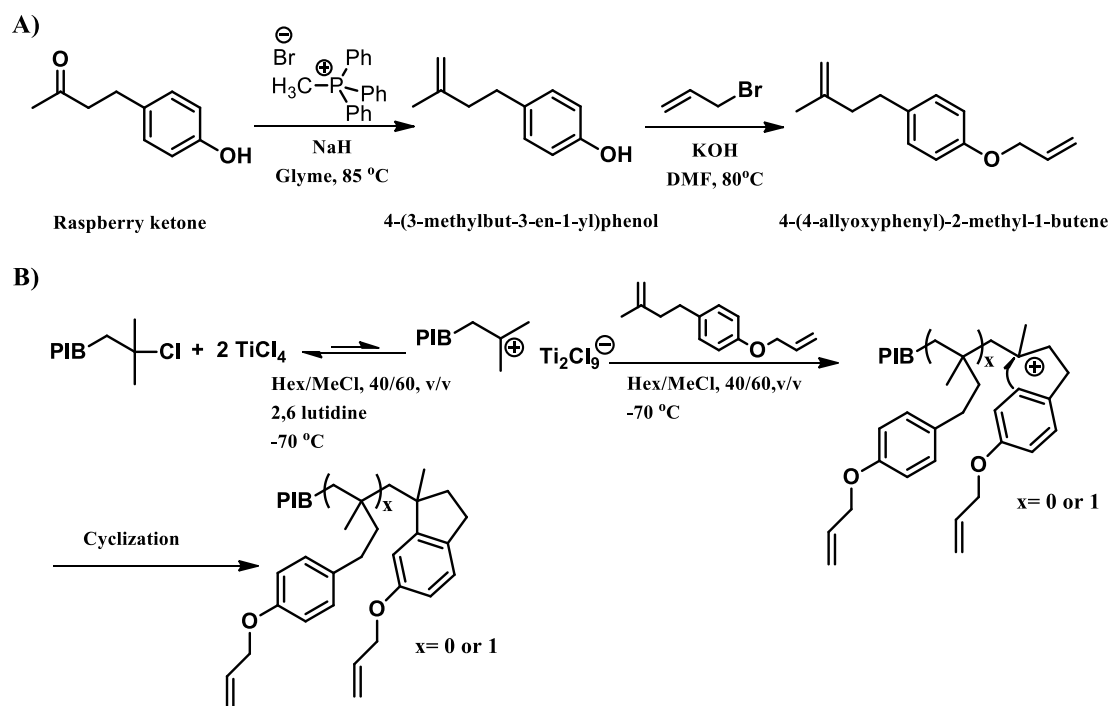
Scheme 5.1 Synthesis of A) allyloxyphenyl-functional comonomer, 4-(4-allyloxyphenyl)-2-methyl-1-butene and B) allyloxyphenyl-terminated PIB synthesized therefrom by end-capping living PIB at full IB conversion.

5.3 Experimental

Materials. Hexane (anhydrous, 95%), methanol (anhydrous, 99.8%), methylene chloride (anhydrous, 99.8%), titanium tetrachloride (TiCl$_4$) (99.9%), 2,6-lutidine

158

(99.5%), methyltriphenylphosphonium bromide (98%), sodium hydride (60% in mineral oil), 1,2-dimethoxyethane (anhydrous, 99.9%), allyl bromide (reagent plus, 99%), 4-(4-hydroxyphenyl)-2-butanone (raspberry ketone, 99%), tetrahydrofuran (THF) (anhydrous, 99.9%), chloroform (anhydrous, 99.9%), and dichloromethane-d_2 (CD_2Cl_2) were purchased from Sigma-Aldrich and used as received. Magnesium sulphate ($MgSO_4$) (anhydrous), diethyl ether (anhydrous), potassium hydroxide (KOH), dimethylformamide (DMF, HPLC, 99.9%), chloroform-d ($CDCl_3$) were purchased and used as received from Fisher Scientific. Isobutylene (IB, BOC Gases) and methyl chloride (Gas and Supply) were dried by passing the gasses through columns of $CaSO_4$/molecular sieves/$CaCl_2$ and condensed within a N_2-atmosphere glovebox immediately prior to use. The difunctional initiator, 5-*tert*-butyl-1,3-di(1-chloro-1-methylethyl)benzene (*t*-Bu-*m*-DCC), was synthesized as previously reported[31] and stored at 0 °C.

Instrumentation. Nuclear magnetic resonance (NMR) spectra were obtained using a 600 MHz Bruker AVANCE III NMR (TopSpin 3.1) spectrometer. All ^{1}H chemical shifts were referenced to TMS (0 ppm). Samples were prepared by dissolving the polymer in either chloroform-d or dichloromethane-d_2 (5-7%, w/v) and charging this solution to a 5 mm NMR tube. For quantitative integration, 16 transients were acquired using a pulse delay of 27.3 s. In all cases, the signal due to the phenyl protons of the initiator (7.17 ppm, 2H, singlet) was chosen as an internal reference for functionality analysis.

Number-average molecular weights ($\overline{M_n}$) and polydispersities (PDI = ($\overline{M_w}/\overline{M_n}$) were determined using a gel-permeation chromatography (GPC) system consisting of a

Waters Alliance 2695 separations module, an online multi-angle laser light scattering (MALLS) detector fitted with a gallium arsenide laser (power: 20 mW) operating at 658 nm (miniDAWN TREOS, Wyatt Technology Inc.), an interferometric refractometer (Optilab rEX, Wyatt Technology Inc.) operating at 35°C and 685 nm, and two PLgel (Polymer Laboratories Inc.) mixed E columns (pore size range 50-10^3 Å, 3 μm bead size). Freshly distilled THF served as the mobile phase and was delivered at a flow rate of 1.0 mL/min. Sample concentrations were ca. 15-20 mg of polymer/mL of THF, and the injection volume was 100μL. The detector signals were simultaneously recorded using ASTRA software (Wyatt Technology Inc.), and absolute molecular weights were determined by MALLS using a *dn/dc* calculated from the refractive index detector response and assuming 100% mass recovery from the columns.

Matrix-assisted laser desorption/ionization time-of-flight mass spectrometry (MALDI-TOF MS) was performed using a Bruker Microflex LRF MALDI-TOF mass spectrometer equipped with a nitrogen laser (337 nm) possessing a 60 Hz repetition rate and 50 µJ energy output. The PIB samples were prepared using the dried droplet method: separately prepared THF solutions of DCTB matrix (20 mg/mL), PIB sample (10 mg/mL), and AgTFA cationizing agent (10 mg/mL), were mixed in a volumetric ratio of matrix/sample/cationizing agent = 4:1:0.2, and a 0.5 µL aliquot was applied to a MALDI sample target for analysis. The spectrum was obtained in the positive ion mode utilizing the Reflector mode micro-channel plate detector and was generated as the sum of 900-1000 shots.

Synthesis of allyoxyphenyl-functional comonomer, 4-(4-allyloxyphenyl)-2-methyl-1-butene. Raspberry ketone was converted to 4-(3-methylbut-3-en-1-yl)phenol using a Wittig reaction performed using a modification of a literature procedure. [32] To an l L 3-neck round bottom flask, equipped with a reflux condenser, magnetic stirrer, and dry N_2 inlet and outlet, were charged with 500 mL dry glyme and 35.72 g (0.1 mol) of methyltriphenylphosphonium bromide, forming a milky suspension. Then 4.85 g of NaH (60% in mineral oil, 0.12 mol effective NaH) was added, and the mixture was stirred for 6 h at room temperature. Finally, 14.78 g (0.09 mol) of raspberry ketone was added. After 9 h of refluxing at 85 °C, the mixture was allowed to cool to room temperature, and DI water was added to neutralize excess NaH. The contents were extracted with diethyl ether, and the ether was removed by rotary evaporation yielding a brown oil, 4-(3-methylbut-3-en-1-yl)phenol.

4-(4-Allyloxyphenyl)-2-methyl-1-butene was next synthesized by reaction of 4-(3-methylbut-3-en-1-yl)phenolate with allyl bromide. Typically, 14.6 g (0.09 mol) of 4-(3-methylbut-3-en-1-yl)phenol, 15.6 mL (0.18 mol) of allyl bromide, and 10.1 g (0.18 mol) of KOH were combined in 200 mL of DMF and heated to reflux in a 80°C oil bath. After 16 h, the reaction was cooled, and the product was extracted into diethyl ether. The resulting solution was washed with deionized water and dried over $MgSO_4$. Removal of ether using rotary evaporation yielded a brown oil and some white crystals identified as triphenylphosphine oxide. The latter is slightly soluble in the intermediate phenol but insoluble in the less polar 4-(4-allyloxyphenyl)-2-methyl-1-butene. The brown oil was purified by trituration with hexane. Removal of hexane gave a yellow oil. The yellow oil

161

was vacuum distilled, and the fraction distilling around 140°C was collected to provide 10.3 g of a colorless liquid (yield 56.6%.)

Synthesis of allyoxyphenyl-terminated PIB. Copolymerization reactions were performed within a N_2-atmosphere glovebox equipped with cryostated heptane bath. Various conditions were investigated including solvent polarity, temperature, and comonomer/chain end ratio. A typical procedure for synthesis of difunctional allyoxyphenyl-terminated-PIB was as follows: To a 500 mL 4-neck round-bottom flask, equipped with an overhead stirrer, thermocouple, and ReactIR probe, and immersed in the heptane bath, were added 70 mL hexane, 105 mL methyl chloride, 0.117 mL (1.00 mmol) 2,6-lutidine, 1.44 g (5.00 mmol) *b*DCC, and 24.2 mL (16.9 g, 0.301 mol) IB. The mixture was equilibrated to -70°C with stirring, and polymerization was initiated by the addition of 0.23 mL (2.2 mmol) $TiCl_4$, followed by a second addition of 0.23mL after 8 min. Full monomer conversion was reached in 45 min according to FTIR data. At full monomer conversion, 4.05g (20.0 mmol) 4-(4-allyloxyphenyl)-2-methyl-1-butene comonomer was charged to the reaction (2 eq per chain end). The copolymerization was allowed to proceed for 3 h. At the end of this time, the catalyst was destroyed by addition of excess pre-chilled methanol. The contents of the reaction flask were allowed to warm to room temperature, and after evaporation of methyl chloride, the polymer solution was washed with methanol and then collected by precipitation into methanol. The precipitate was collected by redissolution in fresh hexane; the solution was washed with DI water, dried over $MgSO_4$, and then vacuum stripped. Residual solvent was removed under vacuum at 40°C to yield pure phenyl allyl ether terminated PIB.

162

5.4 Results and Discussion

Synthesis of 4-(4-allyloxyphenyl)-2-methyl-1-butene comonomer. The Wittig

reaction provides the convenient preparation of an alkene by reaction of an aldehyde or

ketone with an ylide generated from a phosphonium salt. ^{1}H NMR was used to

characterize the starting material, raspberry ketone (Figure 5.1A), and the intermediate,

"raspberry olefin" (Figure 5.1B.) Formation of the olefin was revealed by the appearance

of olefinic proton resonances at 4.70 ppm (doublet), and upfield shift of methyl group

(from 2.14 to 1.74 ppm). Several major resonances are present in the 7.39-7.76 ppm

region of the spectrum, due to the phenyl protons of triphenylphosphine oxide (TPPO), a

by-product of the Wittig reaction that is known to be hard to remove. The boiling point of

the obtained "raspberry olefin" is above 260°C, which suggests that distillation even

under high vacuum might require excessively high temperature. It was therefore decided

to proceed to the next step without separation of TPPO, which should not interfere with

the allylation reaction. It was also expected that introduction of the ally group will

decrease the polarity and boiling point, which will ease the purification process.

4-(4-Allyloxyphenyl)-2-methyl-1-butene comonomer was finally achieved by

allylation using allyl bromide. Evidence of formation of 4-(4-Allyloxyphenyl)-2-methyl-

1-butene was given by the disappearance of the phenolic proton resonance at 8.47 ppm,

as well as the appearance of resonances at 6.05 (octet), 5.40 and 5.27 (doublet of

doublets), and 4.51 ppm (doublet) due to the addition of the allyl moiety, as shown in

Figure 5.1C.

Synthesis of allyloxyphenyl-terminated PIB. Scheme 5.1B shows the route for end-capping of living PIB with the sterically hindered comonomer, 4-(4-allyloxyphenyl)-2-methyl-1-butene. The end-capped product, allyloxyphenyl-terminated PIB, was obtained by directly charging an excess (2 equiv per chain end) of 4-(4-allyloxyphenyl)-2-methyl-1-butene to TiCl$_4$-catalyzed living polyisobutylene in 40/60 (v/v) hexane/methyl chloride at -70 °C. The comonomer was added immediately upon reaching complete IB conversion as indicated by FTIR monitoring (at least 6 but not more than 10 monomer half-lives), to avoid possible spontaneous termination processes such as chain end rearrangement. Figure 5.2B shows the ^{1}H NMR spectrum of the resulting PIB bearing allyloxyphenyl end groups after 3 h of reaction.

Evidence of the formation of the copolymerized product was given by the appearance of chemical shifts of the comonomer moiety, including resonances at 2.01 and 2.13 (both singlets), 3.30 and 3.78 (both doublets), 4.51 (doublet), 5.26 (doublet), 5.40 (doublet), 6.04 (octet), 6.83 (doublet), and 7.08 ppm (doublet) due to the allyloxyphenyl moieties. Significantly, the spectrum shows no evidence of unreacted (un-capped) PIB chain ends. If these chain ends were present, they would appear either in the form of *tert*-Cl, characterized by resonances at 1.68 and 1.96 ppm due to the *gem*-dimethyl and methylene protons adjacent to the chloride group or as *exo* or *endo* olefin, characterized by olefinic proton resonances in the 4.6-5.2 ppm range. Integration of the allyloxyphenyl resonances (see integration data, Figure 5.2B) in comparison with the aromatic initiator resonance at 7.17 ppm indicated an average of 1.22 comonomer units per chain end group. Thus, most chain ends were capped with a single comonomer unit,

164

but a small fraction of the chain ends were capped with two consecutive comonomer units.

No further comonomer addition to the chain end was observed after 3 h, even though a significant amount of comonomer remained unreacted (i.e., 2-1.22 = 0.78 comonomer units per chain end remained). This suggests operation of an absolute termination mechanism during polymerization of AMB. This mechanism cannot be collapse of $AMB^{\oplus}Ti_2Cl_9{}^{\mathsf{S}}$ ion pairs because even if irreversible, this mechanism would form *tert*-chloride end groups, which were not observed. It is also evident from the spectrum that termination cannot involve β-H abstraction to form olefin chain ends since no olefinic proton peaks were observed.

Consideration of the carbocationic polymerization of styrenic monomers provided a suggestion as to the nature of the termination mechanism. For styrenic monomers, if the concentration of monomer is low, chain transfer to counterion by electrophilic aromatic substitution (EAS) at the penultimate phenyl ring may occur via a cyclic transition, a process termed "backbiting." Several features of the AMB comonomer and the process suggested that a similar mechanism was operable here. A two-carbon tether separates the alkene and the phenyl ring, which provides for an entropically favorable 5-membered transition for EAS. The allyloxy group causes the ring to be strongly activated toward EAS. With regard to process conditions, comonomer concentration is low in order to limit homopolymerization, and the presence of the proton trap 2,6-lutidine would render the reaction irreversible. Thus we propose that a backbiting-type mechanism, as shown in Scheme 5.1B), might occur with AMB to terminate the polymerization by forming a

165

stable five-membered ring product. Since homopolymerization is competitive with backbiting, low monomer concentration as used herein favors the latter reaction. In fact, for most chains backbiting indeed occurred after only one comonomer addition; however, approximately 22% of the chains were able to add a second unit before backbiting occurred. It is possible that a small fraction of chains achieved three (or more) comonomer additions prior to backbiting, but as we will report, the concentration of such products is below the level of detection. Thus, for the difunctional polymers produced here, we propose that the final end-capped product is a mixture of three species. The dominant species possesses a single, cyclized AMB unit at each chain end. A first minor species possesses a single, cyclized AMB unit at one chain end and two AMB units at the other chain end, with the penultimate unit homopolymerized and the ultimate unit cyclized. A second minor species possesses two AMB units at each chain end, one homopolymerized and one cyclized.

^{13}C, APT, and 2D gradient HSQC and HMBC NMR were used to confirm the proposed structure of the copolymerized product and to validate the reaction mechanism. APT (Figure 5.3) distinguishes carbon atoms with respect to number of attached hydrogen nuclei; methyl and methine carbons (odd number of hydrogen nuclei) display a positive signal and methylene and quarternary carbons (even number of hydrogen nuclei) display a negative signal. 2D HSQC (Figure 5.4) identifies direct (one-bond) C-H correlations. In the aromatic region of the HSQC spectrum (Figure 5.4B), besides the phenyl ring of the initiator residue, cross peaks 7.08 and 129.4 ppm, 6.82 and 114.8 ppm, 6.92 and 129.3 ppm, 6.04 and 133.7 ppm, 5.40 and 117.5 ppm, 5.25 and 117.6 ppm are

166

connected. In the aliphatic region (Figure 5.4A) cross peaks, 3.30 and 34.0 ppm, 2.00 and 56.0 ppm, 2.10 and 55.6 ppm, 1.83 and 59.0 ppm, 1.62 and 32.2 ppm are connected. In HMBC, Figure 5.5. 1-bond C-H correlations are removed, and only 2- and higher-bond correlations are shown. One signature aromatic CH (chemical shift r in the ^{1}H NMR and chemical shift 25 in the APT NMR) showed correlations at 6.92, 6.82, 3.30, and 2.00 ppm; while a corresponding aromatic CH from the homopolymerized comonomer unit, chemical shift i in the ^{1}H NMR and chemical shift 13 in the APT NMR, showed correlations at 7.08, 6.82, and 2.10 ppm. Such differences provided strong evidence that the aliphatic moiety adjacent to the phenyl ring of an AMB unit is dramatically different between two consecutive AMB units at a single chain end; the proposed five-membered ring within the ultimate AMB unit is perfectly consistent with these data. Furthermore, the downfield shift of the two methylene groups adjacent to the phenyl allyl ether was in turn due to the electron withdrawing effect of the aromatic ring since they were brought into closer proximity.

Effect of solvent polarity on the chain end functionality was studied by repeating end-capping experiments in two less polar solvent systems, 50/50 and 60/40 (v/v) Hex/MeCl. As solvent polarity was decreased, the number of comonomer units added to each chain end decreased only slightly, at the expense of longer reactions time. For example, the average number of comonomer units added to each chain end in 50/50 (v/v) Hex/MeCl system reached 1.10 after 8 h; while it reached 1.08 after 15 h in the 50/50 (v/v) Hex/MeCl system.

Figure 5.6 shows GPC traces for difunctional PIB immediately prior to addition of 4-(4-allyloxyphenyl)-2-methyl-1-butene and after copolymerization. Number-average molecular weights (and polydispersities) calculated from the chromatograms were 3.4×10^3 g/mol (PDI=1.22) immediately before and 4.3×10^3 g/mol (PDI=1.20) after copolymerization. The chromatograms slightly shifted to lower elution volume after copolymerization due to the addition of the bulky comonomer unit.

End group analysis. MALDI-TOF MS provided definition evidence for the proposed mechanism of end-capping. The MALDI-TOF mass spectra of 4K allyloxyphenyl PIB are shown in Figure 5.7. The sample displayed three major distributions of polymeric species, each distribution associated with Ag cations from the AgTFA cationizing agent, differing from each other only by the number of isobutylene repeat units. The data from each distribution were analyzed by linear regression of a plot of mass-to-charge ratio (M/z, assumed to be 1), measured at the maximum of each peak of the major distribution, versus degree of polymerization (DP), Figure 5.8. The slope of each plot is theoretically equivalent to the exact mass of the isobutylene repeat unit, 56.06 Da. The *y*-intercept is theoretically equivalent to $f \times EG + I + C$, where f is the functionality of the polymer (2 for mono addition at each chain end, 3 for mono addition at one chain end and double addition at the other chain end, 4 for double addition at each PIB chain end); EG is the exact mass of the comonomer, 4-(4-allyloxyphenyl)-2-methyl-1-butene; I is the exact mass of the *b*DCC initiator residue; and C is the exact mass (106.91 Da) of the major isotope of the associated Ag cation.

MALDI-TOF MS data for each distribution of 4K allyloxyphenyl PIB, analyzed in this manner, are summarized in Table 5.2. In all cases, the measured value of the repeat unit molecular weight (M_{ru}) was within 0.1% of the theoretical value (56.06 Da), and the measured value of $f \times EG+I+C$ was within 0.2% of the theoretical value. The observed close agreement between measured and theoretical values provides strong evidence that 1) a maximum of two comonomer units added to any given PIB chain end indicating that backbiting/cyclization is kinetically favored relative to comonomer homopolymerization, and 2) other termination mechanisms, particularly ion pair collapse to form *tert*-chloride chain ends, were absent.

Table 5.2 also lists M_n and PDI data obtained from MALDI-TOF-MS. In all cases, these values are lower than the corresponding values obtained from GPC analysis (Table 5.1). This is a common observation and reflects the fact that polymer chains with higher molecular weight are more difficult to desorb/ionize and thus are under-represented at the detector.

5.5 Conclusions

We have demonstrated that copolymerization of a sterically hindered comonomer, 4-(4-allyloxyphenyl)-2-methyl-1-butene, with living PIB at full IB monomer conversion produces allyloxyphenyl-terminated PIB. Owing to the bulkiness of the comonomer, combined with a low comonomer concentration, homopolymerization of the comonomer was limited. Under these conditions, termination by EAS backbiting of the carbocation at the *ortho* position of the aromatic ring, to form a five-membered ring, is kinetically favorable relative to comonomer homopolymerization. MALDI-TOF mass spectral

analysis provided strong evidence that a maximum of two comonomer units are added to a given PIB chain end. The advantage of this method is that telechelic PIB prepolymers can be achieved *via* copolymerization, which avoids the high Lewis acid concentrations typically required for other chain end functionalization methods, particularly alkylation of alkoxybenzenes. The obtained allyloxyphenyl PIB is a valuable intermediate toward several products including primary hydroxyl PIB (via hydroboration/oxidation) and phenyl glycidyl ether PIB *via* direct epoxidation with *m*CPBA, or it may be used directly in thiol-ene "click" chemistry to form networks or for further chain end functionalization.

Finally, AMB represents only one example of a family of comonomers that may be produced from the intermediate 4-(3-methylbut-3-en-1-yl)phenol. The phenolic moiety enables the ready preparation, via the Williamson route, of many sterically hindered comonomers with various functional groups for synthesis of telechelic PIB prepolymers other than phenyl allyl ether functionality.

5.6 Acknowledgements

5.7 References

(1)   Hancsók, J.; Bartha, L.; Baladincz, J.; Kocsis, Z., *Lubr. Sci.* **1999,** *11* (3), 297-

310.

(2)   Wang, K. S.; Osborne, J. L.; Hunt, J. A.; Nelson, M. K., Google Patents: 1996.

(3)   Tripathy, R.; Ojha, U.; Faust, R., *Macromolecules* **2011,** *44* (17), 6800-6809.

(4)   Puskas, J. E.; Chen, Y.; Dahman, Y.; Padavan, D., *J. Polym. Sci., Part A: Polym.
Chem.* **2004,** *42* (13), 3091-3109.

(5)   Simison, K. L.; Stokes, C. D.; Harrison, J. J.; Storey, R. F., *Macromolecules*
2006, *39* (7), 2481-2487.

(6)   Morgan, D. L.; Stokes, C. D.; Meierhoefer, M. A.; Storey, R. F., *Macromolecules*
2009, *42* (7), 2344-2352.

(7)   Ummadisetty, S.; Morgan, D. L.; Stokes, C. D.; Storey, R. F., *Macromolecules*
2011, *44* (20), 7901-7910.

(8)   Ummadisetty, S.; Morgan, D. L.; Stokes, C. D.; Harrison, J. J.; Campbell, C. G.;
Storey, R. F., *Macromol. Symp.* **2013,** *323* (1), 6-17.

(9)   Ummadisetty, S.; Storey, R. F., *Macromolecules* **2013,** *46* (6), 2049-2059.

(10)   De, P.; Faust, R., *Macromolecules* **2006,** *39* (20), 6861-6870.

(11)   Ivan, B.; Kennedy, J. P., *J. Polym. Sci., Part A: Polym. Chem.* **1990,** *28*, 16.

(12)   Roth, M.; Mayr, H., *Macromolecules* **1996,** *29* (19), 6104-6109.

(13)   Martinez-Castro, N.; Morgan, D. L.; Storey, R. F., *Macromolecules* **2009,** *42* (14),
4963-4971.

(14)   Morgan, D. L.; Storey, R. F., *Macromolecules* **2010,** *43* (3), 1329-1340.

(15)   Hadjikyriacou, S.; Faust, R., *Macromolecules* **1999,** *32* (20), 6393-6399.

(16)   Martinez-Castro, N.; Lanzendörfer, M. G.; Müller, A. H. E.; Cho, J. C.; Acar, M. H.; Faust, R., *Macromolecules* **2003,** *36* (19), 6985-6994.

(17)   Storey, R. F.; Stokes, C. D.; Harrison, J. J., *Macromolecules* **2005,** *38* (11), 4618-4624.

(18)   Morgan, D. L.; Storey, R. F., *Macromolecules* **2009,** *42* (18), 6844-6847.

(19)   Morgan, D. L.; Martinez-Castro, N.; Storey, R. F., *Macromolecules* **2010,** *43* (21), 8724-8740.

(20)   Roche, C. P.; Brei, M. R.; Yang, B.; Storey, R. F., *ACS Macro Lett.* **2014,** *3* (12), 1230-1234.

(21)   Yang, B.; Storey, R. F., *Polym. Chem.* **2015,** *6* (20), 3764-3774.

(22)   Döhler, D.; Michael, P.; Binder, W. H., *Macromolecules* **2012,** *45* (8), 3335-3345.

(23)   Hirao, A.; Hayashi, M.; Loykulnant, S.; Sugiyama, K.; Ryu, S.; Haraguchi, N.; Matsuo, A.; Higashihara, T., *Prog. Polym. Sci.* **2005,** *30* (2), 111-182.

(24)   Higashihara, T.; Sakurai, T.; Hirao, A., *Macromolecules* **2009,** *42* (16), 6006-6014.

(25)   Hirao, A.; Inoue, K.; Higashihara, T.; Hayashi, M., *Polym. J.* **2008,** *40* (10), 923-941.

(26)   Higashihara, T.; Feng, D.; Faust, R., *Macromolecules* **2006,** *39*, 5275-5279.

(27)   Feldthusen, J.; Iván, B.; Müller, A. H. E., *Macromolecules* **1998,** *31* (3), 578-585.

(28)   Cho, J. C.; Cheng, G.; Feng, D.; Faust, R.; Richard, R.; Schwarz, M.; Chan, K.; Boden, M., *Biomacromolecules* **2006,** *7*, 11.

(29)   Sipos, L.; De, P.; Faust, R., *Macromolecules* **2003,** *36* (22), 8282-8290.

(30)   Aoshima, S.; Kanaoka, S., *Chem. Rev.* **2009,** *109* (11), 5245-5287.

(31)   Storey, R. F.; Choate, K. R., *Macromolecules* **1997,** *30* (17), 4799-4806.

(32)   Kennedy, J. P.; Ross, L. R.; Lackey, J. E.; Nuyken, O., *Polym. Bull. 4* (1), 67-74.

5.8 Tables and Figures for Chapter V

Table 5.1

Molecular weight and polydispersity of difunctional *tert*-Cl PIB and allyloxyphenyl PIB.

Sample	M_n (g/mol)	PDI
PIB-di-Cl	3,400	1.22
PIB phenyl allyl ether	4,300	1.20

Table 5.2

MALDI-TOF MS data of 4K allyloxyphenyl PIB[a]

Component	MW_{theo} $f\times EG+I+C$[b]	MW_{exp} $f\times EG+I+C$	Diff.	M_n	PDI	M_{ru}[c]
1 [raspberry]/[CE]	727.31	727.86	0.55	1666	1.07	56.11
1.5 [raspberry]/[CE]	929.51	930.15	0.64	2011	1.04	56.13
2 [raspberry]/[CE]	1131.65	1134.25	2.60	2234	1.06	56.08

[a]Unit for molecular weight is Da; [b]*f*=chain end functionality, EG = end group, I = initiator, C = Ag cation; [c]ru is repeat unit.
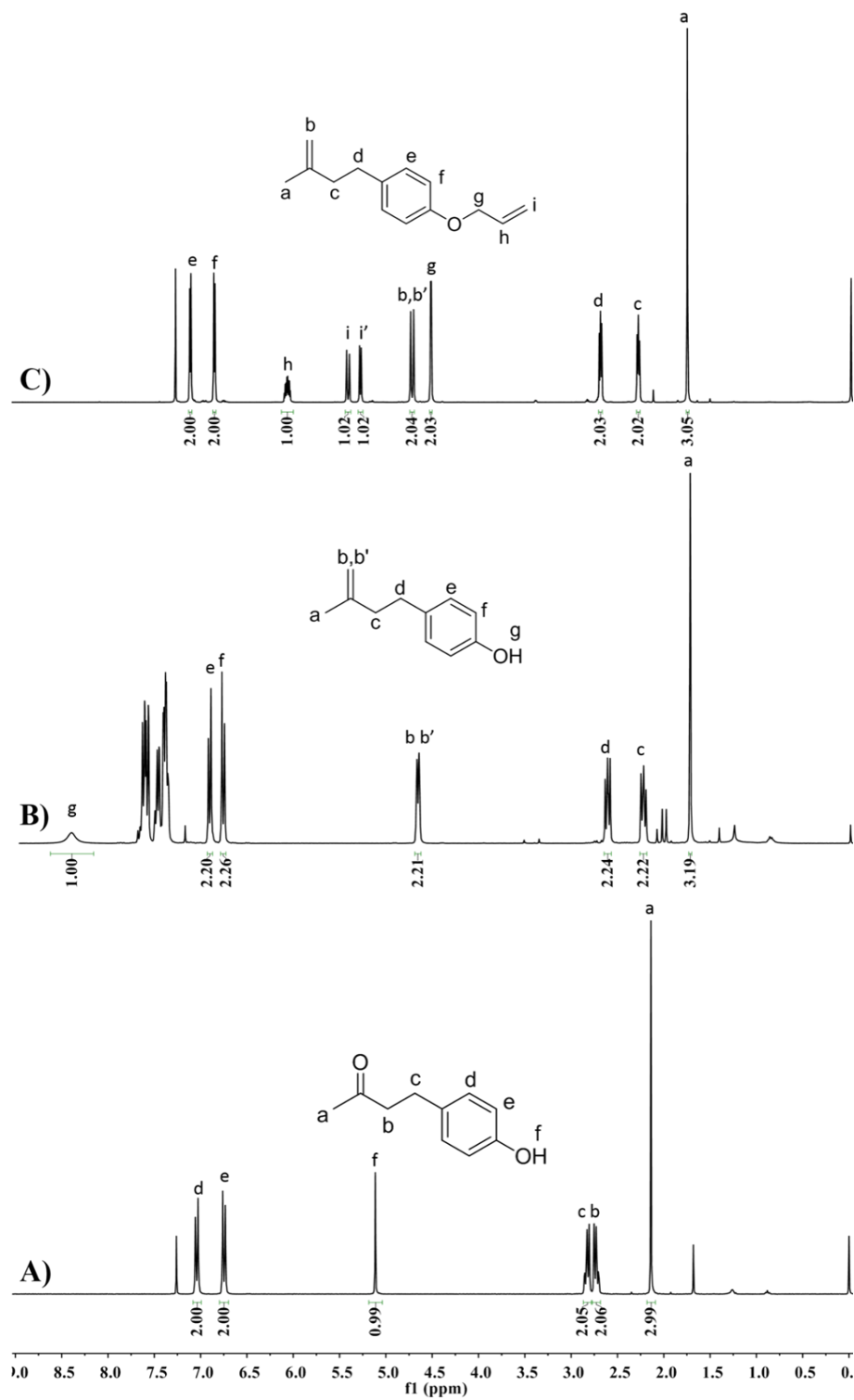
Figure 5.1 ^{1}H NMR (600 MHz, CDCl$_3$, 25°C) spectra of A) raspberry ketone, B) "raspberry olefin"(4-(3-methylbut-3-en-1-yl)phenol), and C) 4-(4-allyloxyphenyl)-2-methyl-1-butene.

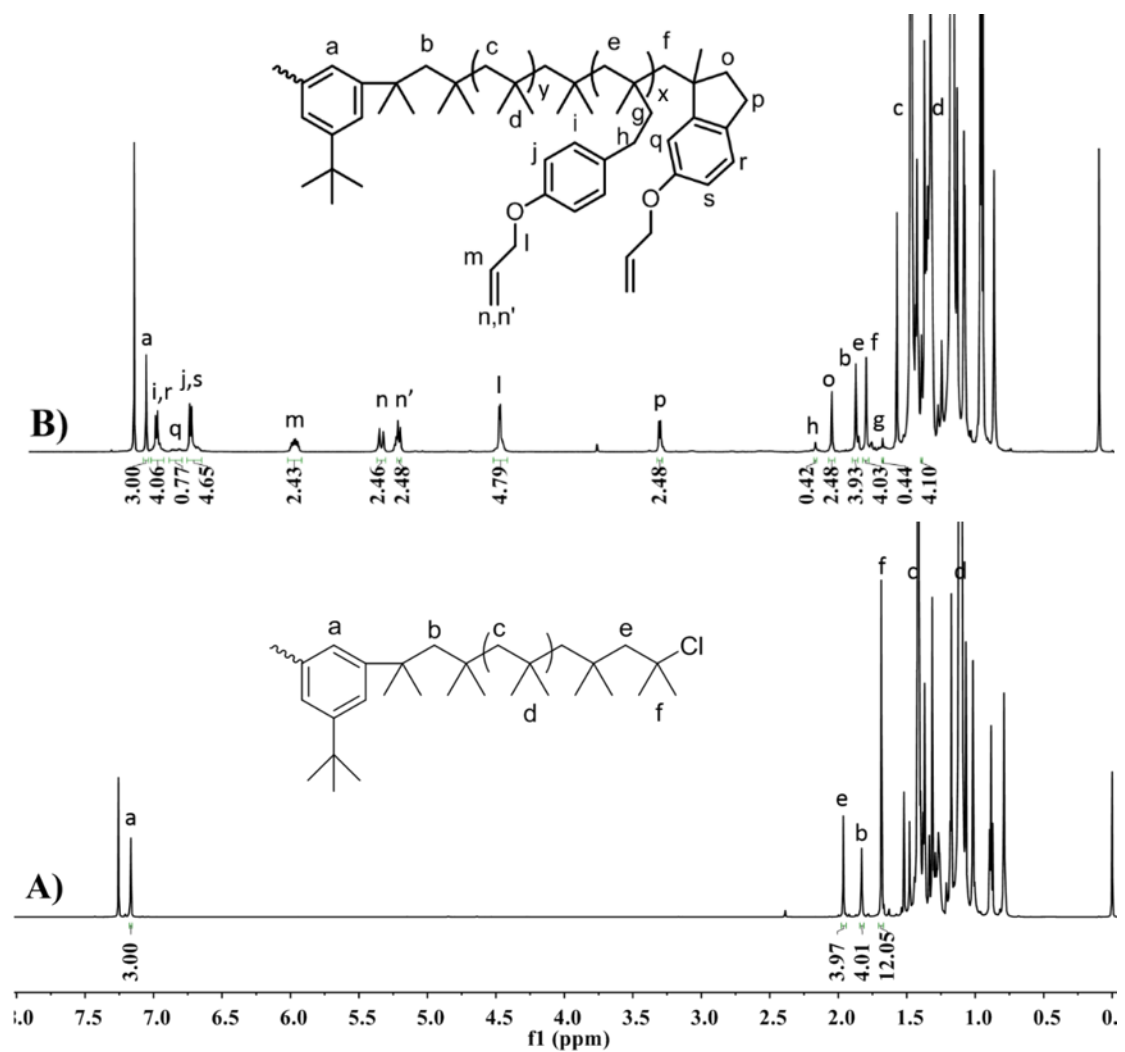Figure 5.2 ^{1}H NMR (600 MHz, CDCl$_3$, 25°C) spectra of A) difunctonal *tert*-Cl terminated PIB and B) allyoxyphenyl-terminated PIB.

176

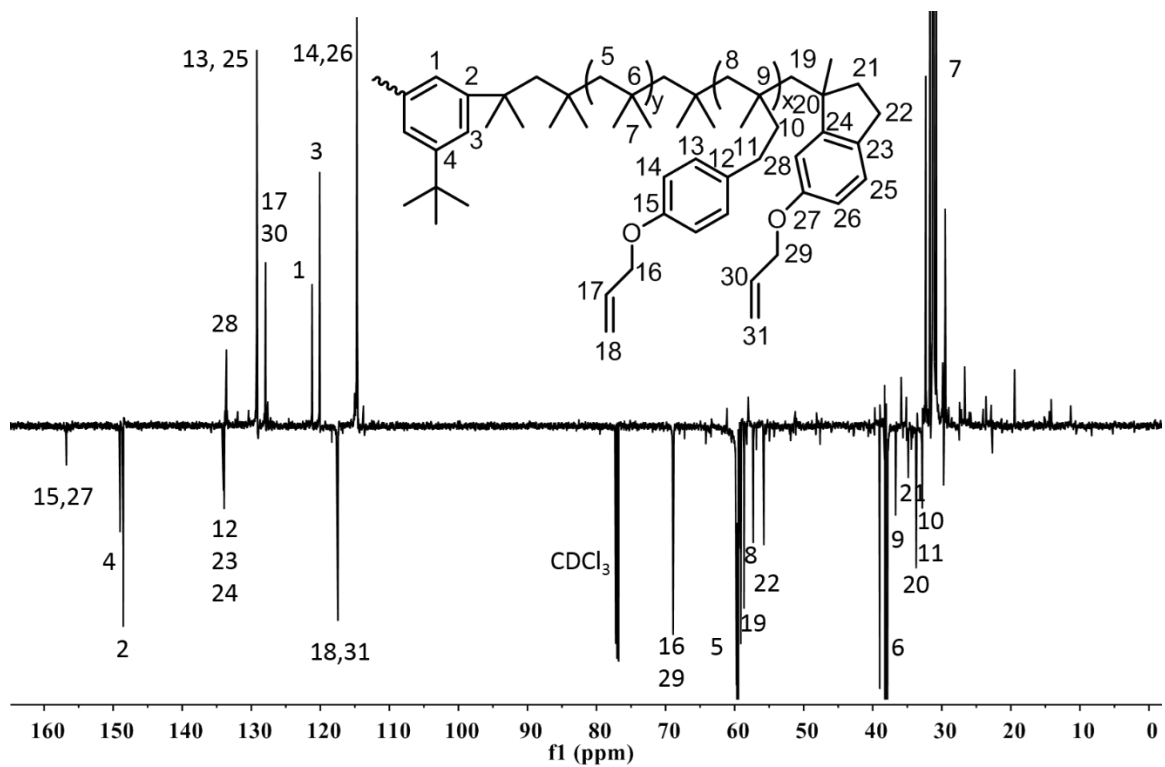Figure 5.3 APT NMR spectrum of allyloxyphenyl PIB.
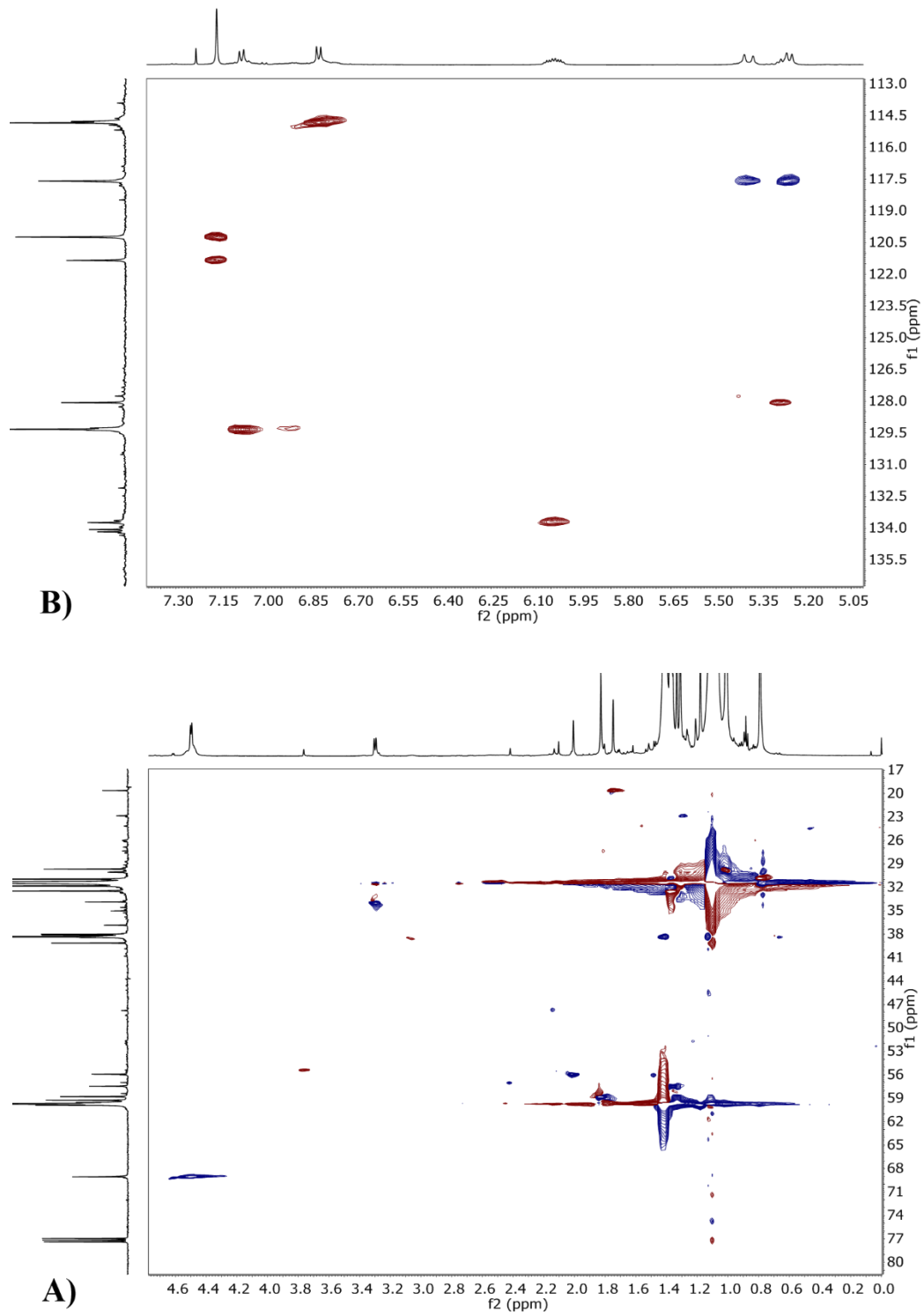
Figure 5.4 2D gradient HSQC NMR spectra of allyloxyphenyl PIB: A) aliphatic region and B) aromatic region.
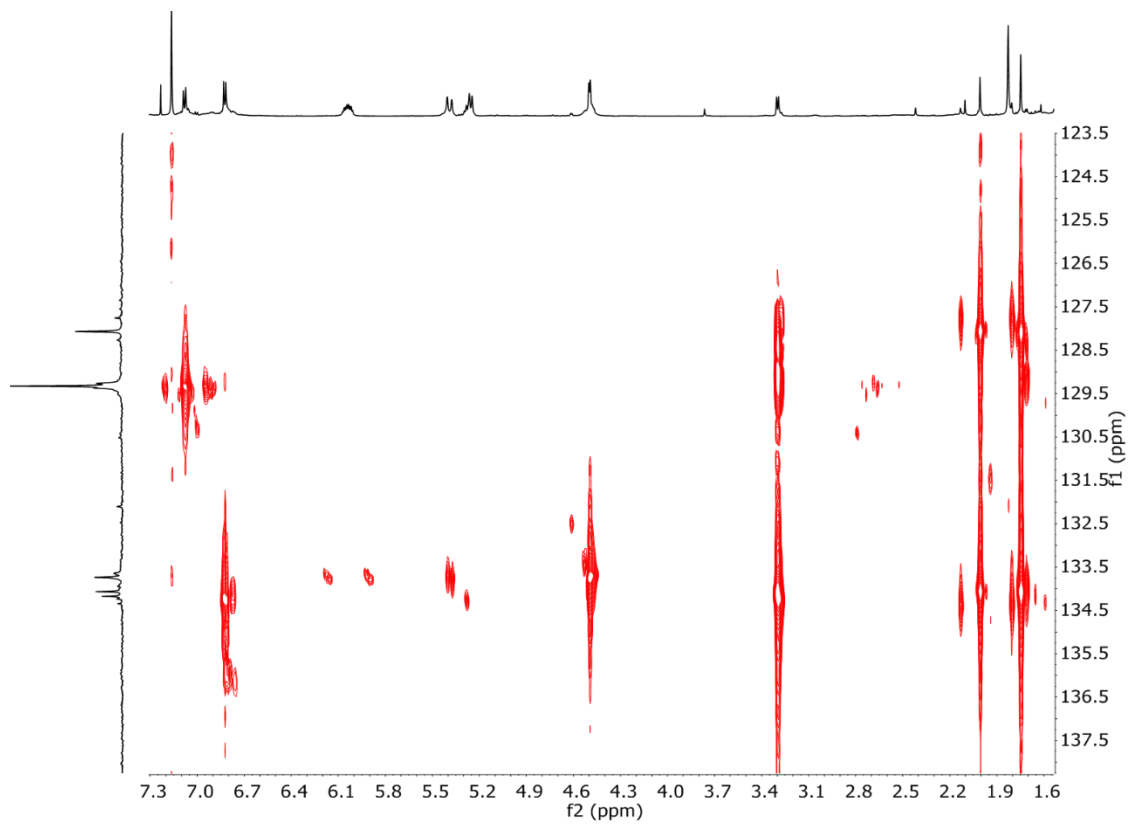
Figure 5.5 2D HMBC NMR spectra of allyloxyphenyl PIB.
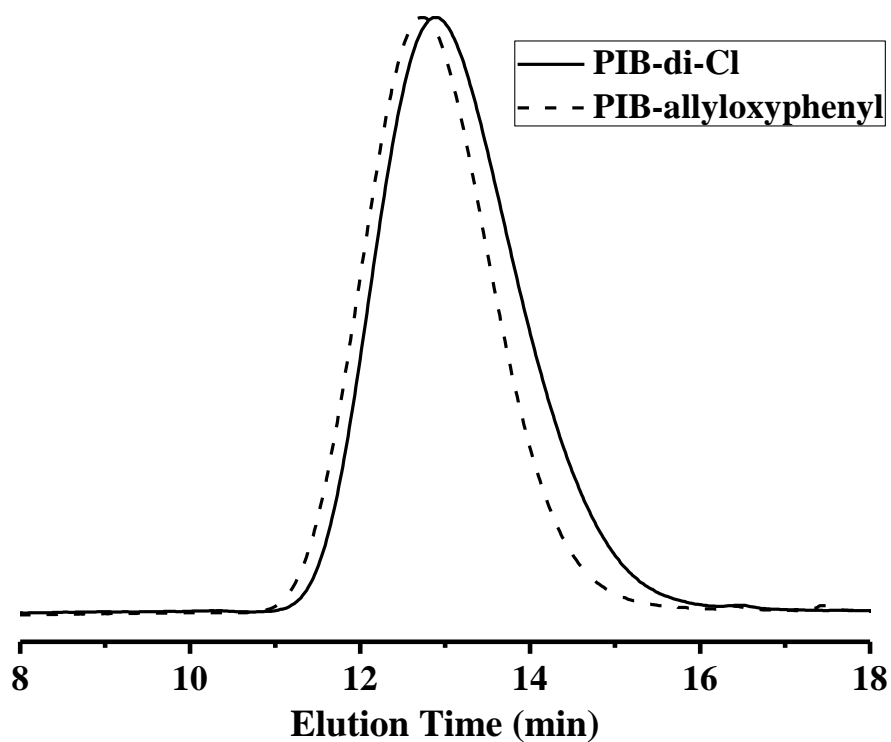
Figure 5.6 GPC trace of difunctonal *tert*-chloride PIB prior to addition of 4-(4-allyloxyphenyl)-2-methyl-1-butene (solid) and allyloxyphenyl-terminated PIB after copolymerization/end-capping (dash.)
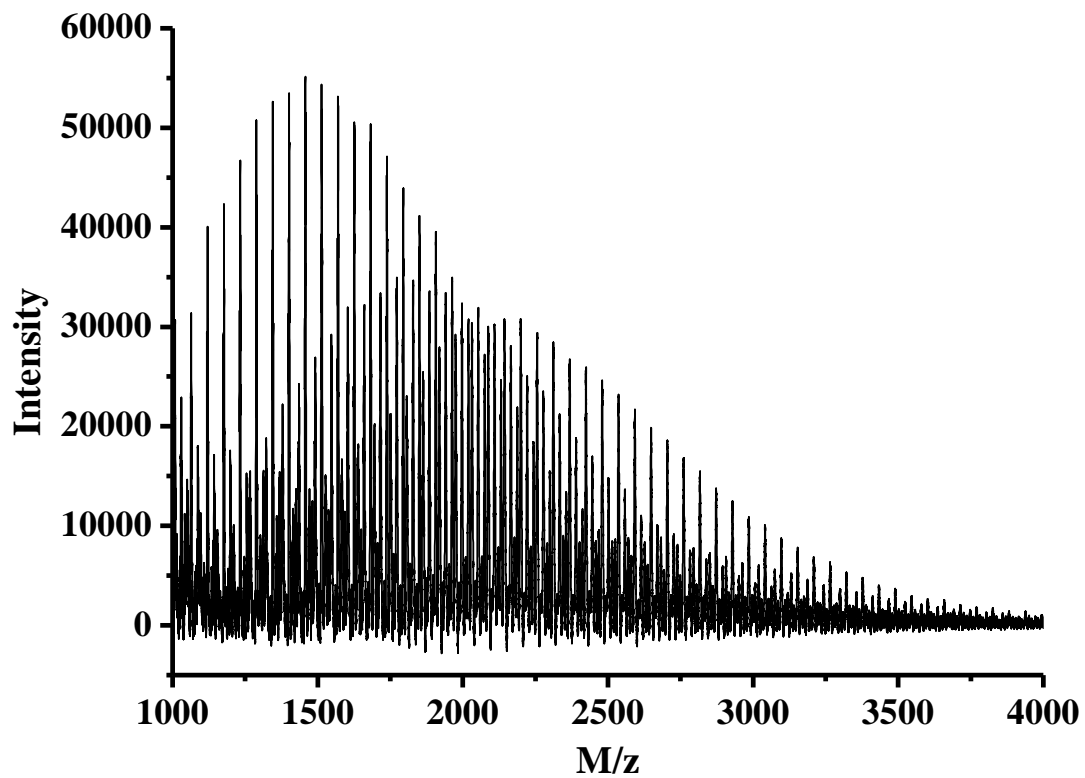
Figure 5.7 MALDI-TOF mass spectra of 4K allyloxyphenyl PIB.

Prepared by the dried droplet method using DCTB as the matrix, AgTFA as the cationizing agent, and THF as the solvent.

Figure 5.8 Linear regression plots of MALDI-TOF mass spectrum of 4K allyloxyphenyl PIB.

CHAPTER VI – SYNTHESIS OF POLYISOBUTYLENE BOTTLEBRUSH

POLYMERS *VIA* RING-OPENING METATHESIS POLYMERIZATION

6.1 Abstract

Polyisobutylene (PIB)-based bottlebrush polymers were synthesized *via* ring-opening metathesis polymerization (ROMP) of norbornene-and oxanorbornene-terminated PIB macromonomers (MMs) initiated by Grubbs third generation catalyst ((H_2IMes)-$(pyr)_2(Cl)_2Ru=CHPh$) (G3). While b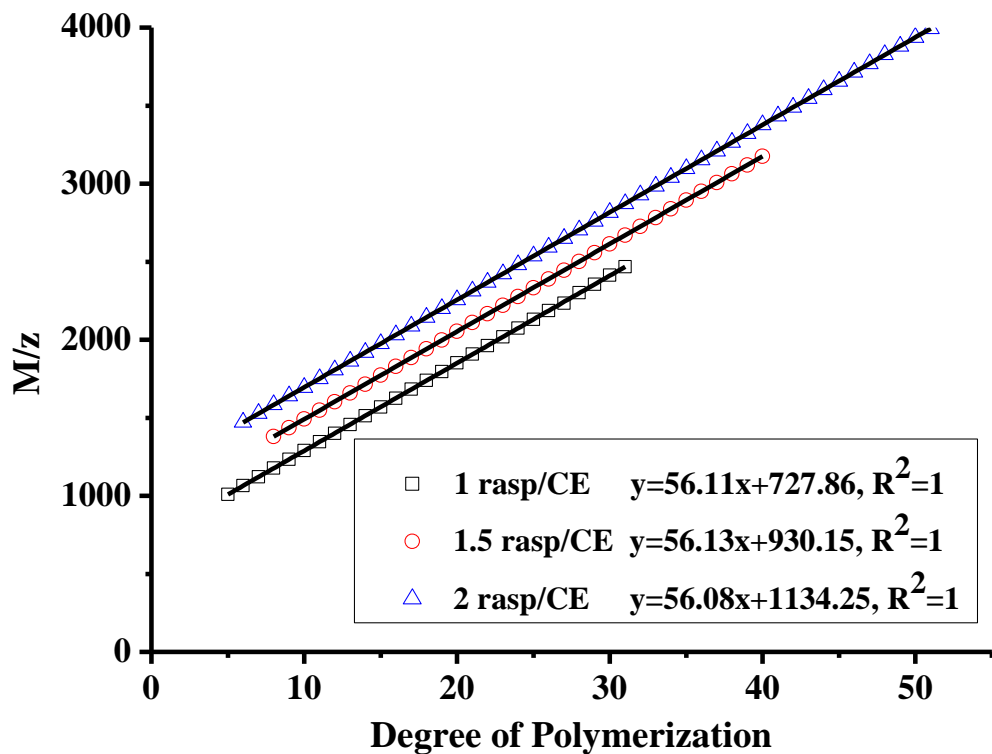oth prepolymers reached greater than 97% conversion as measured by ^1H NMR, the rate of propagation of PIB norbornene was measured to be 2.9 times greater than that of PIB oxanorbornene prepolymer of similar molecular weight. The slower rate of propagation was attributed to the complex effect between the electron rich oxygen bridge and G3, which slowed but didn't inhibit polymerization of oxanorbornene-functional PIB. Both types of prepolymers demonstrated controlled/"living" polymerization behavior, and brush polymers with molecular weight up to ~700 kg/mol were achieved.

6.2 Introduction

Most of the MMs polymerized by ROMP are prepared using reversible deactivation radical polymerization (RDRP) or anionic polymerization technique to achieve precise molecular weights and near quantitative end group functionality. [1-2] However, to the best of our knowledge, no preparation of such MMs have been reported by living carbocationic polymerization (LCP), more specifically, norbornene-functional PIB MMs. The only literature reports regarding PIB and ROMP pertains to ruthenium catalyst recycling by binding PIB to the N-heterocyclic carbine (NHC) ligand of 2nd generation Grubbs catalyst. [3] PIB is a polymer with unique properties, including high

flexibility and energy damping, good thermal and oxidative stability, low gas permeability, good chemical and solvent resistance, and good biocompatibility. [4] It would be of great importance to introduce such good properties to bottlebrush polymers for desired applications. Recently, the synthesis of PIB brush polymers have been reported by RAFT polymerization of PIB acrylate MMs. [5] However, this approach required long reaction times (>24 h) and high initiator concentrations to achieve high conversion. Furthermore, the Đ of obtained PIB brushes was greater than 2.0.

With the development of LCP of PIB, a broad family of PIB MMs have been reported, such as (meth)acrylates [6-8] and epoxides. [9] However, to our knowledge, there are no literature reports on the synthesis of norbornene functional PIBs. Recent work by our lab in chain end functionalization of PIB by combining end-quenching of living PIB with post-polymerization modifications offers promising new routes for facile synthesis of functionalized PIBs with quantitative end group conversion, precise controlled molecular weights, narrow Đ. [10-13]

Herein, this work demonstrates a novel synthetic route towards norbornene-functional PIB MMs by nucleophilic substitution of PIB-Br with *exo*-(oxa)norbornene imides as shown in Scheme 6.1C. Secondly, we report the facile synthesis of various high molecular weight brush polymers with controlled MW and narrow Đ. Meanwhile, the effect of norbornene bridge group on the ROMP kinetics of PIB norbornene and PIB oxanorborne MMs initiated by G3 catalyst is investigated by both ^{1}H NMR and SEC kinetic analysis.
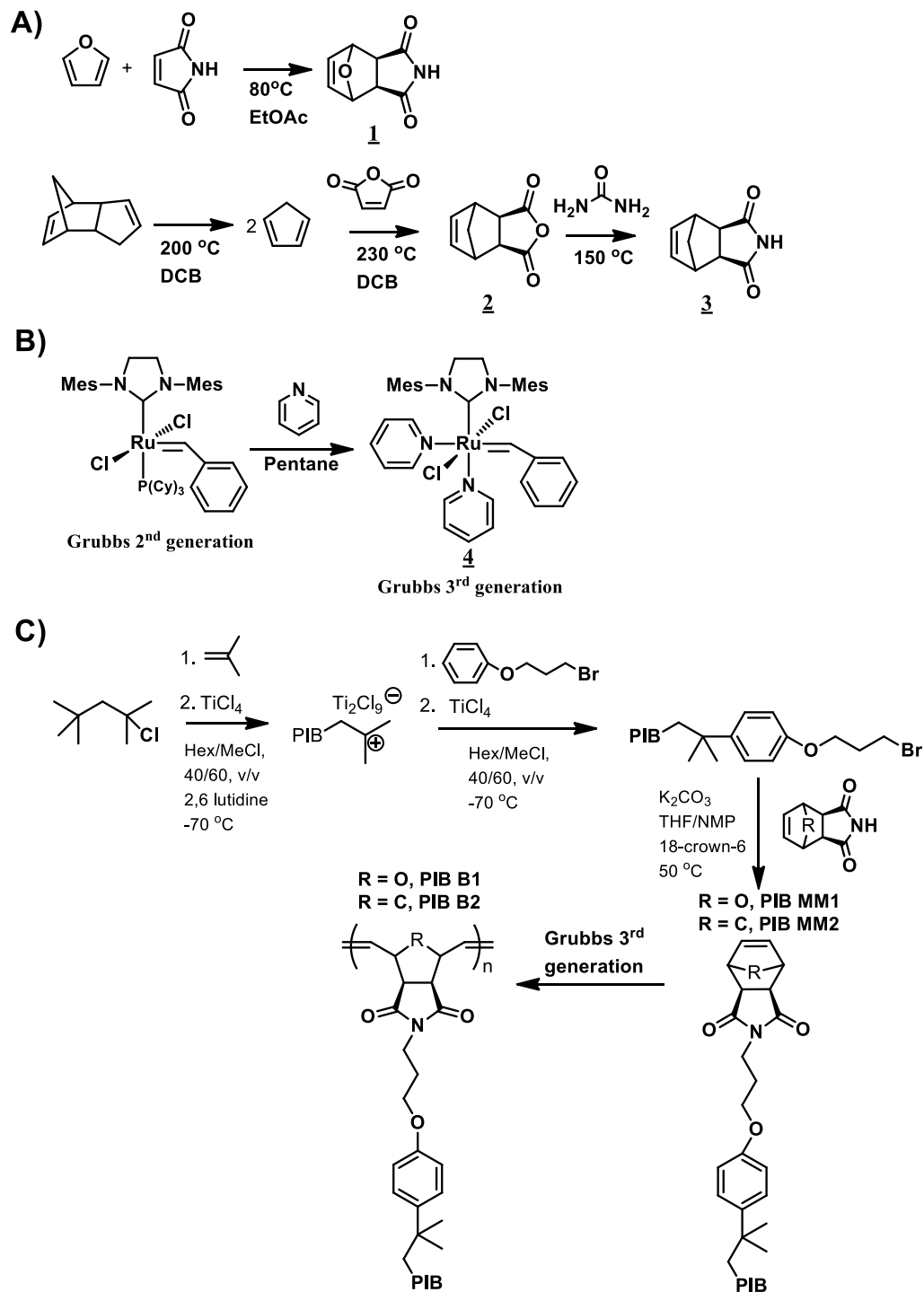
Scheme 6.1 Synthesis of A) *exo*-7-oxanorbornene-5,6-dicarboximide and *exo*-5-norbornene-2,3-dicarboximide, B) third generation Grubbs catalyst, and C) PIB norbornene and PIB oxanorborene MMs and their corresponding bottlebrush polymers *via* ROMP.

6.3 Experimental

Materials. Hexane (anhydrous, 95%), methanol (anhydrous, 99.8%), methylene chloride (anhydrous, 99.8%), titanium tetrachloride (TiCl$_4$) (99.9%), 2,6-lutidine (99.5%), anisole (anhydrous, 99.7%), (3-bromopropoxy)benzene (anhydrous, 98%), tetrahydrofuran (THF) (anhydrous, 99.9%), ethyl vinyl ether (99%), maleimide (99%), pentane, dichloromethane-d$_2$ (CD$_2$Cl$_2$), diethyl ether, furan (99%), 2nd generation Grubbs catalyst, pyridine(99%), potassium carbonate (K$_2$CO$_3$), ethyl acetate (99%), maleic anhydride (99%), maleic anhydride (99%), dicyclopentadiene (99%), urea (99%), toluene (99%), 1,2-dichlorobenzene, and silver trifluoroacetic acid (AgTFA) were purchased from Sigma-Aldrich and used as received. *Trans*-2-[3-(4-*t*-butylphenyl)-2-methyl-2-propenylidene]malononitrile (DTCB) was purchased from Tokyo Chemical Industry Co. and used as received. Magnesium sulfate (MgSO$_4$) (anhydrous), sulfuric acid (98%), chloroform-d (CDCl$_3$) were purchased and used as received from Fisher Scientific. Acetonitrile-d$_3$ (99.8%) were purchased from Cambridge Isotopes and used as received. Isobutylene (IB, BOC Gases) and methyl chloride (Gas and Supply) were dried by passing the gaseous reagent through a column of CaSO$_4$/molecular sieves/CaCl$_2$ and condensing within a N$_2$-atmosphere glovebox immediately prior to use. The mono-functional initiator, 2-chloro-2,4,4-trimethylpentane (TMPCl) was synthesized by bubbling HCl gas through neat 2,4,4-trimethyl-1-pentene (Sigma-Aldrich Co.) at 0°C and was stored at 0 °C prior to use.

Instrumentation. Nuclear magnetic resonance (^{1}H NMR and ^{13}C NMR) experiments were performed on a Varian 300 or Bruker Ascend 600.13 MHz (TopSpin 3.5) spectrometer. All ^{1}H chemical shifts were referenced to TMS (0 ppm), and all ^{13}C

shifts were referenced to CDCl$_3$ (77.16 ppm). Samples were prepared by dissolving the polymer in either chloroform-d or acetonitrile-d$_3$ (5-7%, w/v) and charging this solution to a 5 mm NMR tube. For quantitative proton integration, 16 transients were acquired using a pulse delay of 27.3 s. In the end group analysis, the signal due to the ultimate methylene protons adjacent to the phenoxy moiety (1.79 ppm, 1H, singlet) was chosen as an internal reference for functionality analysis.

Real-time Fourier transform infrared (RT-FTIR) monitoring of isobutylene polymerizations was performed using a ReactIR 45m (Mettler-Toledo) integrated with a N$_2$-atmosphere glovebox (MBraun Labmaster 130) equipped with a cryostated heptane bath. Isobutylene conversion during polymerization was determined by monitoring the area above a two-point baseline of the absorbance at 887 cm^{-1}, associated with the =CH$_2$ wag of isobutylene.

Number-average molecular weights (M$_n$) and polydispersities (PDI = M$_w$/M$_n$) were determined using a gel-permeation chromatography (GPC) system consisting of a Waters Alliance 2695 separations module, an online multi-angle laser light scattering (MALLS) detector fitted with a gallium arsenide laser (power: 20 mW) operating at 658 nm (miniDAWN TREOS, Wyatt Technology Inc.), an interferometric refractometer (Optilab rEX, Wyatt Technology Inc.) operating at 35°C and 685 nm, and two PLgel (Polymer Laboratories Inc.) mixed E columns (pore size range 50-10^3 Å, 3 μm bead size). Freshly distilled THF served as the mobile phase and was delivered at a flow rate of 1.0 mL/min. Sample concentrations were ca. 15-20 mg of polymer/mL of THF, and the injection volume was 100μL. The detector signals were simultaneously recorded using ASTRA software (Wyatt Technology Inc.), and absolute molecular weights were

determined by MALLS using a *dn/dc* calculated from the refractive index detector response and assuming 100% mass recovery from the columns.

Matrix-assisted laser desorption/ionization time-of-flight mass spectrometry (MALDI-TOF MS) was performed using a Bruker Microflex LRF MALDI-TOF mass spectrometer equipped with a nitrogen laser (337 nm) possessing a 60 Hz repetition rate and 50 µJ energy output. The PIB samples were prepared using the dried droplet method: separately prepared THF solutions of DCTB matrix (20 mg/mL), PIB sample (10 mg/mL), and AgTFA cationizing agent (10 mg/mL), were mixed in a volumetric ratio of matrix/sample/cationizing agent = 4:1:0.2, and a 0.5 µL aliquot was applied to a MALDI sample target for analysis. The spectrum was obtained in the positive ion mode utilizing the Reflector mode micro-channel plate detector and was generated as the sum of 900-1000 shots.

Thermal property testing. The thermal degradation properties were investigated by thermogravimetric analysis (TGA), using a Q 500 (TA Instrument) thermogravimetric analyzer. The furnace atmosphere was defined by 10 mL/min N_2. Samples were prepared by loading a platinum sample pan with 10-20 mg of material. The samples were subjected to a temperature ramp of 10 $^{\circ}$C/min from 30 to 600°C. The degradation temperature was defined as the temperature at which 10% weight loss had occurred.

Exo-7-oxanorbornene-5,6-dicarboximide (1). A solution of maleimide (4.75g, 48.9 mmol) and freshly distilled furan (25.0 mL, 343 mmol) in EtOAc (100 mL) was prepared in a 250 mL 3-necked round bottomed flask equipped with magnetic stir bar and reflux condenser. The reaction was purged with N_2 for 30 min before heating at 80 °C overnight (18 h). The reaction was then cooled to room temperature and pentane (50 mL)

added followed by cooling to -10 °C for 6 hours affording (*1*) (6.69 g, 83%) as colorless crystals; mp 168-170 °C dec. ^{1}H NMR (300 MHz, CD$_3$CN): δ 8.88 (s, 1H), 6.49 (s, 2H), 5.14 (s, 2H), 2.84 (s, 2H). ^{13}C NMR (75 MHz, CD$_3$CN): δ 178.34, 137.78, 82.24, 50.02.

Exo-5-norbornene-2,3-dicarboxylic anhydride (2). Briefly, a 500 mL 3-necked round bottomed flask equipped with magnetic stir bar, condenser, and addition funnel, was charged with maleic anhydride (98.06 g, 1.00 mol) and 1,2-dichlorobenzene (100 mL) and heated to 200 °C. Subsequently, a solution of dicyclopentadiene (69.41 g, 0.525 mol) in 1,2-dichlorobenzene (40 mL) was added dropwise over 1 h while maintaining the reaction temperature at 200 °C. The reaction was then heated at 230 °C for 2.5 h, followed by cooling to room temperature (12 h). The resulting crystals were isolated by vacuum filtration and recrystallized three additional times from toluene to give >99% exo (*2*) (46.4 g, 28%) as needle-like crystals. ^{1}H NMR (300 MHz, CDCl$_3$): δ 6.29 (s, 2H), 3.41 (s, 2H), 2.97 (s, 2H), 1.63 (d, *J* = 9.8 Hz, 1H), 1.40 (d, *J* = 10.1 Hz, 1H).

Exo-5-norbornene-2,3-dicarboximide (3). exo-5-norbornene-2,3,-dicarboxylic anhydride (41.20 g, 251 mmol) and urea (16.58 g, 276 mmol) were weighted into a 250 mL round bottomed flask equipped with magnetic stir bar and reflux condenser. The setup was evacuated of air and backfilled with argon before heating at 150 °C for 2h. Melting of the reactants was accompanied by vigorous evolution of gas which was vented using an oil bubbler. The crude product was purified by first dissolving in water (700 mL) at 90 °C, followed by recrystallization at room temperature giving (*3*) (31.60 g, 77%) as off-white crystals that were dried overnight *in-vacuo*; mp 163-164 °C. ^{1}H NMR (300 MHz, CDCl$_3$): δ 8.57 (s, 1H), 6.26 (s, 2H), 3.27 (s, 2H), 2.71 (s, 2H), 1.55 (d, *J* =

10.0 Hz, 1H), 1.43 (d, J = 9.6 Hz, 1H). ^{13}C NMR (75 MHz, CDCl$_3$): δ 178.76, 137.94, 49.36, 45.31, 43.10.

Third generation Grubb's catalyst (4). Second generation Grubb's catalyst (500 mg, 0.12 mmol) was weighed into a scintillation vial containing a small magnetic stir bar followed by the addition of pyridine (0.474 mL, 5.88 mmol) in the presence of air. After 5 min, pentane (20 mL) was added to the vial resulting in precipitation of a bright green solid. The vial was placed in the refrigerator (5 °C) overnight upon which the green 3rd generation Grubbs catalyst (*4*) was isolated by vacuum filtration and washed with pentane (20 mL) before drying *in-vacuo*. (*4*) was subsequently stored under argon in the dark at 5 °C. Yield: 400 mg, 93%.

Monofunctional primary bromide-terminated PIB precursor (PIB-Br). Monofunctinal PIB Br precursor was synthesized by living isobutylene polymerization/phenoxy quenching. Polymerization and quenching reactions were performed within a N$_2$-atmosphere glovebox equipped with a cryostated heptane bath. Synthesis of 4K PIB Br was carried out as follows: To a 1 L 4-neck round-bottom flask, equipped with an overhead stirrer, thermocouple, and ReactIR probe, and immersed in the heptane bath, were added 131 mL hexane, 196 mL methyl chloride, 0.15 mL (1.3 mmol) 2, 6-lutidine, 3.40 mL (20.0 mmol, 2.97 g) TMPCl, and 105 mL (1.31 mol) IB. The mixture was equilibrated to -70°C with stirring, and polymerization was initiated by the addition of 0.82 mL (7.5 mmol) TiCl$_4$. Essentially full monomer conversion was reached in 42 min according to RT-FTIR data, at which time 9.5 mL (60.0 mmol) 3-bromopropoxybenzene was charged to the reaction (2 eq per chain end). Additional TiCl$_4$ (3.67 mL, 33.4 mmol) was added to catalyze the quenching reaction, resulting in a

total TiCl$_4$ concentration of 2 eq per chain end. The quenching reaction was allowed to proceed for 5 h. At the end of this time, the catalyst was destroyed by careful addition of excess prechilled methanol (~ 30 mL). The resulting polymer solution was washed with methanol and then precipitated into 1.5 L of methanol and acetone solution (methanol/acetone, v/v, 95/5). The precipitate was collected by re-dissolution in fresh hexane; the solution was washed with DI water, dried over MgSO$_4$, and then vacuum stripped. Residual solvent was removed under vacuum at 50°C to yield pure primary bromide terminated PIB precursor **5** (M$_n$ = 4,200 g/mol, Đ =1.23.)

Monofunctional PIB oxanorbornene (PIB MM1) and PIB norbornene (PIB MM2) macromonomers. Monofunctional primary bromide-terminated PIB precursor (PIB-mono-Br, 15.1 g, M$_n$=4,200 g/mol, PDI=1.23) was dissolved in 200 mL of freshly distilled THF and was then transferred to a 500 mL one-neck round bottom flask. To the stirred solution were added 40 mL of anhydrous N-methyl-2-pyrrolidone (NMP), 1.77 g (10.8 mmol mL) *exo*-5-norbornene-2,3-dicarboximide (*3*), 2.47 g (17.9 mmol) potassium carbonate, and 1.89 g (7.16 mmol) 18-crown-6. The mixture was heated at 50 °C under a dry N$_2$ atmosphere for 10 h. Upon completion of the reaction, the THF was vacuum stripped, and the polymer was dissolved in hexane. The resulting solution was filtered through a filter paper and slowly added into excess methanol to precipitate the polymer. The precipitate was redissolved in fresh hexane, and the resulting solution was washed with DI water, dried over MgSO$_4$, and then vacuum stripped at room temperature to obtain pure PIB MM2 (M$_n$ = 4,500 g/mol, PDI = 1.21). PIB MM1 prepolymer (M$_n$ = 4,500 g/mol, Đ = 1.22) was prepared by following the similar procedure.

PIB bottlebrushes via ROMP of exo-(oxa)norbornene-functional PIB. A representative procedure is as follows: PIB MM2 (500 mg, 1.1 x 10^{-4} mol, 100 eq.) was weighed into a vial equipped with magnetic stir bar and pierceable cap. 4.0 mL of a 9:1 (v:v) mixture of CH_2Cl_2 and hexane was then added and the vial degassed via four freeze-pump-thaw cycles and backfilled with argon. A stock solution of third generation Grubb's catalyst (G3) was next prepared by weighing 9.05 mg of G3 into a separate vial equipped with pierceable cap and the vial evacuated/refilled with argon four times. 1.0 mL of previously degassed 9:1 (v:v) CH_2Cl_2:Hexane (four x freeze-pump-thaw cycles) was added to the vial containing G3 using an argon-purged gastight syringe. The polymerization was initiated by the addition of 89 mL of G3 stock solution (1.1 x 10^{-6} mol, 1 eq.) to the vial of PIB MM2 using an argon-purged gas-tight syringe and subsequent aliquots (50 mL) were taken at timed intervals and terminated by addition to vials containing 300 mL of CH_2Cl_2 and 2-3 drops of ethyl vinyl ether.

6.4 Results and Discussion

Synthesis of exo-5-norbornene and exo-7-oxanorbornene precursors. Two norbornene dicarboximide precursors (*1* and *3*) were prepared via Diels Alder reaction. *Exo*-7-oxanorbornene-5,6-dicarboximide (*1*) is a direct combination of furan and maleimide while *exo*-5-norbornene-2,3-dicarboximide (*3*) was prepared by reacting urea with a Diels-Alder product of cyclopentadiene and maleic anhydride. The two precursors differ only at the bridge connecting C3 and C6, which is an ether for (*1*), and methylene for (*3*). This bridge moiety is designed to study the effect of the binding of an electron rich atom, such as oxygen, to the Ru=C of the third generation Grubbs catalyst on the rate of propagation and final conversion of ROMP.

The structures of both norbornene precursors were confirmed by ^{1}H and ^{13}C

NMR. The structure of the intermediate to precursor (*3*), *exo*-5-norbornene-2,3-

dicarboxylic anhydride (*2*), was also confirmed by ^{1}H NMR. Figure 6.1A-C illustrates the

^{1}H spectra of the precursors and the intermediate. All three spectra are consistent with the

expected structures and feature three prominent singlets of equal intensity (2 protons

each) representing alkene (a), C3/C6 bridgehead methine (b), and C4/C5 bridgehead

methine (c) protons. In addition, the spectra of compounds (*2)* and (*3)* show a doublet of

doublets representing the two protons (d, d′) of the C7 methylene bridge, and the spectra

of the two precursors exhibit a broad downfield singlet due to the imide proton. For

example, for precursor (*1*) (Figure 6.1A), the alkene protons appear as a sharp singlet at

6.49 ppm; the C3/C6 methine protons at the oxygen bridgehead appear at 5.14 ppm, and

the C4/C5 methine protons at the oxanorbornene-maleimide bridgehead appear at 2.84

ppm. For precursor (*3*) (Figure 6.2C), the alkene and bridgehead protons were identified

similarly. Major differences in the spectrum of (*3*) compared to (*1*) are the appearance of

methylene protons in the 1.43-1.55 ppm range correlated to the C7 carbon bridge and the

upfield shift to 3.27 ppm of the C3/C6 bridgehead methine protons due to change from an

electron withdrawing oxygen atom to an electron donating methylene group. For both

precursors, the integrated intensity of the imide proton was lower than the theoretical

value due to proton-deuterium exchange with solvent.

^{13}C NMR spectroscopy provided further confirmation of the structure of both

precursors as shown in Figure 6.2. For example, in Figure 6.2A, peaks at 137.8, 82.2, and

49.4 ppm were observed for the alkene, C3/C6 bridgehead, and C4/C5 bridgehead

carbons, respectively of the oxanorbornene precursor. Moving to the norbornene

193

precursor (Figure 6.2B), the major differences observed were the appearance of the methylene peak at 49.4 ppm, and the upfield shift of the C3/C6 peak to 43.1 ppm.

Synthesis of PIB norbornene and PIB oxanorbornene macromonomers. First, primary bromide-terminated PIB was prepared by end-quenching of living carbocationic polymerization of PIB at full IB monomer conversion with (3-bromopropoxy)benzene. PIB (oxa)norbornene macromonomers were then synthesized by nucleophilic substitution reaction of PIB Br with precursors (*1*) or (*3*), as shown in Scheme 6.1C. A mild reaction temperature of 50°C was adopted to prevent decomposition of the (oxa)norbornene moiety *via* retro Diels-Alder reaction. The weak base potassium carbonate was used to prevent the E_2 elimination of HBr which would form unreactive PIB olefinic chain ends. Reaction was carried out in 5/1 (v/v) THF/NMP cosolvent mixture; the small portion of polar NMP was used to increase the solubility of the norbornene precursors in THF. The reaction rate was greatly improved by the addition of an 18-crown-6 phase transfer catalyst.

The structures of both macromonomers were confirmed by ^{1}H and ^{13}C NMR. Figure 6.3B and 6.3C show the ^{1}H spectra of the oxanorbornene and norbornene macromonomers, respectively. Quantitative substitution of primary bromide for oxanorbornene was demonstrated in Figure 6.3B by the appearance of resonances with the theoretically predicted intensities at 6.50 (s), 5.25 (s), and 2. 82 (s) ppm due to the addition of the oxanorbornene moiety. Similarly, evidence of quantitative conversion to PIB norbornene was demonstrated in Figure 6.3C by resonances of appropriate intensity appearing at 6.29 (s), 3.28 (s), and 2.68 (s) ppm due to the addition of the norbornene

moiety. The peak due to the methylene bridge of PIB norbornene was overlapped by the intense methylene groups from the PIB backbone.

^{13}C NMR spectroscropy further verified the structure for both macromonomers; Figure 6.4A and 6.4B show the spectra of the oxanorbornene and norbornene macromonomers, respectively. For example, in Figure 6.4A, peaks at 176.3, 136.7, 81.1, and 47.6 ppm correspond to the carbonyl, alkene, C3/C6 bridgehead methine, and C4/C5 bridgeheand methine carbons, respectively. With respect to the norbornene macromonomer (Figure 6.4B), the major differences observed were the appearance of the methylene peak of the carbon bridge at 48.0 ppm, and the upfield shift of the C3/C6 methine carbons to 43.0 ppm.

Molecular weight and dispersity (Đ) of both PIB oxanorbornene and PIB norbornene macromonomers were investigated by GPC, as shown in Figure 6.5. The refractive index traces show that upon addition of the *exo*-(oxa)norbornene moiety, the elution volume stays almost unchanged in comparison with the starting PIB Br, which indicates no chain coupling or degradation has occurred during post-polymerization modification. The molecular weight and Đ are listed in Table 6.1 with the M_n calculated by NMR in close agreement with the values obtained by GPC.

End group analysis. MALDI-TOF MS provided a second method to determine molecular weight, polydispersity, and end-functionality. The MALDI-TOF mass spectra of 4K mono-functional PIB oxanorbornene and PIB norbornene macromonomers are shown in Figure 6.6A and 6.6B, respectively. Each sample displayed a single, major distribution of polymeric species, associated with Ag cations from the AgTFA cationizing agent, differing from each other only by the number of isobutylene repeat

units. The data from each mass spectrum were analyzed by linear regression of a plot of mass-to-charge ratio (M/z, assumed to be 1), measured at the maximum of each peak of the major distribution, versus degree of polymerization (DP). The slope of this plot is theoretically equivalent to the exact mass of the isobutylene repeat unit, 56.06 Da. The y-intercept is theoretically equivalent to $f \times EG+I+C$, where f is the functionality of the polymer (1 in this study), EG is the exact mass of the (oxa)norborene moiety, I is the exact mass of the TMPCl initiator residue (*sec*-butyl in this case), and C is the exact mass (106.91 Da) of the major isotope of the associated Ag cation.

MALDI-TOF MS data for both of the difunctional PIB (oxa)norbornene macromonomers, analyzed in this manner, are summarized in Table 6.2. In all cases, the measured value of the repeat unit molecular weight (M_{ru}) was within 0.1% of the theoretical value (56.06 Da), and the measured value of $f \times EG+I+C$ was within 2% of the theoretical value. The observed close agreement between measured and theoretical values provides strong evidence that the synthesized difunctional PIB macromonomers possess the expected structure and end-group functionality. Table 6.2 also lists M_n and Đ data obtained from MALDI-TOF-MS. In all cases, these values are lower than the corresponding values obtained from GPC analysis (Table 6.1). This is a common observation and reflects the fact that polymer chains with higher molecular weight are more difficult to desorb/ionize and thus are under-represented at the detector.

Homopolymerization of PIB norbornene and PIB oxanorbornene macromonomers. The homopolymerization of PIB oxanorbornene (PIB MM1)and PIB norbornene (PIB MM2) macromonomerswas was carried out using Grubbs' third generation catalyst owing to its improved functional group tolerance and ability to

196

achieve high monomer conversions in very short reaction times. As shown in Figure 6.7A

and 6.7B, high conversion was indeed achieved for both macromonomers PIB MM1 and

PIB MM2 as confirmed using ^{1}H NMR by monitoring the disappearance of the alkene

proton chemical shifts at 6.50 and 6.29 ppm, respectively, as well as the increase of

chemical shifts at 5.00-5.90 ppm which correspond to the *cis* and *trans* double bonds on

the backbone of the homopolymers. Figure 6.7A and 6.7B illustrate the ^{1}H NMR spectra

of PIB brush polymers PIB B1 and PIB B2. The data show that the rate of propagation

for macromonomer PIB MM2 was faster than that of PIB MM1, since the alkene proton

peak of PIB MM2 completely disappeared after 12.5 min; whereas it took at least 35 min

for PIB MM1. For macromonomer PIB MM1, the ether bridge within the oxanorbornene

moiety played an essential role in slowing the rate of propagation. The ether oxygen is a

strong electron donating group, which coordinates with the electrophilic Ru and thus

competes with the insertion of oxanorbornene olefin into Ru=C. However, this

interference effect was not strong enough to inhibit the ROMP of PIB MM1, with the

polymerization still proceeded to high conversion.

Controlled/living ROMP.^{1}H NMR kinetic study. The controlled/ "living" ROMP

of macromonomers PIB MM1 and PIB MM2 were investigated using both ^{1}H NMR and

GPC. The macromonomer conversions were calculated by monitoring the relative

integration of (oxa)norbornene olefin relative to the aromatic protons from the phenoxy

moiety of the macromonomers, which remain constant. Conversions obtained from [1]H

NMR were used to calculate propagation rate constants and half-lives (Table 6.3). The

conversion vs time plots (Figure 6.8A) showed that the polymerization rate for PIB MM2

was faster than that of PIB MM1 as the conversion of PIB MM2 reached 97% in 8.7 min, while it took 24.6 min for PIB MM1 to achieve a similar conversion.

The semilogarithmic kinetic plots (Figure 6.8B) showed a linear relationship between ln[1/(1-p)] and reaction time, indicating the third generation Grubbs catalyst-mediated ROMP proceeds in a pseudo first-order, controlled/"living" fashion. The slope of PIB MM2 is 2.9 times greater than that of PIB MM1.

SEC kinetics study. An alternative kinetic study was conducted using an SEC technique. The sampling procedure included taking aliquots of the reaction mixture and injecting them into a solution containing ethyl vinyl ether to terminate the polymerization at each time point. The aliquots taken in the ^{1}H NMR study were used for SEC analysis as well. Figure 6.9A and 6.9B illustrate the SEC traces of ROMP of PIB MM1 and PIB MM2 at various times. The data clearly demonstrate that as the reaction proceeds, the macromonomer peak area decreases steadily, while the brush peak area steadily increases. The position of the brush peak also shifts to lower elution volumes, quickly at first and then more gradually. Conversions were determined *via* SEC by comparing the integrated area of the PIB MM1 or PIB MM2 peak at each aliquot with the integrated area of the PIB MM1 or PIB MM2 peak immediately before the addition of the G3 catalyst, in the refractive index (RI) traces (Figure 6.9A and 6.9B). Similar to the aforementioned ^{1}H NMR kinetics analysis, propagation rate constants and half-lives were calculated from conversions determined by SEC. The conversion vs time (Figure 6.10A) and semilogarithmic kinetic plots (Figure 6.10B) obtained by SEC kinetic analysis demonstrated the same trend observed in the ^{1}H NMR kinetics analysis, indicating same

trend for propagation rate constant and half-lives as well. The propagation rate of PIB

MM2 is 2.2 times greater than that of PIB MM1.

Since ROMP proceeds in a controlled/"living" fashion, molecular weights of the

bottlebrush polymers can be precisely controlled by varying the molar ratio of

[macromonomer]$_0$/[G3]$_0$. In a second study, PIB MM2 macromonomer was chosen as an

example due to its faster rate of polymerization, and polymerizations were allowed to

reach complete conversion. The plot of molar feed ratio vs degree of polymerization

(Figure 6.10C) shows a linear increase of molecular weight with the feed ratio, and the

slope of the M_n vs [PIB MM2]$_0$/[G3]$_0$ is approximate the same to the M_n of the starting

macromonomer PIB MM2 further confirming the controlled polymerization. In addition,

narrow monomodal SEC curves demonstrated the facile control of polymerization

(Figure 6.10D).

6.5 Conclusions

Novel (oxa)norbornene end-functional PIBs were prepared by reacting *exo-*

(oxa)norbornene imide with PIB Br obtained by end-quenching of living carbocationic

polymerization of PIB with (3-bromopropoxy)benzene. Third generation Grubbs catalyst-

mediated ROMP of both PIB oxanorbornene and PIB norbornene macromonomers *via* a

grafting "through" methodology was conducted successfully at room temperature,

producing PIB bottlebrush polymers with controlled molecular weights and low

dispersities (Đ=1.01). It was demonstrated that PIB brushes with high molecular weight

(700 kDa) could be achieved by varying the feed ratio of the [(oxa)norbornene]$_0$/[G3]$_0$;

even higher molecular weight could be achieved by further increasing the latter ratio,

since no termination or G3 catalyst degradation was observed even at very high macromonomer conversions.

ROMP kinetics studied using both ^{1}H NMR and SEC analysis showed pseudo first-order kinetic behavior for both PIB oxanorbornene and PIB norbornene macromonomers. Both methods demonstrated that the ROMP propagation rate of PIB norbornene is at least 2.2 times greater than that of PIB oxanorborne macromonomer with similar molecular weight. The slower rate of propagation was ascribed to the complex effect between the electron rich oxygen atom and G3, which interfered with, but didn't inhibit, the interaction of Ru=C with the polymerizable oxanorbornene moiety. It was likely due to the proximity of the olefin moiety to the ether bridge that still gave the opportunity for the olefin terminal group to insert into the Ru=C center allowing ROMP to occur, but at a slower rate.

ROMP of PIB (oxa)norbornene prepolymers promises an effective, fast, and facile method for the preparation of PIB brushes. Owing to the exceptional properties of PIB itself, such as good flexibility and damping, good thermal and oxidative stability, chemical and solvent resistance, and biocompatibility, PIB brushes have the potential to be applied in the fields of rheology modifiers, super-soft elastomers, vibration or noise damping materials, and polymer therapeutics.

6.6 Acknowledgements

6.7 References

(1)   Hawker, C. J.; Bosman, A. W.; Harth, E., *Chem. Rev.* **2001,** *101* (12), 3661-3688.

(2)   Matyjaszewski, K.; Xia, J., *Chem. Rev.* **2001,** *101* (9), 2921-2990.

(3)   Al-Hashimi, M.; Bakar, M. D. A.; Elsaid, K.; Bergbreiter, D. E.; Bazzi, H. S., *RSC Adv.* **2014,** *4* (82), 43766-43771.

(4)   Erdodi, G.; Kennedy, J. P., *Prog. Polym. Sci.* **2006,** *31* (1), 1-18.

(5)   Malins, E. L.; Waterson, C.; Becer, C. R., *J. Polym. Sci., Part A: Polym. Chem.* **2016,** *54* (5), 634-643.

(6)   Roche, C. P.; Brei, M. R.; Yang, B.; Storey, R. F., *ACS Macro Lett.* **2014,** *3* (12), 1230-1234.

(7)   Yang, B.; Parada, C. M.; Storey, R. F., *Macromolecules* **2016,** *49* (17), 6173-6185.

(8)   Tripathy, R.; Ojha, U.; Faust, R., *Macromolecules* **2009,** *42* (12), 3958-3964.

(9)   Ojha, U.; Rajkhowa, R.; Agnihotra, S. R.; Faust, R., *Macromolecules* **2008,** *41* (11), 3832-3841.

(10)   Yang, B.; Storey, R. F., *Polym. Chem.* **2015,** *6* (20), 3764-3774.

(11)   Morgan, D. L.; Martinez-Castro, N.; Storey, R. F., *Macromolecules* **2010,** *43* (21), 8724-8740.

(12)   Morgan, D. L.; Storey, R. F., *Macromolecules* **2009,** *42* (18), 6844-6847.

(13)   Ummadisetty, S.; Storey, R. F., *Macromolecules* **2013,** *46* (6), 2049-2059.

6.8 Tables and Figures for Chapter VI

Table 6.1

Molecular weight and dispersity of 4K mono-functional PIB oxanorbornene and PIB norbornene macromonomers.

Sample	Funct.	$M_{n,NMR}$ (g/mol)	$M_{n,GPC}$ (g/mol)	Đ
4K PIB Br	1	4,040	4,200	1.23
4K PIB oxanorbornene	1	4,420	4,500	1.22
4K PIB norbornene	1	4,400	4,500	1.21

Table 6.2 MALDI-TOF MS data for mono-functional PIB oxanorbornene and PIB norbornene macromonomers[a]

Sample	MW_{theo} $f{\times}EG{+}I{+}C$[b]	MW_{exp} $f{\times}EG{+}I{+}C$	Diff.	M_n	Đ	M_{ru}[c]
4K PIB oxanorbornene	462.09	452.72	9.37	1621	1.14	56.12
4K PIB norbornene	460.11	463.15	3.04	1996	1.13	56.11

[a]Unit for molecular weight is Da; [b]f=chain end functionality, EG = end group, I = initiator, C = Ag cation; [c]ru is repeat unit.

Table 6.3

Summary of ROMP kinetic analysis of macromonomers.

MM	molar ratio [MM]/[G3]	^{1}H NMR						SEC		
		k_{app} (min^{-1})^a	$t_{1/2}$ (min)^b	% conv^c	k_{app} (min^{-1})^d	$t_{1/2}$ (min)	% conv^e	BB M_n (kDa)^f	BB $M_{n,theo}$ (kDa)^g	Đ
PIB MM1	100:1	0.14	4.95	97	0.079	8.77	89	403	401	1.03
	100:1	0.40	1.73	97	0.17	4.08	87	387	392	1.01
	50:1	/	/	/	/	/	/	195	/	1.02
PIB MM2	75:1	/	/	/	/	/	/	309	/	1.01
	125:1	/	/	/	/	/	/	542	/	1,02
	150:1	/	/	/	/	/	/	712	/	1.04

^{a}Calculated from slope of the semilogarithimic plot by ^{1}H NMR first-order kinetic analysis. ^{b}Calculated using equation $t_{1/2} = \ln 2/k_{app}$. ^{c}Measured by monitoring olefin consumption using ^{1}H NMR spectra. ^{d}Calculated from slope of the semilogarithimic plot by SEC first-order kinetic analysis. ^{e}Measured using SEC by monitoring the integrations of the MM peaks in the RI trace. ^{f}Measured by SEC using absolute MW determined by light scattering. ^{g}Calculated using the formaula $M_{n,theo} = M_{n,MM} * conv * ([MM]_0/[G]_0)$.
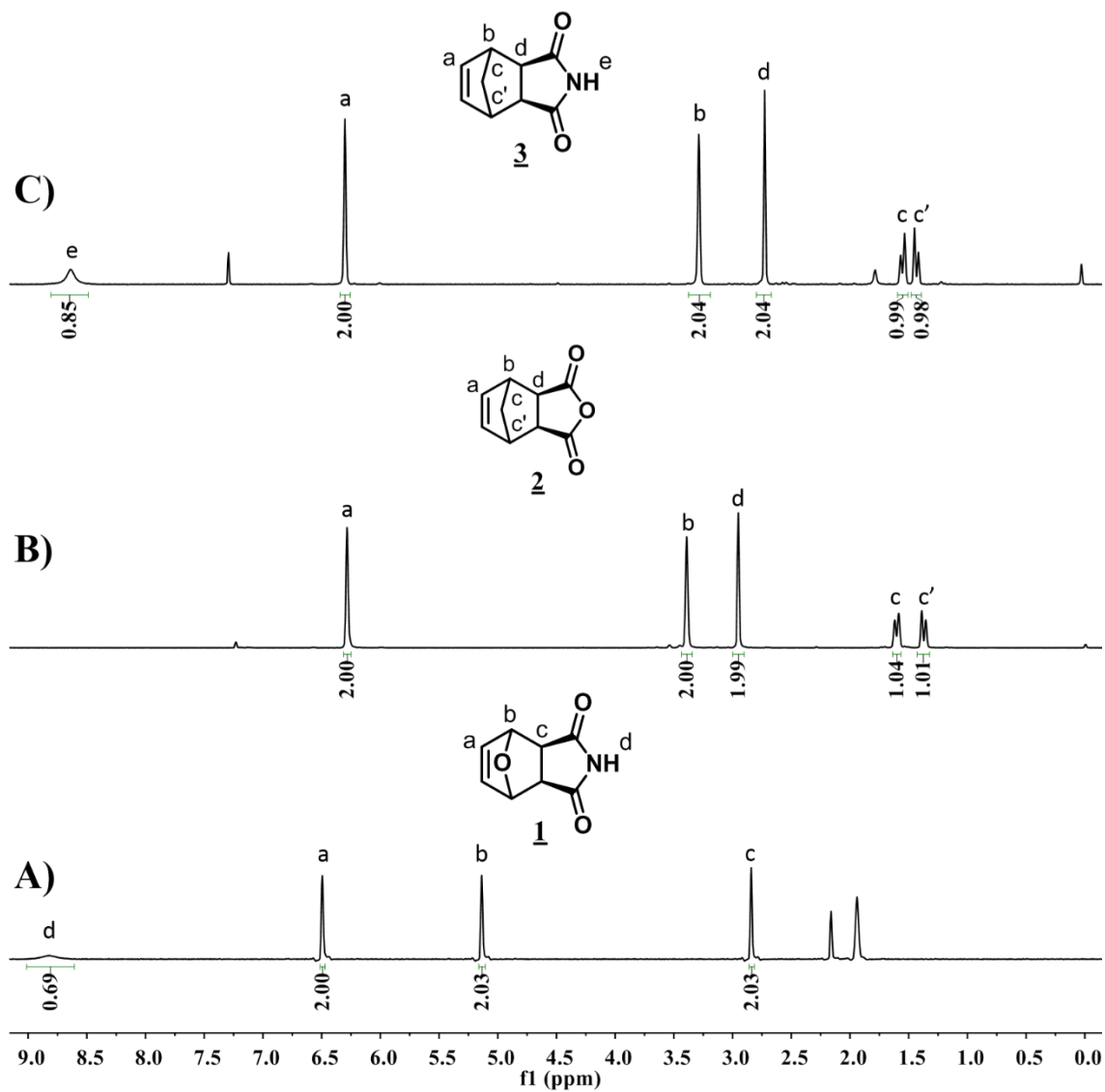
Figure 6.1 ^{1}H NMR spectra (300 MHz, 25°C) of A) *exo*-7-oxanorbornene-5,6-dicarboximide **1** in CD$_3$CN, B) *exo*-5-norbornene-2,3-dicarboxylic anhydride **2** in CDCl$_3$, and C) *exo*-5-norbornene-2,3-dicarboximide **3** in CDCl$_3$.
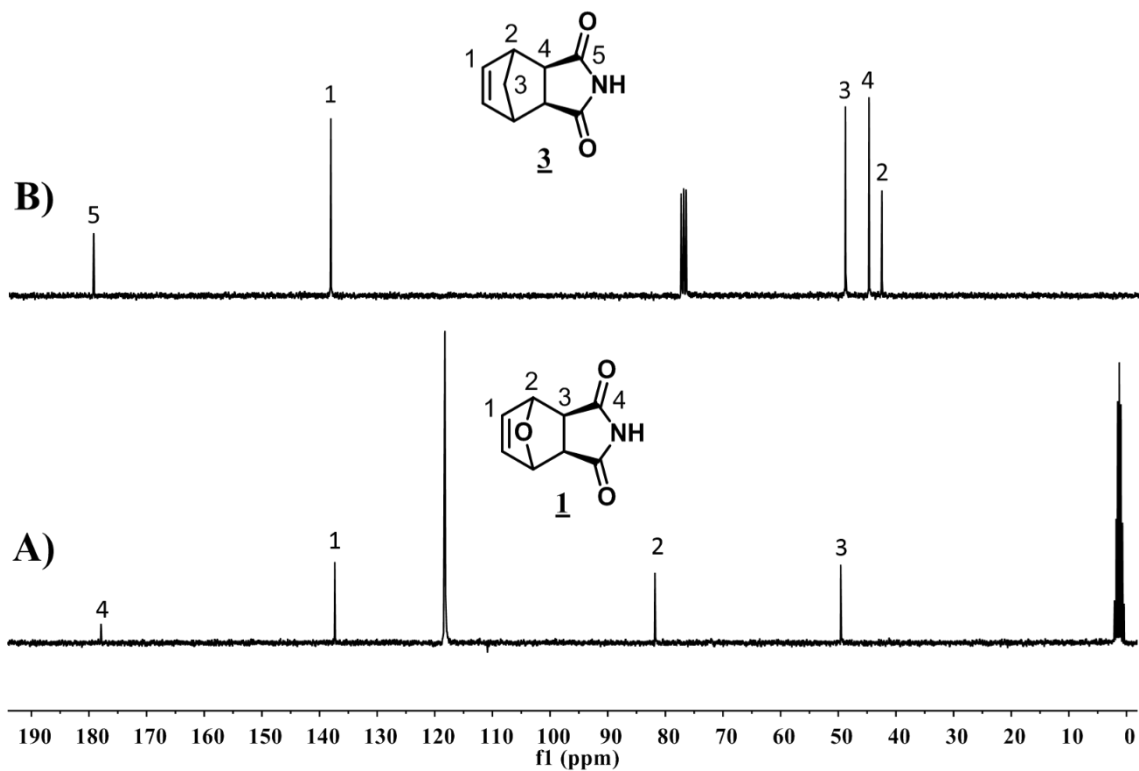
Figure 6.2 ^{13}C NMR spectra (75 MHz, 25°C) of A) *exo*-7-oxanorbornene-5,6-dicarboximide **1** in CD$_3$CN and B) *exo*-5-norbornene-2,3-dicarboximide **3** in CDCl$_3$.
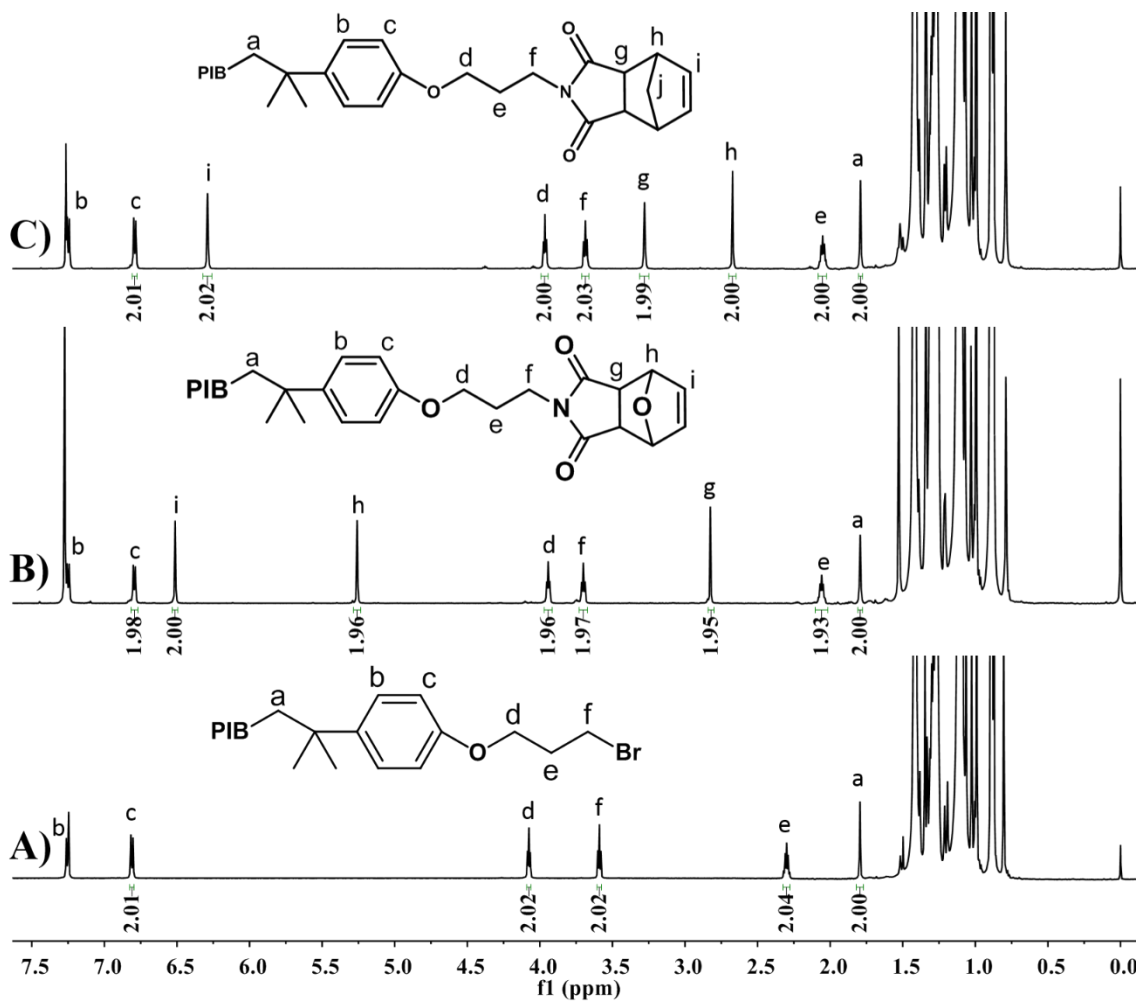
Figure 6.3 ^{1}H NMR spectra (600 MHz, 25°C, CDCl$_3$) of monofunctional A) PIB Br, B) PIB oxanorbornene macromonomer, and C) PIB norbornene macromonomer.
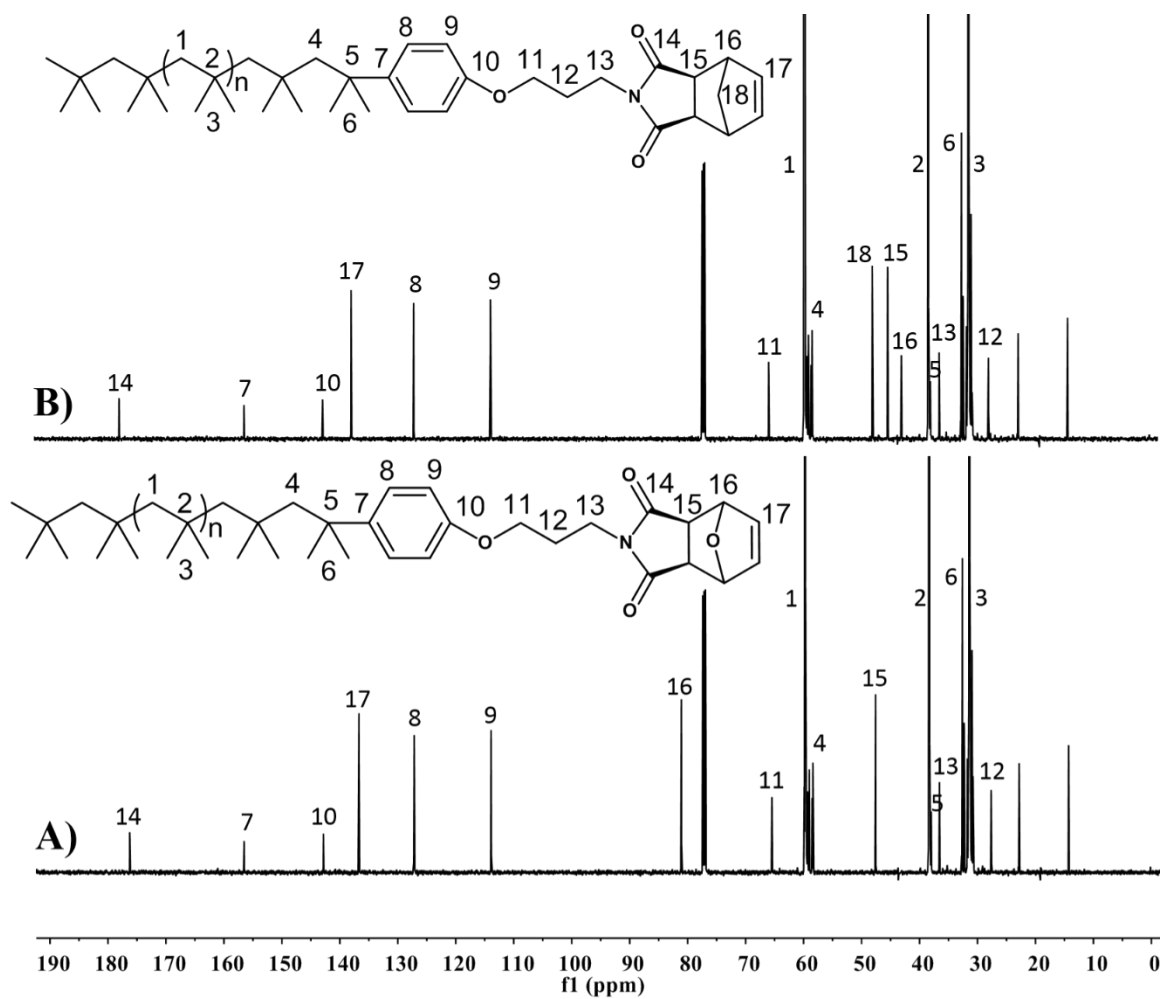
Figure 6.4 ^{13}C NMR spectra (150 MHz, 25 °C, CDCl$_3$) of monofunctional A) PIB oxanorbornene macromonomer; and B) PIB norbornene macromonomer.
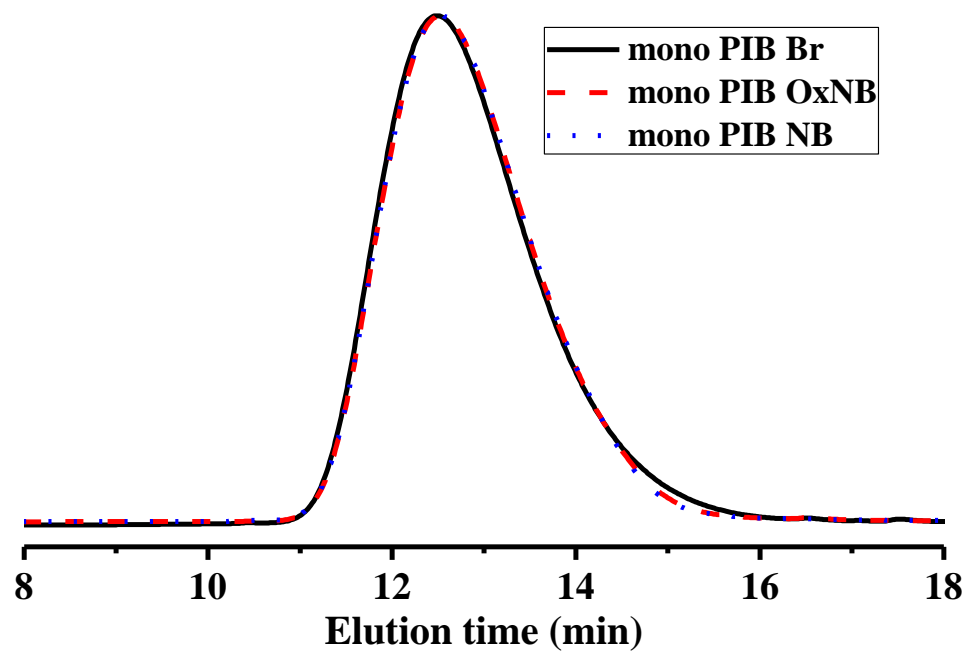
Figure 6.5 GPC refractive index traces of mono-functional PIB Br (solid) and PIB oxanorbornene (dashed) and PIB norbornene (dot) macromonomers.
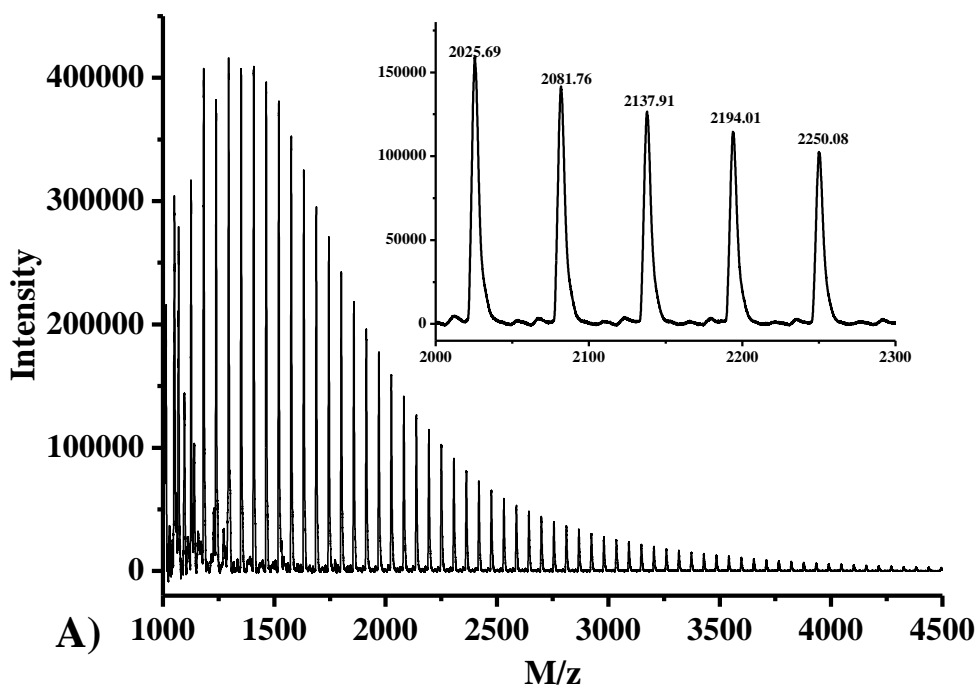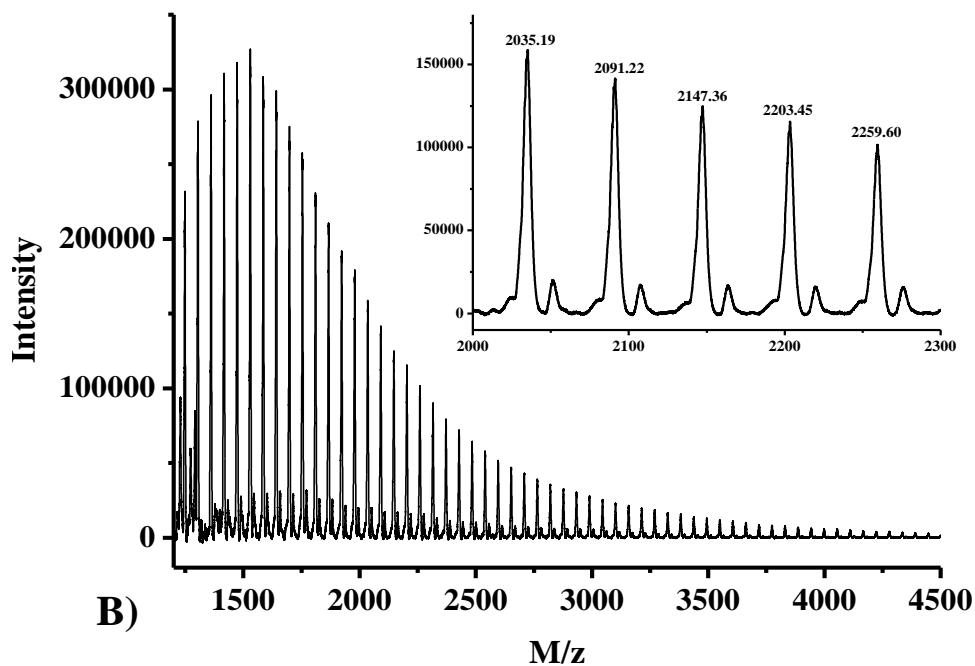
Figure 6.6 MALDI-TOF mass spectra of 4K mono-functional A) PIB oxanorbornene, and B) PIB norbornene prepolymers prepared by the dried droplet method using DCTB as the matrix, AgTFA as the cationizing agent, and THF as the solvent.
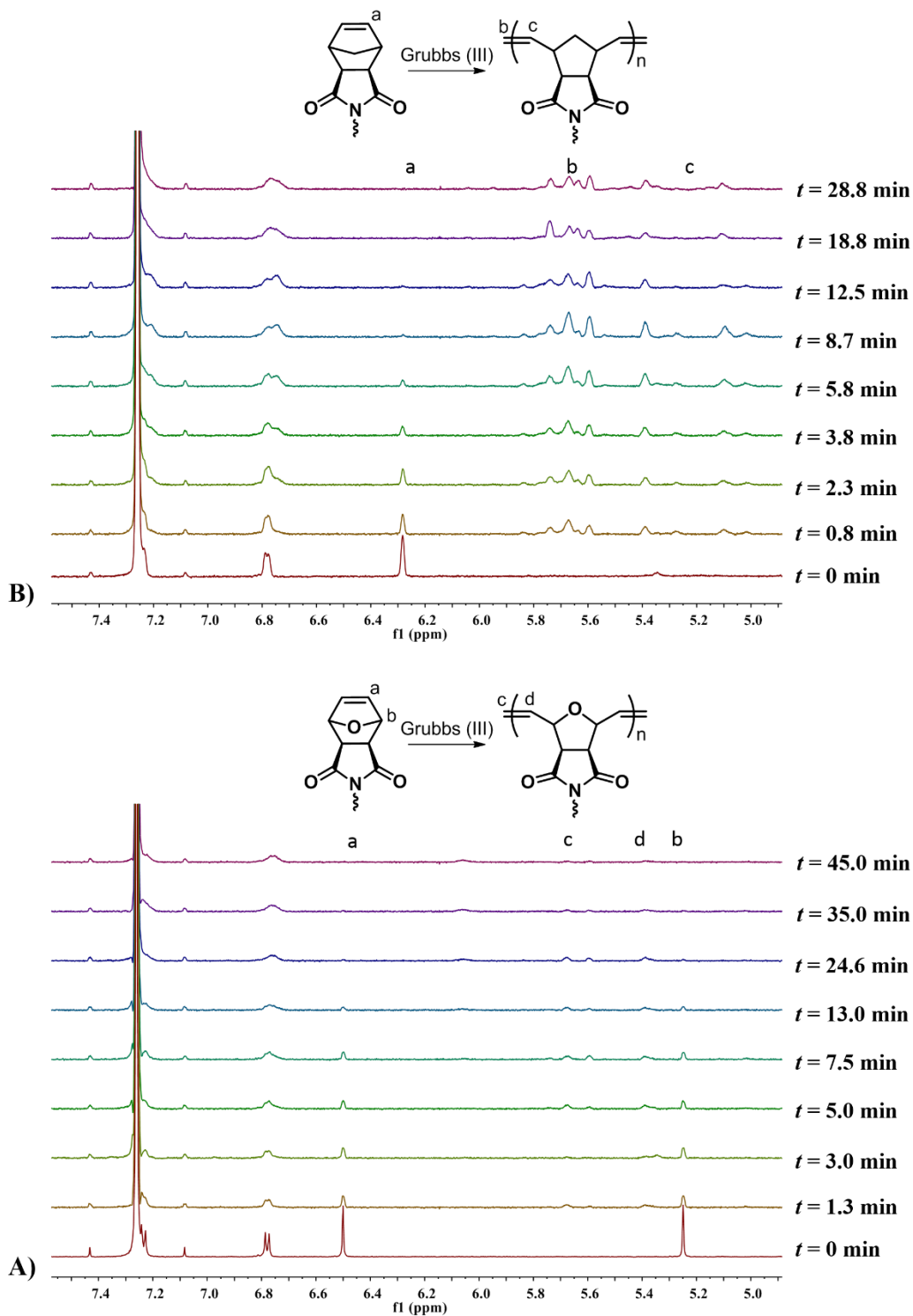
Figure 6.7 ^{1}H NMR spectra of ROMP of A) PIB oxonorbornene and B) PIB norbornene macromonomerat at various reaction times.
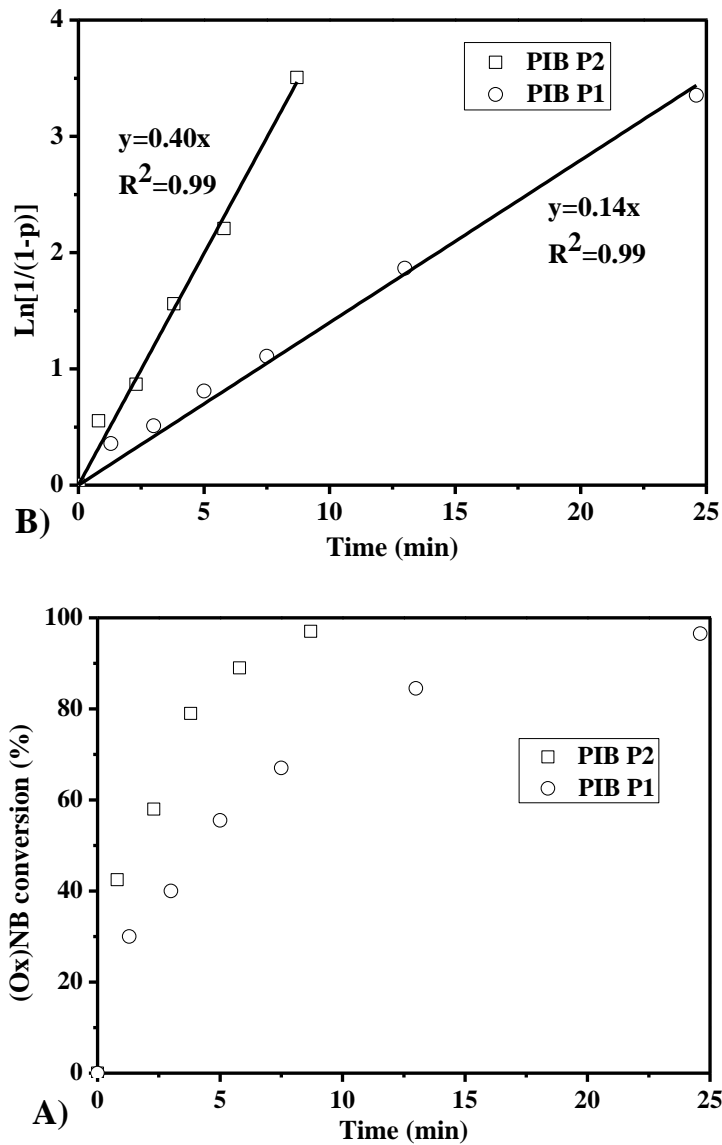
Figure 6.8 ^{1}H NMR kinetic analysis of ROMP of PIB MM1 and PIB MM2 with G3 catalyst (macromonomer:G3 = 100:1 (mol:mol), in CH$_2$Cl$_2$, at room temperature): A) conversion vs time plot; B) semilogarithmic kinetic plots.
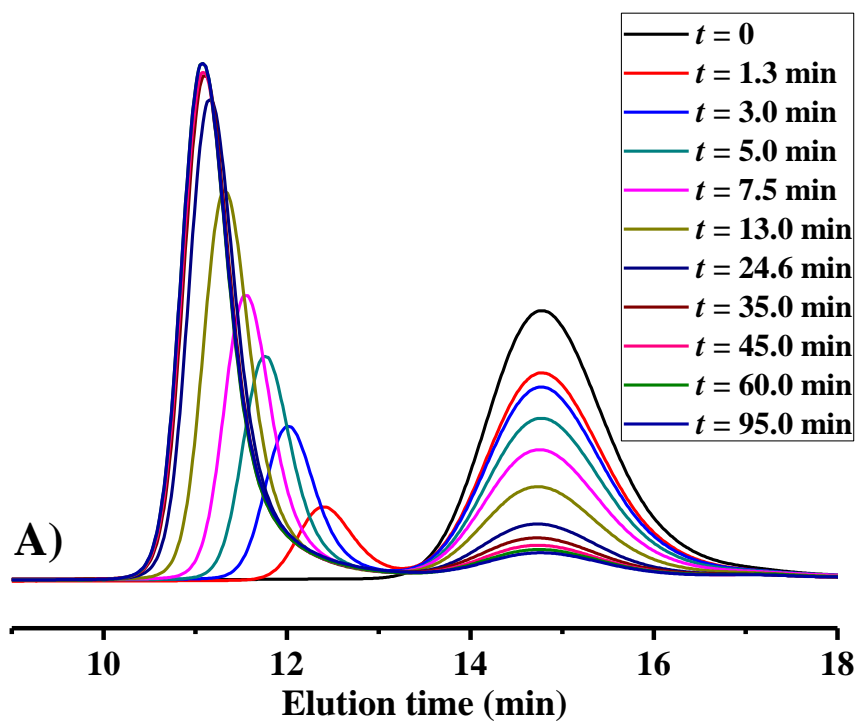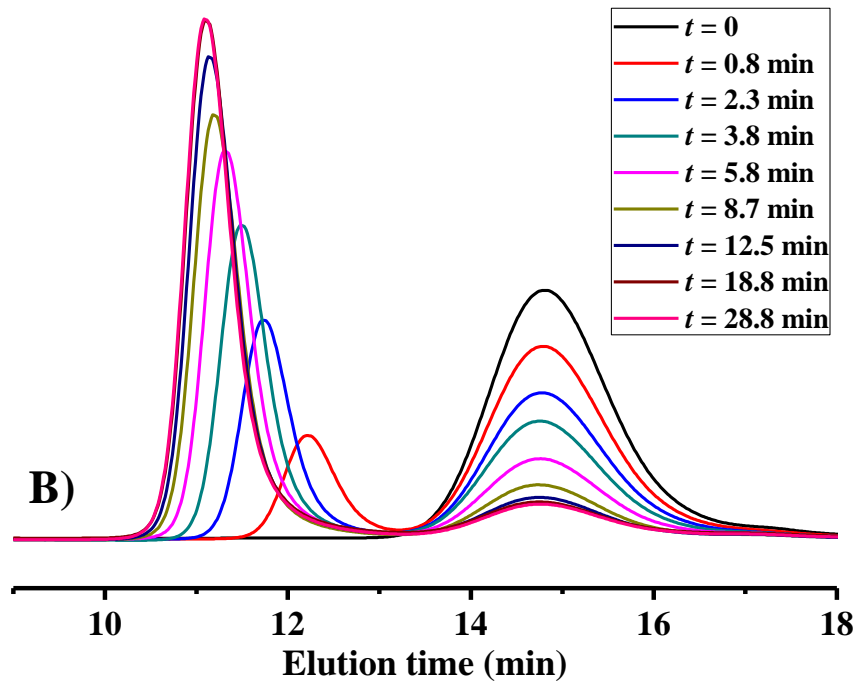
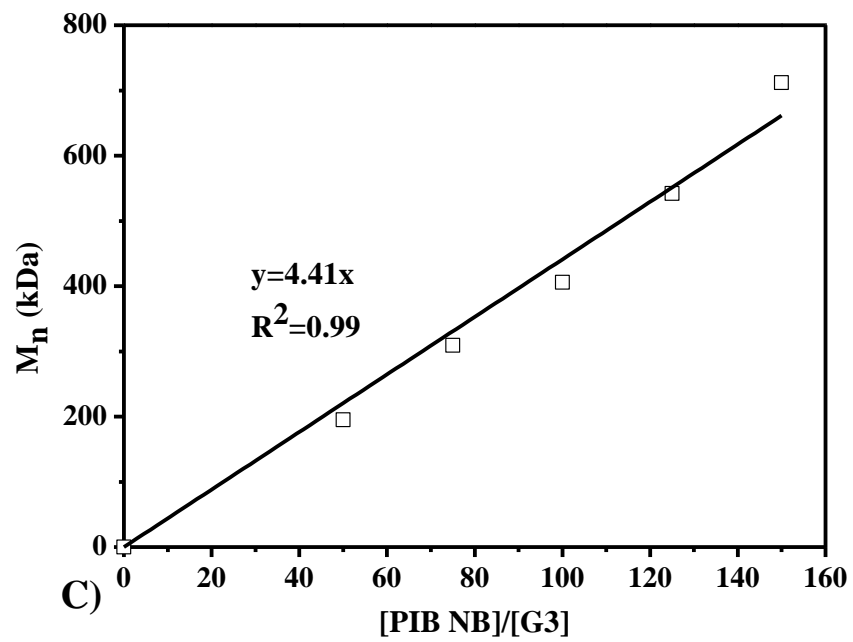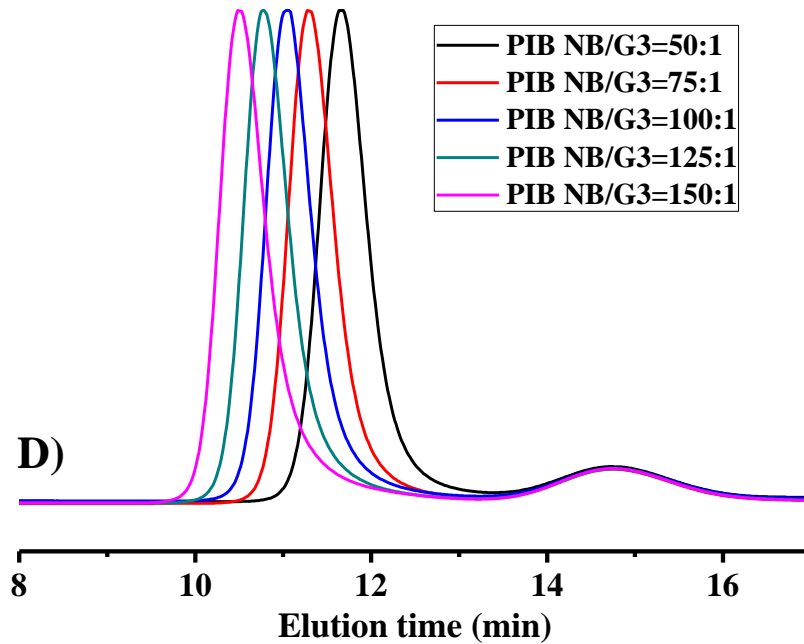Figure 6.9 SEC traces of the kinetic study of ROMP of macromonomers A) PIB MM and B) PIB MM2. The peaks at longer retention times (ca. 14.8 min) correspond to residual macromonomers.
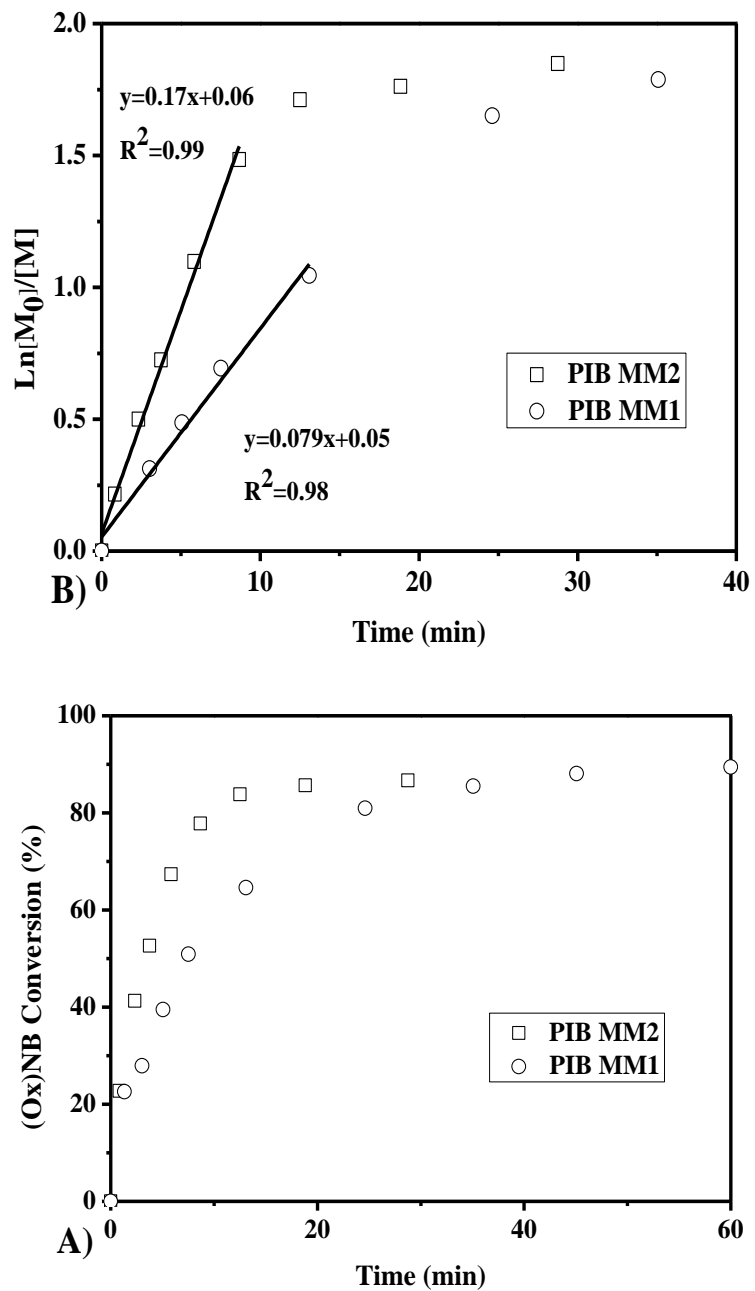
Figure 6.10 Kinetics of ROMP of PIB MM1 and PIB MM2 using Grubbs' third-generation catalyst (macromonomer:G3 = 100:1 (mol:mol), in CH_2Cl_2, at room temperature.

A) conversion vs time plots, B) semilogarithmic kinetic plots, C.) Mn vs [PIB MM2]$_0$/[G3]$_0$ plot, and SEC traces of ROMP of PIB

MM2 with various PIB MM2]$_0$/[G3]$_0$ values after 2 h of reaction.